Université Fédérale
Toulouse Midi-Pyrénées

THÈSE

En vue de l'obtention du
DOCTORAT DE L'UNIVERSITÉ DE TOULOUSE

Délivré par l'Université Toulouse 3 - Paul Sabatier

Présentée et soutenue par

Marcin Jakub DOMAGALA

Le 17 février 2022

Caractérisation d'un nouvel anticorps ciblant les macrophages associés aux tumeurs

---

Ecole doctorale : **BSB - Biologie, Santé, Biotechnologies**

Spécialité : **CANCEROLOGIE**

Unité de recherche :
CRCT - Centre de Recherche en Cancérologie de Toulouse

Thèse dirigée par
Mary POUPOT

Jury

M. Antonio SICA, Rapporteur
M. Alan RAMSAY, Rapporteur
Mme Fatima TEIXEIRA-CLERC, Rapporteure
M. Jean-Pierre DELORD, Examinateur
M. Jean-Jacques FOURNIÉ, Examinateur
Mme Mary POUPOT, Directrice de thèse

Acknowledgements

Looking back at the finished manuscript of my thesis I would like to thank with all my heart, everyone I met during the journey of my PhD. The dream, I thought at times will never come to fruition.

First, I would like to thank all the members of my thesis jury, including Prof. Jean-Pierre Delord who accepted the role of the chairman of the jury; Prof. Antonio Sica, Dr. Alan Ramsay, and Dr. Fatima Teixeira-Clerc who also dedicated their time to review my thesis manuscript.

I can't also forget about the members of my thesis committee: Dr. François Canonne-Hergaux and Dr. Frédéric Lagarrigue. Thank you for your valuable feedback!

Then I would like to thank my dear Team 9/NoLYMIT of CRCT. With your kindness and openness, you all have created a great working environment!

Mary Poupot, my thesis director. I will not be able to thank you enough for entrusting this PhD project to me. Since the beginning you showed me a constant support and patience, not even once losing your temper! Even when forced to deal with my clumsiness when it comes to solving the complexities of administration or my last-minute corrections of this manuscript. I admire your honesty and integrity. Also, thank you for introducing me to pottery!

Jean-Jacques Fournié – for welcoming me in His Team and remaining a constant inspiration. It is truly a rare occasion to find a person with such a charisma, brilliance and integrity. I am also truly grateful for you being an examiner during my defense!

Camille Laurent – some people can't even say they had one good team-leader, in my case I was lucky to have two of them! Camille I wanted to especially thank you for your feedback before the defense – it helped me a lot.

Anne – you have always showed me your kindness, patiently answering my numerous questions (especially the ones concerning CLL) and giving a valuable feedback! I can't forget your encouragement for me to speak French. I wish I could also understand your language better, to fully appreciate your great sense of humor. Finally, you have the best pronunciation of Polish words, even peculiar ones like Mszczonów

Christine – I really appreciate your good heart and approach to life! I will try to always apply the breathing technique you shared with me, to help me deal with pre-presentation stress.

Pauline – I wanted to thank you for everything. You are truly a lovely soul with incredible goodwill, eagerness to help and unmatched ability to multi-task.

Don-Marc – huge thanks for answering my never-ending questions, especially scientific ones, but also sharing many good stories. Your diligence and will when it comes to your job, will always remain an inspiration for me.

Olivia – I will never forget your warmness and smile, that always made me feel at home. Big thanks for help the experiments, especially microscopy and dreaded electroporation. I hope I will finally be able to apply at least a percent of your sense of organization and composure.

Sophie – I will always remain grateful for our collaboration on the project! You are a great person and I am happy you have found a good position in the north

Sarah – thank you for many great memories, I hope you are satisfied with your new job!

Cathy – even if we didn't have time to know each other well, I really appreciate your good energy.

Especially big thanks to dear Carla, Chloé and Nico – my dear companions, who also shared with me their own ups and downs of PhD journey. You are truly remained the best sports!

Chloé – I remember I was a bit afraid that there might remain some reserve between each other in the beginning. Gladly I could not be more mistaken. You turned out to be a great person, who showed me a lot of support and heart.

Carla – sometimes I don't know, what I would have done without you! You allowed me to find some true connections in France. You are truly the best! I am sure you will do exceptional on your defense and find an interesting post-doc in Switzerland.

Nico – thank you for our long discussions, both scientific ones and also geekier oriented. I truly keep my fingers crossed for your soon to be finished PhD and unfold of your scientific carrier!

Fabien – thank you for your kindness, steadiness and willingness to help!

Benoit – big thanks to the best organizer of all the social event and thus a countless great memories! I am really happy, that despite only few months in CRCT, you have remained an integral part of "our group"

Julie – you will always remain a member of team 9 for me. Thank you for keeping us constantly motivated to keep our run routine, organization of social events and bringing delicious home-made pastries☺

Gabriele – I think you have been the first one, who welcomed me truly in the team. I will always remain thankful for that! I hope you have found your place, after finishing your PhD.

I wanted to also thank a "new members" of the Team: Léa, Marion, Nicolas and Amandine (I will say it again – your brownie remain an important factor in finishing this thesis manuscript in its the most critical moments!).

Beside, huge thanks to all the collaborator during my scientific journey, in particular: Bastien Gerby, Vincent Fregona and Manon Bayet from Team IGAALD; Vera Pancaldi, Nina Verstraete, Malvina Marku, and Alexis Coullomb from Team NetB(IO)^2; Laetitia Ligat, Frédéric Pont, Frédéric Pont, Juan-Pablo Cerapio Arroyo, Carine Valle, Emeline Sarot, Emeline Sarot from Pole Technologique of CRCT; Carine Froment, Véronique Le Cabec and Thibaut Sanchez of IPBS; and finally Rudi Baron of TTT.

Besides, big thanks to all people who allowed me to enjoy my stay in France, that in the end might be longer than I expected. Thanks to you this time allowed me to feel like at home.

Collective thanks to our great adventure group of Carla-Guillaume, Chloé-Remi, Benoit-Romain, Nico, Julie for countless memorable journeys!

Huge thanks to Carla, Guillaume and Benoit for showing me climbing – the first sport that I truly enjoy, which helped me also to remain focused☺

Steffen and Rebecca – I will remain grateful that our paths crossed during the last few months of my PhD journey. It is rare to get along so easily. You are truly an incredible couple!

Carine and Maud my great companions during journey to Canada.

Tę drugą część podziękowań chciałbym zadedykować moim wszystkich drogim duszyczkom z Polski, która w pewnym sense, na zawsze pozostanie moim domem!

Po pierwsze wielkie podziękowania dla moich kochanych rodziców! Mamo i Tato – wasze ciągłę wsparcie i wiara pomogły mi nie raz w tej drodze. Dziękuję także mojemu bratu Barkowi, bratowej Katarzynie i babci Józefie. Nie mogę także pominąć mojej drugiej rodzine: Marlenie, Bolesławowi, Magdzie, Karolinie i

Łukaszowi. Chciałem podziękować także pozostałej części mojej rodziny: Marysi (nigdy nie zapomnę, ile razy mnie inspirowałaś do nowych wyzwań, które myślę że w dużej mierze przyczyniły się do tego, gdzie teraz jestem) i Radkowi, Joli, Piotrowi, Ani i Rafałowi, a także drogim przyjaciołom rodziców: Halinie, Ewie, Marzenie, Marysi i Zenkowi.

W końcu chciałbym podziękować moim ukochanym przyjaciołom – Masajowi, Doro, Gabrieli, Izie (no ej Zizi) i Robertowi. Dziękuje, że mimo dzielącej nas odległości mogę ciągle liczyć na Was i Wasze wsparcie. Naprawdę nie wiem, co bym bez Was zrobił <3! Wielkie podziękowania dla moich drogich znajomych: Izie, Konie, Kosiowi, Krystynie, Ewie, Przemkowi, Karolowi i Natalii oraz wszystkich pozostałych, których spotkałem na swojej drodze.

W końcu chciałbym podziekować mojemu Kochanemu Tomkowi, który od lat towarzyszy mi w naszym wspólnym życiu. Kocham Cię i dziękuję, że jesteś!

Résumé

Les macrophages associés aux tumeurs (TAM) sont une des principales populations cellulaires du microenvironnement tumoral. Ils favorisent la croissance et les métastases tumorales et confèrent aux cellules cancéreuses une résistance à l'apoptose, aux attaques du système immunitaire et à la thérapie. Le ciblage thérapeutique des TAM dans les cancers reste difficile, en raison de leur grande plasticité et de l'absence de marqueurs exclusifs. L'équipe 9 du CRCT a alors développé un anticorps monoclonal appelé 6-25, en utilisant des cellules de type Nurse-like (NLC) comme modèle de TAM. Les NLC sont le type de TAM rencontrés dans la leucémie lymphoïde chronique (LLC), sont cruciales pour la survie des cellules leucémiques et peuvent être facilement générées in vitro. L'anticorps 6-25 a été caractérisé pour se lier spécifiquement aux TAM de différentes tumeurs en reconnaissant la protéine sidéroflexine-3 (SFXN3) à leur surface. L'anticorps 6-25 et sa cible ont été brevetés (WO2018/020000 et WO2018/19990).

L'objectif global de cette thèse était de caractériser davantage la spécificité et le potentiel thérapeutique de l'anticorps 6-25 ainsi que le rôle biologique de sa cible, la SFXN3. La première partie de la thèse visait à évaluer la fonctionnalité de l'anticorps 6-25. La version IgG1 nue de l'anticorps 6-25 n'a montré aucune toxicité envers les PBMC provenant à la fois de donneurs sains et de patients atteints de LLC. Il n'a pas causé de déplétion des NLC et n'a montré qu'un effet mineur sur le phénotype de ces cellules et des macrophages dérivés des monocytes (MDM) in vitro. Cependant, l'anticorps 6 25 s'est avéré être efficacement internalisé par les NLC.

La deuxième partie de la thèse a été consacrée à la cible proposée reconnue par l'anticorps 6-25, la SFXN3. En raison du manque général d'informations concernant SFXN3, la caractérisation plus approfondie de son expression dans les macrophages a été étudiée. De nombreuses expériences sur MDM traitées avec divers agents polarisants M1 et M2, ont prouvé que la cible du 6 25 est spécifiquement exprimée à la surface des macrophages de type M2. Les résultats obtenus lors du criblage de la cible 6-25 sur MDM ont en outre été utilisés pour étudier son modèle d'expression dans la NLC. L'augmentation de l'expression de la cible du 6-25 à la surface des NLC a été corrélée à leurs fonctions protectrices, ce qui en fait un marqueur de TAM pro-tumoraux. De plus, des expériences sur la polarisation des NLC ont permis de mieux comprendre le rôle du TNF et de l'IL-10 sur la biologie de ces cellules et en particulier la fonction protectrice vis-à-vis des cellules cancéreuses LLC.

La réalisation des expériences complémentaires sur la cible reconnue par l'anticorps 6 25 a conduit à la remise en cause initiale et finalement à la disqualification de la SFXN3 en tant qu'épitope potentiel. La ré-identification ultérieure de la cible a été effectuée à l'aide d'une immunoprécipitation optimisée/spectrométrie de masse quantitative (IP-MS) et d'une approche RNAseq, qui a fourni la liste des cibles potentielles. Dans le processus de criblage, le récepteur du folate β (FRβ) a été identifié comme la cible de l'anticorps 6-25.

Les résultats présentés dans cette thèse montrent que l'anticorps 6-25 représente une voie prometteuse pour cibler les TAM. Le FRβ a été montré comme étant un marqueur M2 spécifique des TAM. En raison des propriétés fonctionnelles du 6 25, y compris une spécificité élevée et une internalisation lors de la liaison aux macrophages de type M2, une version conjuguée à une drogue (ADC) de celui-ci a été générée. Comme les premières expériences avec le 6-25 ADC ont montré des résultats prometteurs de déplétion des macrophages exprimant le FRβ, elles seront poursuivies à l'avenir. Toujours en perspective, les expériences in vivo avec l'anticorps 6-25 sont prévues pour évaluer son efficacité dans la modulation du TME, afin d'améliorer les résultats de la thérapie anticancéreuse.

Abstract

Tumor-associated macrophages (TAM) belong to the major cell population of tumor microenvironment where they support tumor growth and metastasis, and also confer cancer cells resistance to apoptosis, immune system attacks and therapy. Therapeutic targeting of TAM in cancer remains challenging, owing to their high plasticity and lack of exclusive markers. To address these problems, Team 9 of CRCT developed the monoclonal antibody called 6-25, using Nurse-like cells (NLCs) as the model of TAM. NLCs are the type of TAM encountered in chronic lymphocytic leukemia (CLL), are crucial for the survival of cancer B-CLL cells and can be easily generated in vitro. The 6-25 antibody has been further characterized to specifically bind to TAM of different human malignancies by recognizing sideroflexin-3 (SFXN3) protein on their surface. Both 6-25 antibody and its target have been patented (WO2018/020000 and WO2018/19990).

The overall aim of this thesis was to further characterize specificity and therapeutic potential of 6-25 antibody and also biological role of its target – SFXN3. The first part of the thesis aimed to evaluate the functionality of the 6-25 antibody. Naked, IgG1 version of 6-25 antibody showed no toxicity toward PBMC from both healthy donor and CLL patients. It did not cause depletion of NLCs and showed only minor effect on the phenotype of monocyte-derived macrophages (MDM) in vitro. On the other hand, 6 25 antibody turned out to be efficiently internalized by NLCs.

The second part of the thesis was dedicated to the proposed target recognized by 6-25 antibody – SFXN3. Because of overall lack of information regarding SFXN3, the more in-depth characterization of its expression in macrophages have been studied. Numerous experiments on MDM treated with various M1 and M2 polarizing agents, proved that 6 25 target is specifically expressed on the surface of M2-like macrophages and its level could be abolished after administration of TNF and to lesser extent with IFN-γ and LPS. Results obtained during screening of 6-25 target on MDM were further used to study its expression pattern in NLC. Upregulation of 6-25 target on the surface of NLCs was consistently correlated with their protective functions, making it a marker of protumoral-TAM. Additionally, experiments on NLC polarization led to gaining an insight into the role of TNF and IL-10 on the biology of these cells and in particular the protective function toward cancer CLL cells. Performing the additional experiments on the target recognized by 6-25 antibody, led to initially question and finally disqualification of SFXN3 as the potential epitope. Subsequent target re-identification was done using optimized immunoprecipitation, quantitative mass spectrometry (IP-MS) and RNAseq approach, which provided the list of potential

antibody targets. In the process of screening, folate receptor β (FRβ) was identified as the target of 6-25 antibody. This result was successfully validated by: 1 – knock-out (KO) of FRβ gene (FOLR2) in primary macrophages, and 2 – overexpression of FOLR2 in HEK-T cells (wild type HEK-T cells do not express 6-25 target).

Results presented in this thesis show that the 6-25 antibody represents a promising way of targeting TAM. They also fully support FRβ, as a specific M2 marker of TAM. Because of functional properties of 6-25, including high specificity and internalization upon binding to M2-like macrophages, antibody-drug conjugate (ADC) version of it have been generated. As initial experiments with 6-25 ADC showed promising results in depletion of macrophages expressing FRβ, they will be continued in the future. Also in perspective, the in vivo experiments with 6-25 antibody are planned to evaluate its efficacy in modulating tumor microenvironment (TME), in order to improve the outcomes of anticancer therapy.

Table of content

Acknowledgements 2

Résumé 6

Abstract 8

1 Introduction 15

1.1 The Role of Tumor Microenvironment in Cancer 15

1.1.1 Formation of tumor stroma 16

1.1.2 Cancer-related inflammation (CRI) 17

1.2 Role of macrophages in oncogenesis 23

1.2.1 Origin and physiological roles of macrophages 23

1.2.2 Pathological functions of macrophages 24

1.2.3 Macrophages in cancer 25

1.3 Targeting of TAM 28

1.3.1 Differentiation and Depletion 30

1.3.2 Reprogramming 32

1.3.3 Inhibition of recruitment 35

1.3.4 Conclusions 37

1.4 Chronic lymphocytic leukemia 37

1.4.1 Epidemiology of CLL 38

1.4.2 Classification of CLL 38

1.4.3 Pathophysiology 39

1.4.4 B cell signaling and life cycle of CLL cells 40

1.4.5 Importance of TME and proliferation centers 40

1.4.6 Nurse-like cells (NLC) 42
1.4.7 Targeting of nurse-like cells in CLL 44
1.5 Aim of the thesis 47
2 Material and methods 48
2.1 Cell culture in vitro 48
2.1.1 Primary cell culture 48
2.1.2 Cell lines 51
2.1.3 Cryopreservation of cells 51
2.2 Flow cytometry 51
2.2.1 Basic cell staining 53
2.2.2 6-25 staining 54
2.2.3 Data acquisition and analysis 54
2.3 Statistical analysis 54
2.4 Western blot analysis 54
2.5 Ribonucleoprotein-mediated CRISPR-Cas9 gRNA delivery to primary myeloid cells 55
2.6 RNAseq analysis 56
2.6.1 RNA isolation and quality control 56
2.6.2 RNA sequencing 56
2.6.3 Differential gene expression (DGE) analysis 56
2.7 IP-MS validation of 6-25 target 56
2.7.1 Immunoprecipitation 57
2.7.2 Protein digestion and MS analysis 57
2.7.3 MS-based protein identification and label-free quantification 58
3 Study I) specificity of the 6-25 antibody 60
3.1 Specificity of the 6-25 antibody toward primary blood cells 60

3.1.1 Expression of the target on autologous NLC, NLC from patient after relapse and heterologous NLC. 62
3.2 Screening of AML cell line with the 6-25 antibody 65
3.3 Modulation of the 6-25 target in human monocyte-derived macrophages (MDM) 67
3.3.1 Expression of the 6-25 target by MDM – effect of CSF-1, IL-34 and GM-CSF 67
3.3.2 The 6-25 target is a specific marker of M2-like macrophages and is upregulated by CSF1R activation 69
3.3.3 The 6-25 target expression is abrogated by TNF 71
3.3.4 Conclusions 76
4 Study II) The 6-25 target – a marker of protective NLC 77
4.1 Kinetic of the 6-25 target expression in NLC 77
4.2 Connection of 6-25 target expression on NLC with viability of cancer B-CLL cells 79
4.3 Publication on Interplay between TNF and IL-10 on phenotype of CLL cells. 83
4.4 Conclusions 99
5 Study III) Determination of the 6-25 target 99
5.1 Invalidation of SFXN3 as the target of the 6-25 antibody 99
5.1.1 Immunofluorescence with the 6-25 mAb and commercial anti-SFXN3 antibodies 101
5.1.2 KO of SFXN3 in primary monocytes and macrophages, ultimate target invalidation 104
5.2 Identification of a new target recognized by the 6-25 antibody 105
5.2.1 Differential gene expression (DGE) analysis of MDM after treatment with TNF 105
5.2.2 Immunoprecipitation of M2 MDM membrane proteins with 6-25 antibody combined with quantitative mass spectrometry 107
5.2.3 Validation of the new 6-25 target 109
5.3 Conclusions 112
6 Study IV) Functionality of the 6-25 antibody 113

6.1 Effect of naked 6-25 antibody on the viability of the primary human cells 113
6.2 Effect of naked 6-25 antibody on the maturation and polarization of macrophages 116
6.3 Internalization of 6-25 antibody 119
6.4 Conclusions 120
7 Discussion 121
7.1 Expression of FRβ 122
7.2 Phenotype of FRβ$^+$ macrophages 124
7.3 Role of folate and FRβ in macrophages 125
7.4 Current state of FRβ-centered therapies 125
7.5 Perspectives for study of therapeutic potential of 6-25 mAb 127
7.5.1 Prognostic value of FRβ and 6-25 mAb in CLL 128
8 Bibliography 130
List of figures 147
List of abbreviations 148

1 Introduction

1.1 The Role of Tumor Microenvironment in Cancer

For a long time, cancer research and therapy have been centered on deciphering the complexity of oncogenesis from the perspective of cancer cells itself. It has led to better understanding the mechanisms leading to emergence of the cancer cells, but also their heterogeneity, ability to evade immune-surveillance and resist therapeutic targeting. Nonetheless, this knowledge made evident that cancer cell focused approach is not enough to efficiently control the disease. It has been known for a long time that oncogenesis, beside cancer cells, involves also non-tumoral cells and extracellular components, which all form a complex ecosystem [1]. Already in 1863 Rudolf Virchow discovered leukocytes infiltrating neoplastic tissue thereby finding connection between tumor and inflammation [2]. Later in 1899 Pagets developed the theory of "seed and soil", where he proposed that spread of cancer cells (seed) is controlled by cooperation with the host organ (soil) [3]. Interestingly, these concepts are still being explored leading to better understanding of biological mechanisms controlling the cancerogenesis. With an advent of more advanced methods it has been finally possible to uncover a multitude of cell types infiltrating tumors, their phenotypes and functions, spatial distribution and density [1]. Among cells found in tumors we can distinguish - immune cells: T and B lymphocytes, NK cells, macrophages, MDSC, neutrophils, basophils, eosinophils, mast cells; stromal cells: fibroblast, mesenchymal stromal cells, osteoblasts and chondrocytes and non-stromal cells: endothelial cells, pericytes, adipocytes [4] and neurons [5]. Additionally, stromal cells with extracellular matrix (ECM) are constituting tumor stroma (some consider stroma to be formed also by blood vessels and inflammatory cells). All of these components together are forming the so-called tumor microenvironment (TME) [4,6]. TME can be further divided into different niches, to signify stimuli influencing/controlling particular part of the tumor: hypoxic niche, acidic niche, immune microenvironment, metabolism microenvironment, innervated microenvironment and mechanical microenvironment.[5] It has been accepted that TME has a crucial influence on multiple hallmarks of cancer, actively supporting all stages of oncogenesis and also having central role in cancer resistance to the treatment. Additional layer of complexity comes from the observation that TME is constantly changing along with cancer cells, adapting to new situations and stages of the cancer. Thus TME of metastases differ from the environment of primary tumor [3,7]. Continuous focus on deciphering the interplay of TME with

tumor cells and finding a way to efficiently target components of TME seems to be a key in better controlling the disease and improving curative efficiency of cancer therapy [4].

Recently the concept of TME is being revisited/expanded, with the emergence of the tumor-organismal environment (TOE) containing a multilayer view on TME [8].

1.1.1 Formation of tumor stroma

Tumor stroma is composed of extracellular matrix and stromal cells and is one of the essential components of TME serving as a scaffold for tumoral and non-tumoral cells. Amount of stroma between the tumors shows extreme variations depending on the nature of the malignancy. At one side of the spectrum there are solid tumors, where stroma can represent up to ~90% of the tumor mass, as in case of some of the breast, pancreas and stomach carcinomas, whereas in case of hematological malignancies its content is much smaller [9] and often restricted to lymphoid organs [10] . Dependency of the solid tumors from the stroma, comes from the nature of surrounding tissue, that restricts availability of the nutrients and oxygen. It has been established that if the tumor is growing beyond 1-2 mm, it requires establishment of nutrients influx, removal of metabolism byproducts and gas exchange for its further growth [9]. As mentioned previously the observation of complexity of tumor stroma and inflammatory processes has been made already in the XIX century. It was however much later, in the 1970s that molecular mechanisms underlying the formation of TME were uncovered. Researchers showed that mechanisms of tumor stroma formation share striking similarities to regenerative processes found in wound healing and chronic inflammatory diseases like rheumatoid arthritis (RA) or psoriasis [4,11]. As a continuation of these discoveries, in 1986 Dvorak came up with a very picturesque concept, describing tumors as a “wounds that do not heal” [9,11,12]. He pointed out that tumor microvasculature is characterized by incredible hyperpermeability, which can be compared to injured blood vessel. The crucial factor responsible for this state is vascular permeability factor (VPF)[9]. VPF was later identified to be VEGF [12]. Action of VEGF leads to extravasation/leaking of vascular exudate rich in plasma proteins and clotting agents into the tumor proximity. Tumor cells itself are also able to release substantial amount of tissue factors and enzymes that after mixing with this vascular exudate lead to formation of fibrin gel serving as an early/provisional stroma and a perfect medium for subsequent infiltration of accessory cells/non-cancer cells [9]. Early stroma is subjected to constant remodeling, overgrowth of new blood vessels/angiogenesis/vasculo- and arterio- genesis. With degradation of fibrin, the stroma forms granulation tissue, rich in blood vessels. The last stage of this process is connected to “resorption of vasculature and synthesis of collagen resulting in formation of dense

and fibrous connective tissue" that in case of cancer is called desmoplasia. Desmoplasia corresponds to scar tissue in wound healing process [11,12].

Recently Dvorak has refined the previous concept of "wound that never heals" taking into account the heterogeneity of the tumor. As distinctive parts of the tumor might be in the different stages of tumorigenesis/healing, there might be a presence of "stable" parts, where tumor cells are embedded in mature, poorly vascular stroma representing "healed" parts. On the other hand, the invading front of the tumor keeps initiating previously described healing cycle, with release of permeability factors and fibrin gel deposition [11,12]. The similarity between tumor and regenerative processes is reflected not only on the phenotypic/protein level, but also on the gene expression level. Microarray analysis of murine models of renal cell carcinoma and renal regeneration and repair, showed 77% of similarity in overexpressed genes. The common genes were implicated in regenerative processes, cell proliferation and immune responses [13].

Profound observation of molecular mechanisms harnessed by cancer to sustain its growth and progression, shows striking analogies with one utilized by physiological cells, suggesting that cancer cells do not rely on cancer-specific tools. Instead, they hijack tools normally utilized in physiological processes. It holds a very important implication that the knowledge of the physiological processes can be used to better understand and fight cancer [11–14].

1.1.2 Cancer-related inflammation (CRI)

1.1.2.1 *Physiological role of inflammation*

Inflammation is a defensive response involving recruitment and activation of immune cells in order to re-establish tissue homeostasis [15,16]. While this process is most often associated with fighting the infection, it is equally important in controlling the damage and regenerating the tissue after injury [15,17]. In physiological conditions (often referred as acute inflammation), the process leads to elimination of noxious material, resolution of inflammation followed by initiation of repair phase and restoration of homeostasis. On the mechanistic level the inflammation response starts with detection of pathogen-associated molecular patterns (PAMP) or damage-associated molecular pattern (DAMP), that activates macrophages and mast-cells, which in turn secrete: pro-inflammatory cytokines, vasoactive amines and eicosanoids[18]. These pro-inflammatory mediators cause dilatation and increased permeability of blood vessels, followed by recruitment of leukocytes. First lane of defense is represented by polymorphonuclear neutrophils, which

are specialized in phagocytosis and release of enzymes that destroy the pathogen. Subsequently the inflamed site is cleared from apoptotic neutrophils by monocytes and macrophages. Clearance of dying cells and additional release of lipid-derived resolvins and protectins, contribute to quenching of the inflammation. Resolving inflammation is a crucial phase, that allows the regenerative processes to further restore the local homeostasis [15].

The physiological inflammation response proceeds in a highly-programmed manner. However, if any stage of the process is disturbed or the response is unable to neutralize the triggering agent it may convert into chronic inflammation. This pathological condition may eventually lead to fibrosis, formation of granulomas or development of auto-immunological conditions [15].

1.1.2.2 *Chronic inflammation in cancer*

Inflammatory processes are nowadays recognized to play a crucial role in the cancerogenesis. While acute inflammation, especially at the early steps of tumor formation might play an anti-tumoral role, it changes into chronic state upon failure to remove the source of the response [18]. Process of chronic inflammation often referred to as "smoldering inflammation" [19] is recognized as one of the main driver and hallmark of oncogenesis, that allows tumors to acquire all the characteristics of cancer and escape immune-surveillance [15,16]. Inflammation in cancer is characterized as non-resolving and involves constant presence of various immune cells like tumor-associated macrophages, MDSCs, Tregs, but also inflammatory mediators, including: cytokines, chemokines, vasoactive amines and prostaglandins[18].

It is important to mention that the tumor environment is especially non-hospitable, characterized by hypoxia, acidosis, scarce of nutrients and growth factors, but also surveillance from the immune system [16]. To counterbalance these adversities inflammation can promote cancer both directly and indirectly.

Direct promotional effect of inflammation is based on the supply of cytokines to cancer cells that can serve as growth factors, enabling cell proliferation and resistance to cell death. This is especially crucial at the early stage of survival of transformed clones. [16]. Additionally, inflammation can shape plasticity of cancer cells by inducing epithelial-mesenchymal transition and expression of adhesion molecules, thus promoting metastasis processes [21].

Indirectly, inflammation can promote cancer by constantly shaping the TME, which include controlling of cellular composition and maintaining immunosuppressive status of TME to protect malignant cells from

immune attacks [1,18,21], activation of accessory cells to promote angiogenesis and ECM remodeling, thus modifying availability of key metabolites and facilitating metastasis process [16].

Importance of CRI in cancer promotion has been proven by the numerous experiments and clinical studies of both murine and human tumors. In general, modulation of immune responses by the transfer of immune cells or induction of cytokines promotes progression of the disease, while targeting of immune cells and mediators of inflammation can impair cancer metastasis. Also limiting inflammation by administration of non-steroid anti-inflammatory drugs (NSAIDs) proved to lower the incidence or mortality of some malignancies [16].

1.1.2.2.1 Chronic inflammation in cancer initiation

There are two main pathways connecting inflammation with cancer initiation and establishment of immunosuppressive TME – extrinsic (microenvironment driven) and intrinsic one[17,18] or tumor-elicited inflammation (TEI) [14,18].

Extrinsic pathway involves chronic inflammatory processes induced long before tumor formation. They can be an effect of: bacterial/viral infection or autoimmune disease, environmental pollution, but also unhealthy lifestyle – including tobacco smoking or obesity [16,18]. These stimuli induce an inflammatory milieu involving: constant activation of master-regulatory transcription factor (TF) NF-κB, presence of pro-inflammatory cytokines including Il-1, IL-6, TNF and reactive-oxygen species (ROS) or reactive-nitrogen species (RNS). ROS and RNS can induce genetic mutations in the adjacent cells that may affect the function of oncogenes and tumor-suppressor genes. Long-term exposure to these conditions may lead to malignant transformation of the cells [16,21,22]. It is recognized that chronic inflammation caused by infection or autoimmunity is responsible for induction of about 20% of the malignancies, usually at the same site of the body. One of the examples is inflammatory bowel disease (IBD) that may predispose to colorectal cancer (CRC) [16,20]. On the other hand, a relatively common skin condition like psoriasis is not considered to increase the risk of skin cancer [23], but is associated with increased risk of development and mortality of cancer at the other sides of the body [24]. Inhalation of fine particles, asbestos or tobacco smoke is also responsible for site specific inflammation and may lead to development of malignancies related to respiratory system. On the other hand, conditions like obesity and hyperglycemia are associated with induction of systemic inflammation, thus increasing the risk of developing malignancies in the various sites of the body [16].

While extrinsic pathway remain an important driver of tumorogenesis, a majority of the primary tumors and cancers form without pre-existent inflammation [16,25]. Instead the tumor itself can promote an inflammatory environment to further drive it's progression, **which is referred to as tumor-elicited inflammation (TEI)** [14,18] or intrinsic pathway [17,18].

In the intrinsic pathway, the tumor cells themselves initiate the inflammation by the action of mutated oncogenes. These oncogenes are not only leading to neoplastic transformation, but are also responsible for expression of pro-inflammatory mediators that attract immune cells, further prolonging their survival and retention. RET, RAS and MYC are the main oncogenes that drive formation of inflammatory responses/milieu. For example, activation of protein tyrosine kinases like RET, drives expression of among others: colony-stimulating factors (CSFs) that attracts leukocytes to the tumor site, subsequently increasing their survival and differentiation; chemokines CLL2 and CCL20 that attracts monocytes and dendritic cells; IL-1β – which is one of the main pro-inflammatory cytokines; COX2 responsible for synthesis of prostaglandins; IL8/CXCL8 – chemokine that drives angiogenesis and CXCR4 attracting lymphocytes [21,22].

Tumor-elicited inflammation can be also induced as a side-effect of nascent tumor formation. As previously mentioned growing tumors tend to induce angiogenic responses, as the oxygen demands from the near vessels are insufficient. The lack of oxygen causes formation of hypoxic niche in the tumor and stabilization of hypoxia-inducible factors (HIFs). These transcription factors cause induction of a plethora of genes, implicated in processes like: angiogenesis, cell survival and proliferation. At the same time HIFs support reprogramming of metabolism of cancer cells to rely mainly on glycolysis. It is important to mention that even in normoxic regions of the tumor, cancer cells are undergoing glycolytic switch to generate energy. This process is referred to as aerobic glycolysis [26] or Warburg's effect [6]. Even though glycolysis generates low net ATP in comparison to oxidative phosphorylation, it allow cancer cells to accumulate metabolic intermediates to build macromolecules for biosynthesis and to support quick cell proliferation [7]. One of the side effects of these phenomenon is release of a substantial amount of lactate by cancer cells, which lowers the pH of surrounding tissue and leads to formation of acidic niche[26]. Both hypoxia and acidosis may cause cells death and release of DAMPs that further fuel inflammation and wound-healing processes [7]. Additionally, acidosis is important in repolarization of immune cells, promoting Th2 responses in TME to further attenuate anti-tumor processes. These cascades of events contribute to non-resolving inflammation state and finally formation of pro-tumoral TME [18].

1.1.2.2.2 Establishment and types of TME

Irrespective of the pathway leading to cancer initiation, CRI leads to recruitment of a rich population of tumor-promoting inflammatory cells. By the action of selective pressure of inflammatory molecules present in TME, the recruited cells will adopt pro-tumoral roles, helping to enforce the supportive character of TME [27].

Depending on the genetic background and phenotype of the tumor, the TME can have a different proportion and spatial distribution of specific subtypes of immune and stromal cells [27]. We can differentiate immunologically "hot" tumors, strongly infiltrated with cytotoxic T lymphocytes (CTLs) and CD103+ DC, that in some cases can even lead to formation of tertiary lymphoid structures in the tumor. Neoplastic cells in these tumors are characterized by high genetic instability that may lead to release of numerous neoantigens that further increase overall immunogenicity. In general these tumors are representing favorable prognosis, as anti-tumoral potential of CTLs can be reactivated therapeutically [27].

On the other hand, immunologically "cold" tumors can be distinguished. They are characterized by exclusion of CTLs from the tumor core and prominent infiltration with tumor-associated macrophages (TAM), monocyte-derived suppressor cells (MDSC) and regulatory T cells (Tregs) [27]. These cells are especially important for establishment of an immunosuppressive environment by a potent inhibition of anti-tumor responses of adaptive immunity [21,27]. They can block antigen presentation by DC, inhibit proliferation and activation by T and B lymphocytes [28]. Additionally, "cold" tumors are characterized to be more genetically stable – poor in neoantigens and generally harder to target by immune system or therapy [27].

Presented information signifies the importance of classification of not only an absolute number of immune cells in the tumor, but also their activation status and spatial distribution [1].

1.1.2.2.3 CRI and TME in tumor progression and metastasis

With the tumor growth and progression the diseases can approach an invasive and finally metastasis state [7]. Establishment of cancer metastasis is a critical event in tumorogenesis, as metastatic disease is responsible for 90% of overall cancer-related mortality. Numerous clinical studies spot the role of inflammation and TME in driving cancer spreading in the body. Also long term administration of NSAID have shown to decrease colonization events and help remove micrometastases [16].

Depending on the tumor progression that leads to metastasis begins with disruption of the basal membrane or ECM capsule around the tumor, that can be further breached by cancer cells. Remodeling of the ECM is mostly induced by the action of TAMs, which release among others matrix metaloproteinases MMP, facilitating local invasion or spread through blood or lymphatic vessels [16]. In general, the metastasis process is highly inefficient and among numerous cancer cells that leave primary tumor only few will succeed in colonizing a new site. It might be caused from both intrinsic characteristic of cancer cells, but also from the properties of the potential seeding site, that might not support the metastasis growth [16,28].

In order to increase the chances of a successful metastatic event, cancer cells need to be properly conditioned by either intrinsic genetic factors or influence of TME. It is important to mention that cancer-stem cells (CSC) are much more likely to colonize distant tissues, as they are more plastic and resistant in comparison to remaining primary tumor cells. Inflammatory milieu of the tumor can stimulate NF-κB and STAT3 signalling that induce stemness of cancer cells and increase proportion of CSC in the tumor [16]. This process is partially overlapping with induction of epithelial-mesenchymal transition (EMT) of cancer cells that drastically increases their migratory capabilities [16] and stemness [28]. Upon colonizing a distant site, under the influence of "new" TME cancer cells often undergo reverse transition, back to epithelial phenotype in order to form a secondary tumor. This illustrates how TME can influence plasticity of malignant cells [28].

Additionally, as metastasis happens mostly by lymphatic or blood vessels, cancer needs to be able to attach to vessel walls and further intravasate. For that they need to be able to express specific adhesion molecules, including integrins and chemokine receptors that confer tropism of cancer cells to specific tissue [16]. For example in case of melanoma cells, expression of CCR7 will be associated with lymph-node metastasis, while CCR9 with targeting of small intestine [21].

Another interesting mechanism that increases efficiency of metastasis is an ability of cancer cells to form complexes with other cancer cells, monocytes or neutrophils. These complexes are not only more likely to evade immune attacks, but also have a broader tissue tropism [16].

CRI is not restricted to the tumor site though, as the neoplastic disorders are associated with defective inflammatory responses at the other parts of the body [2]. The systemic inflammatory processes along the factor released by the tumor cells itself are essential for establishment of pre-metastatic niches at distant

parts of the body. It has been shown that before arrival of neoplastic cells, potential metastatic sites can be already colonized by inflammatory cells, that will first prepare permissive environment [28].

1.2 Role of macrophages in oncogenesis

Macrophages represent a major population of the immune cells within the TME and their presence is usually associated with a bad prognosis. Understanding both the origin and physiological roles of macrophages provide improved insight into their role in cancer. It also shows the importance of macrophages-targeting specificity when it comes to development of new anti-TAM therapies.

1.2.1 Origin and physiological roles of macrophages

There are two main sources of macrophages in the body: tissue resident ones and derived from circulating cells, including monocytes and bone-marrow progenitors. It was recently shown that most resident macrophages (MPs) in normal tissues are not only derived from bone marrow (BM) progenitors, as previously thought, but also from yolk sac or fetal liver, and are maintained by self-renewal [29,30]. However, during adult life, the rate of resident MPs can also be maintained by the infiltration of monocytes or early bone-marrow progenitors, with exception for/of microglia in the brain [31,32]. Monocytes from blood and bone marrow are therefore able to infiltrate tissues and to differentiate into specific tissue MPs but whether they can be considered as tissue-resident MPs is still a debate. In human blood, three main monocyte populations have been identified, a classical one, $CD14^{++}CD16^{-}$, a non-classical one, $CD14^{int}CD16^{+}$, and an intermediate one, $CD14^{+}CD16^{+}$ [33]. These two latter populations are differentiated from a uniform population $CD14^{++}CD16^{-}$ egressing from the bone marrow [34].

Resident macrophages display key roles in growth, tissue development, homeostasis and remodelling, and have site-specific phenotypes and functions. It was proposed that the specialization of the resident MPs takes place inside the target tissue due to close contacts with tissue-specific cells as well as to soluble factors in the tissue environment [35]. Microglia, in the brain and spinal cord, contribute to synaptic maturation during brain development and clearance of immature or defective neuronal synapses [36]. In the lung, alveolar MPs mediate approximately 30% of the surfactant lipid metabolism Langerhans cells with cutaneous MPs in the skin are specialized in the formation of the extracellular matrix and in the skin layer differentiation. Cardiac-resident MPs are required during heart development and take part in the regulation of the cardiac rhythm [37]. Kupffer cells in the liver are involved in the modulation of metabolism in hepatocytes, preventing the pathogenic accumulation of lipids [38]. Tissue-resident MPs located in the

red-pulp region of the spleen have important functions in iron processing connected with the clearance of damaged red blood cells and the erythropoiesis [39,40]. White-pulp of the spleen also contains specialized MPs in both T cells zones and B-cell follicles. Role of the latter, called tangible MPs is especially important, as they remove apoptotic B-cells cumulating during germinal selection, thus preventing inflammation and autoimmunity [41].

Apart from physiological functions, monocytes/MPs also participate in infection/inflammation contexts, tissue repair and cancer.

1.2.2 Pathological functions of macrophages

MPs are very plastic cells which are able to respond to molecular or cellular signals from the tissue environment. The molecular signals can be endocrine or paracrine signals originating from phagocytosed cells or microorganisms and from the extracellular matrix/proteins. MPs can also directly interact with other tissue-resident cells such as immune cells recruited during injury. Indeed, monocytes and MPs are recruited from the bone marrow to the tissue injury site via the chemoattractant CCL2 secreted by resident MPs, endothelial cells, myocytes and fibroblasts [42]. In humans, classical monocytes ($CD14^{+}CD16^{-}$) display a high expression of CCR2 and are involved in responses to bacterial infection and inflammation, inflame masome signaling and in low density lipoprotein uptake. In contrast, non-classical monocytes ($CD14^{int}CD16^{+}$) display a high expression of genes involved in cytoskeletal dynamics, tissue invasion during inflammation and genes suggesting terminal differentiation and cellular maturity [43].

Monocytes-derived and tissue-resident MPs therefore co-localize to take part in healing and then to the resolution, thanks to the production of cytotoxic and pro-inflammatory mediators, clearance of invading microorganisms or removal of apoptotic and damaged cells [44]. On arrival at the injury site, blood-derived MPs can adopt a pro-inflammatory/M1/classical or anti-inflammatory/M2/alternative phenotype depending on the cytokines that are present in the microenvironment [45,46]. Regarding the plasticity of MPs, although the framework of M1/M2 polarization is a very useful system for in vitro studies, it is unclear how similar clear-cut phenotypes can be appended during in vivo injury and repair [47]. This M1/M2 paradigm is well pictured by the high expression of M2 markers by tissue-resident MPs compared to the mature phenotype of monocyte-derived MPs [48,49]. Early on after damage or injury, infiltrated Ly6C+ monocytes scavenge apoptotic debris or pathogens or infected cells thanks to the expression of pattern recognition receptors (PRR), Toll like receptors (TLR), scavenger receptors and Fc receptors that respectively recognize

microbial antigens, danger signals, or immunoglobulins. These events lead to activation of transcription factors such as interferon (IFN) regulatory factors and nuclear factor kappa B (NFκB), inducing an M1 polarization and initiation of the inflammatory response [50]. These blood-derived M1 MPs then release pro-inflammatory cytokines (e.g., IL-1β, IL-6, IL-12, IL-23, and TNF-α) and type-1 cell-attracting chemokines (e.g., CXCL9 and CXCL10), favoring the recruitment of more macrophages and leukocytes to help with injury resolution [51]. Once the acute injury has been resolved, MPs are in charge of suppressing inflammation and initiating wound repair. After clearing debris, MPs produce growth factors and mediators which abrogate the pro-inflammatory function of T cells and other immune cells [52]. This is accompanied by a progressive repolarization of the blood-derived MPs towards a phenotype and functions increasingly similar to those of homeostatic tissue-resident MPs [53].

Pro- and anti-inflammatory pathways in MPs are induced by activation of specific plasma membrane receptors. If IFN-γ mediates the classical/M1 activation with upregulation of MHCII antigens, induction of nitric oxide synthase (iNOS) and production of pro-inflammatory molecules, interleukin-4 and -13 (IL-4 and IL-13) induce the alternative/M2 phenotype characterized by upregulation of CD206, transglutaminase 2, arginase and production of IL-10 and chemokines such as CCL17, CCL22 and CCL24 [51,54]. Like other immune cells, specific functions of MPs are therefore coupled to specific phenotypes even considering their plasticity, MPs can display intermediate phenotypes in certain inflammatory diseases and cancer [55,56].

1.2.3 Macrophages in cancer

MPs in cancer are called tumor associated macrophages (TAM) and represent one of the major cellular component of the TME. They play a major role in tumor growth, metastatic dissemination, and therapy failure by inhibiting anti-tumor immune responses, promoting angiogenesis and extracellular matrix remodeling and providing nutrients for cancer cells. High TAM infiltration is generally correlated with poor outcomes in several types of cancer [57].

1.2.3.1 *Origin and phenotype of TAM*

Until recently, TAM were considered to originate exclusively from blood-derived MPs undergoing differentiation upon tissue infiltration in response to chemokine and growth factors produced by stromal and tumor cells in the TME. Colony-stimulating factor 1 (CSF-1), vascular endothelial growth factor A (VEGF-A) and different CCL, especially CCL-2 [43,56,58] were found to act as chemotactic molecules for monocytes in various cancers [59–61]. However, evidence shows that tissue-resident MPs can coexist in

tumors with blood-derived MPs and their phenotype can rapidly evolve depending on the stage of the tumor and the characteristics of the molecular and cellular actors in the TME.

Depending on the tumor stage, state of microenvironment (oxygen ratio), TAMs phenotype is distributed somewhere in between M1 and M2 of the polarization spectrum, depending on the tumor stage and microenvironmental context. While generally considered to be protumoral, macrophages can exhibit some anti-tumoral activity, especially at the early stages of the tumor formation [18,57]. Also in vitro experiments demonstrated that macrophages activated with M1 promoting cytokines or bacterial products, including LPS can kill malignant cells [57,62]. For example, IFN-γ can polarize resident MPs towards an M1 phenotype and promotes maturation of blood derived-M1 MPs. These MPs release pro-inflammatory factors that activate Th1 and Th17 immune responses and can also produce TNF-related apoptosis-inducing ligand (TRAIL) that result in TRAIL-induced cancer cell apoptosis [62]. However, during most of the oncogenesis, especially in more advanced tumors, TAMs show strong protumoral influence and are characterized by M2 directed polarization. This polarization occurs thanks to anti-inflammatory mediators produced by the tumor cell and by stromal and immune cells in the TME, including MPs themselves. CSF-1, CCLs -2, -3, -14 and ILs -4, -10, -13 are common tumor-derived factors driving recruitment, proliferation and M2-polarization of MPs [63–65]. Other factors are more specific to the type of cancer such as prostate cancer-derived cathelicidin-related antimicrobial peptide [65] or hypoxic cancer cell-derived cytokines Oncosatin-M and Eotaxin [66]. Besides, migration-stimulating factor (MSF) and CXCL12 can be secreted by MPs to promote self-polarization [67–69]. Finally, low pH, hypoxia-inducible factors (HIF-1α and 2α), high-mobility group box 1 protein (HMGB1), extracellular ATP or tumor-derived ECM components are also potential factors that promote M2 polarization [69,70].

1.2.3.2 *Pro-tumoral function of TAMs*

There are several pro-tumoral functions displayed by TAMs at practically all stages of tumorogenesis. These cells are essential in maintenance of immunosuppressive TME, especially by inhibiting adaptive anti-cancer responses [18]. First of all TAM-derived TGF-β decreases antigen presentation and migration of DC, increasing their apoptosis at the same time [71]. IL10 and TGF-β released by macrophages can directly suppress recruitment and functions of cytotoxic CD8 T-cells and natural killer cells [72,73]. Also IL-10, alone or in concert with IL-6, causes upregulation of macrophage B7-H4 expression, responsible for suppression of tumor-associated antigen-specific T cell immunity [74]. Moreover, IL-10 and PGE2 can induce expression of immune-checkpoint ligands (PD-L1) in myeloid cells which can inhibit cytolytic T lymphocytes responses

[75,76]. Finally, IL-10 acts in an autocrine circuit in TAM to restrain their expression of IL-12 and also inhibits the release of IFN-γ [68]. Production of CCL17 and CCL22 by TAM promotes infiltration of Th2 and Treg populations in tumors, that are another important immunosuppressive cells [71]. TAM-derived prostaglandin E2 (PGE2), indoleamine 2,3-dioxygenase (IDO) and arginase 1 (ARG1) play important roles in further suppression of cytolytic T lymphocytes and in the induction of Treg function [71,77,78]. TAMs are also a potent producers of reactive oxygen species (ROS) and reactive nitrogen species (RNS), that are not only an important inducers DNA damage, but are also leading to modification of MHC on the surface of tumor cells. This reaction might lower binding of antigenic peptides to MHC and thus recognition of malignant cells by CTL [79]. All of these effect combined lead to situation where TAM form almost a "physical barrier", completely excluding CD8 T cells from the center of the tumor, leading to formation of previously described "cold" tumors [27].

TAM can secrete IL-17 and IL-23 that promote cancer cell proliferation. IL-23 signaling in tumor cells is important for the intra-tumoral production of downstream cytokines, which are either direct (IL-6, IL-22) or indirect (IL-17A) STAT3 activators [80]. IL-6 produced by TAM also promotes tumor cells proliferation and invasive potential via STAT3 signalling [81]. TAMs also represent an important source of iron, which is essential for tumor cell division, growth and survival [82]. TAM also take part in the promotion of the formation of blood vessels within the tumor providing nutrition for tumor growth [83]. Several pro-angiogenic factors such as TGF-β, VEGF, PDGF are produced by TAM in the TME, especially in hypoxia conditions [84]. CCL18 produced by TAM promote synergically with VEGF the endothelial cell migration and angiogenesis [85]. Other chemokines such as CXCL1, 8, 12, 13 and CCL2, 5 produced by TAM help with the angiogenic switch in tumor tissues [51].

TAM are also responsible for production of TNF which is a key player in NFκB upregulation, and induces migration and invasion potential of cancer cells, which is essential for subsequent metastasis [82]. Various metalloproteinases (MMPs) and cathepsins produced by TAM are crucial for ECM remodeling and that further allows cancer cells dissemination [86,87]. Some chemokines such as CCL18 produced by TAM, can induce clusterization of integrins in cancer cells, increasing their adherence to ECM and promoting migration and metastasis [88]. A mouse study showed that mouse MPs-derived insulin growth factor 1 (IGF-1) induces migration of epithelial ovarian cell lines [89]. Finally, it has been shown that MPs-derived microRNA (miR-223) also regulates tumor invasion [90]. Additionally, TAM plays an active role in induction

of ETM of tumor cells, by both direct interaction and release of specific molecules, like EGF that induces the transition by activating the EGFR/ERK1/2 signalling pathway [91].

Pro-tumoral functions of TAMs lead also to cancer cell resistance to various therapies. TAM-derived exosomes have been shown as involved in mediating the resistance of gastric cancer cells to cisplatin [79]. Endocrine resistance in breast cancer cells can be increased by TAM-derived CCL2 through activation of the PI3K/Akt/mTOR signalling pathway [64]. Autophagy in hepatocellular carcinomas cells can be induced by TAM leading to oxaliplatin resistance [92]. It was recently shown that depletion of TAM by an anti-CSF1R enhanced the anti-tumor effect of docetaxel in a murine epithelial ovarian cancer [79]. High levels of TAM in the TME was also shown to increase the resistance of tumor cells to Padeliporfin, Vascular-targeted photodynamic (VTP) therapy in a prostate mouse model [93]. Anticancer immunotherapies may also be reduced by TAM when their suppression of TME correlates with an increase of DC-vaccination therapy in a malignant mesothelioma mouse model [94]. Finally TAMs are getting recognition for the low frequency of response to Immune Checkpoint Blockade (ICB) therapies, as they limit both CD8 T cell infiltration and activity [95–97].

Adapted and updated from our review on Cancer Cells Resistance Shaping by Tumor Infiltrating Myeloid Cells [98]

1.3 Targeting of TAM

As mentioned previously, classical anticancer therapy has been mostly focused on chirurgical removal of the tumors, systemic treatment involving chemo- or radiotherapy and finally targeted treatment focusing on specific mechanisms driving tumor cells survival and proliferation. Unfortunately, these treatments are often associated with low efficiency, egress of multi-drug resistant clones of cancer cells that leads to relapse and further cancer progression [18].

To overcome the shortcomings of current cancer treatment, the focus has been shifted from cancer cells to TME. As it has been proven numerous times that TME is crucial for tumor immune evasion and failure of anti-cancer therapy [1,4,28]. Additionally, it has been shown that in the right circumstances, tumor-infiltrating cells have capabilities to normalize growth of cancer cells. Immune cells of TME also have a big anti-cancer potential, that after efficient re-activation might lead to a long lasting and efficient way of controlling the progress or even treating the disease [4,28]. Beside, targeting of TME represents a good

therapeutic target, as accessory cells of TME are genetically stable in comparison to tumor cells, thus lowering the chance of developing resistance[1].

Reactivation of the immune system to fight cancer cells is extensively studied, yielding first successes in the form of immune checkpoint inhibitors (ICI) and specific CAR T cells. These relatively new therapies led to some spectacular results in melanoma, non-small cell lung cancer (NSCLC), and other cancers that were previously associated with poor prognosis [99]. While undoubtedly, these therapies can be considered a breakthrough in the field of oncology, they show efficacy in a very limited number of patients [100,101], and especially in case of CAR T cells are associated with significant expenses, further limiting their accessibility [101].

Limited efficiency of ICB is sought in the presence of immunosuppressive cells of TME. It further stresses the importance of targeting the remaining populations of TME, especially innate immunity cells [101]. Among these cells, TAM are cited as one of the most numerous and influential groups [23,57] and their presence in TME is partially responsible for failure of many anticancer therapies [102,103]. Various therapeutic approaches targeting TAM are being developed right now. We can differentiate three main strategies, aiming to: deplete TAM population; re-educate TAM to reverse their pro-tumoral phenotype and actively attack tumor cells; inhibit recruitment of monocytes/TAM to the tumor site [104,105]. Illustration 1 summarizes main strategies to target TAM presented in chapters below.

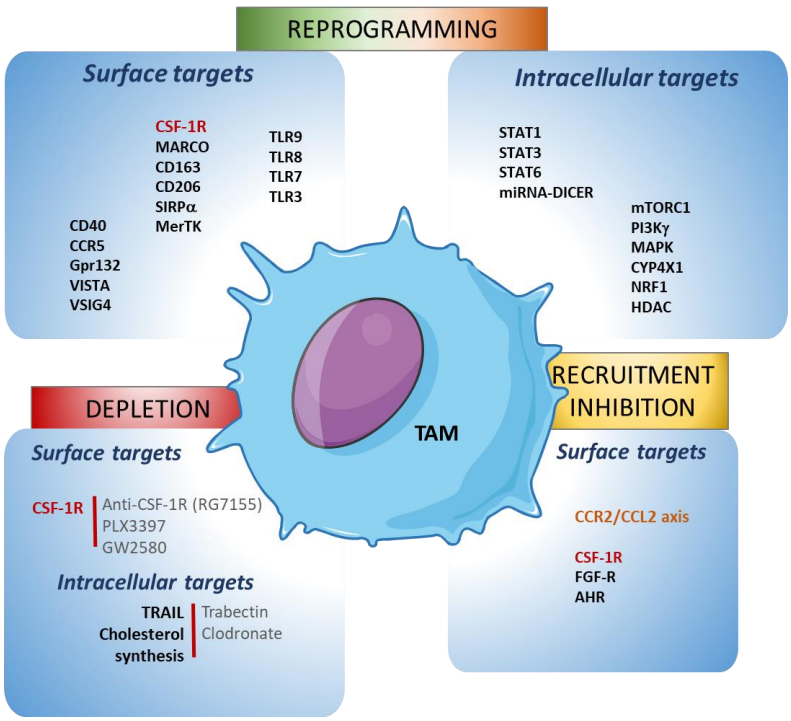

Illustration 1. Main therapeutic strategies aiming to reprogram, eliminate or inhibit recruitment of TAM. *Main targets for each approach are listed with distinction to extra- or intracellular localization. Adapted from* [106].

1.3.1 Differentiation and Depletion

Strategies based around TAMs depletion, represent the main body of focus regarding clinical trials. They are centered on targeting of CSF1R (CD115). CSF-R1 is expressed on monocytes, macrophages and some DC. It is a tyrosine kinase receptor, having two native ligands CSF-1 and IL-34, and upon activation it leads to signaling cascade promoting survival, proliferation and differentiation of monocytes and macrophages [107]. Several antagonists and antibodies to CSF1R were developed for the therapeutic modulation of infiltrating TAMs and tested in preclinical models. In a preclinical breast cancer model, anti-mouse CSF1R antibodies were shown to deplete macrophages and to reduce tumor size [108]. Treatment with RG7155l, a humanized monoclonal antibody, was associated with a reduction in tumor-infiltrating TAMs and an increase in infiltration of effector T-cells in a fibrosarcoma mouse model, as well as in colorectal cancer and cancer patients with advanced tenosynovial giant cell tumors [107]. Alongside antibodies blocking CSF1R, small-molecule antagonists to CSF1R, capable of penetrating the blood–brain barrier, were developed. For example, tests with PLX3397 (pexidartinib) were associated with a reduction in the number of tumor-associated microglia and glioblastoma invasions in glioma mouse models [109]. Moreover, PLX3397 was able

to potentiate the therapeutic effects of radiotherapy in a preclinical mouse xenograft model of intracranial human glioblastoma through the neutralization of CSF-1, which was upregulated by radiotherapy [110]. In an ovarian cancer model, GW2580 - selective CSF1R inhibitor, induced a reduction of ascite volume and a decrease in the number of infiltrating macrophages [111]. In a phase II clinical trial, patients with recurrent glioblastoma displayed a good tolerance to GW2580, but only 8% of 37 patients showed a six-month progression-free survival [112]. To enhance the potential of these inhibitors, combination strategies with conventional chemotherapy were proposed. The efficacy of paclitaxel in a mammary adenocarcinoma mouse model was enhanced by the blockade of CSF1R/CSF-1, with paclitaxel upregulating the production of CSF-1 [113]. On the other hand, phase I study using a combination of a monoclonal anti-CSF1R with paclitaxel in patients with advanced and metastatic solid tumors revealed TAM depletion but no clinically relevant anti-tumor activity [114]. Combination of GW2580 with another chemotherapeutic - gemcitabine, showed a synergistic effect in mouse model of pancreatic adenocarcinoma. Action of GW2580 allowed to stop production of cytidine deaminase by TAM – an enzyme that was responsible for cancer cell resistance to gemcitabine [115]. More recently, combination of anti-CSF1R with docetaxel (microtubule-stabilizing agent) led to TAM depletion in a murine epithelial ovarian cancer model, which improved the anti-cancer effect of docetaxel [116]. Finally, it was shown that CSF1R targeting by the BLZ945 inhibitor (more potent and selective inhibitor of CSF1R) in a mouse model of glioma, led to significant decrease of tumor size. Interestingly, while the CSF1R blockade led to depletion of macrophages in the peripheral tissues, it did not affect viability of the TAM in the tumor. It has been shown that the TAM has been rescued by factors produced by cancer cells, including: GM-CSF, IFN-γ and CXCL10, that however led to loss of M2 protective phenotype of macrophages [117].

Another way to deplete TAMs is to use bisphosphonates (BPs), which induce apoptosis of myeloid cells by inhibiting the essential farnesyl diphosphate synthase, a key enzyme for cholesterol synthesis and protein prenylation. These compounds have a high affinity for bone hydroxyapatite, where they are internalized by bone osteoclasts leading to their apoptosis, and they are, thus, indicated as treatment in pathologies with abnormal bone resorption such as osteoporosis or multiple myeloma [118]. However, all tissue-resident macrophages, including TAMs, can be targeted by BPs such as clodronate using a proper formulation and administration strategy [119]. In case of cancer treatment clodronate is used as encapsulated in liposomal formulation, which not only prolong its half-life in circulation, but further target it toward mononuclear phagocytic system (APS) and thus macrophages [119]. Clodronate is approved to use in the clinics, showing

to lower the incidence of bone and visceral metastasis in human mammary carcinomas treated with a combination of clodronate/chemo- or hormonal therapy [120]. Zoledronate, another type of BPs reduced skeletal-related events in patients with pancreatic cancer and improved overall survival in patients with bone metastases [121]. Effect of BPs is still studied in pre-clinical models, to check their usefulness in other types of cancers showing positive results correlated with TAM depletion [122]. In a murine xenograft model for cutaneous T-cell lymphoma, the reduction of tumor growth was associated with a decrease in pSTAT3 and macrophage number [123]; the same association was observed in other preclinical mouse models of bone metastasis from lung cancer [124], lung metastasis from breast cancer [125], or melanoma xenograft models [126].

Finally, trabectedin a tetrahydroisoquinoline alkaloid based chemotherapeutic, approved for the treatment of advanced-stage tissue sarcoma and relapsed ovarian cancer, was shown to also cause a partial depletion of circulating monocytes and TAMs [127]. Trabectedin is a DNA-binding agent isolated from a sea squid. It can bind to a minor DNA groove of DNA, inhibit DNA repair and transcription, and induce cell cycle arrest [128]. Trabectedin activates a TRAIL-dependent pathway of apoptosis, and myeloid cells, especially monocytes express high level of TRAIL receptor, which makes them sensitive to TRAIL-triggered apoptosis [129].

1.3.2 Reprogramming

Even if TAMs generally display a pro-tumor role, they can potentially be converted to directly kill cancer cells or mobilize the immune system against the malignant cells. TAMs can be reprogrammed toward a tumoricidal phenotype by the targeting of surface markers, signaling molecules, or by modifications of their metabolism. Several markers at the surface of TAMs can be targeted to switch their phenotype such as the scavenger receptor MARCO, TLRs, MerTK, CD40, or CCR5 [78,130–133]. The pattern recognition scavenger receptor MARCO has been implicated in various human cancers, and has been finally identified to be specifically expressed by a subset of TAM [130]. Use of an anti-MARCO monoclonal antibody with modified Fc receptor, showed anti-tumor activity in breast and colon carcinoma, and also in melanoma models. It turned out that by binding to inhibitory Fc-receptor (FcγRIIB), mAb led to reprogramming of TAMs populations to a pro-inflammatory phenotype, leading to tumor regression [130]. The pro-inflammatory phenotype can also be activated by specific ligands of TLRs or of CD40. Some TLR synthetic ligands were tested in cancer, such as the TLR3 agonist Poly(I:C) which activates the NF-κB pathway, leading to pro-inflammatory M1 polarization with production of type I IFN [134]. Intratumoral delivery of a TLR9 agonist,

such as cytosine–phosphate–guanine oligodeoxynucleotides (CpG ODN), or a TLR7/8 agonist (R848) showed a tumoricidal activity in mouse models of melanoma and breast cancer [131,135]. Clinical trials with IMQ and a DNA-based TLR9 immunomodulator in metastatic cancer also showed histological tumor regression and an increase in lymphoid immune infiltration [136]. TLRs can also be activated by sensing bacterial ligands such as the attenuated ΔactA/ΔinlB strain of Listeria monocytogenes, which, when introduced into the aggressive ID8-Defb29/Vegf-A murine ovarian carcinoma, is preferentially phagocytosed by TAMs inducing their anti-tumoral phenotype [137]. CD40 is also an important receptor at the TAM surface, as its ligation with the CD40 ligand at the T-cell surface stimulates T-cell–based anti-tumor responses. In preclinical studies, a rat anti-mouse CD40 antibody showed remarkable therapeutic activity in the treatment of $CD40^+$ B-cell lymphomas [138]. The first class of modified anti-CD40 antibody, presenting five point mutations in the Fc domain (CP-870,893), showed efficient immunostimulation of effector T-cells in mouse models but little clinical effect in advanced cancer patients [139]. Recently, the same CD40 agonist was shown to increase pancreatic carcinoma sensitivity to chemotherapy in a PDAC mouse model associated with a switch of infiltrated macrophages due to an increase in CCL2 expression and IFN-γ in these mice [133]. This last study opened promising perspectives for combination therapies. CCR5 antagonists such as maraviroc provided an anti-tumor effect in a phase I trial in patients with liver metastasis of advanced refractory colorectal cancer correlated with a macrophage repolarization [132]. Furthermore, a majority of cancer cells express a high amount of CD47 at their surface, which interacts with signal regulatory protein alpha SIRPα on myeloid cells such as macrophages, to transmit the “do not eat me” signal. This inhibition of phagocytosis of autologous cells exists in homeostatic conditions by the prevention of myosin IIA accumulation at the phagocytic synapse. Anti-CD47 antibodies or engineered SIRPα–Fc fusion were shown to restore macrophage ability to phagocytose cancer cells and prime cytotoxic CD8 T-cells, leading to the tumor regression in several tumor models and in clinical trials. Two anti-CD47 antibodies (Hu5F9-G4 and CC-90002) and one soluble recombinant SIRPα-crystallizable fragment (Fc) fusion protein (TTI-621) were tested in phase I clinical trials in AML and other hematological malignancies, pediatric brain tumors, and some multiple solid tumors (trial numbers NCT02678338 and NCT03957096). To minimize the off-target toxicity (transient anemia), bispecific antibodies targeting both CD47 and tumor-associated antigens were recently developed, yielding promising results [140].

Specific pathways involving STAT3 or STAT6 characteristic of an anti-inflammatory response can be targeted to modify M2 characteristics of TAMs. For instance, through its ligation to the IL-10 receptor,

IL-10 and IL-6 induce the activation of STAT3 necessary to drive an anti-inflammatory effect. Formerly, microtubule-stabilizing agents such as paclitaxel were shown to promote polarization of MDSC to macrophages with the M1 phenotype via suppression of STAT3 phosphorylation [141]. The STAT3 axis was then more specifically targeted with an intravenous injection of a STAT3–small interfering RNA (siRNA)–CpG conjugate which was shown to silence the immune suppressor gene STAT3, reprogramming the functions of TAMs correlated with an immune-mediated tumor rejection [142]. A recent in vitro study showed that corosolic acid, packaged within long-circulating liposomes and coupled to an anti-CD163 antibody, inhibited the activation of STAT3 in human M2 type macrophages and their IL-10-induced gene expression [143]. In the same way, STAT6, one of the major signal transducers activated by IL-13, involved in M2 polarization, can be inhibited by different synthetic molecules (AS1517499, TMC-264, A771726), leading to an inhibition of tumor growth in the 4T1 mammary tumor model and modification of genetic markers for TAM infiltration [144]. Furthermore, microRNA (miRNA)-155 is best characterized as a pro-inflammatory miRNA since it enhances M1-like macrophage activation by decreasing inhibitors of pro-inflammatory responses and targets the IL-13 receptor to reduce alternative macrophage activation [144]. Currently, several miRNAs are implicated in the regulation of macrophage activation and polarization in cancer [145], and developments of pharmacological formulations that either suppress or enhance the activity of selected miRNAs to reprogram the TAM phenotype are emerging. For instance, targeting of miRNA-processing enzyme DICER in macrophages with lysozyme-M-driven Cre prompts M1-like TAM reprogramming in lung carcinoma and MC38 tumors [146]. The switch of M2 TAMs toward an M1-like phenotype can also be driven by rapamycin, which is an mTORC1-specific inhibitor, inducing an anti-tumor effect in a hepatocarcinoma mouse model [147]. Moreover, inhibitors of PI3kγ, a molecule upstream of mTOR, are able to promote TAM-immunostimulatory responses in several cancer models [148]. Activation of MAPKs via production of ROS, thanks to a copper chelator, CuNG (N-(2-hydroxy acetophenone) glycinate), can convert suppressive TAMs toward a pro-inflammatory phenotype [149]. M1 genes such as iNOS and CXCL9 can also be upregulated concomitantly with the downregulated expression of M2 genes, arginase-1 and CD206, thanks to the inhibition of the CYP4X1 monooxygenase or the activation of the autophagy-induced RelB/p52 by flavonoids in glioma or hepatocellular carcinoma models [150,151]. Several synthetic molecules can also actively reverse the M2 phenotype of TAMs such as TMP195, an HDAC inhibitor, in breast cancer mouse models, or paclitaxel, an anti-microtubule agent, in patients with ovarian carcinoma [152,153]. Combination strategies were also reported to have a good effect on TAMs reprogramming. Anti-CD40 was combined with anti-CSF1R to create a pro-inflammatory environment eliciting T-cell responses

before depletion of TAMs [154] or with chemotherapies such as imatinib (tyrosine kinase inhibitor) with strong tumor regression in a gastrointestinal tumor mouse model [154]. A TLR9 agonist (IMO-2055) combined with chemotherapies and anti-VEGF showed anti-tumor activity in advanced or metastatic lung cancer [155]. Moreover, TLR9 agonists were also able to enhance radiofrequency-induced CTL responses, potentiating the inhibition of primary tumor growth and lung metastasis [156]. Regulating macrophage mitochondrial function is another way to activate the reprogramming of TAMs. Indeed, downregulation of the gene encoding pyruvate dehydrogenase is avoided by dampening the nuclear respiratory factor 1 degradation under hypoxia, which minimizes the Warburg effect and promotes M1 polarization of TAMs [157]. Moreover, cancer cells secrete lots of lactate through glycolysis, which is recognized by Gpr132 at the surface of TAMs and promotes M2 polarization. PPARγ agonists, which are suppressive for the Gpr132 axis, or siRNA silencing of Gpr132, was successfully used to desensitize TAMs to lactate stimulation in a breast tumor model [158,159]. Finally, recent studies identified novel drug targets for further investigation in the future.

For instance, loss of Gadd45b, a gene involved in the regulation of growth and apoptosis in myeloid cells, restored activation of pro-inflammatory functions of TAMs and intra-tumor immune infiltration in a fibrosarcoma mouse model [160]. Interfering with angiopoietin family molecules might be an effective strategy for reprogramming TAM polarization in NSCLC [161]. CaMKK2 was defined as a new myeloid-selective checkpoint and could be blocked to facilitate a favorable reprogramming of immune cells in the TME [162]. Several studies also proposed to reprogram the energetic metabolism in TAMs, in which fatty-acid oxidation is preponderant, decreasing lipid and cholesterol intake and metabolism [163,164].

Another interesting approach allowing to harness pro-tumoral potential of TAM is development of chimeric antigen receptor macrophages (CAR-Ms). Based on pre-clinical experiments, CAR-Ms were shown to efficiently phagocyte cancer cells in a directed manner. Additionally, they possess stable M1 phenotype and ability to convert other bystander M2 macrophages into M1 side of the spectrum, thus leading to disruption of pro-tumoral microenvironment [165]. Further development of CAR-Ms should soon yield the first results of its efficacy in the clinical trials.

1.3.3 Inhibition of recruitment

Modulation of the recruitment of monocytes and macrophages to the tumor site in order to disrupt TAM populations, represents a promising complementary therapeutic strategy. Inhibition of the CCR2/CCL2-axis is a major focus in this field as it represents the main pathway responsible for monocyte recruitment.

Targeting of CCR2/CCL2 pathway showed positive outcomes in various experimental cancer models [166–170]. In contrast to animal studies, clinical translation proved to be problematic. Clinical trials with agents depleting CCL2 (carlumab or CNTO888) or blocking CCR2 (MLN1202) showed poor therapeutic responses when used as monotherapies [171,172]. While administration of an anti-CCL2 antibody initially showed response, leading to decreased levels of CCL2, in a long term it led to significant elevation of this chemokine. Further precaution must be taken, as discontinuation of CCL2 therapy in murine models of breast cancer showed increased monocyte mobilization and tumor progression [172]. Phase I and II clinical trials with carlumab were carried out in patients with different types of tumors and indicated that CCL2 levels were only partially suppressed, leading to lack of therapeutic effect [173,174]. On the other hand, the blockage of CCR2 by small-molecule drug PF-04136309 in combination with folfirinox chemotherapy in a phase Ib clinical trial in patients with pancreatic cancer led to promising outcomes. While monotherapy turned out to be ineffective, 97% of patients with the combined treatment showed an objective tumor response and remaining patients showed a local tumor response [175]. To lower the chance of negative outcomes of direct inhibition of CCR2/CCL2 pathway, it has been proposed to target pathways responsible for upregulation of CCR2 on the cells. It was observed that, in a mouse model of glioblastoma, TAMs express aryl hydrocarbon receptor (AHR), which, upon activation by tumor released kynurenine (KYN), upregulates CCR2 expression. Blocking the AHR led to decreased TAM infiltration and tumor growth with concomitant increased survival of the animals [73].

Targeting of CSF1R also showed a decrease in macrophage/monocyte recruitment [176]. In spite of this, numerous clinical trials showed a limited therapeutic effect when CSF1R was targeted alone [177], with the exception of benign tenosynovial giant cell tumors, where a decrease in TAM infiltration and disease stabilization was achieved [178]. Efficacy of CSF1R inhibitors is still being tested in anticancer therapies, also in the form of broad-spectrum kinase inhibitors such as chiauranib (CSF1R, VEGF1-3, PDGFRα, c-Kit, Aurora B inhibitor) [179] and pexidartinib (CSF1R, KIT, FTL3 inhibitor), with potential anticancer results [180]. Research on a mouse model of lung adenocarcinoma showed that FGF released by CAF can induce TAM recruitment. Blocking of FGF receptor (FGF-R) with the Fgfr tyrosine kinase family inhibitor AZD4547 showed strong TAM abolishment and tumor regression, making this receptor a potential therapeutic target [181]. In addition, targeting other important molecules for monocyte/macrophage recruitment in cancer, i.e., catecholamines by 6-hydroxydopamine [182] and complement components such as C5a, may also bring positive results [183].

Adapted and updated from our review on Latest Advances in Targeting the Tumor Microenvironment for Tumor Suppression [106]

1.3.4 Conclusions

Several strategies have been proposed to target TAM, including: inhibition of recruitment, reprogramming into an antitumor phenotype, blocking of functions or depletion of these cells [104,105]. Targeting of CSF1R-CSF1 axis remains the leading approach, showing mixed responses in the clinic, with most promising effect in diffuse-type tenosynovial giant cell tumors [178,184]. Problem of this approach is associated with targeting apart from TAMs, also monocytes and tissue macrophages [99]. Similar situation concern administration of Clodronate and other BPs, which potentially target the whole mononuclear phagocytic system (MPS) [119]. Blocking of CCL2 axis responsible for recruitment of monocytes to the tissue sites, has been associated with low efficiency and intensified monocytes mobilization upon the treatment termination [171,172]. Alternative to "systemic" targeting of macrophages, would be therapies aiming to address only discrete populations of pro-tumoral TAMs. Unfortunately, specific targeting of macrophages remains a major challenge, mostly because of the remarkable plasticity of these cells, and shortage of exclusive markers. Emergence of a relatively new macrophage-specific markers like: MARCO [130], VISTA[185], Tyro3, Axl and MerTK[186] may offer a more accurate TAM-targeting in the future, opening a possibility for more precise elimination or reprogramming of TAM. Also continuation of finding new specific markers of TAM should remain a priority.

1.4 Chronic lymphocytic leukemia

TME is often associated with solid tumors, but it plays an equally important role in case of blood cancers. While the amount of tumor stroma and location of TME elements may differ drastically in comparison to localized tumors[9], all the interactions between cancer cells and accessory cells are also present in hematological malignancies. One of such examples can be observed in case of chronic lymphocytic leukemia (CLL)[187].

CLL belongs to the group of B cells malignancies and is characterized by the accumulation of small, CD5+, CD19+ mature-appearing neoplastic lymphocytes in the circulation and both primary and secondary lymphoid organs. Depending on the stage of the disease it leads to lymphocytosis, lymphadenopathy or

splenomegaly. CLL is an extremely heterogenous disease. Freshly diagnosed patient might require only monitoring of the disease, otherwise remaining fully active for decades. On the other side, there are individuals, who will progress rapidly, which despite treatment might lead to death. In most cases however, patients land somewhere in between of these two extremes [187]. 5-year relative survival of CLL is around 87.2% [188].

1.4.1 Epidemiology of CLL

CLL is stated as a most frequent adult leukemia of "western world", with frequency reaching around 0,06% of population in Europe and United States to around 0,01% in people of Asian and Pacific Islands descent in US [187]. The median age of CLL diagnosis ranges from 70-72 years and risk of the disease development is 2-times higher in men, than women [187]. CLL is almost always preceded by an indolent stage called monoclonal B-cell lymphocytosis of CLL phenotype (CLL-like MBL). People with more than 500 of CLL-like B cells clones/ul of blood might develop therapy-requiring CLL, with frequency of 1-2%/year. Interestingly few CLL-like MBL/ul of blood can be already detected in 7-14% of Western adults > 40 years old. In comparison, for Taiwan population, this level reaches only 1.3% [189]. Additionally, first degree relatives of people with CLL have up to 8.5 higher risk of developing the disease [187]. These results signify importance of genetic background in CLL initiation.

1.4.2 Classification of CLL

CLL B cells are characterized by expression of CD19+, CD5+, CD23+ and CD200 (which helps differentiating them from mantle lymphoma cancer cells), but low expression of CD20 and lack of CD10 [187]. CLL can be divided into 2 distinct groups based on the presence of unmutated (U-CLL) or mutated (M-CLL) immunoglobulin heavy-chain variable region gene (IGHV), thus reflecting typical maturation stage of B cells. CLL B cells with unmutated IGVH come from the cells which did not undergo the somatic hypermutation upon differentiation in germinal center zone. Hence, they are less mature leading to more aggressive disease with worse prognosis. On the other hand, CLL B cells with mutated IGVH represent the cells from post-germinal centers, expressing immunoglobulins after somatic hypermutation or in some cases also class switching (Illustration 2).

Additionally, there are plethora of flow cytometry markers with prognostic value, regarding agresivness of the disease, likelihood of treatment necessity etc. These include: CD49d [190,191], CD38, ZAP70, CD69 [192]. Also measurement of b2-microglobulin (β2-m) levels in the serum, represents an important predictive value,

and since this protein is constitutively released by CLL B cells it can be used to evaluate overall burden of cancer cells and thus response to therapy [193].

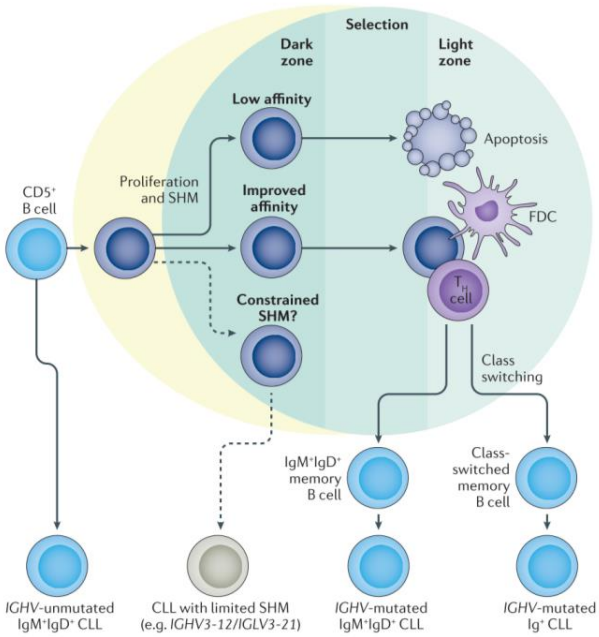

Illustration 2. U-CLL and M-CLL classification depends on maturation status of CLL cells. *Unmutated or mutated status of CLL cells, depends on the maturation stage from which malignant clone originates. Naïve B cell before somatic hypermutation (SHM) can give rise to U-CLL cell, analogically more mature B cell, after SHM and class switching can potentially lead to M-CLL cell expressing IgG. Adapted from [187], permission granted via RightsLink.*

1.4.3 Pathophysiology

CLL is associated with plethora of chromosomal alternations, somatic mutations, epigenetic modifications and miRNAs expression. Around 80% of patients have one of 4 chromosomal abnormalities: a deletion in chromosome 13q14.3 (del(13q)), del(11q), del(17q) and trisomy 12. Del(13q) is present in >50% of patients and is associated with positive prognosis. Alternations in this region are connected to expression of BCL2 gene, that has big implication in resistance to apoptosis and cell cycle progression. Del(11q) is detected in around 18% of patients and is usually connected to mutation in ATM gene. Del(17q) is found in 7% of patients, leading to loss of tumor suppressor gene TP53 [187]. Finally, trisomy 12 occur in 20% of patients, is frequently associated with NOTCH1 mutations [194]. Both Del(11q) and del(17q) are both associated with adverse prognosis [187,195], while trisomy 12 with intermediate one [187,194].

1.4.4 B cell signaling and life cycle of CLL cells

B cell receptor (BCR) signaling is required for survival of mature B cells and is also active in CLL B cells. It is composed of two parts: a membrane bound immunoglobulin (IgD, IgM, IgA, IgG or IgE) that serves as antigen-binding subunit and heterodimeric Ig-γ (CD79A)/Ig-β(CD79B), that is responsible for a signal transduction through SRC-family kinase-dependent phosphorylation (predominantly LYN) and spleen tyrosine kinase (SYK)[187]. CD19 serves as a co-receptor for BCR leading to Pi3K-AKT-mTOR, NFκβ and ERK activation [187]. In CLL, malignant B cells can maintain continuous activation of BCR through engagement of autoantigen. Interestingly, BCR signaling in CLL can lead to completely opposite outcomes, from B cell activation that increases survival and proliferation to cell anergy. Outcomes of BCR engagement depends on which downstream pathway will be activated afterwards. In general, BCR signaling leads to cell activation in U-CLL and cell anergy in M-CLL. While the reason for cell anergy is not clearly known, it might be an outcome of chronic BCR activation with lack of proper T-cell engagement. Also, the difference in genetic and epigenetic background might be involved. Nevertheless, the cell anergy, at least partially explains the usual indolent character of M-CLL[100]. Another difference between M and U-CLL B cells is the repertoire and level of response to autoantigen recognized by BCR. In M-CLL, BCR signalling pathway show constant phosphorylation, and binding of antigens like β-(1,6)-glucans or rheumatoid factors (RF) lead to only mild response. On the other hand BCRs in U-CLL show high specificity toward much wider repertoire of targets, including: MYHIIA, vimentin, but also single and double-stranded DNA, oxidized low-density lipoprotein and bacterial antigens, like lipo-polysaccaride (LPS). Also, binding of the antigens in case of U-CLL b cells is leading to strong activation, especially in the presence of CD38 and ZAP70 [196].

Beside direct activation of CLL B-cells, BCR control also activity of various surface receptors on cancer cells, including integrins. One of integrin modulated by BCR is α4β1 integrin composed of CD49d (alpha 4) and CD29 (beta 1), resulting in binding to vascular cell adhesion protein 1 (VCAM1) and fibronectin [100], thus facilitating cell-cell and cell-ECM interaction respectively [190].

1.4.5 Importance of TME and proliferation centers

CLL represents quite a unique setting to observe dependency of cancer cells from TME. Because of their mature phenotype, CLL cells are unable to survive and proliferate on their own, instead they need to migrate from peripheral blood (PB) to lymphoid organs in order to obtain appropriate stimuli. These spots are mostly located in the lymph nodes (LN), are called proliferation centers (PC) and represents one of the hallmarks of CLL [187]. CLL cells migration to PC is driven by chemokine gradient created by non-malignant

cells of TME. Mechanistically the main receptor responsible for CLL cells migration is CXC-chemokine receptor 4 (CXCR4), which binds CXC-chemokine ligand 12 (CXCL12), and CC-chemokine receptor 7 (CCR7), which binds CC-chemokine ligand 19 and 21 (CCL19/CCL21) [187].

Following the chemokine gradient, CLL cells enter lymphoid organs. In there, CLL B cells encounters various accessory cells, including: T-cells, Nurse-like cells and mesenchymal-derived stromal cells (MSCs). T-cells provide cancer cells with multiple proliferation stimuli, including engagement of CD40 by CD40L and release of IL-2, IL-4 and IL-10. It has been shown that IL-4 can upregulate expression of surface IgM on cancer cells, thus improving interaction with autoantigens. In turn, presence of autoantigens on both stromal cells and NLC [196] and stimulation from T cells, lead to proliferation of cancer cells (the role of NLC in the CLL pathophysiology will be discussed in detail in the next chapter). MSCs also supports cancer cell survival through release of CXCL12, WNT and directly by VCAM1 and CD49d/CD29 interaction. Activated cancer cells in turn release CLL2-4 to recruit more T-cells, and monocytes that will differentiate into NLC, thus further strengthening the TME [187,197].

Looking globally, at any given moment only few percent of CLL B cells reside in the proliferation centers. After activation and proliferation in LN, cancer cells return to circulation where they acquire resting status or be driven into anergy. Returning to circulation will cause CLL cells to upregulate expression of CXCR4 and surface IgM. After reaching certain level, the cells can again follow the CXCL12 gradient that will lead them back to LN, thus repeating the cycle. The "activation cycle" of CLL B cells can be followed by the CXCR4/CD5 expression pattern [198]. Engagement of CXCR4 with CXCL12 leads to its downregulation, thus CLL B cell right after leaving proliferation centers are $CXCR4^{dim}$ and $CD5^{bright}$ and resting cells are $CXCR4^{int/bright}$ and $CD5^{int/dim}$ respectively [187,198] (Illustration 3). The role of CD5 in this process is not exactly clear, however it has been suggested that CD5 might prevent negative BCR signaling and also induce expression of CCR7, activation of STAT3 and expression of IL-10 [197]. CCR7 is crucial for homing to LN [198] and IL-10 has a very important role in CLL, as it not only increase survival of cancer cells themselves [187,199], but also induce immunosuppressive environment and polarization of NLC.

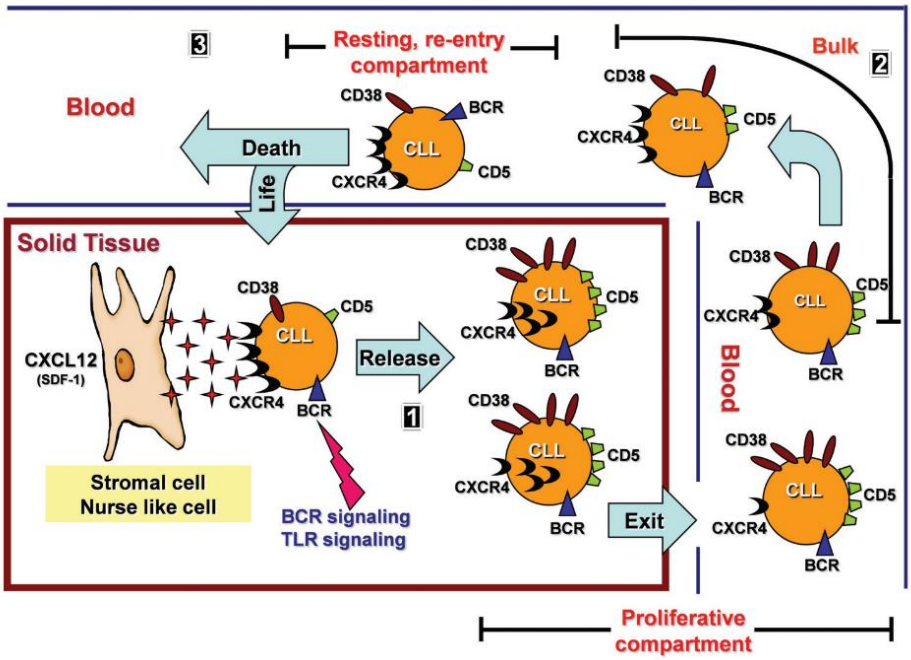

Illustration 3 Representation of hypothetical model of CLL cell lifecycle, *signifying migration of cancer cells between proliferation center (solid tissue) and blood stream. 1) CLL cell enter proliferation center, and get in contact with accessory cells, including NLC, stromal cells and T cells. There cancer cells get activated, proliferate and upregulate expression of CD5 and downregulate CXCR4. $CD5^{high}CXCR4^{dim}$ cancer cells reach the blood stream. 2) in the bloodstream CLL cells gradually lose expression of CD5 and upregulate CXCR4, leading to $CD5^{int}CXCR4^{int}$ and finally $CD5^{dim}CXCR4^{high}$ populations. 3) $CD5^{dim}CXCR4^{high}$ cells will most likely detect CXCL12 gradient and re-enter the proliferation center/solid tissue to repeat the cycle (otherwise they die from exhaustion). Adapted from* [198]

1.4.6 Nurse-like cells (NLC)

Nurse-like cells represent one of the main component of CLL-specific TME found in lymphoid organs, especially LN where they participate in formation of "proliferation centers", as introduced previously. NLC differentiate from CD14+ monocytes, attracted to the tissue site, mostly by cancer cells producing chemokines like CCR2 [200,201]. The exact factors involved in NLC differentiation and maturation remains unknown, none the less CSF-1[202,203], extracellular nicotinamide phosphoribosyltransferase (NAMPT) produced by CLL cells[204], HMGB1[205] released by dying CLL cells and direct contact with CLL B cells are all necessary [206]. NLC can be obtained *in vitro* during long-term culture of PBMC isolated from blood of CLL patient. PBMC culture leads to outgrowth of large, adherent NLC with numerous cancer cells attached to their surface. Sometimes also pseudo-emperipolesis process can be observed, where CLL B cells are crawling under the macrophages without being internalized (Illustration 4). This phenomenon also granted NLC their name, based on nurse cells present in the thymus, which display emperipolesis and have a crucial

role in thymocytes maturation [201]. Furthermore, transcriptomic analyses of monocytes, M1, M2 macrophages, TAM and NLC revealed that NLC show very close resemblance to M2-like TAM. Thus NLC can be classified as specialized form of tumor-associated macrophages in CLL[207]. Recently also term leukemia-associated macrophages (LAM) is quite often utilized in context of blood malignancies [208]. NLC can be characterized by expression of $CD14^{+}$, $CD68^{+}$, $CD163^{++}$ and $CD206^{+}$ markers [201,209].

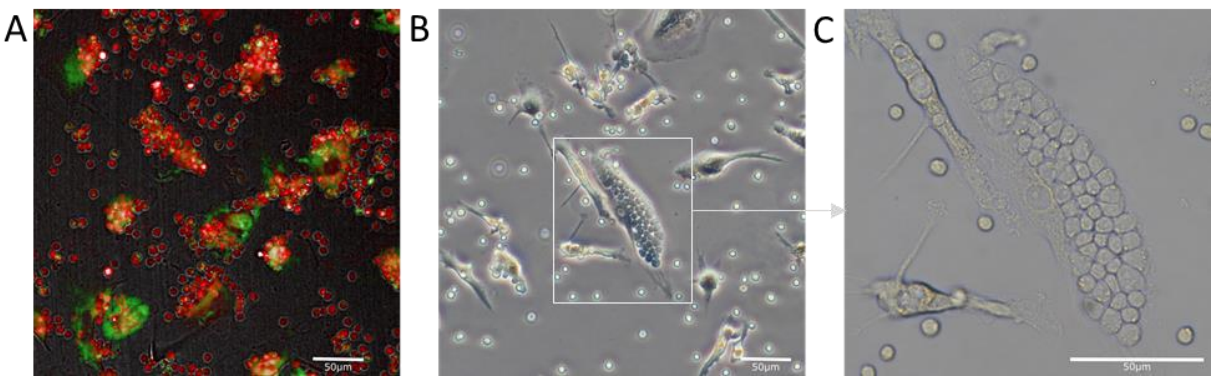

Illustration 4. Visualization of interaction between CLL cells and NLCs. *A) Picture of NLCs (green) and CLL cells (red), 120 min after initiation of co-culture. Live-cell imaging with Operetta CLS High Content, x20 objective. B, C) Bright-field imaging of pseudo-emperipolesis event, with small round CLL cells gathered below big, adherent NLC. Most of the floating cells were removed by pipetting, right before taking the picture. B) ×20 objective, C) ×40 objective with focus on the indicated area on picture B.*

Similarly, to TAM, NLCs perform various processes to support cancer cells. Perhaps the most prominent function of NLCs is protecting CLL B cells from spontaneous apoptosis. NLCs are the main producers of SDF-1 (CXCL12), that beside stimulating survival of malignant cells, is also attracting cancer cells to the proliferation centers [187,201]. Beside NLC are protecting CLL B cells by expressing B cell-activating factor (BAFF), a proliferation-inducing ligand (APRIL) [210], B cell-attracting chemokine (BCA-1 or CXCL13), WNT5A [187,201] and BDNF [211]. Even though APRIL continue to appear as an important molecule for CLL survival, some studies question its role in the process [212]. Apart from soluble factors, the NLC protective function is also mediated by direct contact mediated through CD31-CD38[196] and CD2-CD58 (lymphocyte function-associated antigen 3/LFA3) interaction between macrophages and cancer cells respectively [206]. Beside, NLCs together with stromal cells are believed to be a source of autoantigen, necessary for stimulation of BCR signaling on cancer cells [213]. Similarly to other TAM, NLCs are believed to also participate in formation of immunosuppressive TME, as they are shown to produce: IL-10, CCL18, IL-6, IL-8 and also IDO [204].

Beside participation in pathophysiological function of CLL B cells, NLCs can also protect cancer cells from therapeutic insult. In vitro studies showed, that CLL cells co-cultured with NLCs were more likely to survive treatment with idelalisib [202], ibrutinib, chlorambucil or dexamethasone [214].

In general, NLCs infiltration is associated with worse prognosis in CLL. Absolute monocyte count (AMC), which can indirectly reflect the number of NLCs in the LNs is associated with shorter time to first therapy (TTT) and overall survival (OS) [215]. In accordance, abundance of soluble CD163 (sCD163) in the blood of the patients is associated with disease progression and bad prognosis. Soluble CD163 can be used as a more direct indicator of NLCs infiltration level in the proliferation centers [214].

1.4.7 Targeting of nurse-like cells in CLL

NLCs represent an important therapeutic target, given their significance in the pathophysiology of CLL and resistance to treatment. So far no therapeutics directly targeting NLC in CLL has been approved. Nonetheless, multiple candidates indirectly affecting NLC are available. The first example of a drug indirectly modulating NLC is Ibrutinib. Ibrutinib belongs to the new generation of drugs for the treatment of CLL. It is an irreversible inhibitor of Bruton's tyrosin kinase (BTK), that shows exceptional efficacy in the clinics. Ibrutinib action causes impairment of BCR and NF-κβ signaling, which in turn modify mobility and adherence of the cancer cells, limiting access to prosurvival TME and finally leading to cell apoptosis [187]. Ibrutinib exhibit also immunomodulatory functions, leading to normalization of T cells populations and inhibition of BTK expressed by NLCs. Interestingly treatment with ibrutinib potentiates M2 phenotype of NLCs by: blocking STAT1 phosphorylation with concomitant activation of STAT6; increased expression of CD163 and CD206; stimulation of IL-10 expression. It also decreases the phagocytic potential of NLCs by downregulation of Macrophage-1 antigen (MAC1)/CD11b/CD18 expression [216]. However, it was not shown if ibrutinib can also affect the efferocytosis process which is an especially relevant form of phagocytosis in tumorogenesis [217]. *In vitro* studies on monocyte to macrophage differentiation upon treatment with ibrutinib, showed: promotion of spindle shape morphology of mature cells; decrease expression of CD11b; increased oxidative metabolism. On the other hand, it did not change the expression of important M2 markers, like CD163 and CD206 [218]. In the end, better characterization of the effect of ibrutinib on NLCs function is required, especially as these cells are suggested to be an important factor in the resistance to this treatment. So far the results imply that ibrutinib, actually promote protective phenotype of NLCs and alternative targeting of these cells would help improve the outcome of the therapy in case of resistant patients.

All the drugs presented below are not yet approved in the clinic for treatment of CLL and have been mentioned upon general TAM targeting. The first one - Lenalidomide is an immunomodulatory agent (IMID) with non-defined molecular mechanism of action, involving increased actin polymerization and cell adhesion. This agent turned out to affect several cell types forming TME of CLL, including monocytes and NLCs. It is believed to indirectly decrease CLL B cell viability by: inhibiting migration of monocytes toward LN and repolarizing NLCs toward M1-like, anti-neoplastic phenotype, with increased ability to activate T-cells. On the other hand, results presented in the paper showed also increased proliferation and number of NLC upon treatment with Lenalidomide followed by stronger adhesion of cancer B cells to NLCs – which is one of the hallmarks of protective function of these cells. Also decrease of CD163 marker presented by the authors is negligible [219]. Additionally, use of Lenalidomide in clinical trials showed a high incidence of severe adverse effects [220]. In one of the phase III clinical trials of elderly patients with CLL, Lenalidomide showed therapeutic activity in the subset of patients. However, there was no improvement of PFS compared to Chlorambucil, and increased mortality of the patients in Lenalidomide led to early termination of the trial [221].

Trabectedin, described in a previous chapter, has been also proposed as an immunomodulatory drug that could be used in CLL. It showed activity to selectively kill CLL B cells and Mo-MDSC. Additionally, this drug, turned out to modulate function of immune cells of CLL TME, activating anti-tumoral activity of both T cells are macrophages. Trabectedin can also promote M1-like polarization of macrophages, inducing expression of many proinflammatory genes and impairing protective function of NLCs, serving as another potential drug to indirectly affect NLCs and TME of CLL [128]. While first clinical trials with Trabectedin in combination with Venetoclax for the treatment of CLL patients with resistance to BTK inhibition was terminated due to lack of participants, it will potentially lead to future attempts [222].

Another compound, that could be used in the treatment of CLL is Lurbinectedin (PM01183) – and analoque of Trabectedin. This compound is a selective inhibitor of protein-coding genes transcription, that leads to cell apoptosis. Both cancer B-cells and non-malignant immune cells dispaly increased sensitivity to the drug. It was shown, that Lubrinectedin can also change the profile of cytokine produced by monocytes and NLC, with increased production of IL-1β – which is overall a marker of good prognosis in CLL [223].

All of the drugs presented above affect NLCs by modulating their phenotype and potentially disrupting their nursing properties toward CLL cells. However, they are working on the broad spectrum of cell types,

displaying low specificity. More direct approach in targeting of NLCs could involve targeting of CSF1R signaling or treatment with Clodronate. For example, treatment of primary CLL samples *in vitro* with agents blocking CSF1R signaling, led to depletion of NLCs, increased mortality of cancer cells and also sensitization of cells to idelalisib and ibrutinib in case of resistant cells [202,203]. Also in vivo treatment of leukemic Eμ-TCL1 mouse model with Clodronate resulted in: depletion of both monocytic and M2 macrophage populations; stimulation of proinflammatory cytokines production including GM-CSF; increased number of DCs – all of which led to decreased survival of CLL B cells [224].

Finally, an interesting strategy in disruption of NLCs properties, could be achieved by repolarization of TME with use of cytokines, like IFN-γ. One study on in vitro effect of IFN-γ, showed that NLCs could be partially repolarized into M1-side of the spectrum, leading to decreased viability of CLL cells and increased antibody-dependent cell phagocytosis (ADCP) potential of NLCs [225].

All things considered, targeting of NLCs display similar problems, as in case of TAM in other cancer – overall lack of specificity. It leads to not only weaker response to therapy, but also might increase toxicity as seen with drugs like Lenalidomide. If we consider that in most cases targeting of TME, including TAM should be used in combination with agents targeting cancer cells, it is necessary limit side-effects of the complementary treatment. For that, it remains crucial to find specific markers for TAM in different types of cancers.

1.5 Aim of the thesis

Tumor-associated macrophages (TAMs) belong to the major cell population of tumor microenvironment where they support tumor growth and metastasis, and also confer cancer cells resistance to apoptosis, immune system attacks and therapy. Therapeutic targeting of TAM in cancer remains challenging, owing to their high plasticity and lack of exclusive markers. To address these problems, Team 9 of CRCT used a Hybridoma technology, immunizing mice with Nurse-like cells (NLCs) as a model of TAM. NLCs are the type of TAM encountered in chronic lymphocytic leukemia (CLL), are crucial for the survival of cancer B-CLL cells and can be easily generated in vitro. This approach resulted in generation of monoclonal antibody, called 6-25, that was further characterized to specifically bind to TAM of different human malignancies by recognizing sideroflexin-3 (SFXN3) protein on their surface. Both 6-25 antibody and its target have been patented (WO2018/020000 and WO2018/19990). SFXN3 represented a very interesting and unique target as it is a poorly defined, ubiquitous inner-membrane mitochondrial protein, that for an unknown reason was detected on the subpopulation of TAM.

The overall aim of this thesis was to further characterize 1) the specificity and therapeutic potential of 6-25 antibody toward TAM *in vitro* and 2) study the biology of 6-25 target (SFXN3), a potential new marker of TAM. These results will further support project aiming to use 6-25 antibody to target TAM in human malignancies, in order to improve the outcome of anticancer therapies.

2 Material and methods

2.1 Cell culture in vitro

Both primary cells after isolation and cell lines cultured in the complete medium containing: RPMI 1640 with GlutaMAX (Gibco, France) supplemented with 10% of FBS (Life Technologies, France) and 100 µg/ml of penicillin/streptomycin (Sigma-Aldrich, France). Only in the case of HEL92, THP-1, HEP-G2 and HEK-T cells, DMEM with GlutaMAX (Gibco, France) was used instead. All cultures were performed in Tissue Culture Treated Plates (Corning, USA). Cells were kept in 37°C, at the atmosphere of 5% CO2.

2.1.1 Primary cell culture

2.1.1.1 *Chronic lymphocytic leukemia (CLL) cells*

Peripheral blood samples from CLL Patients were obtained from the Hematology Department with informed consent and referenced in the INSERM cell bank. According to French law, the INSERM cell bank has been registered with the Ministry of Higher Education and Research (DC-2013-1903) after being approved by the ethic committee (Comité de Protection des Personnes Sud-Ouest et Outremer II). Clinical and Biological annotations of the samples have been reported to the Comité National Informatique et Liberté (the Data Processing and Liberties National Committee). Blood samples were collected from previously untreated patients, if not stated otherwise. PBMC from CLL patient's blood were isolated by density-gradient centrifugation on Ficoll-PaqueTM PLUS (GE Healthcare, Sweden). If not stated otherwise, CLL PBMC were plated freshly after isolation at 10×10^6 c/mL and maintained for 12-14 days to allow maturation of NLCs. Culture of cells at such high concentration, allows to generate sufficient number of NLCs for downstream processing, and limits spontaneous apoptosis of CLL cells during early days of the culture.

Experiments for flow cytometry analysis of NLCs were performed in 6-well plates in 4 mL of complete medium. To evaluate phenotype and viability of CLL cells only, cultures were downscaled to 48- or 96-well plates.

2.1.1.1.1 CLL B cells isolation

CLL cells were isolated from fresh or frozen PBMC, using EasySep™ Human B Cell Enrichment Kit II Without CD43 Depletion (STEMcell, France) for negative cell selection, according to manufacturer instructions.

Purity and viability of the cells after isolation were evaluated by flow cytometry, following staining with anti-CD5/CD19 antibodies and Annexin-V/7-AAD respectively. For each experiment both values exceeded 95% (data not shown).

2.1.1.2 *Normal human PBMC*

Normal human PBMC were isolated from healthy donor buffy coats, using density-gradient centrifugation on Ficoll-PaqueTM PLUS (GE Healthcare, Sweden). Whole PBMC were used for further in vitro culture or for subsequent isolation of CD14+ monocytes.

PBMC for toxicity assay with the 6-25 mAb, were used freshly after isolation. Cells were cultured at 1 × 10^6 c/mL, in 0.5 mL of complete medium, per well of 24-well plate.

2.1.1.3 *Isolation of $CD14^+$ monocytes*

Isolation of $CD14^+$ monocytes from normal human PBMC was performed using CD14 MicroBeads positive selection kit and MS/LS columns (Miltenyi Biotec, France), according to the adjusted manufacturer's protocol. In the process of optimization, the amount of positive selection beads was reduced 6-times leading to: retention of satisfactory cell yield, reduced monocyte clumping and improved cell purity. Following the isolation, cell purity was measured by flow cytometry following staining with α-CD14 antibody. Isolated monocytes were used right away for subsequent generation of monocyte-derived macrophages (MDM) or heterologous NLC.

For experiments with RNP (ribonucleoprotein) CRISPR Cas9 gene knock-out, monocytes were also isolated with RosetteSep negative selection kit (STEM cell, France) according to the manufacturer's protocol.

2.1.1.4 *Monocyte-derived macrophages (MDM) differentiation*

In order to study expression pattern of the 6-25 target, multiple protocols of generation of MDM were tested. As a result of optimization a following protocol was chosen for further experiments - monocytes after isolation were seeded in a 12-well plate, at 0.5 × 10^6 c/mL in 1.5mL of complete medium..

To obtain M1 or M2-like macrophages, monocytes were activated with 50 ng/mL of GM-CSF (research grade) or 25ng/mL CSF-1 (premium grade) respectively. In both cases cytokines were administrated at day 0 and again on day 3. On day 6, half of the culture medium was replaced and cells were supplemented with 10 ng/mL of IFN-γ to generate M1 macrophages or 25 ng/mL of IL-4 and IL-13 to generate M2 macrophages (Illustration 5). In case of M1 MDM, 18h later, cells were treated with 10ng/mL of LPS.

In chapter 3.3.1 and 3.3.2, IL-34 was used at 50 ng/mL with the same schedule as CSF-1 and GM-CSF. In case of TNF treatment, the cytokine was added at 10ng/mL at day 0, 3 or 6 (according to descriptions in specific chapters). All cytokines were bought at Miltenyi, and after resuspension, aliquoted at 0.1 mg/mL and stored in -20°C.

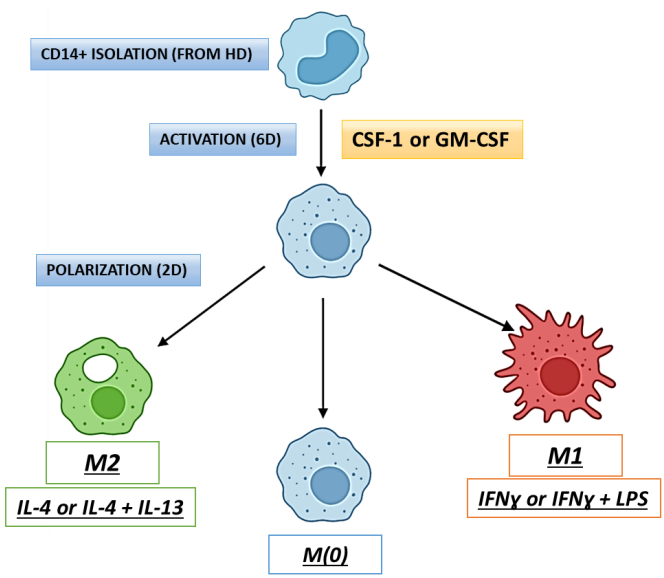

Illustration 5. Scheme of generation classical M0, M1 or M2-MDM. To obtain M1 and M2 macrophages, monocytes were activated with GM-CSF and CSF-1 respectively.

2.1.1.5 *NLC and MDM detachment protocol*

Non-enzymatic detachment was performed using Versene solution (0.48 mM EDTA in PBS, Gibco, France). In case of NLCs, non-adherent cells were first removed by gentle pippeting. Then remaining cells were washed twice with cold PBS, covered with Versene solution and incubated at 4°C for 20-40 min (depending on the degree of cell rounding). Subsequently FBS was added as a protectant, and cells were gently scrapped with 2-position, 16 cm cell scraper (Sarstedt, USA).

Enzymatic detachment was performed using Accutase® Cell Detachment Solution (Ozyme, Biolegend). Briefly, cells were washed twice with PBS at RT, covered with pre-warmed Accutase solution and placed on orbital rocker, in cell culture incubator (37°C, 5% CO_2) for 15-20 min. Afterwards FBS was added, and if needed cells were gently scrapped (analogically as in non-enzymatic procedure).

For both procedures cell rounding and detachment were controlled with bright-field microscopy (BFM). Following cell detachment, cells were centrifuged (200g, 5min, RT), counted and re-suspended in appropriate buffer for subsequent assay.

Note: non-enzymatic procedure was used in chapter 3.1, 4.1, 6.2 and 6.3. Enzymatic procedure was used for remaining experiments as it was characterized with better cell recovery. As both procedure can affect cell phenotype, only one technique was used in given set of experiments.

2.1.2 Cell lines

Various cell lines used for screening of the 6-25 target expression, including: MV4-11, THP-1, HEP-G2, HMC-1, HEL92 were purchased previously from the ATCC collection. MOLM-14, OCI-AML-3, U-373 and U-937 cells were a kind gift of Dr. Thomas Farge (Team METAML, CRCT, France). HEK-T cells used for overexpression of the FOLR2 gene, were a kind gift of Pauline Herviou (Team RNAreg, CRCT, France). All cell lines were split every 2-3 days, until reaching passage 20-25, before returning for fresh frozen vial. In case of adherent cultures, cells were treated with trypsin for 5-10 min in 37°C, followed by inactivation of the enzyme with FBS.

2.1.3 Cryopreservation of cells

For cryopreservation procedures: cell lines, CLL PBMC for isolation of CLL cells and purified CLL cells were re-suspended in cold, freshly prepared FBS containing 10% of DMSO. CLL PBMC for whole PBMC culture and isolated human CD14+ cells were suspended in cold Cryostor CM10 medium (STEMCELL Technologies, France). 1-1.5mL aliquots were placed in Cryotubes, transferred to a cryofreezing container (Mr. Frosty, Nalgene) and placed in a −80 °C freezer (short term) or in liquid nitrogen (long term). Note: only Cryostor CM10 medium allowed to obtain viable monocytes after thawing procedure. Nevertheless, NLC from cryopreserved CLL PBMC showed reduced yield and modified phenotype, hence their use was limited to the necessary minimum.

2.2 Flow cytometry

List of antibodies used for phenotyping of normal human PBMC, CLL and myeloid cells.

Target	Fluorochrome	Company	Clone	Cat. number	Dilution	Isotype
PBMC						
CD3	BV510	BD Horizon™	HIT3a	564713	50	Mouse IgG2a, κ
CD4	BV421	BD Horizon™	RPA-T4	562424	50	Mouse IgG1, κ

CD5	PE-Cy7	BioLegend	UCHT2	300622	200	Mouse IgG1 κ
CD8	PE	Beckman Coulter	B9.11	A07757	50	Mouse IgG1 κ
CD56	PE	MACS Miltenyi Biotec	AF12-7H3	130-090-755	50	mouse IgG1κ
CD19	BV421	BD Horizon™	HIB19	562440	200	Mouse IgG1, κ
CLL B-cells						
CD5	PE-Cy7	Sony	UCHT2	RT2103110	200	Mouse IgG1, κ
CD19	BV421	Sony	HIB19	RT2111170	200	Mouse IgG1, κ
CD19	PE-Cy7	BD Pharmingen™	SJ25C1	557835	50	Mouse IgG1, κ
Myeloid cells						
CD11c	BV421	BD Pharmingen	B-ly6	562561	50	Mouse IgG1, κ
FR-β	PE	Biolegend	94b/FOLR2	391703	50	Mouse IgG1, κ
CD115	BV421	Sony	9-4D2-1E4	RT2336610	50	Rat IgG1, κ
CD14	PE-Cy7	BD Pharmingen	M5E2	557742	50	Mouse IgG2a κ
CD14	APC/Cy7	BioLegend	M5E2	301820	50	Mouse IgG2a κ
CD14	PE-Cy7	Sony	HCD14	RT2228090	50	Mouse IgG1, κ
CD16	PE	BD Biosciences	3G8	560995	50	Mouse IgG1, κ
CD16	PE-Cy7	Beckman Coulter	3G8	6607118	50	Mouse IgG1, κ
CD163	APC	BioLegend	RM3/1	326509	50	Mouse IgG1, κ
CD163	FITC	Sony	GHI/61	RT2268090	50	Mouse IgG1, κ
CD163	Alexa Fluor 488	R&DSystem	215927	FAB1607G-100	50	Mouse IgG1, κ
CD169	APC	Sony	7-239	RT2330040	50	Mouse IgG1, κ
CD204	BV421	BD Pharmingen	U23-56	742438	50	Mouse IgG1, κ
CD204	PE	BD	U23-56	566251	50	Mouse IgG1, κ
CD206	BV421	Sony	15_2	RT2205630	50	Mouse IgG1, κ
CD206	PE	Beckman Coulter	3.29B1.10	PN IM2741	50	Mouse IgG1
CD206	unconjugated	Sony	15_2	RT2205510		Mouse IgG1, κ
CD209 (DC-SIGN)	FITC	BD	DCN46	561764	50	Mouse IgG2b, κ
CD64	PE	BioLegend	10.1	305008	50	Mouse IgG1, κ
CD64	PE	BD Pharmingen	10.1	305008	50	Mouse IgG1, κ
CD64	BV605	Sony	10.1	RT2125170	50	Mouse IgG1, κ
CD68	APC/Cy7	BioLegend	Y1/82A	333822	50	Mouse IgG2b κ
CD71	APC-Cy7	Sony	CY1G4	RT2270550	50	Mouse IgG2a, κ
CD86	BV421	Sony	BU63	RT2471060	50	Mouse IgG1, κ
HLA-DR	PE-Cy7	BioLegend	L243	307616	50	Mouse IgG2a κ
HLA-DR	FITC	BioLegend	L243	307604	50	Mouse IgG2a κ
HLA-DR	FITC	Sony	L243	RT2138020	50	Mouse IgG2a, κ
MARCO	PE	Life Technologies	PLK-1	12-5447-42	50	Mouse IgG3
MARCO	PE-Cy7	life techno	PLK-1	25-5447-41	50	Mouse IgG3

Isotype controls						
	Alexa Fluor 488	Novus Biologics	60024B	IC1051G	50	Rabbit
	PE	Sony	MOPC-21	RT2600560	50	Mouse IgG1, κ
	PE-Cy7	Sony	MOPC-21	RT2600630	50	Mouse IgG1, κ
	FITC	Sony	MOPC-21	RT2600540	50	Mouse IgG1, κ
	Alexa Fluor 488	Sony	MOPC-21	RT2600645	50	Mouse IgG1, κ
	BV421	Sony	MOPC-21	RT2600790	50	Mouse IgG1, κ
	Alexa Fluor 488	Sony	MOPC-21	RT2600660	50	Mouse IgG1, κ
	BV605	Sony	MOPC-173	RT2601345	50	Mouse IgG2a κ
	BV421	Sony	MOPC-21	RT2600790	50	Mouse IgG1, κ
	BV421	Sony	RTK2071	RT2602145	50	Rat IgG1, κ
	PE	Life Technologies	B10	12-4742-41	50	Mouse IgG3
	APC	ozyme		BLE400120	50	Mouse IgG1, κ
	BV421	BD		562438	50	Mouse IgG1, κ
	BV605	Sony	MOPC-21	RT2600810	50	Mouse IgG1, κ
	CF633	in-house stained				Mouse IgG1, κ
	CF633	in-house stained				Human IgG1
	PE-Cy7	BD Pharmingen	MOPC-173	560906	200	Mouse IgG2a κ
Secondary antibodies						
anti-mouse IgG	FITC	Invitrogen		31543	200	Goat F(ab)2
anti-human IgG	Alexa Fluor 488	Invitrogen		H10120	200	Goat F(ab)2

2.2.1 Basic cell staining

Collected macrophages were re-suspended in flow cytometry staining buffer (2% FBS, 1mM EDTA in PBS) containing 2.5 µg/mL of Human BD Fc Block™ (BD Pharminge, France) and incubated for 15 min at 4°C. Subsequently cells were stained with antibodies at saturating concentrations, for 20 min at 4°C. After washing, cells were re-suspended in PBS, containing 0.8 µg/mL 7-AAD (Sony, USA) and immediately analyzed by flow cytometry.

For CLL cell viability analysis, flow cytometry staining buffer contained no EDTA. After Fc Block incubation, cells were stained with 1 µg/ml of CD5 and CD19 antibodies for 20 min at 4°C. Next cells were washed in Annexin-V buffer and stained with Annexin-V-FITC according to manufacturer protocol. 5 minutes before the analysis cells were re-suspended in Annexin-V buffer containing 0.8 µg/mL 7-AAD.

2.2.2 6-25 staining

Indirect staining with 6-25 antibody

During early experiments an unconjugated version of 6-25 mAb was used. Briefly, after Fc block incubation, cells were incubated with 10ug/mL of 6-25 mAb for 30 min at 4°C. After washing cells were incubated with goat anti-mouse II-antibody for 20 min at 4°C. Next, cells were incubated with a specific antibody mix for 20 min at 4°C. After washing, cells were re-suspended in PBS, containing 0.8 µg/mL 7-AAD (Sony, USA) and immediately analyzed by flow cytometry. Protocol used in chapter 3, 4.1 and 6.3.

Direct staining with 6-25 antibody

In order to perform direct staining, 6-25 antibody was coupled with CF633 fluorophore, using Mix-n-Stain™ CF®633 Antibody Labeling Kit manufacturer instruction. During 6-25 conjugation, also matching isotype control antibody was prepared. Every new batch of antibody was tested by flow cytometry on M2-MDM or NLCs, to ensure consistency of the staining. 6-25 after labelling was used in the same fashion as other commercial antibodies conjugated with fluorophore.

2.2.3 Data acquisition and analysis

All presented results were acquired on an LSRII flow cytometer (BD Biosciences, France). Obtained data was analyzed by Flow Logic 700.2A (Inivai Technologies, Australia), further calculations were performed in Graph Pad Prism 9.1.2 or Microsoft Excel 2016.

2.3 Statistical analysis

All statistical analyses were performed using Graph Pad Prism 9.1.2.

2.4 Western blot analysis

Cell for preparation of lysates, were washed ×2 in PBS and lysed with RIPA buffer supplemented with protease inhibitors (Roche), for 15 minutes at 4°C. Cell lysates were centrifuged at 10000g for 15 min at 4°C. Supernatants were collected and protein concentration was evaluated with BCA assay. Then appropriate amount of protein was mixed with Laemmli Sample Buffer (Bio-Rad #161-0747: 62.5 mM Tris-HCl, pH 6.8, 10% glycerol, 1% LDS, 0.005% Bromophenol Blue) and heated at 60°C for 15 min. Samples were then resolved by SDS-PAGE, during ~2h at 120V, using in-house prepared 4/12% gel. After separation, proteins were transferred to Nitrocellulose membrane using wet transfer procedure (400 mA, 2h, 4°C). Afterwards, membrane was incubated in blocking buffer (5% milk, in TBS-T) for 1h at RT. Then membrane was incubated with primary antibody, O/N at 4°C, followed by ×4 washing with TBS-T. Next, membrane

was incubated with appropriate secondary antibody conjugated with HRP, for 1-2h at RT. After ×4 washing in TBS-T, followed by ×1 wash in TBS, membrane was covered in ECL™ Western Blotting Detection Reagents (Amersham™, GE Healthcare, Sweden) reagent for 5 minutes, and chemiluminescence was detected by ChemiDoc Imaging System (Biorad, Germany).

Target	Species	Clonality	Cat. number	Dilution factor	Company
Primary					
SFXN3	Rabbit	polyclonal	HPA008028	1000	Ozyme
SFXN3	Rabbit	monoclonal	ab181163	1000	Abcam
SFXN3	Rabbit	polyclonal	A12298	2000	Abclonal
chimeric 6-25	Chimeric (human Fc fragment)	monoclonal	-	10µg/mL	-
Secondary					
anti-rabbit	Goat		#7074	5000	Cell signalling
anti-mouse	Horse		#7076	5000	Cell signalling
anti-human	Goat			5000	Sigma

2.5 Ribonucleoprotein-mediated CRISPR-Cas9 gRNA delivery to primary myeloid cells

In order to obtain gene KO in primary monocytes or MDM we used Ribonucleoprotein (RNP)-mediated CRISPR-Cas9 gRNA delivery. To target specific gene of interest (SFXN3, FOLR2) we used predesigned crRNA sequences https://eu.idtdna.com/site/order/designtool/index/CRISPR_PREDESIGN, provided by Integrated DNA Technologies (IDT). For each gene we used three different crRNA targeting different coding region.

Before each experiment a freshly isolated human monocytes were activated with 25 ng/mL of CSF-1 and cultured in complete medium without antibiotic. In case of experiment on monocytes, cells were used 16h after isolation. For mature MDM, cells were allowed to grow for 5-6 days in medium with CSF-1. At the day of electroporation, RNP complexes were prepared, according to protocol provided by IDT and Thermo Fisher. Briefly, crRNA and tracrRNA were reconstituted in IDTE buffer (IDT, USA). Then crRNA:tracrRNA duplexes were mixed in equimolar concentrations, followed by heating at 95°C for 5 min. Generated duplexes (gRNA) were used freshly, or were stored at -20°C for up to 6 months. Then each gRNA was mixed with Cas9 protein at a 1:1.2 molar ratio and incubated at 37°C for 15-20 min. Afterward obtained RNP complex was moved to RT. In the meantime, cells for electroporation were detached, washed with PBS, counted by haemocytometer and resuspended in buffer T (monocytes) or buffer R (mature MDM) at desired quantity. Usually from 1-5 × 10^6 cells were used per 100µl Neon electroporation tip. Afterwards, RNP complex and cells were mixed together, aspirated by Neon Tip and electroporated by Neon Transfection System, using 1900V, 20ms, single pulse. Following electroporation cells were plated in 12-

well plate at 1 × 10^6c/mL in 1mL of medium and placed in cell culture incubator. 90 min later, old medium was replaced to remove traces of electroporation buffer. Afterwards, cells were cultured for 4-5 days, before analyzing effectiveness of gene KO.

2.6 RNAseq analysis

RNAseq analysis was performed to detect differentially expressed genes in CSF-1 activated MDM, upon a treatment with TNF (that was previously shown to abrogate 6-25 target expression, as measured by FC).

2.6.1 RNA isolation and quality control

Total RNA from CSF-1 activated MDM (5 control and 5 TNF treated groups) at day 8 of culture were isolated using Direct-zol™ RNA MiniPrep (Zymo Research, France), according to manufacturer instruction and stored in -80°C until further processing. Before sequencing, quality control of RNA was performed with Fragment analyzer (Agilent) and concentration of the RNA was evaluated using Ribogreen.

2.6.2 RNA sequencing

Total RNA after quality control was subjected to: purification of mRNA, temperature fragmentation, generation of cDNA by reverse transcription, adapter ligation and indexing and finally amplification. Next RNA library was sequenced using NextSeq 550 Illumina system, with 2 × 75bp paired-end reads and 25M reads per sample.

2.6.3 Differential gene expression (DGE) analysis

Raw data after sequencing was subjected to normalization and batch corrections with ComBat algorithm (sva R package). Generated datasets were then collapsed using Fred's Softwares algorithm. A pathway-centric approach using SES was then applied based on four curated databases from Fred's Softwares: KEGG, Reactome (reactome_2018803), Gene OntologyCellular Component (C5_CC), and MSigDB Hallmarks (H. Fred's Software source codes and databases are available at: https://sites. google.com/site/fredsoftwares/products. A gene-centric approach was applied to identify DEGs using limma R package with a p-value of 0.05.

2.7 IP-MS validation of 6-25 target

To re-identify protein recognized by 6-25 mAb, IP-MS approach was applied.

2.7.1 Immunoprecipitation

For IP, CSF-1 activated MDM at day 8 of the culture were taken. ~ 15 × 10^6 cells per sample were used. Expression of 6-25 target was confirmed each time, using FC. At day 8 of culture, cells were washed with PBS and subsequently lysed with RIPA buffer supplemented with Benzonase (2mM) and protease inhibitors (Roche), for 15 minutes at 4°C. Cell lysates were centrifuged at 10000g for 15 min at 4°C. Supernatants were collected and protein concentration was evaluated with BCA assay. 1,5mg of supernatant with concentration of 1mg/mL was mixed with 10µg of 6-25 antibody (6-25 condition) or isotype control antibody (IC condition) and incubated O/N at 4°C on the rocker. Next day samples were mixed with 0.5 mg of Pierce Protein A Magnetic Beads and incubated further for 4 h at 4°C on the rocker unit. Subsequently magnetic beads were washed 5 times with RIPA buffer (with 0,25x detergent content), re-suspended in 30µl of ×4 Laemmli Sample Buffer (Bio-Rad #161-0747: 62.5 mM Tris-HCl, pH 6.8, 10% glycerol, 1% LDS, 0.005% Bromophenol Blue), incubated for 30 min in 37°C and subsequently frozen in -20°C before further processing.

2.7.2 Protein digestion and MS analysis

For mass spectrometry analysis, samples immunoprecipitated with 6-25 antibody (6-25 condition) or isotype control antibody (IC condition), prepared in quadruple biological replicates for each condition, in 30µl of ×4 Laemmli buffer, were reduced with 1M DTT (to final conc. of 25 mM) during 30 min at 56°C under agitation, cooled to room temperature and alkylated with 1M iodoacetamide (to final conc. 60 mM) during 30 min in the dark. Each reduced/alkylated protein sample was then digested using the S-Trap™ Mini spin column protocol [225]. Briefly, equivalent volume of 10% SDS were added to each sample in order to reach 5% SDS final concentration. Undissolved matter was removed by centrifugation for 8 min at 13,000g. 12% aqueous phosphoric acid was added at 1:10 to the protein sample for a final concentration of ~1.2% phosphoric acid followed by seven volumes of S-Trap binding buffer (90% methanol, 100 mM TEAB, pH 7.1). After gentle mixing, the protein solution was loaded onto an S-Trap filter in several times, each separated by a 4,000 g centrifugation step until all the SDS lysate/S-Trap buffer has passed through the column. Afterwards, the captured proteins were washed six times with 400 µL S-Trap binding buffer. Digestion was performed for 1h at 47°C and then over-night at 37°C by addition of 125 µL of trypsin (Sequencing Grade Modified Trypsin, Promega) at 8ng/µL in 50 mM ammonium bicarbonate. The digested peptides were eluted by addition of 80 µL of 50 mM ammonium bicarbonate and 1 min centrifugation at 4,000 g followed by 80 µL of 0.2% formic acid and 4,000 g centrifugation (1 min) and finally 80 µL of 50%

aqueous acetonitrile containing 0.2% formic acid and a last 1 min centrifugation step at 4,000 g. The pooled eluates were dried down, resuspended with 17µl of 0.05% trifluoroacetic acid (TFA) in 2% acetonitrile (ACN) and sonicated for 10 min before analyzing by online nanoLC using an UltiMate® 3000 RSLCnano LC system (ThermoScientific, Dionex) coupled to an Orbitrap Fusion™ Tribrid™ mass spectrometer (Thermo Scientific, Bremen, Germany) operating in positive mode. Five microliters of each sample were loaded onto a 300 µm ID × 5mm PepMap C18 pre-column (Thermo Scientific, Dionex) at 20 µL/min in 2% ACN, 0.05% TFA. After 3 min of desalting, peptides were on-line separated on a 75 µm ID × 50 cm C18 column (in-house packed with Reprosil C18-AQ Pur 3 µm resin, Dr. Maisch; Proxeon Biosystems, Odense, Denmark) equilibrated in 90% of buffer A (0.2% formic acid (FA)), with a gradient of 10 to 30% of buffer B (80% ACN, 0.2% FA) for 100 min then 30% to 45% for 20 min at a flow rate of 300 nl/min. The instrument was operated in data-dependent acquisition (DDA) mode using a top-speed approach (cycle time of 3 s). Survey scans MS were acquired in the Orbitrap over 350–1400 m/z with a resolution of 120,000 (at 200 m/z), an automatic gain control (AGC) target value of 4e5, and a maximum injection time of 60 ms. Most intense multiply charged ions (2+ to 6+) per survey scan were selected at 1.7 m/z with quadrupole and fragmented by Higher Energy Collisional Dissociation (HCD). The monoisotopic precursor selection was turned on, the intensity threshold for fragmentation was set to 25,000 and the normalized collision energy was set to 28%. The resulting fragments were analysed in the Orbitrap with a resolution of 30,000 (at 200 m/z), an automatic gain control (AGC) target value of 5e4, and a maximum injection time of 54 ms. Dynamic exclusion was used within 60 s with a 10 ppm tolerance, to prevent repetitive selection of the same peptide. For internal calibration the 445.120025 ion was used as lock mass.

2.7.3 MS-based protein identification and label-free quantification

Acquired MS and MS/MS data as raw MS files were converted to the mzDB format [226] using the pwiz-mzdb converter (version 0.9.10, https://github.com/mzdb/pwiz-mzdb) executed with its default parameters. Generated mzDB files were processed with the mzdb-access library (version 0.7, https://github.com/mzdb/mzdb-access) to generate peaklists. Peak lists were searched against Swiss-Prot protein database with *homo sapiens* taxonomy (20,385 sequences) in Mascot search engine (version 2.7.0, Matrix Science, London, UK). Cysteine carbamidomethylation was set as a fixed modification and methionine oxidation as variable modification. Up to two missed trypsin/P cleavages were allowed. Mass tolerances in MS and MS/MS were set to 10 ppm and 20 mmu, respectively. Search results were validated

with a peptide rank=1 and at 1 % FDR both at PSM level (on Adjusted e-Value criterion) and protein sets level (on Modified Mudpit score criterion) using the in-house-developed Proline software version 2.1.2 [226].

For label-free relative quantification across samples, raw MS signal extraction of identified peptides was performed using Proline. The cross-assignment of MS/MS information between runs was enabled (it allows to assign peptide sequences to detected but non-identified features). Each protein intensity was based on the sum of unique peptide intensities and was normalized across all samples by the median intensity. To eliminate false-positive hits from quantitation of low intensity signals, following filters are applied on proteins: the minimum number of values identified by MS/MS (in whole experiment) was set to 2 and the minimum percentage of defined values (in one condition) was set to 50%. After independently replacing missing values for each run with the Gaussian method (random drawing around the median of the intensity values for each protein in a same condition), data were log2-transformed. For pairwise comparison, an unpaired two-tailed Student's t-test was performed and proteins were considered significantly enriched when their absolute log2-transformed fold change was higher than 1 and their p-value lower than 0.05. Volcano plots were drawn to visualize significant protein abundance variations between the two compared conditions. They represent -log10 (p-value) according to the log2 ratio.

3 Study I) specificity of the 6-25 antibody

The 6-25 antibody was developed with the purpose to selectively target pro-tumoral TAM. While the initial experiments confirmed the specificity of antibody toward TAM, not much was known about potential expression of the 6-25 target – SFXN3, on the other cells types. Because SFXN3 is a ubiquitous inner, membrane mitochondrial protein, that for an unknown reason was detected on the surface of subtype of macrophages, we had to use unsupervised approach in further study of the 6-25 mAb specificity. We decided to confirm the previous results on specificity of the antibody and further complement them with analysis of other cell populations present in the blood, including neutrophils or activated version of T-cells. Additionally, we optimized protocol for monocyte-derived macrophage (MDM) culture, to further study expression pattern of the 6-25 target. Finally, we continued the screening of the various cell line with the 6-25 mAb. Apart from giving us more information about the specificity of the 6-25 mAb, the cell line with high expression of the 6-25 target, could serve as an important tool to study the role of the 6-25 target, especially as at that time we were unable to obtain SFXN3 KO in primary NLC or MDM.

3.1 Specificity of the 6-25 antibody toward primary blood cells

Initial studies on the 6-25 antibody, showed that it specifically binds to NLC generated in vitro, without targeting CLL B-cells (Fig. 1A) and normal human PBMC (Fig. 1B), besides slight affinity to monocytes. Additionally, staining with the 6-25 antibody was tested on various cell lines (Fig. 1C), showing no specificity, with exception of weak staining on the MV4-11 cell line. Finally, staining of sections from human tumors with 6-25 antibody, suggested that the antibody can also recognize TAM from different human malignancies (Fig. 1D).

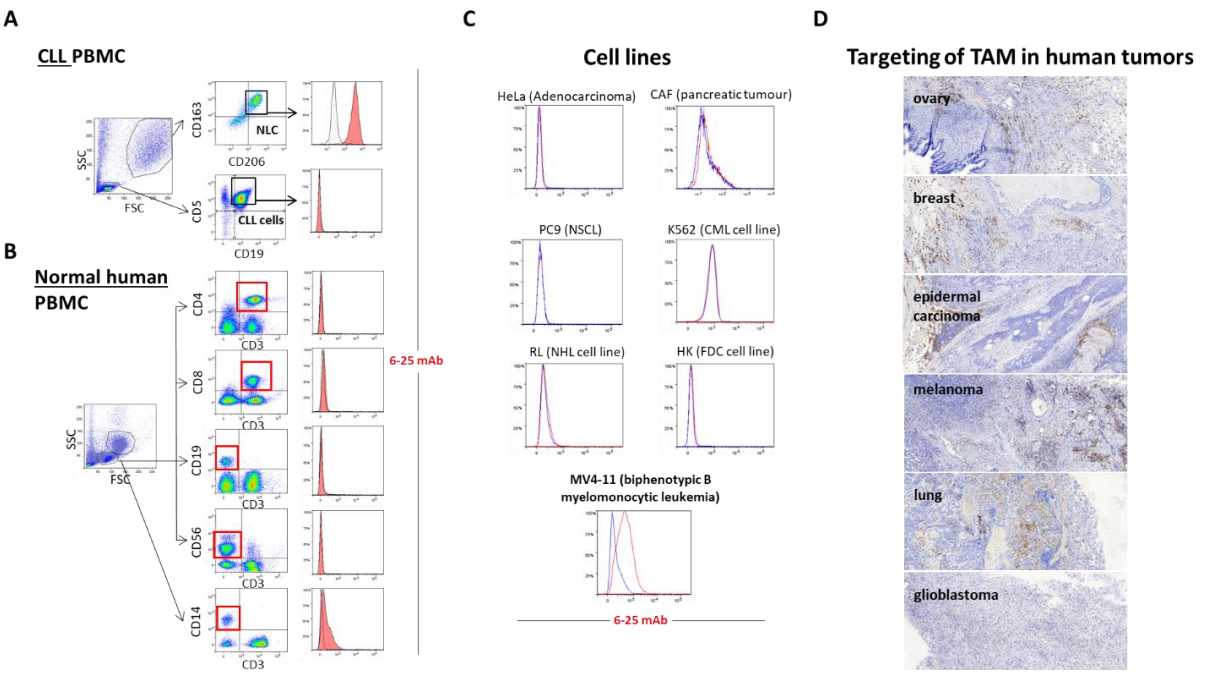

Figure 1. Initial evaluation of 6-25 mAb specificity*. A) flow cytometry analysis of NLCs (CD163⁺, CD206⁺) and CLL cell (CD5⁺, CD19⁺). B) flow cytometry analysis of normal human PBMC: T (CD4⁺ and CD8⁺) and B (CD19⁺) lymphocytes, NK cells (CD56⁺) and monocytes (CD14⁺); C) and various human cell lines. For histogram plot red represents 6-25 and blue isotype signal respectively. D) Immunohistochemistry of tumour biopsies. Hematoxylin – blue staining; 6-25 mAb – brown staining.*

In this part of the project we wanted to further study the specificity of the antibody toward both primary cells and established in vitro cell lines.

First, we have tested staining with the 6-25 mAb on monocytes from CLL patients (Fig. 2A and 2B). Depending on the patient (Fig. 2B) we detected a lack of or dim signal with the antibody, similarly to staining on normal human monocytes (Fig. 1B). Additionally, we performed the staining on normal human neutrophils (Fig. 2C), detecting no signal from the antibody. To be sure that the 6-25 target is not expressed following cell activation (as in the case of monocytes, that upregulate expression of the 6-25 target while differentiating into TAM), we tested staining with 6-25 antibody on primary γδ T cell lines. These cells were obtained by activation with phosphoantigen and IL-2 of naïve γδ T lymphocytes, isolated from normal human PBMC. No staining was detected with the 6-25 mAb on these activated γδ T cells (Fig. 2D).

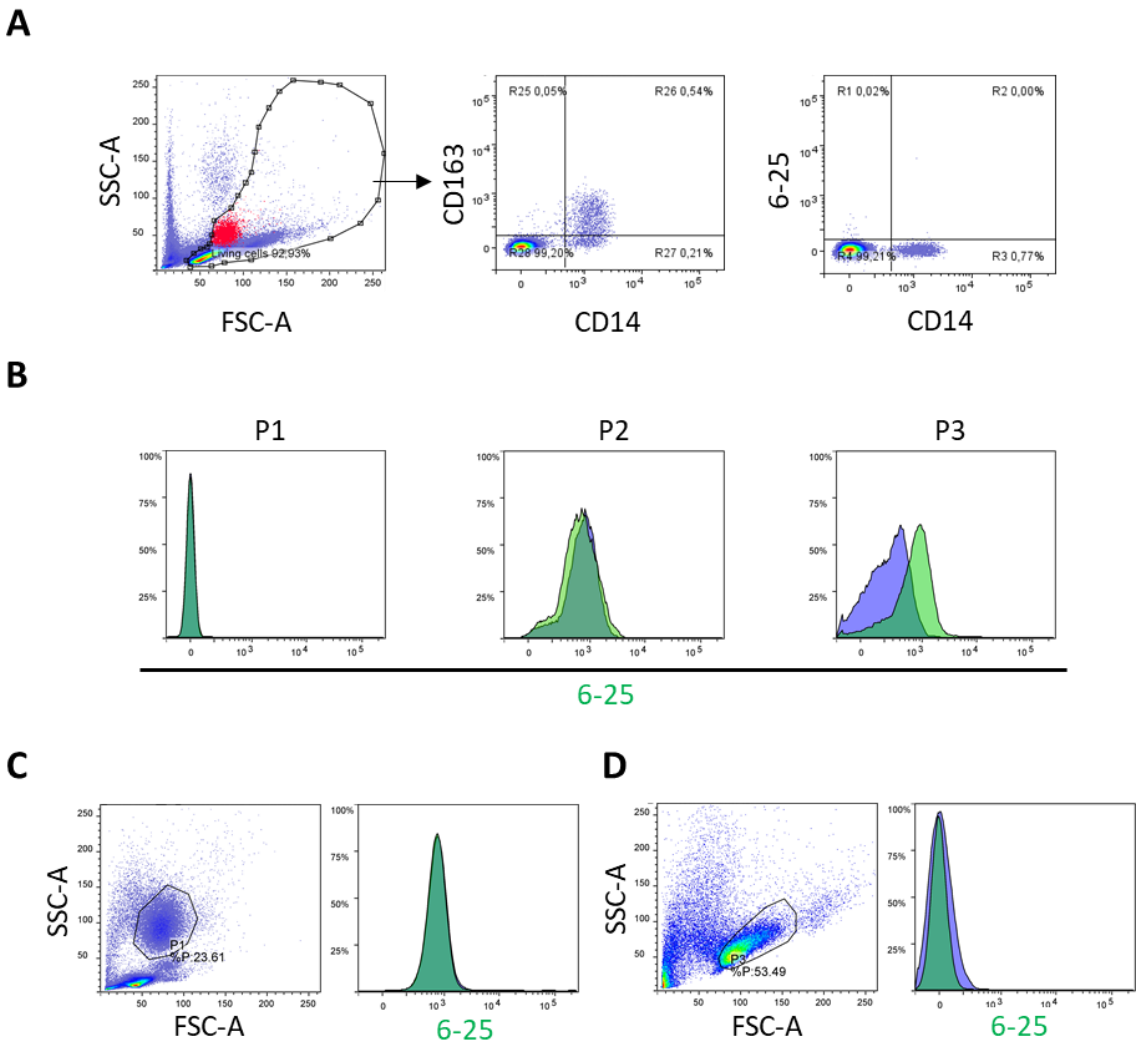

Figure 2 The 6-25 mAb FC analysis of primary human cells. *A) FC analysis of monocytes from CLL PBMC, gating strategy based on CD14 expression (red color on FSC/SSC dotplot depict monocytes after backgating on CD14⁺). Exemplary dotplots representing CD163 and 6-25 staining on CD14+ monocytes. B) FC analysis of 6-25 mAb signal of monocytes from PBMC of three different patients (P1-P3), histogram plots represents 6-25 signal on CD14⁺ gated cells. C) representative FC plots of normal human neutrophils gated based on SSC/FSC difference (D) primary γδ T cell line.*

3.1.1 Expression of the target on autologous NLC, NLC from patient after relapse and heterologous NLC.

NLC represented the main model to study 6-25 mAb in vitro. During our study, we routinely tested the 6-25 staining on NLC derived from various patient samples. By that, we wanted to better characterize

consistency of the 6-25 target expression on these cells, also in relation to other myeloid cell markers. In order to do that, we cultured the CLL PBMC for 14 days and subsequently analyzed the phenotype of the NLCs by flow cytometry (Fig. 3).

For the most part, NLCs gated based on SSC-FSC showed high and uniform expression of 6-25 target (Fig. 3A). It was consistent with upregulation of typical M2 markers of NLC, including: CD163, CD206 and CD14. However, in some cases more heterogeneous, dim or even lack of expression of the 6-25 target of NLC was observed (Fig. 3B). In some cases, gating of NLC based on CD163 and CD206 markers, allowed to distinguish 3 main subpopulations of cells with varying expression of 6-25 target, that was positively correlated with CD163 and CD206 markers (Fig. 3C). Heterogeneity of the 6-25 target expression was further confirmed by confocal microscopy analysis with 6-25 and CD163 co-staining (Fig. 3D). In most cases co-expression of CD163 and 6-25 target on NLCs was observed (Fig. 3D, left picture), but sporadically presence of $CD163^{+}$ and $6\text{-}25^{-}$ was detected (Fig. 3D, right picture). These results suggested that the 6-25 target can be specific to only subpopulation of NLCs and is preferentially co-expressed on more M2-like cells.

CLL PBMC samples for the project were generally taken from untreated patients. Hence, we wanted to confirm that NLC generated from PBMC from patients after relapse can also be recognized by 6-25 mAb. This would be especially important in case of evaluation of therapeutic potential of 6-25 mAb. NLC generated from patient, after relapse from classical fludarabine, cyclophosphamide and rituximab (FCR) therapy, were prepared in the same fashion as before and analyzed by FC (Fig. 3E). Flow cytometry confirmed expression of the 6-25 target on NLCs from this patient.

NLCs can be also generated by co-culture of HD monocytes with isolated CLL cells (heterologous culture). Previous results of the group, confirmed that heterologous NLCs are characterized by similar expression of the surface markers and ability to rescue CLL cells from spontaneous apoptosis in vitro as NLCs from autologous culture. So far they were not analyzed for expression of the 6-25 target though. Exemplary flow cytometry analysis of heterologous NLC (Fig. 3F), revealed that these cells also show expression of the 6-25 target.

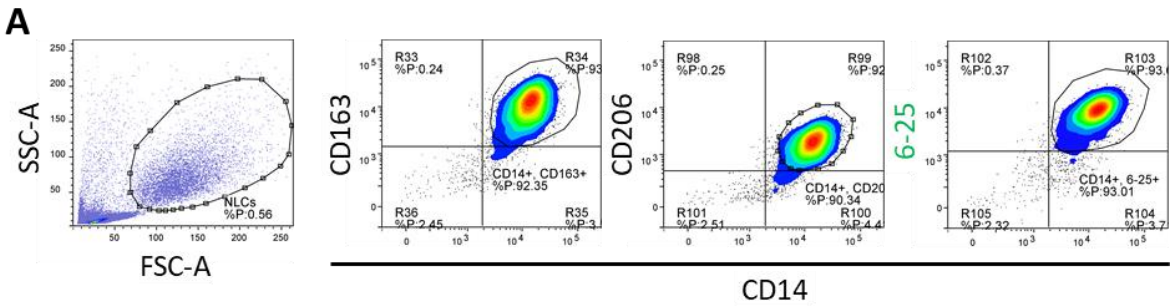
A
SSC-A
FSC-A
NLCs
%P:0.56
CD163
CD14+, CD163+
%P:92.35
CD206
CD14+, CD20
%P:90.34
6-25
CD14+, 6-25+
%P:93.01
CD14

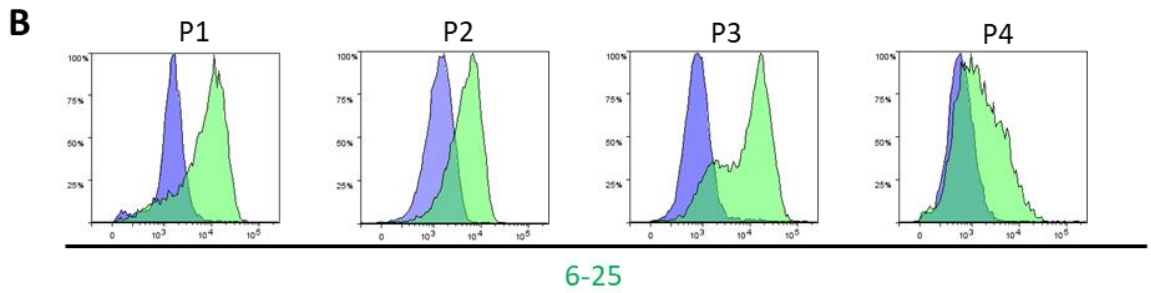
B
P1
P2
P3
P4
6-25

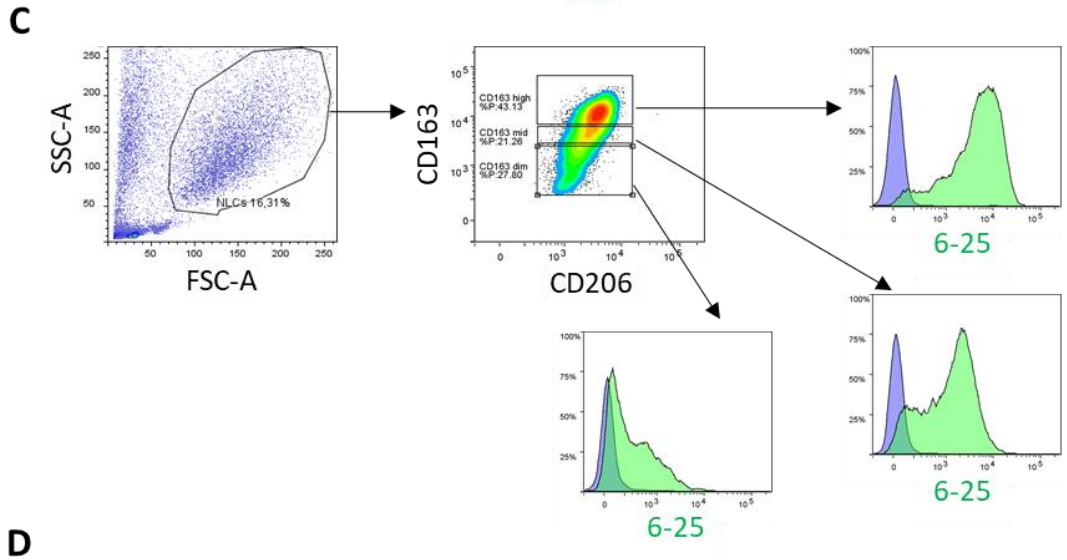
C
SSC-A
FSC-A
NLCs 16,31%
CD163
CD163 high
%P:43.13
CD163 mid
%P:21.26
CD163 dim
%P:27.80
CD206
6-25
6-25
6-25

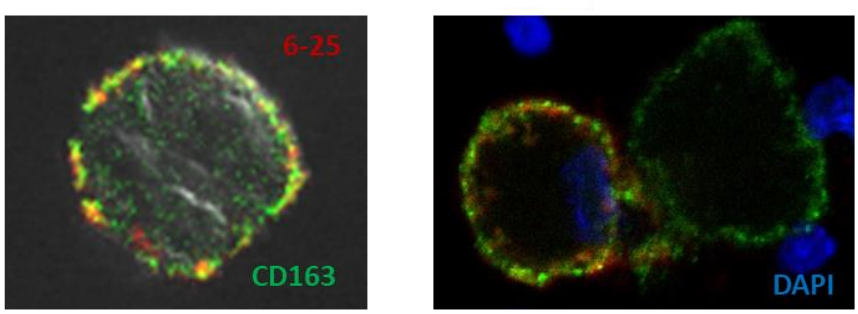
D
6-25
CD163
DAPI

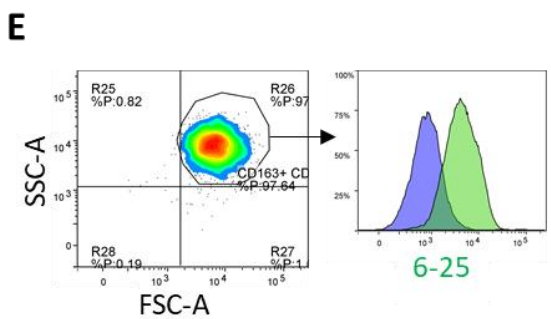
E
SSC-A
FSC-A
CD163+ CD
%P:97.64
6-25

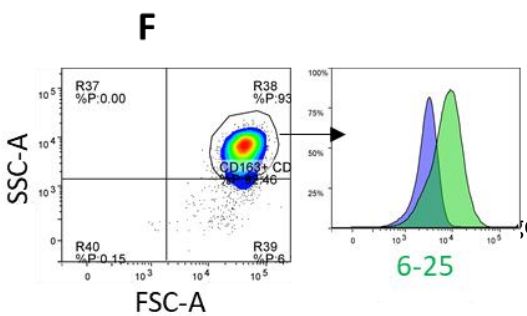
F
SSC-A
FSC-A
6-25

Figure 3. Expression of 6-25 target on NLCs. *A) FC analysis: NLCs were gated based on SSC-A and FSC-A parameters and further classified based on expression of CD14, CD163, CD206. B) FC analysis of 6-25 mAb signal on NLCs generated from PBMC of four different CLL patients (P1-P4), histogram plots represents cells gated on CD163 and CD206. C) Detailed analysis of the 6-25 signal in different subpopulation of NLCs. D) Confocal microscopy analysis of NLC: green – CD163, red – 6-25, blue – DAPI. FC analysis of 6-25 staining on NLC generated from PBMC of patient after relapse and F) NLCs from heterologous co-culture of normal human monocytes with CLL cells.*

In conclusion, autologous and heterologous NLCs generated in vitro, showed high expression of the 6-25 target, which was consistent with the presence of typical M2 markers, like CD163 and CD206. The difference in the expression of the 6-25 target and its potential connection with the functionality on NLC is described in the "chapter 4, study II" of this thesis.

3.2 Screening of AML cell line with the 6-25 antibody

In our work we were interested in finding the cell lines that would express the 6-25 target on their surface, which we could further use as a model to study this molecule in vitro. As previous results showed a dim staining with the 6-25 mAb on MV4-11 cell line (Fig. 1C), we continued to analyze other myeloid cell lines, in particular of acute myeloid leukemia (AML) origin. We included: U-937, THP-1, OCI-AML-13, MOLM-14, U-373 cell lines in the screening, and used MV4-11 cells as a positive control. Results presented on the fig. 4, show no targeting of OCI-AML-3 and U-373 cell lines with the 6-25 antibody. On the other hand, in case of U-937, MOLM-14 and THP-1 cell lines we detected a dim staining with the antibody, that in case of U-937 was comparable with MV4-11.

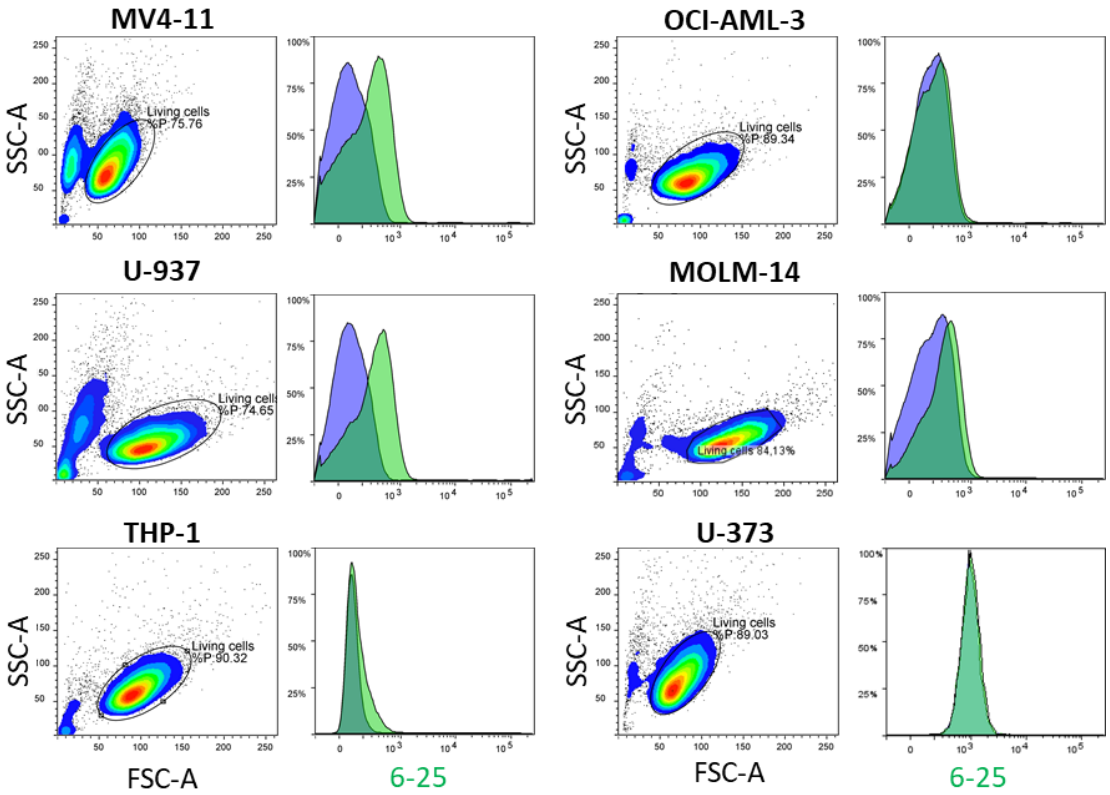

Figure 4. Flow cytometry analysis of the staining of AML cell lines with 6-25 mAb. *Representative FC staining of MV4-11, U-937, THP-1, OCI-AML-13, MOLM-14 and U-373 cell lines. For histogram plots green represents 6-25 and blue IC signal respectively.*

As THP-1 cell line is often used as a model of macrophage differentiation, we attempted to upregulate expression of 6-25 target on these cells, by stimulation with PMA and further M2 polarization with IL-4. In the end however, differentiation of the cells failed to lead to any changes in the expression of the 6-25 target (data not shown).

Additional screening of the AML cell lines, revealed that U-937, MOLM-14 and THP-1 cells are capable of expressing the 6-25 target, with U-937 cells showing comparable staining to MV4-11 cells. These results open a possibility to target AML cells with the 6-25 mAb. While the staining of these cell lines with the 6-25 mAb is nowhere near as high as in case of NLC, there are examples of successful biological therapies where target cell express low level of antigen, including anti-CD20 targeting in CLL [227,228]. Moreover, AML represents a disease with poor overall prognosis and requires finding of a new markers that could improve therapeutic outcome in the future [229]. To pursue this path, it would be also important to evaluate 6-25 mAb staining of primary samples from AML patient.

3.3 Modulation of the 6-25 target in human monocyte-derived macrophages (MDM)

After confirming specificity of 6-25 antibody toward TAM, we wanted to study how to induce and modulate expression of 6-25 target in vitro. However, CLL PBMC model with its relative complexity was not suitable for the task. Moreover, working with the primary cells from CLL patients holds some disadvantages, including high variability of 6-25 target expression, overall low yield of NLCs and time-consuming experiments. Since we did not find a cell line with 6-25 expression comparable to NLCs that could also mimic functionality of these cells, we decided to develop and optimize primary human monocyte-derived macrophage (MDM) model. To obtain maximum information we tested various protocols of MDM differentiation and polarization. We evaluated polarization of macrophages, analyzing various surface markers by flow cytometry and comparison of morphology of the cells by bright-field microscopy.

3.3.1 Expression of the 6-25 target by MDM – effect of CSF-1, IL-34 and GM-CSF

As a starting point of the MDM protocol optimization, we decided to evaluate the effect of CSF-1 and GM-CSF, two of the most important cytokines inducing monocyte differentiation to macrophages [230]. As in the literature there is a lot of confusion involving the role of CSF-1 and GM-CSF itself on the polarization of macrophages [231–233], we decided to optimize protocol, that would allow us to obtain M1 and M2 MDM. First we checked the influence of CSF-1 and GM-CSF alone, on the morphology and phenotype of macrophages. In order to do that we isolated monocytes from HD PBMC and activated them with CSF-1 or GM-CSF. After 8 days of culture we analyzed the cell by flow cytometry (Fig. 5A).

Analysis of MDM obtained from CSF-1 activated monocytes showed high expression of M2 markers – CD163, CD206, but also CD14, CD16, CD64 and HLA-DR. In comparison, GM-CSF stimulated cells showed no expression of CD163, decreased level of CD206, CD14, CD16, but increased expression of CD86 (typical M1 marker). Interestingly, CSF-1, but not GM-CSF led to upregulation of the 6-25 target. Since CSF-1 action stimulated expression of the 6-25 target, we wanted to see, if IL-34 – second ligand of CSF1R (CD115) would have similar effect. We activated monocytes with IL-34 in analogical way to CSF-1 and GM-CSF and analyzed the cells by flow cytometry. Flow cytometry analysis revealed that, IL-34-activated cells were characterized with high expression of CD163, CD206, HLA-DR, and the 6-25 target, thus resembling CSF-1 activated MDM, but with higher expression of CD115, CD86 and decreased expression of CD16.

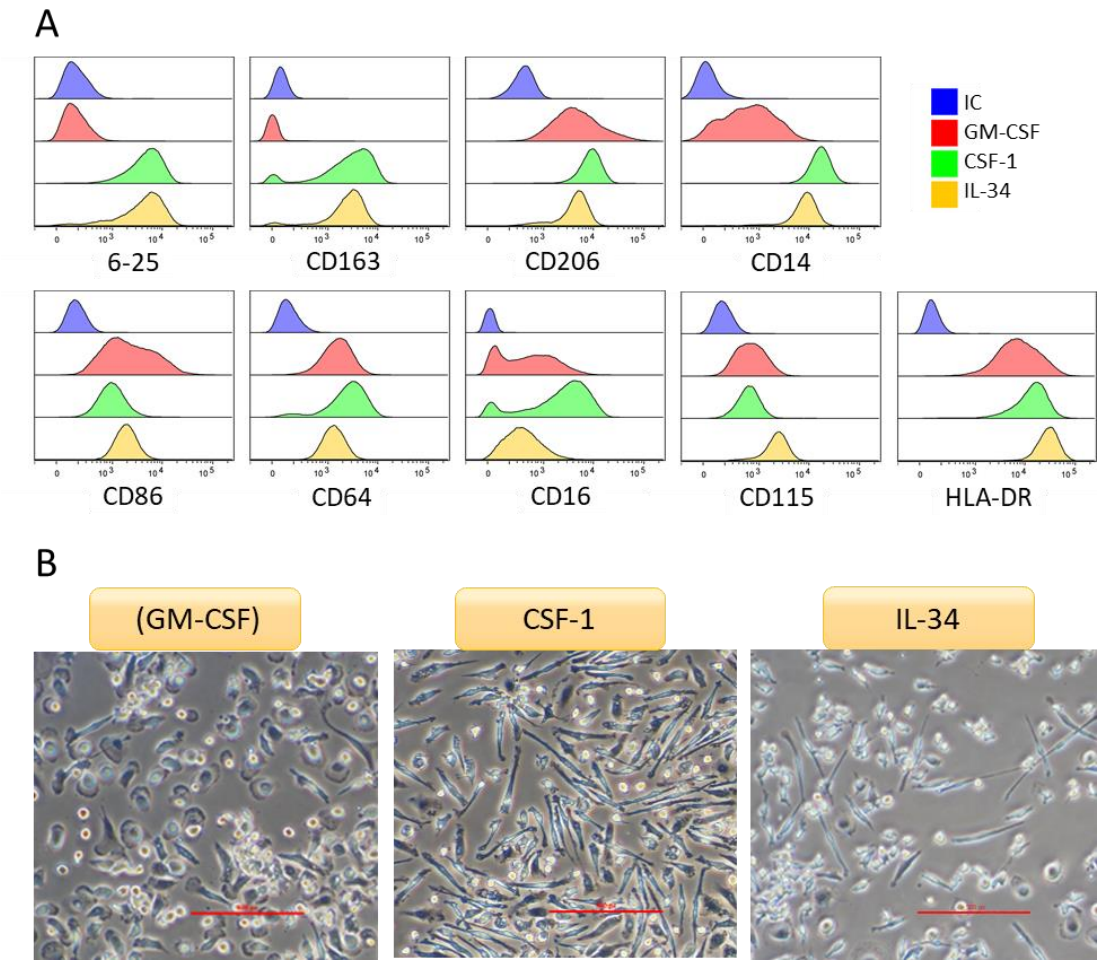

Figure 5. Influence of GM-CSF, CSF-1 and IL-34 on polarization state of MDM and expression of 6-25 target. *A) FC analysis representing histogram overlays between isotype control (blue) and GM-CSF (red), CSF-1 (green), IL-34 (yellow) activated MDM. B) Bright-field microscopy picture of MDM at day 8 of the culture, magnification = ×400.*

Further distinction between GM-CSF, CSF-1 and IL-34 on activation of the monocytes could be also observed in morphology of the cells (Fig. 5B), as GM-CSF activated cells showed more amoeboid shape, while CSF-1 activated cells were characterized by more elongated, spindeloid shape indicative of M2 macrophages [234,235]. IL-34 activation, also led to appearance of spindle-shape like cells, but with higher number of roundish cells that could suggest less mature phenotype [235]. Notion of less differentiated IL-34 activated cells is also supported by the flow cytometry, as these cells were characterized with smaller size and decreased granularity compared to cells stimulated with GM-CSF or CSF-1 (data not shown).

By comparing the effect of CSF-1, IL-34 and GM-CSF on the maturation of MDM we observed that indeed, GM-CSF activation resulted in macrophages with more M1-like phenotype, lacking expression of CD163,

decreased expression of CD206 and increase in the level of CD86. On the other hand, CSF-1 and IL-34 activated cells showed more M2-like phenotype, with high expression of CD163, CD206 and CD14. Additionally, activation with CSF-1 and IL-34 (as oppose to GM-CSF) led to comparable and high expression of the 6-25 target. These results suggest that CSF1R stimulation is necessary for upregulation of the target of the 6-25 antibody.

3.3.2 The 6-25 target is a specific marker of M2-like macrophages and is upregulated by CSF1R activation

Since the 6-25 target seemed to be preferentially expressed on M2-like macrophages, we wanted to further explore this hypothesis. In order to do that, we performed similar experiment to described in chapter 1.3.1, but additionally on day 6 we polarized cells with classical M1 agents (IFN-γ alone or in combination with LPS, added 18 h later) or M2 agents (IL-4 and IL-13) for 2 days. At the end of the maturation process, we collected the cells and analyzed their phenotype by flow cytometry. Results presented on fig. 6, show normalized expression of various myeloid surface markers in comparison to basal conditions ("naïve" macrophages, activated only with CSF-1).

Starting with the results of CSF-1 activated cells, IL-4/IL-13 treated group show moderate upregulation of CD163, 6-25 target, CD11b, CD11c, HLA-DR and strong upregulation of CD206 compared to basal conditions. On the other hand, IFN-γ led to: strong upregulation of CD64, CD86, HLA-DR, mild upregulation of CD11c; strong downregulation of CD163, CD16; moderate downregulation of CD14, CD11b, CD115 and only mild downregulation of CD206 and 6-25 target. Addition of LPS (IFN-γ + LPS condition) resulted in further downregulation of previously mentioned markers, with concomitant decrease of CD64 and CD11c.

In case of Il-34 activation, the effect of secondary polarization is weaker, as compared to CSF-1 activation. There are some interesting changes though, as IFN-γ causes abrogation of CD163 expression in CSF-1 activated cells, but in case of IL-34 cells cause slight upregulation of this marker. Also IL-4/IL-13 polarized, M(IL-34) cells show distinct phenotype, with downregulation of CD14, CD16, CD163, CD64, CD11b and CD11c and slight decrease to 6-25 target. Overall IL-34 activated cells show much higher expression of CD115 (CSF1R) compared with CSF-1 activated cells.

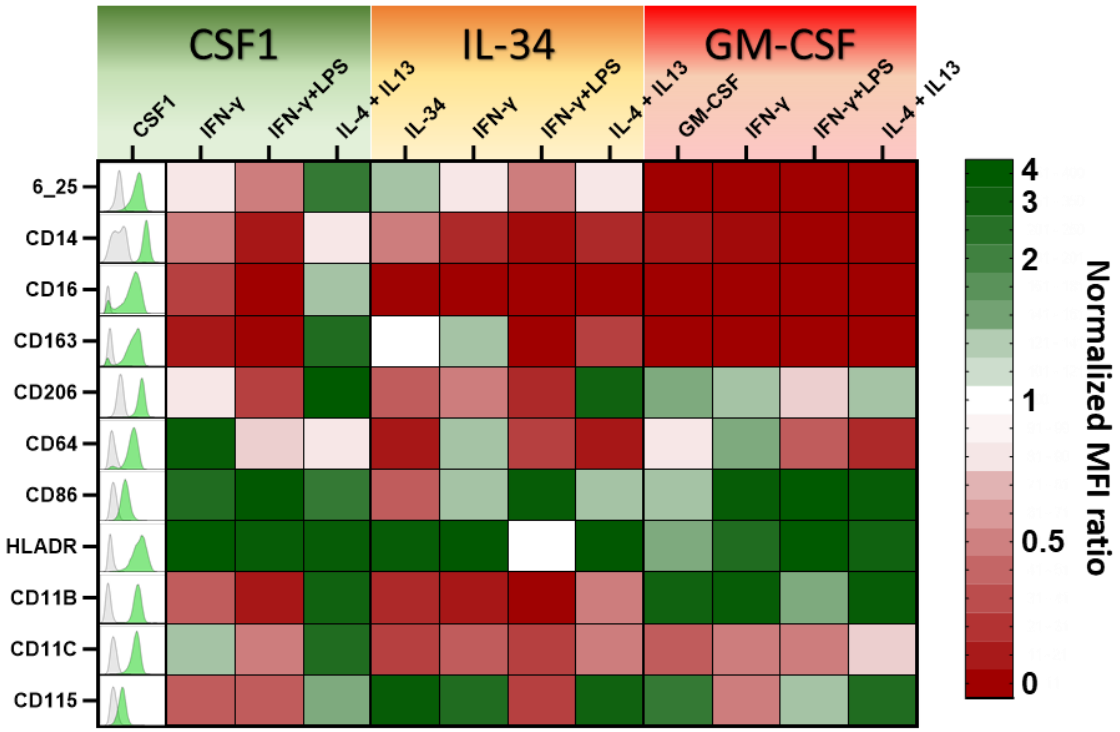

Figure 6. Influence of secondary M1 (IFN-γ or LPS) or M2 (IL-4, IL-13) polarization on expression of 6-25 target in CSF-1, IL-34 or GM-CSF activated MDM. *Heatmap plot with results of 2 independent experiments and MDM from 4 different donors in total. Data from FC analysis was processed as follow: median fluorescence intensity (MFI) ratio between signal from specific antibody and matching IC were calculated; MFI ratio values were normalized for each marker, within cells from each donor, and represented as percentage of basal condition's signal (MDM activated only with CSF-1); geometrical means of combined results were plotted on the heatmap. Green color represent upregulation (non-linear scale) and red color represents downregulation (each tic = 0.1 of basal signal) of each listed marker compared to basal condition. White color depicts signal of basal conditions. Representative histogram for CSF-1 showing basal expression of each tested marker (grey and green represents signal from isotype control and specific antibody respectively.*

Moving to GM-CSF activated macrophages, we observed the least changes upon secondary treatment with classical M1 and M2 agents. Irrespective of secondary stimulation, these cells did not express CD163 and 6-25 and showed very low expression of CD14 and CD16. Treatment with LPS led to slight decrease of the CD206 and CD64 expression, while IL-4 and IL-13 caused downregulation of CD64, and at the same time failed to upregulate CD206.

In conclusion, GM-CSF activated cells seemed to acquire a stable M1-like polarization state, with limited response to secondary treatment. On the other hand, both CSF-1 and IL-34 have similar M2-promoting effect on macrophages activation (at least regarding the expression of surface myeloid markers). At the same time, they maintained cell plasticity, as seen by the changes in MDM phenotype upon administration of M1 and M2 agents.

Regarding the effect of various treatments on 6-25 target expression, we confirmed that activation of CSF1R by either CSF-1 or IL-34 is necessary to induce expression of this molecule. While M2-polarizing agent, IL-4 and IL-13 (but also IL-10 and Dexamethasone – data not shown) can lead to further upregulation of 6-25 target in case of CSF-1 activated cells, they fail to do so in case of IL-34 and GM-CSF activated macrophages. Additionally, we observed overall downregulation of 6-25 target expression upon the treatment of MDM with M1-polarizing agents – IFN-γ and LPS. All these results strongly suggest that the 6-25 target could be categorized as a M2 marker of macrophages.

3.3.3 The 6-25 target expression is abrogated by TNF

The classical protocols usually suggest IFN-γ and LPS to generate M1 macrophages. While IFN-γ role is also indicated in cancerogenesis [236], the effect of LPS stimulation is more relevant in case of bacterial infection. As we were more interested in macrophage polarization in the context of cancer, we decided to evaluate the effect of TNF (another known M1-polarizing agent) on macrophage polarization. TNF has a very prevalent and ambiguous role in oncogenesis [18,237,238], but it was also shown as an important factor that "counterbalances emergence of M2 Tumor Macrophages" [232]. To study the effect of TNF on expression of 6-25 target, but also overall polarization state of macrophages we first performed a test, where we again treated monocytes with CSF-1 secondary M1 or M2-polarizing agents, but additionally challenged the cells with TNF from day 0.

Flow cytometry analysis of the macrophages treated with TNF, revealed changes in the maturation of the cells and subsequent response to classical M1 and M2 polarizing agents (Fig. 7). TNF led to an overall decrease in the expression of CD16, CD163 and CD206. In case of IL-4 polarized cells, we observed more pronounced response to TNF, compared to naïve macrophages (MDM activated only with CSF-1), with strong downregulation of CD16, CD163, CD206, CD14, CD64 but also partial upregulation of CD86. For IFN-γ stimulated cells, additional treatment with TNF led to further decrease of CD16 and CD206. Most strikingly, though, TNF caused also a complete abrogation of the 6-25 target expression in all of the tested conditions.

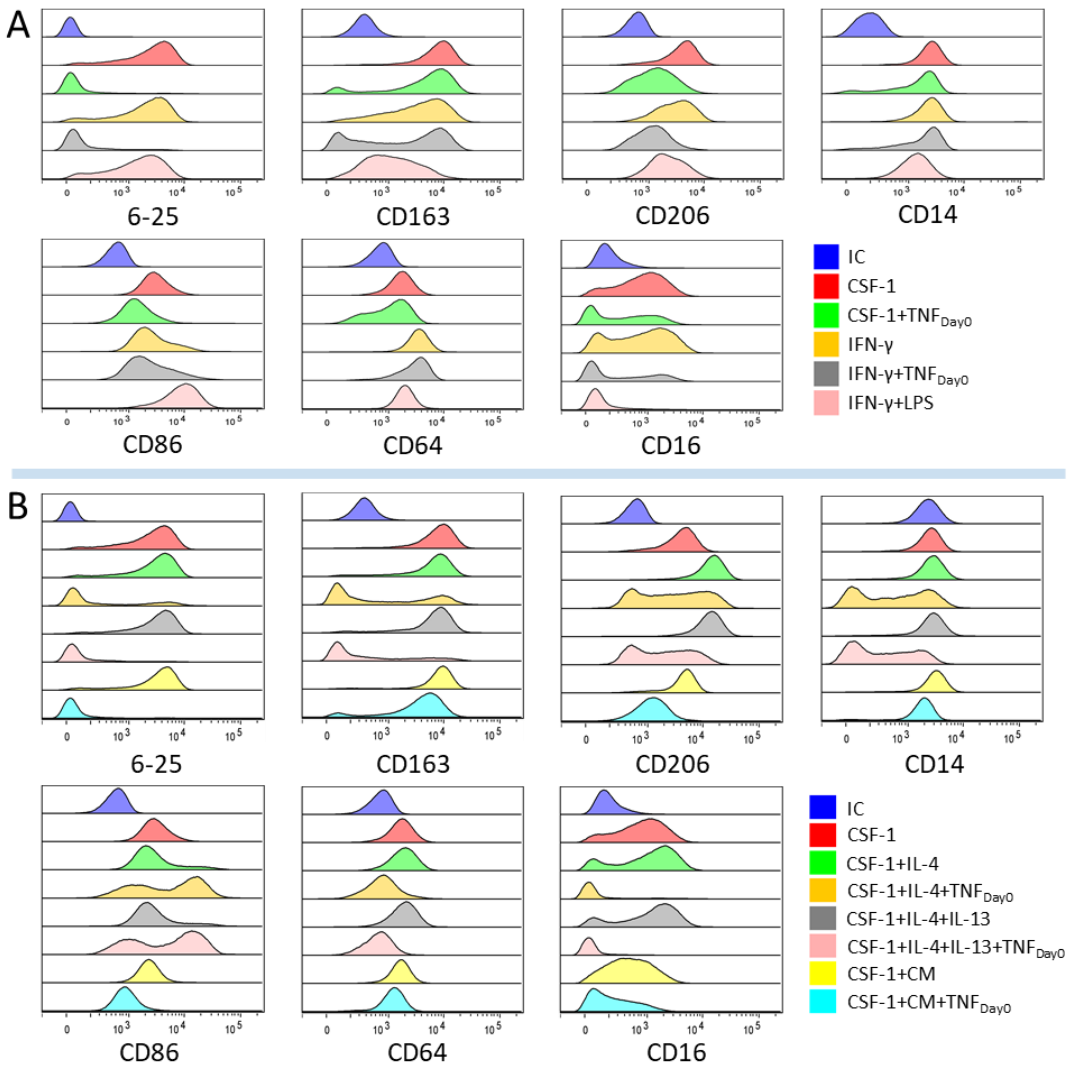

Figure 7. Effect of TNF on maturation and polarization of CSF-1 activated MDM, and expression of 6-25 target*. FC results represented as overlay histograms for each measured marker. A) effect of TNF on M1-polarization of MDM, B) effect of TNF on M2-polarization of MDM. Legends for panels A and B are depicted on the figure.*

Next we wanted to closer evaluate the effect of TNF on expression of the 6-25 target, also in cells initially activated with IL-34 or GM-CSF. Beside treatment at day 0, we also tested the effect of TNF when added from day 3.

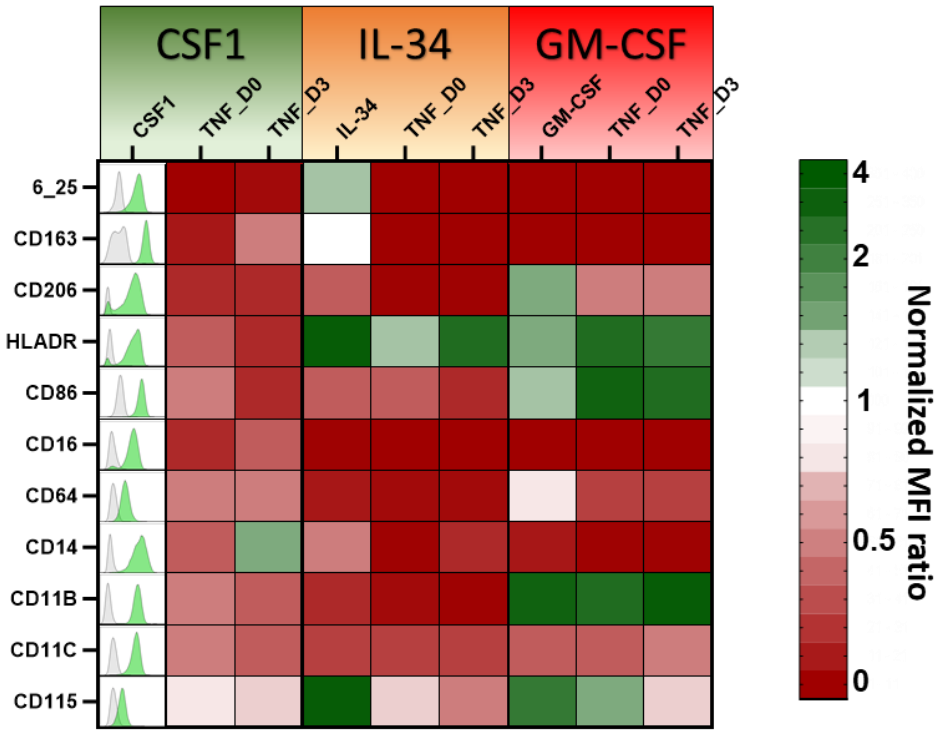

Figure 8. TNF blocks M2-polarization of macrophages induced by CSF-1 and IL-34, and abrogates expression of 6-25 target on MDM*. Heatmap plot with result of 2 independent experiments and MDM from 4 different donors in total. Data from FC analysis was processed as follow: median fluorescence intensity (MFI) ratio between signal from specific antibody and matching IC were calculated; MFI ratio values were normalized for each marker, within cells from each donor, and represented as percentage of basal condition's signal (MDM activated only with CSF-1); geometrical means of combined results were plotted on the heatmap. Green color represents upregulation (non-linear scale) and red color represents downregulation (each tic = 0.1 of basal signal) of each listed marker compared to basal condition. White color depicts signal of basal conditions. Representative histograms for CSF-1 column (grey – isotype control, green – specific antibody signal) show expression of each tested marker in basal conditions.*

Combined results of 2 independent experiments performed with MDM from 4 different donors (Fig. 8), revealed that TNF abrogated the 6-25 target expression in both CSF-1 and IL-34 activated cells when added at day 0 and day 3. It also strongly downregulated expression of most analyzed markers, especially M2-specific: CD163, CD206 but also CD16. On the other hand, TNF treatment showed benign effect on the GM-CSF activated cells, with slight upregulation of HLA-DR, CD86 and downregulation of CD206 and CD64, suggesting further enforcement of M1 polarization.

To further systematize the effect of M1-polarizing agents on the 6-25 target expression we decided to compare the effect of IFN-γ, LPS and TNF on polarization of CSF-1 activated cells. In the previous experiment, IFN-γ and LPS were added late in the process of cell maturation – at day 6, when the 6-25 target was already highly present on the surface of the cells. So this time, we evaluated the effect of the

M1-agents, when added at day 0 or 3. As previously, beside measurement of the 6-25 target we also controlled expression of other surface markers on macrophages. The difference in the effect of IFN-γ, LPS and TNF could be already appreciated by changes in the morphology of the cells, as shown with BF microscopy pictures (Fig. 9A). Overall, LPS treated cells were characterized with roundish morphology and weak attachment to the plastic. TNF treatment increased the proportion of the amoeboid cells. However, the most varied effect was observed in case of treatment with IFN-γ, as when added on: day 0 it led to appearance of elongated macrophages forming colony-like structures; day 3 elongated macrophages in network-like structures and on day 6 firmly attached, flatten amoeboid-like cells. Flow cytometry analysis of MDM phenotype also showed a difference between LPS, TNF and IFN-γ treated MDM, also depending on the time of the treatment (Fig. 9B). Starting from IFN-γ, it led to downregulation of: CD163, CD206, CD14, CD204, CD16 with a concomitant upregulation of CD64 and HLA-DR.

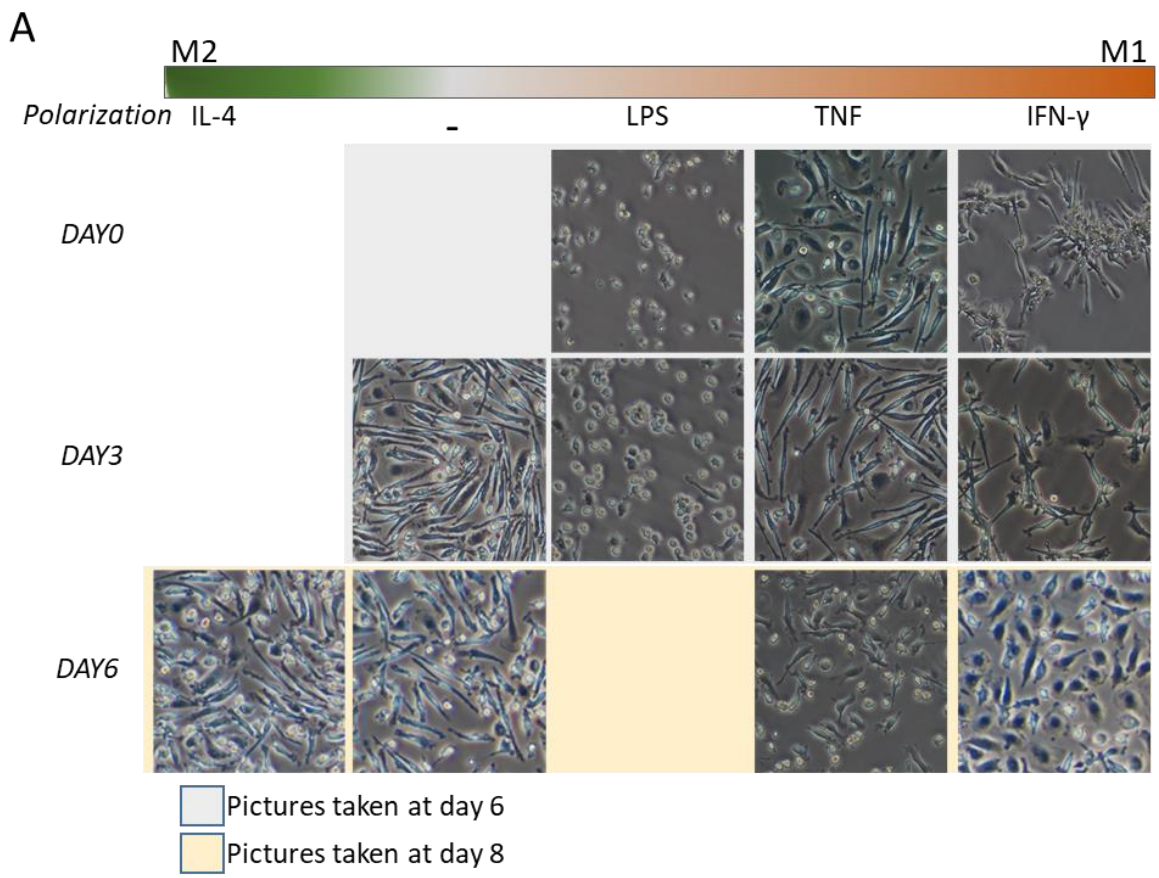

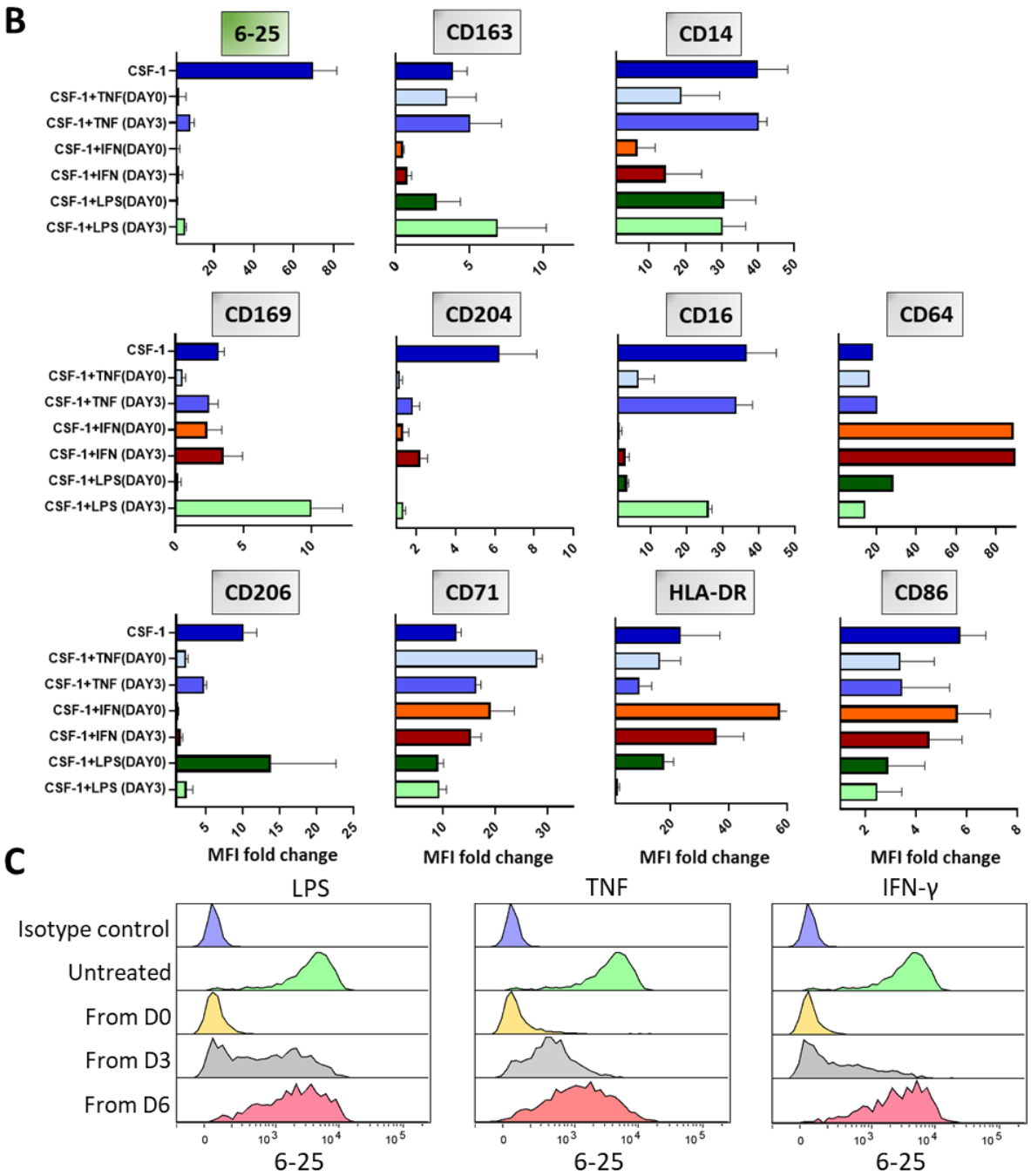

Figure 9. Distinct effect of M1 polarizing agents (LPS, TNF and IFN-γ) on phenotype of CSF-1 activated MDM. *A) Effect of LPS, TNF and IFN-γ administrated at day 0, 3 or 6 on morphology of MDM. IL-4 treated MDM at day 6 as a control of M2 phenotype. Analysis by BF microscopy at day 6 (grey) or 8 (yellow). Representation of M1-M2 spectrum of polarization, adapted from [230]. B) Comparison of MFI fold change of 6-25 target and various myeloid markers, in relation to the type and moment of treatment. Results are mean for 2 independent experiments and MDM from 4 different donors in total. C) Representative histogram plots, showing effect of LPS, TNF or IFN-γ on 6-25 target expression, depending on treatment time.*

Effect of LPS and TNF was less pronounced compared to IFN-γ, leading to downregulation of CD204, CD206 (beside LPS at day 0), HLA-DR (if added from day 3), CD86, CD16 (if added from day 0) and CD169 (if added from day 0). Additionally, LPS led to slight upregulation of CD206 (if added from day 0) and strong upregulation of CD169 (if added from day 3). While LPS, TNF and IFN-γ had various effects on the overall expression on both M2 and M1 macrophages markers, they all led to homogenous downregulation of the 6-25 target expression. This effect was stronger, the earlier the administration of one of the M1 agents (Fig. 9C).

In the end, we observed that LPS, TNF and IFN-γ lead to distinct M1 phenotypes of MDM, as in accordance with official guidelines of macrophages polarization [230]. We confirmed also that all three pro-inflammatory agents have similar effect on downregulation of 6-25 target.

3.3.4 Conclusions

Experiments performed in this chapter showed that the 6-25 target is driven by CSF1-R signaling and can be induced either by CSF-1 or IL-34. Expression of the 6-25 target can be further increased by M2-polarizing agents like IL-4, IL-13, IL-10 or Dexamethasone, but these agents alone do not induce its expression. Next, we have shown that the 6-25 target is a specific M2 marker of macrophages and its level is downregulated by M1-polarizing agents like LPS, TNF or IFN-γ.

We are aware that these analyses are not a definitive study of polarization state of human MDM, which would require additional analyses of: level of intracellular markers, including Arg1, iNOS, IDO; activity of transcriptional factors, like STAT1, STAT3 and STAT6; expression of specific cytokines [230]; phagocytosis index [239] or ability of macrophages to suppress T cell responses [240]. Nevertheless, they allowed us to obtain a reliable model of the 6-25 target expression, and showed overall effect of most common polarization agents on the level of 6-25 target expression, also in relation to other myeloid markers.

4 Study II) The 6-25 target – a marker of protective NLC

After we confirmed the specificity of the 6-25 antibody and explored expression pattern of the 6-25 target in MDM, we decided to turn back, to CLL PBMC model. As this model contains another layer of complexity – notably cancer cells, that can mimic interaction of malignant cells with NLC, we wanted to find a potential connection between the 6-25 target expression and functionality of NLCs. However, first we decided to get a closer look on the kinetic of the 6-25 target expression during maturation process of NLCs.

4.1 Kinetic of the 6-25 target expression in NLC

Since expression of the 6-25 target is highly upregulated during the differentiation of monocytes into NLCs, we wanted to evaluate the kinetic of this process. To do that, we analyzed the phenotype of monocytes by flow cytometry from the moment of CLL PBMC isolation until a late stage of the NLCs culture (day 14-20). During early stage of the culture we analyzed the phenotype daily, then every 2-3 days. Beside analysis of the 6-25 target expression, we measured expression of classical myeloid markers, including CD163 and CD206 (M2 phenotype) and CD11c, CD14 and CD16 (known to be highly expressed also on monocytes) to better follow the maturation of the cells. We further controlled the morphology of the culture by BF microscopy, to observe outgrowth of NLC.

The results of an exemplary analysis presented on the fig. 10 revealed that, during the first 24-48 h of the culture, there is no or a very dim expression of the 6-25 target on differentiating monocytes. Past the initial point, the level of the 6-25 target signal is gradually increasing, reaching maximum between day 9-15 of the culture (Fig. 10 B and C). The increase in the level of the 6-25 target in positively correlated with outgrowth of NLC as observed by BF microscopy (Fig. 10D) and negatively correlated with the MFI ratio of CD14, CD16 and CD11c. It was more difficult to correlate 6-25 target expression with CD163 and CD206. In case of CD163, high fluctuation of the signal during NLCs maturation can be observed (this phenomenon was observed for all 8 experiments), which partially could be explained by potential shedding of the protein, which was reported as a regulatory mechanism for this receptor [214,241]. For CD206 marker, induction was observed after day 2 of the culture, reaching peak at day 3 and then from day 5 keeping stable level on the surface of NLCs.

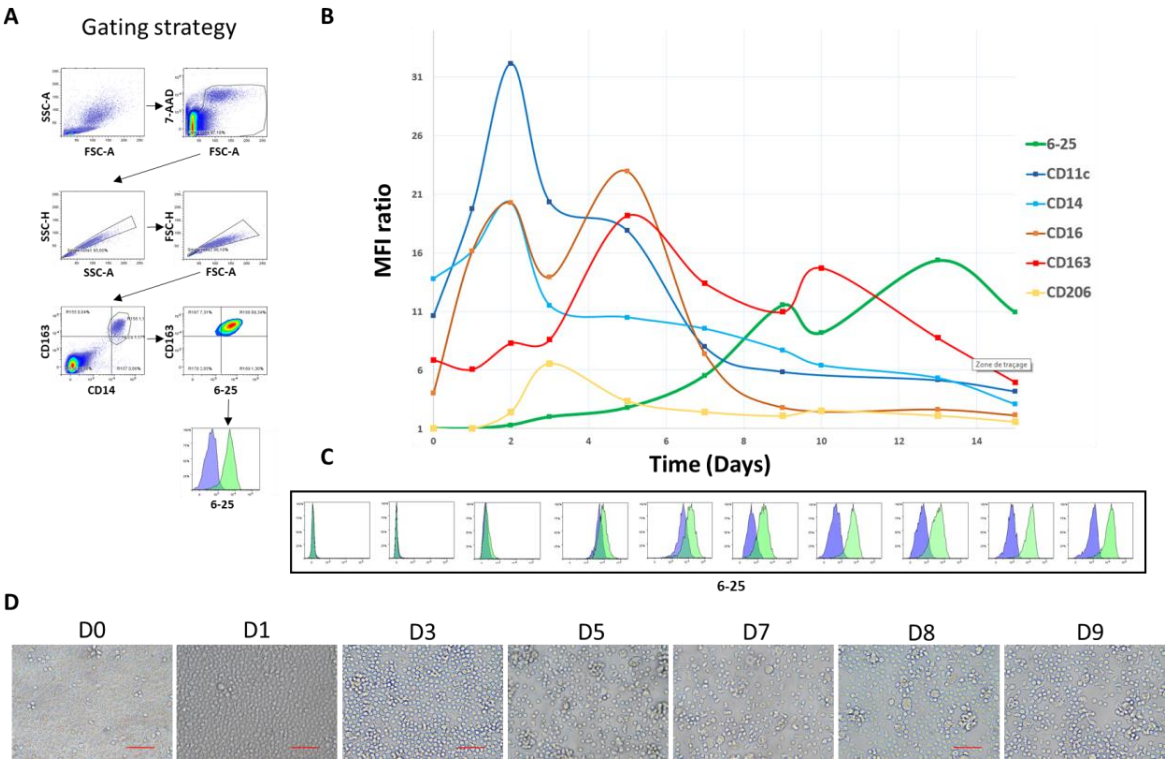

Figure 10. Kinetics of the 6-25 target appearance on the surface monocytes during the maturation into NLC in relation to other myeloid markers. *A) Gating strategy. B) Representative plot with MFI ratio calculated between specific marker and matching isotype control. Measurement point indicated with squares. C) histogram plots representing 6-25 signal (green) overlaid with isotype control (blue), each plot represents 1 measurement point from B). D) BF microscopy pictures of CLL PBMC over the first 9 days of the culture, magnification x400.*

As NLC are known to support viability of CLL cells, we were also measuring changes in the viability and concentration of cancer cells during the culture, to further connect it with changes in the maturation of NLC. Analysis of CLL cell viability by flow cytometry (Annexin V, 7-AAD staining) (Fig. 11) showed, that during the first 3 days of the culture there is a decrease in the viability of the cells, followed by stabilization of this parameter until day 5. Then from day 5-8 viability of cells start to rise, oscillating around 90-95% until the end of the culture. Measurement of the cell concentration by haemocytometer, revealed a continuous drop of the cell number until day 7-8 of the cultures, followed by stabilization of this parameter.

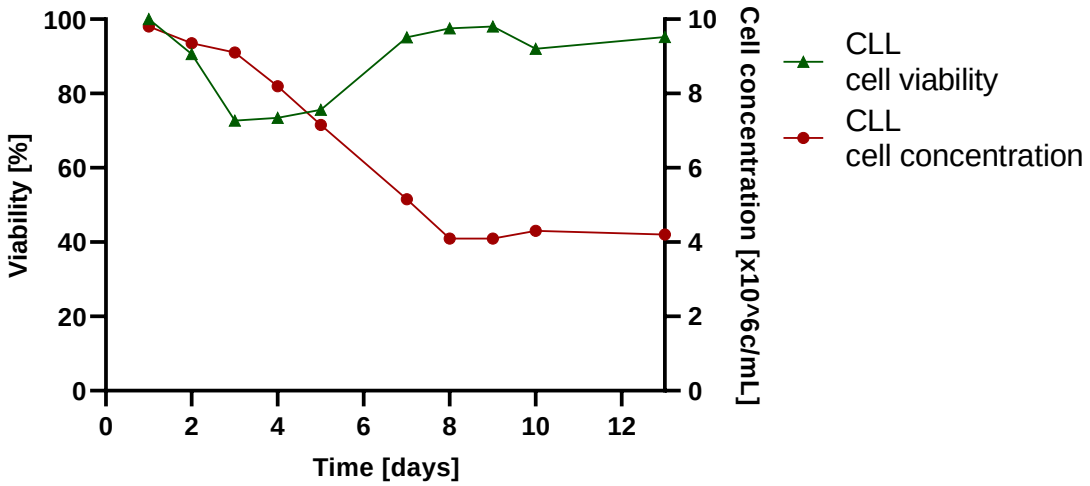

Figure 11 Changes in the viability and CLL cell concentration during typical CLL PBMC culture. *PBMC isolated from the blood of CLL patients, were cultured at 10 × 10^6c/mL. Viability and concentration of the cells were measured at indicated time points, by flow cytometry (Annexin V, 7-AAD staining) and haemocytometer respectively.*

Combining the results of NLC phenotype (Fig. 10) and CLL cells concentration and viability (Fig. 11), we noticed, that stabilization of CLL cell viability and concentration is tightly connected with maturation of NLC. We assumed that from around day 3-8 maturating macrophages are phagocyting dying cancer cells. The intensified phagocytosis is most probably responsible for initial stabilization of cancer cells viability at day 3, while further increase of survival of cancer cells from day 5 is a resultant of both phagocytosis processes, but also anti-apoptotic action of NLC, that start to appear at that time. Based on both analyses we also concluded that the end of maturation of the NLC falls around day 8-10 of the culture, which is also associated with initial stabilization of the 6-25 target level. Results in this chapter suggest that 6-25 target is a marker of NLCs maturation, and its level might indicate their protective functions.

4.2 Connection of 6-25 target expression on NLC with viability of cancer B-CLL cells

As we continued to culture and analyze the CLL PBMC from different patients, we mostly observed NLC expressing a high level of the 6-25 target. In some rare instances however, we noticed that even though maturating monocytes were initially showing an increase in the 6-25 target expression, the level of this molecule started to drop again around day 4—7 of the culture (Fig. 12A). Interestingly, when viability of the CLL cells was measured at day 10 of the culture, a decrease in survival of the cancer cells was noticed in case, where NLC expressed low level of the 6-25 target (Fig. 12B). Additionally, there was no connection between percentage of monocytes at day 0, phenotype of NLC and viability of CLL cells (Fig. 12C).

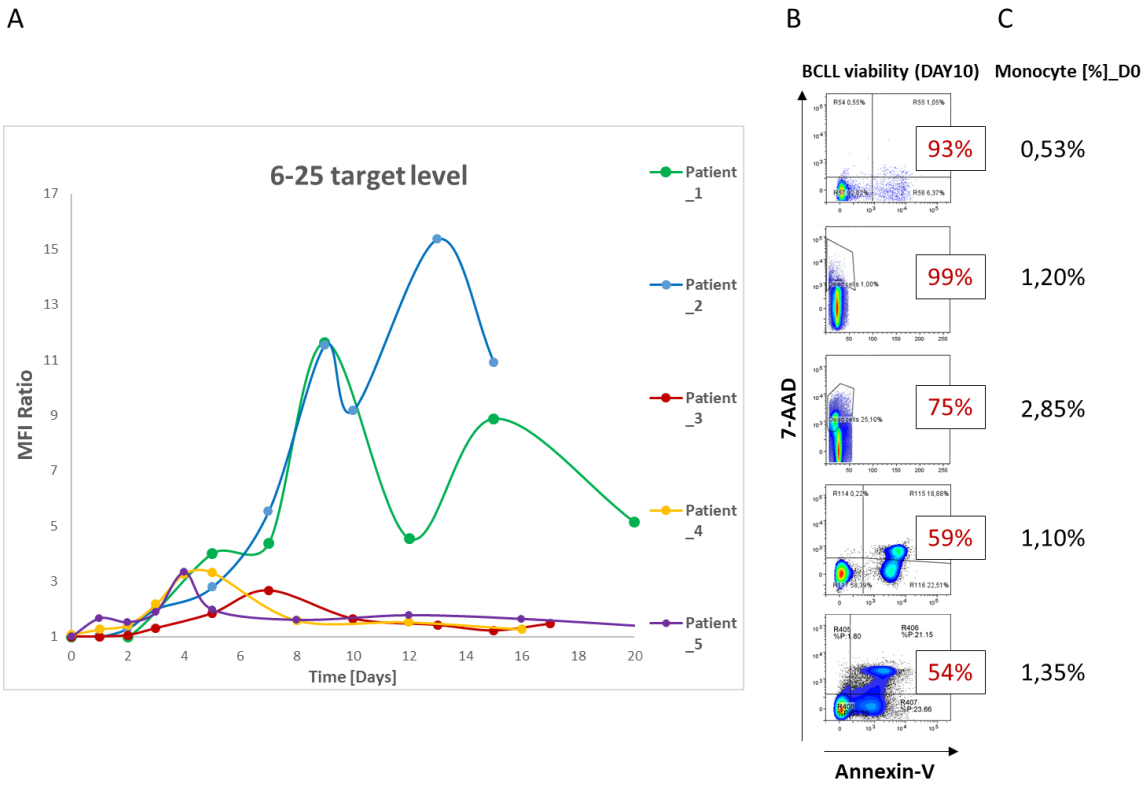

Figure 12. Correlation of the 6-25 target expression on NLC and viability of CLL cells. *A) Kinetics of 6-25 target expression on the surface of maturating NLC, depicted as MFI ratio (between signal from 6-25 and IC antibodies). B) viability of CLL cells at day 10 from the indicated cultures (Annexin V/7-AAD staining, analyzed by FC). C) Initial percentage of monocytes in the CLL PBMC, evaluated by FC (CD14⁺, CD16⁺ staining, data not shown).*

Previously we implied that phagocytosis is partially responsible for stabilization of CLL cell viability *in vitro*. To support this hypothesis, we decided to take a closer look at the viability and cell concentration in the PBMC culture where NLC expressed low level of 6-25 target (Fig. 13). These results showed that the viability of the CLL cells decreases until day 3-5, followed by stabilization phase that last until the end of the culture. At the same time, cell concentration in this culture showed only minor decrease. Comparison of these results to analogical analysis from Fig. 11, show evidence on difference in functionality of NLC in cultures with high and low viability.

These results further support our hypothesis that expression of the 6-25 target might be connected with the protective functionality of NLCs. To confirm the consistency of this finding, we decided to further analyze phenotype of NLC and viability of CLL cells from different samples, focusing on later stages of the cultures (day 10-14). At the end, we gathered the results of PBMC cultures from 34 different CLL patients.

Next we divided the samples into two groups, based on viability of the CLL cells at day 10 of the culture: “High CLL cell viability” – with CLL cells viability > 80% and “Low CLL cell viability” – with CLL cell viability <80% (Fig. 14A). Then we apposed the results of the 6-25 target MFI ratio on NLC from high vs low viability CLL PBMC cultures (Fig. 14B).

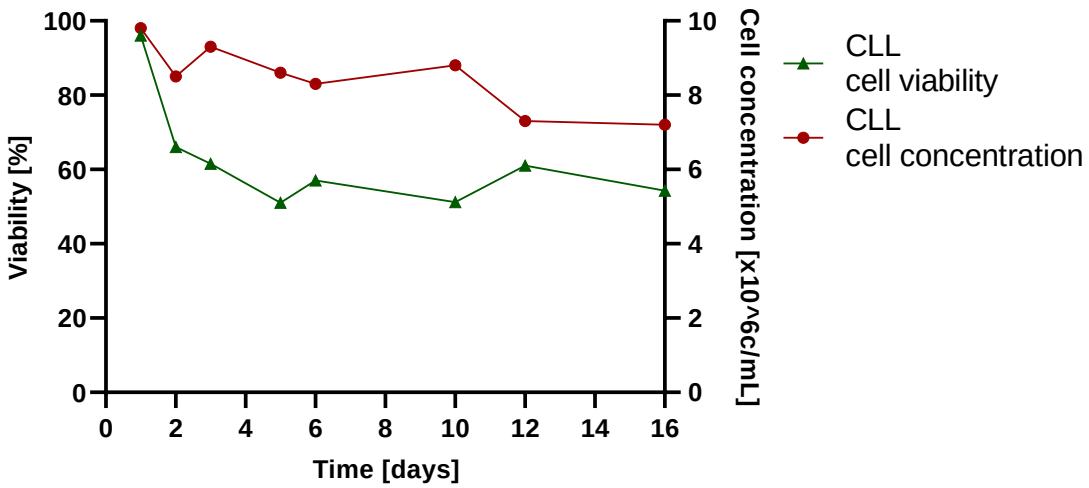

Figure 13. Changes in the viability and CLL cell concentration in CLL PBMC culture from patient 5 (Fig. 12A)*. PBMC isolated from the blood of CLL patients, were cultured at 10 × 10^6c/mL. Viability and concentration of the cells were measured at indicated time points, by flow cytometry (Annexin V, 7-AAD staining) and haemocytometer respectively.*

Based on these analyses we observed a significant decrease in viability of CLL cells in PBMC cultures with NLC expressing low level of the 6-25 target. On the contrary, in the cultures with NLC expressing high expression of the 6-25 target, the viability of the CLL cells remained consistently high. These results further suggested a potential link between the expression of the 6-25 target, protective capabilities of NLC, and thus the viability of cancer cells.

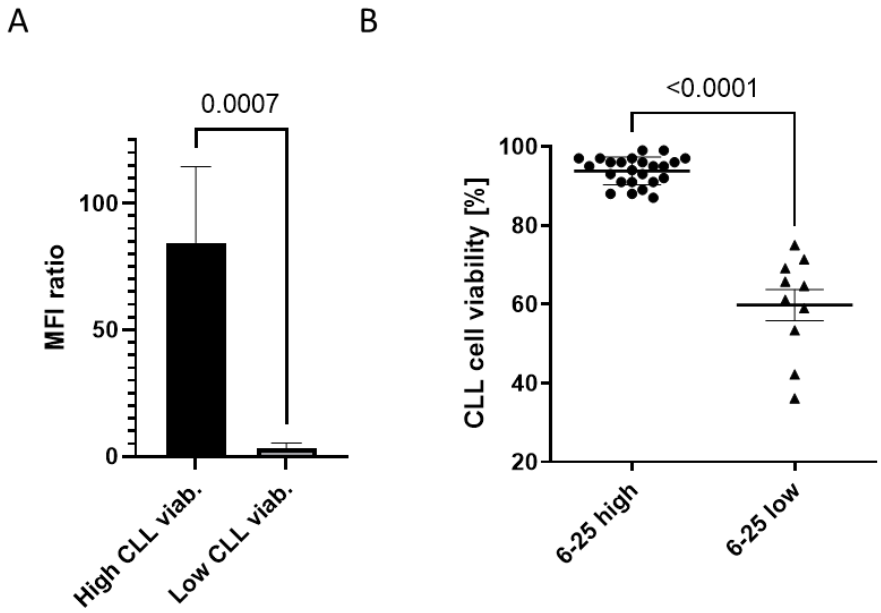

Figure 14. Correlation of 6-25 target expression on NLCs and viability of CLL cells*. Comparison of A) MFI ratio of the 6-25 target on NLC from PBMC cultures with high and low CLL viability. B) relation between expression of 6-25 target on NLC and viability of CLL cells: 6-25 high/low indicates PBMC culture with NLCs expressing high/low level of 6-25 target.*

Beside analysis of the 6-25 target expression, we also characterized the level of other myeloid markers on the surface of these NLC. Afterward, we divided NLC into two groups: protective NLC (cells expressing high level of the 6-25 target) and non-protective NLC (cells expressing low level of the 6-25 target) (Fig. 15). The combined MFI from 8 and 6 independent experiment for protective vs non-protective NLC respectively, showed an upregulation of CD163, CD14, CD209, CD169, CD206 (to lesser extent) and downregulation of CD64, CD86 and CD71. Based on these results, protective NLCs land on the M2-, while non-protective on the M1-side of the polarization spectrum.

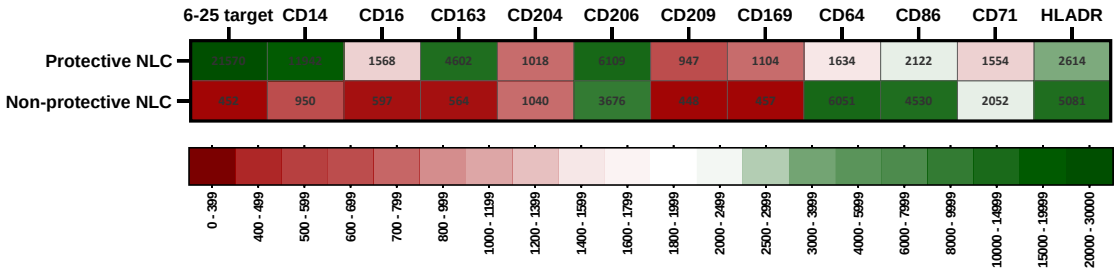

Figure 15. Comparison of phenotype NLCs from high and low viability CLL PBMC cultures. *Phenotype of the cells was analyzed by FC and level of each marker was represented as geometrical mean of MFI from 8 biological replicates for "Protective NLC" group and 6 biological replicates for "Non-protective NLC group".*

Combining previous results, we concluded that 6-25 target is a marker of protective NLC, and that the M2-polarization state of NLC is tightly connected with survival of cancer cells in these cultures.

4.3 Publication on Interplay between TNF and IL-10 on phenotype of CLL cells.

Taking into consideration previous results on the influence of cytokines on the polarization state of MDM, we decided to get insight into the effect of M1 and M2 cytokines on the polarization and functionality of NLCs. As we were still not ready to publish data on the 6-25 target, we decided to classify the NLCs based on the combined level of M2 and M1 markers.

cancers

MDPI

Article

IL-10 Rescues CLL Survival through Repolarization of Inflammatory Nurse-like Cells

Marcin Domagala [1,2,3], Loïc Ysebaert [1,2,3,4], Laetitia Ligat [1,2,3], Frederic Lopez [1,2,3], Jean-Jacques Fournié [1,2,3], Camille Laurent [1,2,3,4] and Mary Poupot [1,2,3,*]

1 Centre de Recherches en Cancérologie de Toulouse, Inserm UMR1037, 31037 Toulouse, France; marcin.domagala@inserm.fr (M.D.); ysebaert.loic@iuct-oncopole.fr (L.Y.); laetitia.ligat@inserm.fr (L.L.); frederic.lopez@inserm.fr (F.L.); jean-jacques.fournie@inserm.fr (J.-J.F.); laurent.c@chu-toulouse.fr (C.L.)
2 Université Toulouse III Paul-Sabatier, 31400 Toulouse, France
3 ERL 5294 CNRS, 31037 Toulouse, France
4 IUCT-O, 31000 Toulouse, France
* Correspondence: mary.poupot@inserm.fr; Tel.: +33-582741662

Simple Summary: In in vitro co-cultures of CLL cells and nurse-like cells (NLC), protection against apoptosis is only provided by M2-like NLC, and not M1-like NLC. In this study, we propose that fine-tuning of NLC polarization (and therefore survival of leukemic cells) is dictated by a balance between IL-10 and TNF.

Abstract: Tumor-associated macrophages (TAMs) in chronic lymphocytic leukemia (CLL) are also called nurse-like cells (NLC), and confer survival signals through the release of soluble factors and cellular contacts. While in most patient samples the presence of NLC in co-cultures guarantees high viability of leukemic cells in vitro, in some cases this protective effect is absent. These macrophages are characterized by an "M1-like phenotype". We show here that their reprogramming towards an M2-like phenotype (tumor-supportive) with IL-10 leads to an increase in leukemic cell survival. Inflammatory cytokines, such as TNF, are also able to depolarize M2-type protective NLC (decreasing CLL cell viability), an effect which is countered by IL-10 or blocking antibodies. Interestingly, both IL-10 and TNF are implied in the pathophysiology of CLL and their elevated level is associated with bad prognosis. We propose that the molecular balance between these two cytokines in CLL niches plays an important role in the maintenance of the protective phenotype of NLCs, and therefore in the survival of CLL cells.

Keywords: Nurse-like cells; polarization; survival; CLL; IL-10; TNF

check for updates

Citation: Domagala, M.; Ysebaert, L.; Ligat, L.; Lopez, F.; Fournié, J.-J.; Laurent, C.; Poupot, M. IL-10 Rescues CLL Survival through Repolarization of Inflammatory Nurse-like Cells. *Cancers* **2022**, *14*, 16. https://doi.org/10.3390/cancers14010016

Academic Editor: Cristina Bottino

Received: 21 October 2021
Accepted: 17 December 2021
Published: 21 December 2021

Publisher's Note: MDPI stays neutral with regard to jurisdictional claims in published maps and institutional affiliations.

Copyright: © 2021 by the authors. Licensee MDPI, Basel, Switzerland. This article is an open access article distributed under the terms and conditions of the Creative Commons Attribution (CC BY) license (https://creativecommons.org/licenses/by/4.0/).

1. Introduction

Nurse-like cells (NLC) are recognized as tumor-associated macrophages (TAMs) found in the lymphoid organs of chronic lymphocytic leukemia (CLL) patients [1]. This disease is the most common B-cell malignancy in the Western world and is characterized by an accumulation of monoclonal $CD5^+$ and mature-appearing B cells in lymphoid tissues and peripheral blood [2]. Numerous studies have shown that CLL cells are especially dependent on their specific tumor microenvironment (TME) and, when cultured in vitro, prone to spontaneous apoptosis. TME of CLL forms a complex medium made up of the extracellular matrix, chemokines, cytokines, and cells including NLC; and has been widely shown to be critical for cancer cell survival, chemoresistance, homing, and proliferation [3–7]. NLC expressing CD68, CD163, and CD206 are found in all tumoral niches [8–10]. They form a survival support for CLL cells, mediated by cell contacts involving different surface molecules such as LFA-3 or galectin-1 [7,11,12] and, controversially, CD31 [13–15]. Moreover, NLC produce pro-survival soluble factors, such as: BAFF, APRIL, SDF-1 (CXCL12), or BDNF [16,17], and can also stimulate the release of CCL3 and CCL4 by leukemic cells to

further strengthen TME [18]. It has been shown that soluble molecules, such as HMGB1 or CSF-1, were involved in NLC differentiation from blood monocytes, [8,19], but that cell contacts between monocytes and CLL cells are also essential [1,10]. However, TAMs, like other macrophages, are highly plastic and readily respond to signals from the microenvironment by fine-tuning their polarization status. Thus, their phenotype will depend on the balance between various pro-M1 factors, such as TNF, IFN-γ, or pro-M2 factors including IL-4, IL-13, or IL-10 [20]. NLC were clearly defined to be closer to the M2 end of the spectrum regarding their phenotype and their pro-survival properties [21] (for review). Unexpectedly, both TNF and IL-10 are implicated in the pathophysiology of CLL, levels of which have been correlated with an adverse prognosis in vivo [22–24]. Indeed, TNF has been listed as an important factor for leukemic proliferation and survival [22,25]. This is not in agreement with the fact that TNF favours the M1 macrophage phenotype, despite the current view of NLC being M2-polarized in the TME. On the other hand, IL-10 thwarts anti-tumoral immune responses, inhibits pro-inflammatory cytokines like TNF, and increases the level of pro-survival molecules such as ICAM-1 on the surface of CLL cells [26–28].

So far, no study has investigated the simultaneous influence of TNF and IL-10 on NLC-mediated protection of CLL cells. We propose here that IL-10 counterbalances the pro-M1 effect of TNF on NLC, thus preserving their pro-niche capacity. We believe that these experiments are useful to understand the impact of TNF and IL-10 on pro-tumoral phenotypes of NLC.

2. Materials and Methods

2.1. Patient's Samples

Peripheral blood samples from CLL Patients were obtained from the Hematology Department with informed consent and referenced in the INSERM cell bank. According to French law, the INSERM cell bank has been registered with the Ministry of Higher Education and Research (DC-2013-1903) after being approved by an ethics committee (Comité de Protection des Personnes Sud-Ouest et Outremer II). Clinical and Biological annotations of the samples have been reported to the Comité National Informatique et Liberté (the Data Processing and Liberties National Comittee). Blood samples were collected from previously untreated patients. PBMC from CLL patients' blood were isolated by density-gradient centrifugation on Ficoll-Paque™ PLUS (GE Healthcare, Sweden). For all experiments except co-culture, fresh PBMC were used. The remaining cells were frozen in Cryostor CM10 (STEMCELL Technologies, France) and stored in liquid nitrogen.

2.2. CLL Cells Isolation

CLL cells were isolated from fresh or frozen PBMC using a negative selection kit—EasySep™ Human B Cell Enrichment Kit II Without CD43 Depletion (STEMcell, Saint Égrève, France), according to the manufacturer's instructions. Purity and viability of the cells after isolation were measured by flow cytometry following staining with CD5/CD19 antibodies and Annexin-V/7-AAD, respectively. For each experiment both values exceeded 95%.

2.3. Cell Cultures

The whole PBMC and isolated CLL cells cultures were cultured in a complete medium: RPMI 1640 with GlutaMAX (Gibco, France) supplemented with 10% of FBS (Life Technologies, France) and 100 µg/mL of penicillin/streptomycin (Sigma-Aldrich, France). Cells were plated at high density (10×10^6 cell/mL) in tissue culture treated plates (Corning, USA), and maintained at 37 °C in a humidified atmosphere with 5% CO_2. In experiments to evaluate the NLC phenotype, cells were cultured in a 4 mL/well of 6-well plates, and to evaluate CLL cells viability, cells were cultured in a 200 µL/well of a 96-well plate or in a 400 µL/well of a 48-well plate in the case of fluorescence microscopy imaging.

2.4. Cytokine Treatment

In order to evaluate the effect of cytokines on the NLC phenotype and CLL cells survival, cells were treated at the indicated time points with 10 ng/mL of human TNF or 50 ng/mL of IL-10 (Miltenyi Biotec, France).

2.4.1. Blocking Antibodies

Blocking antibodies against human TNF or IL-10, and relevant isotype controls were purchased from BD Pharmingen (France). To evaluate the effect of TNF or IL-10 depletion on CLL cells viability and NLC phenotype, PBMC were treated at day zero with a single dose of antibodies alone or in combination at 10 µg/mL, with or without the addition of 10 ng/mL of TNF. The effect of blocking antibodies on CLL cells viability or NLC phenotype was measured on day 12 by flow cytometry.

2.4.2. Co-Culture Experiments

Co-culture experiments were used to imitate CLL cells contact with resident NLC after re-entering the lymph node.

NLC were generated as described above. After 12 to 14 days of culture non-adherent PBMC were separated from adherent NLC by gentle pipetting and washed twice with PBS at room temperature. Subsequently, NLC were co-cultured with purified CLL cells at 10×10^6 cells/mL in 200 µL of complete medium, supplemented with TNF or IL-10. To access basal survival of cancer cells, CLL cells alone were cultured in parallel. CLL cells were co-cultured with NLC from the same (autologous) or different (heterologous) patient. After five days of co-culture, CLL cells viability was measured by flow cytometry using Annexin-V/7-AAD staining.

2.5. Flow Cytometry Analysis

Antibodies against CD5-PC7, CD19-BV421, CD14-PC7, CD16-PE, CD64-PE, CD71-APC-Cy7, CD86-BV421, CD163-FITC, CD169-APC, CD206-BV421, CD209-FITC, and relevant isotype controls were purchased from Sony Biotechnology Europe. 7-AAD and Annexin-V-FITC viability kit were purchased from Miltenyi Biotec, France. Data were acquired on an LSRII flow cytometer (BD Biosciences, France). The obtained results were further analyzed by Flow Logic 700.2A (Inivai Technologies, Australia).

2.5.1. CLL Cells Analysis

On day seven or 12 of culture, floating cells were separated by gentle pipetting and incubated with Human BD Fc Block™ (2.5 µg/mL) in flow cytometry buffer (2% FBS in PBS) for 15 min at 4 °C, followed by staining with 1 µg/mL of CD5 and CD19 antibodies for 20 min at 4 °C. After washing, cells were stained with Annexin-V-FITC according to manufacturer protocol. Following the Annexin-V staining, cells were re-suspended in Annexin-V buffer, containing 7-AAD (0.8 µg/mL) and immediately analyzed by flow cytometry.

2.5.2. NLC Analysis

After 12 or 14 days of CLL PBMC culture, floating cells were harvested and NLC were washed twice with PBS and incubated with 1 mL of Accutase (Biolegend, France) for 20 min in 37 °C. Subsequently, 0.5 mL of FBS was added and cells were further detached with gentle scrapping (Sarstedt, USA). Both floating and adherent cells were further combined, washed in PBS, re-suspended in flow cytometry buffer containing 2.5 µg/mL of Human BD Fc Block™ (BD Biosciences, France) and incubated for 15 min at 4 °C. Subsequently, cells were stained with antibodies at saturating concentrations, for 20 min at 4 °C. After washing, cells were re-suspended in PBS, containing 7-AAD (0.8 µg/mL) and immediately analyzed by flow cytometry.

2.6. Fluorescence Microscopy Imaging

PBMC for fluorescence microscopy analysis were plated in 48-well plates in 400 µL of the complete medium at 10×10^6 cells/mL to allow maturation of NLC. Cytokine treatments and removal of the floating PBMC were cultured according to the co-culture paragraph. Additionally, NLC and isolated CLL cells were stained with specific fluorescent dyes for subsequent visualization of contact between CLL cells and NLC or measurements of phagocytosis during the culture.

2.6.1. Stainings

Visualization of contact between CLL cells and NLC. After removal of floating cells, NLC were stained with mitochondrial MitoView633 (Biotium, USA) or Cell MASK Deep Red plasma membrane dye (Thermo Fisher Scientific, France). Purified CLL cells were stained with cytoplasmic CellTracker Orange CMTMR (Sigma-Aldrich, USA) or CellTrace™ CFSE Cell Proliferation Kit (Thermo Fisher Scientific, France) dye according to the manufacturer's instructions.

Phagocytosis assay. During in vitro CLL culture, NLC can phagocyte dying CLL cells in a process called efferocytosis. To evaluate the phagocytosis capabilities of NLC after cytokine treatment, purified CLL cells were stained with pHrodo dye (Thermo Fisher Scientific, USA). The fluorescence of pHrodo is dependent on pH and increases significantly with acidification of environment (such as in the case of a phagocytosis event). For the pHrodo staining, each 5×10^6 of purified CLL cells were diluted in 500 µL of PBS and mixed with 500 µL of staining buffer (0.1 M of sodium bicarbonate, pH 8.5) containing freshly diluted pHrodo to the final concentration of 20 µg/mL. Cells were incubated in a multiwells plate for 2 h at 37 °C and 5% CO_2. Subsequently, cells were collected and washed twice with a cold complete medium. Next, cells aggregates were removed by passing through a 40 µm nylon filter (Miltenyi Biotec, France), counted with a haemocytometer (Marienfeld, Germany), and plated at 2×10^5 cells/mL of complete medium containing 1 nM of Hoechst 33342 (Life Technologies, USA) with pre-stained NLC.

2.6.2. Image Acquisition

Following the staining, the plates were mounted in Operetta CLS High-Content Analysis System (PerkinElmer, France) equipped with an automated spinning disk fluorescence confocal microscope and analyzed with a 20× objective. Cells were maintained at 37 °C and at 5% of CO_2. Cells morphology and distribution were visualized using bright field (BF) imaging. Depending on the staining: violet, green, orange or red channels were used to visualize cell nuclei, mitochondria, cytoplasm or plasma membrane of the cells. For each well, multiple fields were analysed and images were acquired every 15 min for at least 3 h.

2.6.3. Image Analysis

Calculation of changes in pHrodo intensities within NLC were evaluated by Columbus software (PerkinElmer, France). Briefly, NLC were segmented based on the size, nuclei detection, and plasma membrane staining. The pHrodo intensity values within each NLC cell region were extracted and changes in the pHrodo signal intensities were calculated by subtracting fluorescence values at the first time point from the fluorescence values at the last time point (3 h).

2.7. Statistical Analysis

The Mann–Whitney U test was used for comparison of viability of CLL cells from different cultures (Figure 1B) or MFI ratios of surface markers on NLC (Figure 1E). Paired t-test (Figure 2C,E and Figure 3C) or Wilcoxon test (Figure 3E) were used to determine the differences in viability of CLL cells or MFI ratio in phagocytosis assays. One-way ANOVA with Geisser–Greenhouse correction (Figures 3F and 4B,C,E,F) was used to compare the results after various treatments.

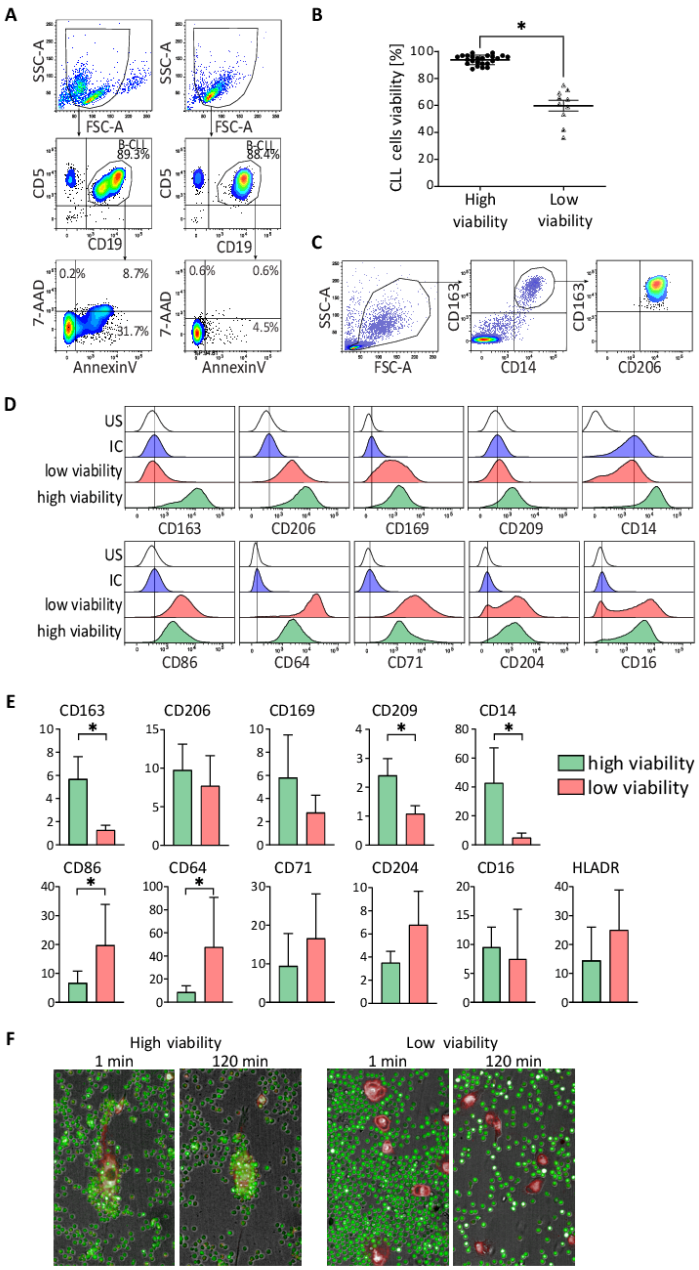

Figure 1. Non protective NLC for CLL cells harbour an M1-like phenotype. (**A**,**B**). Flow cytometry analysis of the percentage of viability (Annexin V/7-AAD negative cells) of CLL cells from cultures of PBMC from CLL patients after 14 days. (One representative experiment (**A**) and data for PBMC

from 35 CLL patients separated in two groups, one with high CLL cells viability and one with low CLL cells viability (**B**)). (**C**–**E**) Surface markers expressed by NLC analysed by flow cytometry at 14 days of cultures of PBMC from CLL patients with low (red) or high (green) in vitro CLL cells viability, comparing to the unstained (US: white) and the isotypic (IC: blue) controls (**D**) one representative experiment; (**E**) compilation of MFI ratios (marker/isotypic control) of five donors. (**F**) Fluorescence imaging of co-cultures of NLC (red staining) and CLL cells (green staining), at 1 min and 120 min, for patients with high (left) and low (right) in vitro viability of CLL cells. * indicates $p < 0.05$.

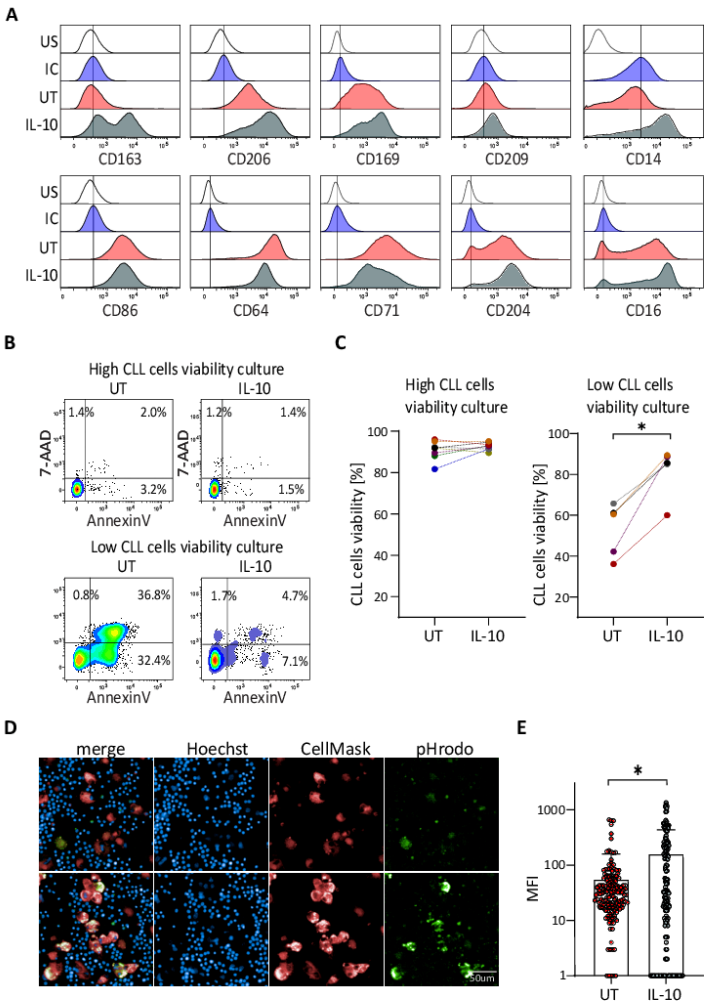

Figure 2. IL-10 rescues viability of CLL cells from patients with low protective NLC. (**A**) Surface markers expressed by NLC analysed by flow cytometry at 14 days of cultures of PBMC from CLL patient with low in vitro CLL cells viability, untreated (UT: red) or treated with IL-10 (grey), comparing to the unstained (US: white) and the isotypic (IC: blue) controls. Representative histograms from five independent experiments. (**B**,**C**) Percentage of the CLL cells viability at 14 days of culture of PBMC from CLL patient with low or high in vitro CLL cells viability untreated (UT) or treated with IL-10

(**B**) one representative experiment; (**C**) eight and five independent experiments for high viability and low viability cultures respectively). (**D**,**E**) Phagocytosis of CLL cells (blue dots) by NLC (red) visualized (**D**) upper: untreated; lower: IL-10 treated and quantified (**E**) thanks to the green pHrodo fluorescence. * indicates $p < 0.05$.

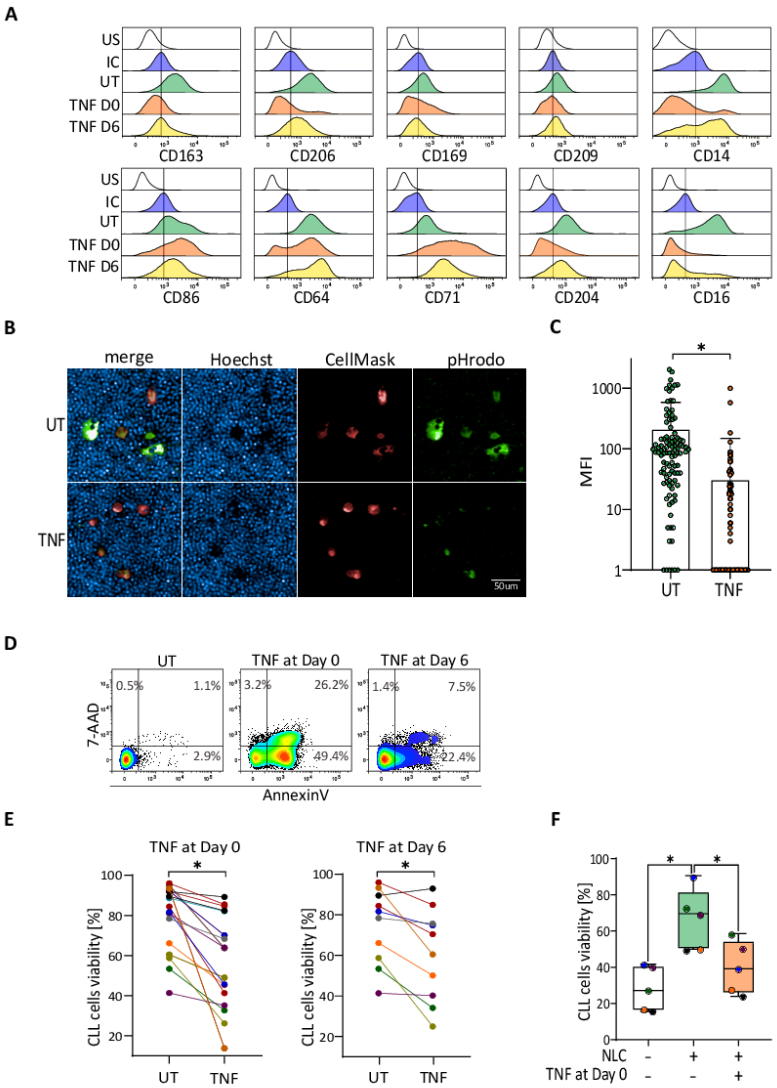

Figure 3. TNF depolarizes protective NLC, leading to a decrease of CLL cells viability. (**A**) Surface markers expressed by NLC analysed by flow cytometry at 14 days of CLL's PBMC cultures incubated or not (UT: green) with TNF at day zero (orange) or at day six (yellow), compared to the unstained (US: white) and the isotypic (IC: blue) controls. Representative histograms from eight independent experiments. (**B**,**C**) Phagocytosis of CLL cells (blue dots) by NLC (red) is visualized. (**B**) upper: untreated; lower: TNF treated and quantified (**C**) thanks to the green pHrodo fluorescence. (**D**,**E**) Percentage

of CLL cells viability at 14 days of culture of CLL PBMC-incubated or not (UT) with TNF at day zero or at day six. (**D**) one representative experiment. (**E**) A total of 19 independent experiments for TNF treatment at day zero and 10 independent experiments at day six. (**F**) Co-culture experiments: percentage of the CLL cells viability cultivated alone (white) or co-cultivated with autologous control NLC (untreated, green) or depolarized NLC (previously treated with TNF; orange). * indicates $p < 0.05$.

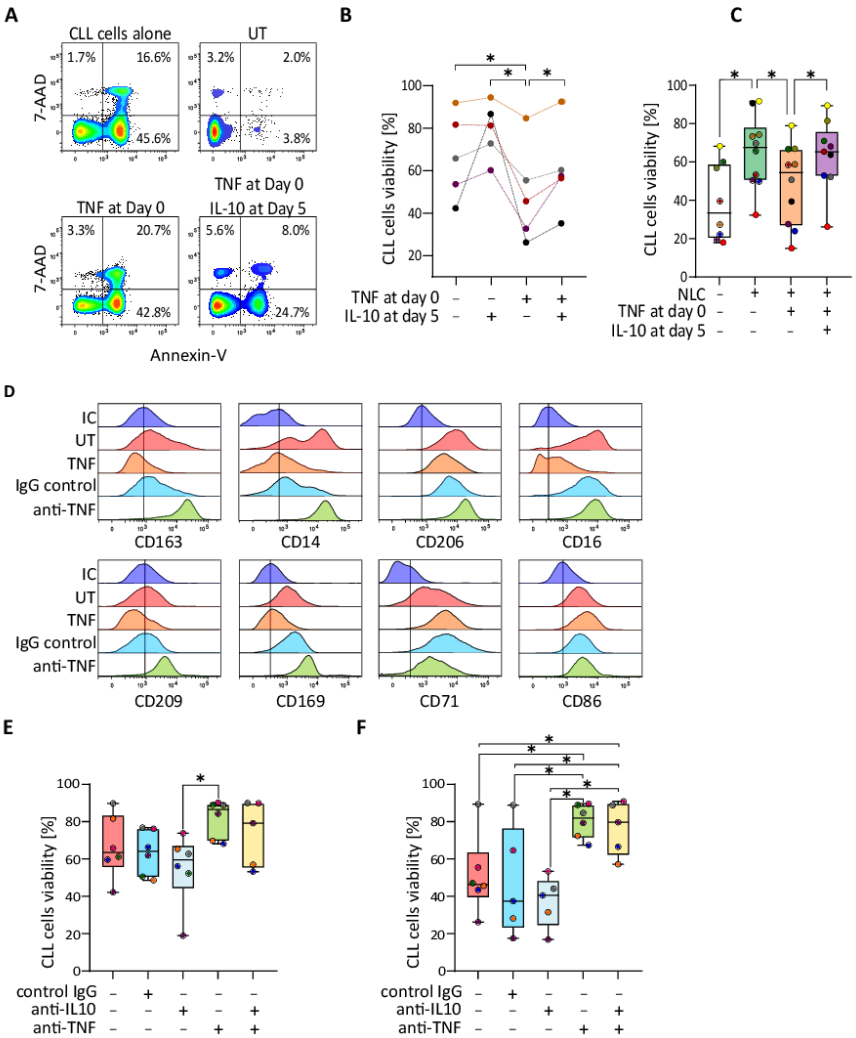

Figure 4. IL-10 repolarizes TNF-depolarized NLC which induce the increase of CLL cells viability. (**A**,**B**) Flow cytometry analysis of the viability (Annexin V/7-AAD negative cells) of CLL cells from cultures of CLL's PBMC incubated or not (UT) with TNF at day zero following by treatment or not with IL-10 at day five. (**A**) one representative experiment; (**B**) five independent experiments. (**C**) Percentage of the CLL cells viability alone (white) or in a CLL's PBMC culture without treatment

(green) or in co-culture with autologous depolarized NLC previously treated with TNF (orange) or with autologous repolarized NLC (treated with TNF at day zero then with IL-10 at day five; purple) (14 independent experiments). (**D**) Surface markers expressed by NLC analysed by flow cytometry at 14 days of CLL's PBMC cultures incubated or not (low viability, UT: red) with TNF at day zero (orange) or with TNF plus an IgG control (blue), or with TNF plus an anti-TNF antibody (green), compared to the isotypic control (IC: dark blue). (**E**,**F**) Percentage of the CLL cells viability at day 14 in CLL's PBMC cultures untreated (**E**) or treated with TNF at day zero (**F**) without antibodies (red) or in the presence of IgG negative control (blue) or anti-IL-10 antibody (grey) or anti-TNF antibody (light green) or the combo anti-IL-10 antibody plus anti-TNF antibody (pale yellow) (nine independent experiments). * indicates $p < 0.05$.

Prior to statistical analyses, the flow cytometry data (presented on Figure 1E), was first transformed into an MFI ratio. Results of the bar plots are shown as mean ± SD. The lines in the middle of the boxes for box and whiskers plots represent median values. All statistical analyses were performed using Graph Pad Prism 9.1.2. The p-values below 0.05 were considered statistically significant.

3. Results

3.1. CLL Cells Viability Depends on M2-like NLCs In Vitro

The culture of CLL cells in the presence of NLC typically allows the cancer cells to maintain high viability in vitro. To our surprise, in some of the CLL PBMC cultures, we observed poor survival of CLL cells, despite the presence of NLC. (Figure 1A,B). In order to elucidate this phenomenon, we decided to analyse the phenotype of NLC by flow cytometry, especially as we didn't observe clear connections between mutational status and lymphocytosis of the patients, and the viability of CLL cells in vitro. To do that, we cultured CLL PBMC for 14 days to allow for the outgrowth of NLC, thanks to contact between monocytes and cancer cells. Then, we investigated the phenotype of NLC by flow cytometry. Classically, NLC are characterized by M2-like phenotype with a high expression of CD163 and CD206 (Figure 1C and Supplementary Figure S1). We further enriched the analysis with several myeloid markers to better distinguish potential differences between NLC from PBMC with low CLL cells in vitro viability (noted: low viability) and from PBMC with high CLL cells in vitro viability (noted: high viability), In comparison to isotypic controls, expression of CD163, CD206, CD169, CD209, and CD14 was higher for NLC from samples with high viability (Figure 1D: green) compared to expression by NLC from samples with low viability (Figure 1D: red). Moreover, expression of CD86, CD64, CD71, and in a smaller proportion of CD204, was higher for NLC from samples with low viability (Figure 1D: red) compared to expression by NLC from samples with high viability (Figure 1D: green). This was observed with at least six different donors from each group (Figure 1E). To confirm that the NLC phenotype analyzed from these two kinds of samples translates into their functionality, we tested the propensity of NLC to attract CLL cells in a protective manner. After 14 days of high or low viability PBMC cultures, floating cells were removed and the remaining NLC were stained with a plasma membrane fluorescent dye. Subsequently, CLL cells were isolated from the frozen PBMC sample, stained with cytoplasmic fluorescent dyes and mixed with NLC. Cells were then visualized by live video-microscopy using an Operetta system. The acquired pictures clearly show a strong grouping of CLL cells around NLC from samples with high viability already after one minute which progresses further until 120 min into the experiment, while NLC from samples with low viability did not induce this phenomenon (Figure 1F and Supplementary Figure S2 for video).

These results prove that NLC from high viability CLL cultures not only display an M2-like phenotype but are also able to attract and facilitate contact with cancer cells, which has been previously shown as the hallmark of their protective functions. On the contrary, NLC from low viability CLL cells cultures are characterized by an M1-like phenotype, with no capacity to attract CLL cells.

3.2. IL-10 Rescues the Viability of CLL Cells in Patient Samples without Protective NLC

IL-10 is known to be an immunosuppressive agent, favouring the M2 phenotype of macrophages. We wanted to know whether this cytokine, naturally produced by CLL cells, could be involved in the protective effect of NLC for CLL cells. PBMC from patients with low CLL cells in vitro viability were cultivated with or without IL-10 for 14 days. Subsequently, the phenotype of NLC was analysed by flow cytometry. Treatment with IL-10 induced an increase of CD163, CD206, CD169, CD14 and weakly of CD209, and a decrease of CD64 and CD71 (Figure 2A). This was in agreement with a switch of the NLC phenotype towards an M2-like phenotype close to that of NLC generated in culture with high CLL cells viability. To go further, the effect of IL-10 was also evaluated on CLL cells viability. IL-10 was shown as having no effect on CLL cells alone (Supplementary Figure S3) or on the viability of CLL cells from samples known to have a high viability. However, IL-10 significantly increased the CLL cells viability in samples with low viability (Figure 2B,C). We then compared phagocytosis capacities of NLC from low viability cultures and NLC from cultures treated with IL-10. Results showed that NLC from IL-10-treated cultures displayed a significantly higher propensity to phagocyte dying CLL cells (efferocytosis) compared to untreated NLC (Figure 2D,E and Supplementary Figure S4 for video).

Thus, the addition of IL-10 in the culture induces an M2-like phenotype of NLC, which in turn leads to increased survival of CLL cells viability.

3.3. TNF-Induced Depolarization Abrogates Pro-Survival Functionality of NLC

TNF is known as a strong pro-inflammatory cytokine polarizing macrophages towards an M1-like state, but has also been linked to an increase of CLL cells viability [22,25]. Thus, we asked the question of whether the treatment of CLL's PBMC cultures with TNF could induce a modification of the NLC phenotype, leading in turn to a decrease in CLL cells viability. This could potentially mimic the phenotype of low viability CLL cultures characterized previously. PBMC from blood samples of CLL patients were cultivated for 14 days in the presence of TNF added either at day zero or at day six of the culture for each sample. NLC phenotype and CLL cells viability were analysed by flow cytometry, while the phagocytic properties of NLC were evaluated by fluorescent microscopy. As shown in Figure 3A, TNF added at the beginning of the culture induced a strong decrease of the expression of CD163, CD206, CD169, CD14, CD16, and CD204; and an increase of CD86, CD64, and CD71. The addition of TNF at day six induced the analogous, although less pronounced, changes for the previously mentioned surface markers (Figure 3A). The depolarization of NLC with other M1 agents, such as IFN-γ and LPS, also changed the final polarization of NLC, but with a distinct pattern and effect on the viability of CLL cells. On the other hand, treatment with IL-10 led to a slight enforcement of the M2 phenotype of NLC (Supplementary Figure S5). We then compared phagocytosis capacity of NLC from high viability cultures and NLC from cultures treated with TNF. Results showed that NLC from untreated cultures displayed a significantly higher propensity to phagocyte dying CLL cells (efferocytosis) compared to NLC treated with TNF (Figure 3B,C). Analysis of the percentage of the viability of CLL cells was done by staining with 7-AAD and Annexin V (Figure 3D). Treatment of the cultures with TNF at day zero or day six induced a significant decrease of the CLL cells viability compared to cultures without treatment (Figure 3E). No direct toxic effect of TNF was observed on CLL cells viability (Supplementary Figure S3). To be sure that the decrease of CLL cells viability was strongly due to the depolarisation of NLC, we performed co-culture experiments. PBMC from the same patients were cultivated for 12 to 14 days in the presence or absence of TNF. Subsequently, floating cells were removed and NLC were further co-cultured with autologous CLL cells isolated from frozen PBMC vials. The viability of isolated CLL cells was then analysed after five days of co-culture. As expected, the viability of CLL cells cultured alone was significantly decreased compared to the condition with M2-like NLCs. Interestingly, the CLL cells viability from the cultures treated with TNF was comparable to that of CLL cells cultured alone, signifying the lack of protective effect of NLC on leukemic cells (Figure 3F).

TNF is therefore able to depolarize protective M2-like NLC into non-protective M1-like NLC.

3.4. IL-10 Repolarizes TNF-Depolarized NLC to Recover the Protective Effect on CLL Cells

We then wondered whether IL-10 could induce the repolarization of TNF-depolarized NLC, which in turn, would result in an increase of CLL cells viability. PBMC from CLL patients were therefore cultivated in the presence of TNF at day zero, then IL-10 was added or not at day five. The CLL cells viability analysis by flow cytometry showed, as expected, a decrease in the viability of cultures treated with TNF, which could be partially countered by co-treatment with IL-10 at day five (Figure 4A,B). At the same time, we showed that low viability CLL cells cultures (Figure 4B: black, purple and green samples) could also be rescued by the addition of IL-10 at day five. Going further, we performed the same experiment of co-culture of freshly isolated CLL cells and TNF-depolarized NLC (TNF at day zero) or IL-10-repolarized NLC (TNF at day zero then IL-10 at day five). As predicted, the presence of protective M2-like NLC in the culture increased the viability of CLL cells, compared to the monocultures of cancer cells. At the same time, the co-culture with TNF-depolarized NLC showed a decrease of cancer cells viability, comparable to the culture of CLL cells alone (Figure 4C: orange block). However, the percentage of CLL cells viability was increased when CLL cells were co-cultivated with IL-10-repolarized NLC (Figure 4C: purple block). To reinforce the message of relevance of IL-10 on the protective function of NLC and thus CLL cells survival, we used blocking antibodies against IL-10 and TNF. First, the phenotype of M1-like NLC cultivated in the presence of anti-TNF or IgG control was analysed by flow cytometry. Expression of CD163, CD14, CD206, CD209, and CD169 which were further decreased by the presence of TNF in the culture, were restored in the presence of anti-TNF compared to the cultures with the IgG control, while expression of CD71 was slightly decreased (Figure 4D). The expression of CD16 and CD86 were similar in the conditions with anti-TNF or IgG control. The percentage of CLL cells viability in the presence of blocking antibodies was also evaluated, revealing that blocking IL-10 in the culture induced a decrease of the viability while blocking TNF increased it slightly (Figure 4E). These effects were even more pronounced if cells were treated with TNF at the beginning of the culture, when the addition of the anti-TNF blocking antibody led to an increase of the viability percentage, while blocking IL-10 led to a small decrease depending on the sample (Figure 4F).

4. Discussion

CLL cells have been shown to be resistant to in vitro apoptosis, in the majority of cases, if cultivated in the presence of NLC [29]. However, in some cases CLL cells display a decrease in survival, even in the presence of NLC. We demonstrated here that NLC obtained from PBMC of these patients can be considered as non-protective for CLL cells, displaying an M1-like phenotype, with a low capacity to attract leukemic cells, and are unable to perform efferocytosis, i.e., phagocytosis of dying cells. However, addition of IL-10 to the cultures of PBMC from these patients led to a significant increase in CLL cells viability. The role of IL-10 in mediating leukemic survival is still controversial, implying a possible involvement in CLL cells maintenance or cell death. IL-10 was involved as provoking apoptosis by decreasing Bcl-2 protein levels or activating STAT1 protein [30,31]. On the contrary, IL-10 was given as a pro-survival cytokine for CLL cells acting as an autocrine growth factor and mediating pro-survival signals through the activation of STAT3 [32–34]. However, nobody asked the question of a possible indirect effect of IL-10 on CLL cells, notably via the microenvironment such as NLC.

Given that IL-10 is a pro-M2 cytokine for myeloid cells and that protective NLC display an M2-like phenotype, this cytokine could maintain and/or polarize NLC towards an M2 protective state to further support leukemic survival. To answer this question, we first generated a model which could mimic cultures with low CLL cells viability. We showed that the addition of TNF in cultures of PBMC from patients with high in vitro CLL cells

viability led to a preclusion of the M2 polarization of blood monocytes into NLC when added at day zero, and to a depolarization of maturating NLC when added at day six of the culture. Even though TNF was shown in some studies as increasing CLL cells viability and correlated with a bad prognosis in patients [22,25], we showed here that it is also able to block or depolarize the M2 protective phenotype of NLC leading to a decrease in leukemic viability (Figure 3). M2 markers such as CD206, CD204, CD169, CD163, and CD16 were abrogated with TNF at day zero and highly decreased with the addition of TNF at day six of the culture with an increase of M1 markers, such as CD86, CD64 and CD71. At the same time, TNF treatment led to a significant decrease of the efferocytosis capacity of NLC. To further exclude the possibility that the effect of TNF might be mediated by other cells present in CLL PBMC culture, we performed experiments with mature NLC co-cultured with freshly isolated CLL cells, in an autologous manner. Co-cultures with TNF- treated NLC led to a decrease in the survival of CLL cells, proving that depolarization of NLC decreases their protective effect. Interestingly, IL-10 was shown here to restore the survival of CLL cells from low viability PBMC cultures by inducing M2 polarization of NLC, and also to rescue CLL cells in PBMC cultures treated with TNF. Furthermore, co-culture experiments with freshly isolated CLL cells and TNF depolarized NLC further repolarized by IL-10 displayed the restoration of protective NLC capacities. Thus, we demonstrated here for the first time that non-protective NLC with an M1-like phenotype can be reoriented towards an M2 protective phenotype thanks to IL-10. This was in agreement with the indirect action of IL-10 on the CLL cells viability via NLC.

Moreover, blocking of TNF in CLL's PBMC cultures increased CLL cells viability, in particular for samples from patients with low in vitro viability. Interestingly, blocking of IL-10 in CLL's PBMC cultures could decrease the CLL cells viability for samples previously displaying high survival of CLL cells, and further decrease survival in initially low viability cultures, especially upon additional treatment with TNF.

All these results, combined with multiple research listing TNF as an important factor for CLL progression, suggest that the TNF and IL-10 interplay constitutes an important axis, allowing both activation of CLL cells by TNF, while at the same time, IL-10 is preserving the M2 protective polarization state of NLC. The M2 polarization of NLC shown by high CD163 staining in lymph nodes was indeed correlated with progressive disease [6]. IL-10 and TNF produced by CLL cells and others in the in vitro culture of PBMC from CLL patients may therefore have an impact on the NLC phenotype and CLL cells viability. IL-10 favours the M2-like protective NLC state and counterbalances the M1-agent TNF, preserving the pro-tumoral effect of NLC on leukemic cells.

Even if in vitro cultures of PBMC from CLL patients do not exactly reflect the CLL microenvironment, it can be sufficiently representative to appreciate the interaction between CLL cells and NLC. No work in the literature has reported concentrations of TNF or IL-10 in lymph nodes. However, TNF was shown as produced by T cells, CLL cells and macrophages in CLL patients [25]; and TNF released by CLL cells was proposed as one of the reasons for dysfunctional hematopoiesis in CLL [35]. IL-10 was also shown to be produced by CLL cells. Interestingly expression of this cytokine was shown to be upregulated by CD5, which is present on the surface of leukemic cells [36]. Additionally, CD5 expression is modulated, dependent on the life cycle of CLL cells. Its expression is increased while CLL cells reside in lymph nodes and, after returning to peripheral blood, CD5 level is gradually downregulated. It would further suggest, that CLL cells express the most of IL-10 while in the lymph nodes, where this cytokine could not only support proliferation of the CLL cells, but also preserve the pro-tumoral polarization state of NLC [36]. In addition, high levels of TNF and IL-10 were measured in the serum of high risk groups of CLL patients [23] with a median of 5.04 pg/mL for IL-10 compared to zero for healthy donors [27,37,38] and 17 to 34 pg/mL for TNF, level for healthy donors being at 5 pg/mL [39]. It is impossible to extrapolate this information to the lymph nodes compartment but we could speculate that cells of TME are continuously producing and using these cytokines. Levels of IL-10 and TNF in serum and/or in lymph nodes of patients

could be therefore linked to the aggressiveness of the disease, and directly linked to NLC polarization, which has a high impact on leukemic cells viability. The amount of these cytokines and more precisely the proportion of IL-10 / TNF produced in the TME can be responsible for the polarization of NLC on which CLL cells viability depends. Classical therapies can also modulate the proportion of these cytokines. Indeed, treatment of patients with ibrutinib enforces M2 phenotype of NLC with exacerbating M2 markers expression, increasing their immunosuppressive profile [34]. Moreover, in vitro treatment of NLC with ibrutinib induces the protection of CLL cells from drug-induced apoptosis partially through the secretion of IL-10 [34]. This results in further support targeting of IL-10 to potentially decrease pro-tumoral function of NLC and TME. Anti-IL-10 in combination with classical therapies in CLL could be beneficial as shown in other diseases such as leukaemia or melanoma [40,41]. In addition, all conventional drugs used in the treatment of CLL could be applied in cultures of CLL cells in vitro to document the types of molecules / cytokines that could be released that induce the depolarization of M2 protective NLC in M1 non-protective NLC.

These results also enforce the possibility of targeting TNF that is associated with disease progression [22,42]. Blocking of TNF could therefore lead to stabilization of the disease, or at least to partial resolution of inflammation. This could be followed by anti-IL10 treatment, combined with targeting of the CLL microenvironment, particularly NLC, to decrease the survival of remaining cancer cells.

5. Conclusions

In this study, we showed that NLC obtained from PBMC of patients with a low in vitro viability of CLL cells can be considered as non-protective for CLL cells, displaying an M1-like phenotype. We also demonstrated that these non-protective NLC or TNF-depolarized NLC can be reoriented towards an M2 protective phenotype thanks to IL-10, confirming the importance of IL-10 in the CLL progression.

Supplementary Materials: The following are available online at https://www.mdpi.com/article/10.3390/cancers14010016/s1, Figure S1: NLC display a phenotype close to M2 macrophages. Figure S2: Video microscopy from a sample with high CLL cells viability. Figure S3: TNF and IL-10 have no effect on the viability of isolated CLL cells. Figure S4: video microscopy with IL-10. Figure S5: TNF, IFN-γ and LPS depolarize NLC toward a M1-like phenotype.

Author Contributions: M.D. performed the experiments and analyzed the data. L.L. and F.L. participated to imaging experiments. L.Y., J.-J.F. and C.L. participated to the discussion of the results. M.P. and M.D. designed the experiments. M.P. supervised the study and wrote the paper. All authors have read and agreed to the published version of the manuscript.

Funding: This work was funded by the Janssen Foundation, Inserm, CNRS, and the Toulouse III University. We are grateful to our healthcare professionals for their boundless investment during the COVID-19 crisis.

Institutional Review Board Statement: The study was conducted according to the guidelines of the Declaration of Helsinki, and approved by the Institutional Review Board (or Ethics Committee) of INSERM (protocol code DC-2013-1903 and date of approval 2013).

Informed Consent Statement: Informed consent was obtained from all subjects involved in the study.

Data Availability Statement: Not applicable.

Conflicts of Interest: The authors declare no conflict of interest.

References

1. Boissard, F.; Fournié, J.-J.; Laurent, C.; Poupot, M.; Ysebaert, L. Nurse like cells: Chronic lymphocytic leukemia associated macrophages. *Leuk. Lymphoma* **2015**, *56*, 1570–1572. [CrossRef]
2. Caligaris-Cappio, F.; Gottardi, D.; Alfarano, A.; Stacchini, A.; Gregoretti, M.G.; Ghia, P.; Bertero, M.T.; Novarino, A.; Bergui, L. The nature of the b lymphocyte in b-chronic lymphocytic leukemia. *Blood Cells* **1993**, *19*, 601–613.

3. Lagneaux, L.; Delforge, A.; Bron, D.; De Bruyn, C.; Stryckmans, P. Chronic lymphocytic leukemic b cells but not normal b cells are rescued from apoptosis by contact with normal bone marrow stromal cells. *Blood* **1998**, *91*, 2387–2396. [CrossRef] [PubMed]
4. Burger, J.A.; Burger, M.; Kipps, T.J. Chronic lymphocytic leukemia b cells express functional cxcr4 chemokine receptors that mediate spontaneous migration beneath bone marrow stromal cells. *Blood* **1999**, *94*, 3658–3667. [CrossRef] [PubMed]
5. Boissard, F.; Fournié, J.-J.; Quillet-Mary, A.; Ysebaert, L.; Poupot, M. Nurse-like cells mediate ibrutinib resistance in chronic lymphocytic leukemia patients. *Blood Cancer J.* **2015**, *5*, e355. [CrossRef] [PubMed]
6. Boissard, F.; Laurent, C.; Ramsay, A.G.; Quillet-Mary, A.; Fournié, J.-J.; Poupot, M.; Ysebaert, L. Nurse-like cells impact on disease progression in chronic lymphocytic leukemia. *Blood Cancer J.* **2016**, *6*, e381. [CrossRef]
7. Boissard, F.; Tosolini, M.; Ligat, L.; Quillet-Mary, A.; Lopez, F.; Fournié, J.-J.; Ysebaert, L.; Poupot, M. Nurse-like cells promote cll survival through LFA-3/CD2 interactions. *Oncotarget* **2017**, *8*, 52225–52236. [CrossRef]
8. Jia, L.; Clear, A.; Liu, F.-T.; Matthews, J.; Uddin, N.; McCarthy, A.; Hoxha, E.; Durance, C.; Iqbal, S.; Gribben, J.G. Extracellular HMGB1 promotes differentiation of nurse-like cells in chronic lymphocytic leukemia. *Blood* **2014**, *123*, 1709–1719. [CrossRef]
9. Ysebaert, L.; Fournié, J.-J. Genomic and Phenotypic Characterization of nurse-like cells that promote drug resistance in chronic lymphocytic leukemia. *Leuk. Lymphoma* **2011**, *52*, 1404–1406. [CrossRef]
10. Tsukada, N.; Burger, J.A.; Zvaifler, N.J.; Kipps, T.J. Distinctive features of "nurselike" cells that differentiate in the context of chronic lymphocytic leukemia. *Blood* **2002**, *99*, 1030–1037. [CrossRef]
11. Talbot, H.; Saada, S.; Barthout, E.; Gallet, P.-F.; Gachard, N.; Abraham, J.; Jaccard, A.; Troutaud, D.; Lalloué, F.; Naves, T.; et al. BDNF Belongs to the nurse-like cell secretome and supports survival of b chronic lymphocytic leukemia cells. *Sci Rep.* **2020**, *10*, 12572. [CrossRef] [PubMed]
12. Croci, D.O.; Morande, P.E.; Dergan-Dylon, S.; Borge, M.; Toscano, M.A.; Stupirski, J.C.; Bezares, R.F.; Avalos, J.S.; Narbaitz, M.; Gamberale, R.; et al. Nurse-like cells control the activity of chronic lymphocytic leukemia b cells via galectin-1. *Leukemia* **2013**, *27*, 1413–1416. [CrossRef] [PubMed]
13. Poggi, A.; Prevosto, C.; Catellani, S.; Rocco, I.; Garuti, A.; Zocchi, M.R. Engagement of CD31 delivers an activating signal that contributes to the survival of chronic lymphocytic leukaemia cells. *Br. J. Haematol.* **2010**, *151*, 252–264. [CrossRef]
14. Tonino, S.H.; Spijker, R.; Luijks, D.M.P.; van Oers, M.H.J.; Kater, A.P. No Convincing evidence for a role of CD31-CD38 interactions in the pathogenesis of chronic lymphocytic leukemia. *Blood* **2008**, *112*, 840–843. [CrossRef]
15. Deaglio, S.; Aydin, S.; Grand, M.M.; Vaisitti, T.; Bergui, L.; D'Arena, G.; Chiorino, G.; Malavasi, F. CD38/CD31 Interactions activate genetic pathways leading to proliferation and migration in chronic lymphocytic leukemia cells. *Mol. Med.* **2010**, *16*, 87–91. [CrossRef]
16. Nishio, M.; Endo, T.; Tsukada, N.; Ohata, J.; Kitada, S.; Reed, J.C.; Zvaifler, N.J.; Kipps, T.J. Nurselike Cells Express BAFF and APRIL, which can promote survival of chronic lymphocytic leukemia cells via a paracrine pathway distinct from that of sdf-1alpha. *Blood* **2005**, *106*, 1012–1020. [CrossRef]
17. Burger, J.A.; Tsukada, N.; Burger, M.; Zvaifler, N.J.; Dell'Aquila, M.; Kipps, T.J. Blood-derived nurse-like cells protect chronic lymphocytic leukemia b cells from spontaneous apoptosis through stromal cell-derived factor-1. *Blood* **2000**, *96*, 2655–2663. [CrossRef] [PubMed]
18. Burger, J.A.; Quiroga, M.P.; Hartmann, E.; Bürkle, A.; Wierda, W.G.; Keating, M.J.; Rosenwald, A. high-level expression of the t-cell chemokines ccl3 and ccl4 by chronic lymphocytic leukemia b cells in nurselike cell cocultures and after BCR stimulation. *Blood* **2009**, *113*, 3050–3058. [CrossRef]
19. Polk, A.; Lu, Y.; Wang, T.; Seymour, E.; Bailey, N.G.; Singer, J.W.; Boonstra, P.S.; Lim, M.S.; Malek, S.; Wilcox, R.A. Colony-stimulating factor-1 receptor is required for nurse-like cell survival in chronic lymphocytic leukemia. *Clin. Cancer Res.* **2016**, *22*, 6118–6128. [CrossRef]
20. Kratochvill, F.; Neale, G.; Haverkamp, J.M.; Van de Velde, L.-A.; Smith, A.M.; Kawauchi, D.; McEvoy, J.; Roussel, M.F.; Dyer, M.A.; Qualls, J.E.; et al. TNF counterbalances the emergence of M2 tumor macrophages. *Cell Rep.* **2015**, *12*, 1902–1914. [CrossRef] [PubMed]
21. Mesaros, O.; Jimbu, L.; Neaga, A.; Popescu, C.; Berceanu, I.; Tomuleasa, C.; Fetica, B.; Zdrenghea, M. Macrophage polarization in chronic lymphocytic leukemia: Nurse-like cells are the caretakers of leukemic cells. *Biomedicines* **2020**, *8*, 516. [CrossRef]
22. Dürr, C.; Hanna, B.S.; Schulz, A.; Lucas, F.; Zucknick, M.; Benner, A.; Clear, A.; Ohl, S.; Öztürk, S.; Zenz, T.; et al. tumor necrosis factor receptor signaling is a driver of chronic lymphocytic leukemia that can be therapeutically targeted by the flavonoid wogonin. *Haematologica* **2018**, *103*, 688–697. [CrossRef] [PubMed]
23. Lech-Maranda, E.; Grzybowska-Izydorczyk, O.; Wyka, K.; Mlynarski, W.; Borowiec, M.; Antosik, K.; Cebula-Obrzut, B.; Makuch-Lasica, H.; Nowak, G.; Klimkiewicz-Wojciechowska, G.; et al. Serum tumor necrosis factor-α and interleukin-10 levels as markers to predict outcome of patients with chronic lymphocytic leukemia in different risk groups defined by the IGHV mutation status. *Arch. Immunol. Exp.* **2012**, *60*, 477–486. [CrossRef]
24. Mainou-Fowler, T.; Miller, S.; Proctor, S.J.; Dickinson, A.M. The levels of TNF alpha, IL4 and IL10 production by T-cells in B-cell chronic lymphocytic leukaemia (B-CLL). *Leuk. Res.* **2001**, *25*, 157–163. [CrossRef]
25. Bojarska-Junak, A.; Hus, I.; Szczepanek, E.W.; Dmoszyńska, A.; Roliński, J. Peripheral blood and bone marrow TNF and TNF receptors in early and advanced stages of B-CLL in correlation with ZAP-70 protein and CD38 antigen. *Leuk. Res.* **2008**, *32*, 225–233. [CrossRef]

26. Rivas, J.R.; Liu, Y.; Alhakeem, S.S.; Eckenrode, J.M.; Marti, F.; Collard, J.P.; Zhang, Y.; Shaaban, K.A.; Muthusamy, N.; Hildebrandt, G.C.; et al. Interleukin-10 suppression enhances t-cell antitumor immunity and responses to checkpoint blockade in chronic lymphocytic leukemia. *Leukemia* **2021**. [CrossRef]
27. DiLillo, D.J.; Weinberg, J.B.; Yoshizaki, A.; Horikawa, M.; Bryant, J.M.; Iwata, Y.; Matsushita, T.; Matta, K.M.; Chen, Y.; Venturi, G.M.; et al. Chronic lymphocytic leukemia and regulatory b cells share il-10 competence and immunosuppressive function. *Leukemia* **2013**, *27*, 170–182. [CrossRef] [PubMed]
28. Schulz, A.; Dürr, C.; Zenz, T.; Döhner, H.; Stilgenbauer, S.; Lichter, P.; Seiffert, M. Lenalidomide reduces survival of chronic lymphocytic leukemia cells in primary cocultures by altering the myeloid microenvironment. *Blood* **2013**, *121*, 2503–2511. [CrossRef]
29. Filip, A.A.; Ciseł, B.; Wąsik-Szczepanek, E. Guilty bystanders: Nurse-like cells as a model of microenvironmental support for leukemic lymphocytes. *Clin. Exp. Med.* **2015**, *15*, 73–83. [CrossRef]
30. Fluckiger, A.C.; Durand, I.; Banchereau, J. Interleukin 10 induces apoptotic cell death of b-chronic lymphocytic leukemia cells. *J. Exp. Med.* **1994**, *179*, 91–99. [CrossRef]
31. Liang, X.; Moseman, E.A.; Farrar, M.A.; Bachanova, V.; Weisdorf, D.J.; Blazar, B.R.; Chen, W. Toll-like Receptor 9 Signaling by CpG-B oligodeoxynucleotides induces an apoptotic pathway in human chronic lymphocytic leukemia b cells. *Blood* **2010**, *115*, 5041–5052. [CrossRef]
32. Kitabayashi, A.; Hirokawa, M.; Miura, A.B. The Role of Interleukin-10 (IL-10) in Chronic B-lymphocytic leukemia: IL-10 prevents leukemic cells from apoptotic cell death. *Int. J. Hematol.* **1995**, *62*, 99–106. [CrossRef]
33. Morabito, F.; Filangeri, M.; Sculli, G.; Oliva, B. In vitro modulation of bcl-2 protein expression, drug-induced apoptosis and cytotoxicity by interleukin-10 in chronic lymphocytic leukemia. *Haematologica* **1998**, *83*, 1046–1048. [PubMed]
34. Fiorcari, S.; Maffei, R.; Audrito, V.; Martinelli, S.; Ten Hacken, E.; Zucchini, P.; Grisendi, G.; Potenza, L.; Luppi, M.; Burger, J.A.; et al. Ibrutinib modifies the function of monocyte/macrophage population in chronic lymphocytic leukemia. *Oncotarget* **2016**, *7*, 65968–65981. [CrossRef] [PubMed]
35. Manso, B.A.; Zhang, H.; Mikkelson, M.G.; Gwin, K.A.; Secreto, C.R.; Ding, W.; Parikh, S.A.; Kay, N.E.; Medina, K.L. Bone Marrow hematopoietic dysfunction in untreated chronic lymphocytic leukemia patients. *Leukemia* **2019**, *33*, 638–652. [CrossRef] [PubMed]
36. Garaud, S.; Morva, A.; Lemoine, S.; Hillion, S.; Bordron, A.; Pers, J.-O.; Berthou, C.; Mageed, R.A.; Renaudineau, Y.; Youinou, P. CD5 promotes IL-10 production in chronic lymphocytic leukemia b cells through STAT3 and NFAT2 activation. *J. Immunol.* **2011**, *186*, 4835–4844. [CrossRef] [PubMed]
37. Pang, N.; Zhang, R.; Li, J.; Zhang, Z.; Yuan, H.; Chen, G.; Zhao, F.; Wang, L.; Cao, H.; Qu, J.; et al. Increased IL-10/IL-17 Ratio is aggravated along with the prognosis of patients with chronic lymphocytic leukemia. *Int. Immunopharmacol.* **2016**, *40*, 57–64. [CrossRef]
38. Kamper, E.F.; Papaphilis, A.D.; Angelopoulou, M.K.; Kopeikina, L.T.; Siakantaris, M.P.; Pangalis, G.A.; Stavridis, J.C. Serum levels of tetranectin, intercellular adhesion molecule-1 and interleukin-10 in b-chronic lymphocytic leukemia. *Clin. Biochem.* **1999**, *32*, 639–645. [CrossRef]
39. Jablonska, E.; Kiersnowska-Rogowska, B.; Rogowski, F.; Parfienczyk, A.; Puzewska, W.; Bukin, M. TNF family molecules in the serum of patients with b-cell chronic lymphocytic leukemia (B-CLL). *Leuk. Lymphoma* **2005**, *46*, 1307–1312. [CrossRef]
40. El Hajj, H.; Hleihel, R.; El Sabban, M.; Bruneau, J.; Zaatari, G.; Cheminant, M.; Marçais, A.; Akkouche, A.; Hasegawa, H.; Hall, W.; et al. Loss of interleukin-10 activates innate immunity to eradicate adult t-cell leukemia-initiating cells. *Haematologica* **2021**, *106*, 1443–1456. [CrossRef]
41. Gordy, J.T.; Luo, K.; Francica, B.; Drake, C.; Markham, R.B. Anti-IL-10-mediated enhancement of antitumor efficacy of a dendritic cell-targeting mip3α-gp100 vaccine in the b16f10 mouse melanoma model is dependent on type i interferons. *J. Immunother.* **2018**, *41*, 181–189. [CrossRef] [PubMed]
42. Spaner, D.E.; Venema, R.; Huang, J.; Norris, P.; Lazarus, A.; Wang, G.; Shi, Y. Association of blood igg with tumor necrosis factor-alpha and clinical course of chronic lymphocytic leukemia. *EBioMedicine* **2018**, *35*, 222–232. [CrossRef] [PubMed]

4.4 Conclusions

Results presented in this paper shed light on the interplay between IL-10 and TNF on the functionality of NLC. Additionally, based on functionality assay of NLCs presented in the paper (cell grouping assay and phagocytosis assay), we confirmed a direct link between the protective role of NLCs and their M2 polarization state, thus confirming that indeed the 6-25 target is a specific marker of pro-tumoral NLC. At the same time, we still do not know if 6-25 have a direct role in pro-tumoral function of NLC, and what that role would be.

5 Study III) Determination of the 6-25 target

6-25 antibody was developed by hybridoma technology, using whole NLC for immunization procedure. This protocol allowed to obtain an antibody, against conformational epitope [242] of potentially unique antigen, but at the same time it created necessity for de novo identification of the target recognized by a given antibody. The initial identification of the 6-25 target was performed by combination of immunoprecipitation (IP) process combined with mass spectrometry (MS) analysis [155]. Briefly, the membrane fraction of NLC (that shown expression of the 6-25 target) were isolated and used for IP against agarose-protein A beads complexed with the 6-25 antibody or isotype control. Subsequently, the eluat from the IP was resolved by SDS-PAGE, protein bands were excised and analyzed by qualitative MS. List of proteins generated with the MS analysis was compared between the 6-25 and Isotype control group. In the process of selection, SFXN3 was chosen as a protein specifically detected in the 6-25 group. Results were further validated by western blot (WB) with whole cell lysates from NLC and human recombinant SFXN3 protein fragment. Immunodetection was performed with the 6-25 antibody and commercial anti-SFXN3 antibody, showing in both cases the signal corresponding to MW of SFXN3 (~35 kDa). It must be mentioned however, that the 6-25 mAb was giving a much weaker signal compared to commercial anti-SFXN3 antibody, even though it was used in higher concentration of (10 µg/mL vs 1µg/mL). Also for the staining with recombinant SFXN3, it was possible to detect the signal only after loading at least 100 ng of pure protein.

5.1 Invalidation of SFXN3 as the target of the 6-25 antibody

During the time of this thesis, we intended to further validate SFXN3 as the target of the 6-25 antibody. First, we performed another round of WB experiments, to confirm the previous findings, and test the 6-25 against the mouse version of the protein. It was important for us to know if the 6-25 antibody is specific

toward the mouse variant of SFXN3, as in perspective we planned to test therapeutic potential of 6-25 mAb in vivo. Comparison of the protein sequence between mouse and human variants of SFXN3 showed 93.8% identity, so there was a good chance that antibody will recognize both versions. We performed immunodetection of previously tested fragment of human recombinant SFXN3 and full length recombinant mouse SFXN3, with the 6-25 mAb and commercial anti-SFXN3 antibody as a positive control (Fig. 16).

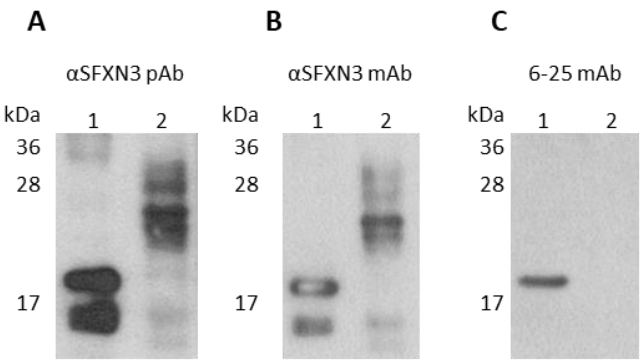

Figure 16. Western blot analysis of 1) fragment of human SFXN3 and 2) mouse SFXN3 recombinant protein*. A) 20 ng of recombinant protein, detection with 1ug/mL rabbit pAb; B) 20 ng of recombinant protein, detection with 1ug/mL of mouse mAb; C) 100 ng of recombinant protein, detection with 6-25 mAb.*

WB analysis revealed that, as expected, commercial antibodies recognized both human and mouse SFXN3. On the other hand, with the 6-25 antibody a dim band was detected only in case of human fragment of SFXN3. Additionally, with the 6-25 antibody signal was observed only using an extremely high amount of recombinant protein – 100 ng, and concentration of the antibody – 10 µg/mL. Next we performed the WB analyses on the lysates from M1- and M2-MDM, but failed to detect any signal with the 6-25 antibody (results not shown).

Based on the WB analyses, we concluded that the 6-25 antibody is specific to the antigen in native conformation, which is lost during downstream processing of the samples. In the end, we had to consider following limitations while further validating SFXN3 as the target of the antibody: 1) at the time we were unable to obtain SFXN3 KO in NLC or primary MDM; 2) the 6-25 works reliably in techniques not involving denaturation, like extracellular staining by flow cytometry or immunofluorescence; 3) commercial anti-SFXN3 antibodies are suitable for WB or

immunohistochemistry, involving antigen denaturation (most probably they recognize linear antigen) and they do not work in flow cytometry; 4) SFXN3 gene is expressed ubiquitously and its expression do not correlate with the 6-25 staining on the surface of the cells; 5) SFXN3 is a membrane protein, and its recombinant versions is likely lacking the native conformation required to study the interaction with the 6-25 by techniques like, surface plasmon resonance (e.g. Biacore).

To overcome these incompatibilities, we decided to try methods that could bypass limitations of both the 6-25 antibody and commercial antibodies against SFXN3, including:

1. immunoprecipitation (IP) of the M2-MDM lysates with the 6-25 antibody and subsequent detection of SFXN3 in the eluat by commercial antibody,
2. isolation of plasma membrane fraction from M2-MDM and detection of SFXN3 with commercial antibody,
3. immunofluorescence detection of intracellular SFXN3 with 6-25 and plasma membrane variant with commercial anti-SFXN3 antibodies.

Note: we were unable to immunoprecipitate SFXN3 with the 6-25 (1) and detect SFXN3 in plasma membrane fraction of M2-MDM (2) with commercial antibody (data now shown).

5.1.1 Immunofluorescence with the 6-25 mAb and commercial anti-SFXN3 antibodies

As both IP and plasma membrane isolation approaches failed in validating SFXN3 as a target of 6-25 antibody, we decided to perform immunofluorescence to attempt detection of mitochondrial SFXN3 with 6-25 antibody and plasma membrane staining with commercial anti-SFXN3 antibody in M2-MDM.

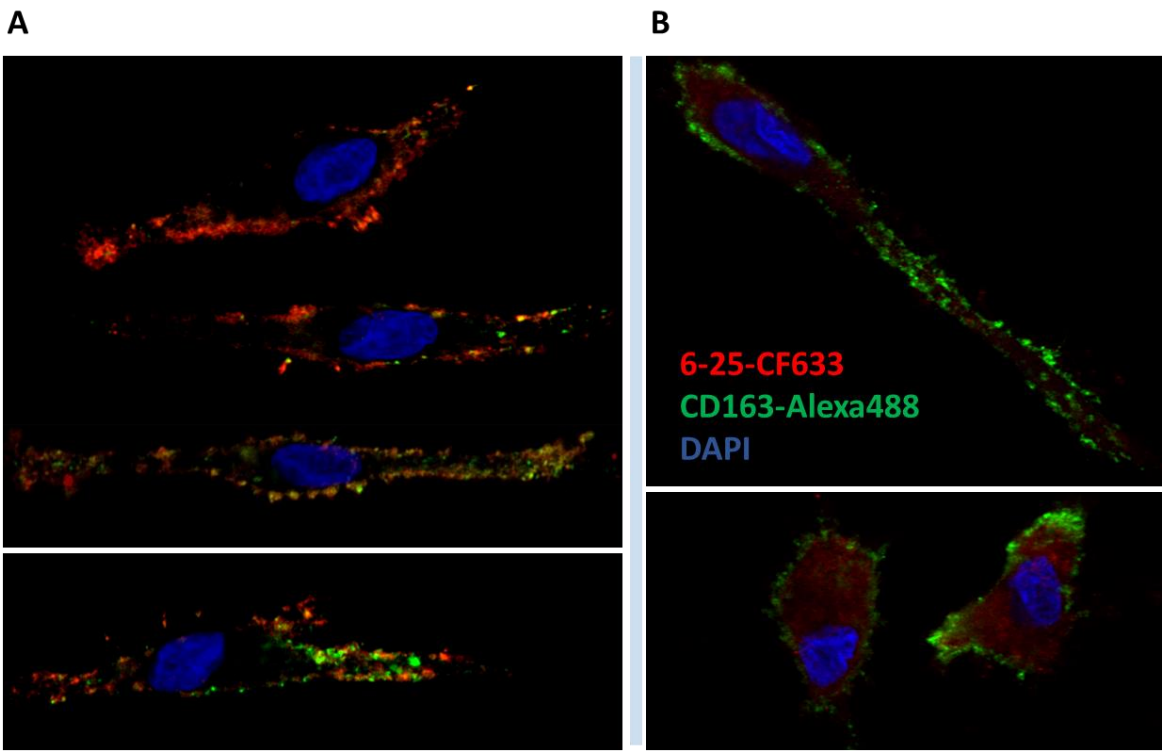

Figure 17. Extracellular and intracellular immunofluorescence labelling of M2-MDM with 6-25 Ab. *A) Plasma membrane staining in native conditions. B) Intracellular staining after fixation and permeabilization. Red signal – 6-25 mAb, green signal - CD163 mAb (control staining of plasma membrane), blue signal - DAPI. Images were acquired with Zeiss 880 confocal microscope, using x63 objective.*

M2-MDM were cultured on glass chamber slides. 8 days after plating cells were stained in the native condition (for plasma membrane staining) or following fixation and permeabilization (intracellular staining), and analyzed using confocal microscope (Fig. 17). Detection of plasma membrane signal with the 6-25 mAb was confirmed with CD163 co-staining (Fig. 17A). Interestingly, results showed only partial co-localization (indicated with orange patches). No signal from the 6-25 mAb detected after intracellular staining (Fig. 17B). Analysis in native conditions showed specific targeting of plasma membrane with the 6-25 mAb, as proved with α-CD163 co-staining. Results on Fig. 17A show M2-MDM co-stained with the 6-25 antibody and plasma membrane control – CD163. As expected, we detected the 6-25 staining localized to the surface of the cells as confirmed by CD163 signal. On the Fig. 17B we attempt to stain mitochondria with 6-25, however we failed to detect specific intracellular signal there. As

intracellular staining of mitochondria requires the sample fixation and permeabilization, we concluded that it might have hindered potential detection with the 6-25 antibody.

In the next set of experiments, 6-25 mAb was replaced with commercial anti-SFXN3 antibody. Results on the Fig. 18A and C, show intracellular signal with commercial antibody, that corresponds to mitochondrial staining. CD163 control signal, proved that there is no plasma membrane staining with anti-SFXN3 antibody (Fig. 18C). We also failed to detect any PM signal with anti-SFXN3 antibody when we stained the cells in native conditions (Fig. 18B).

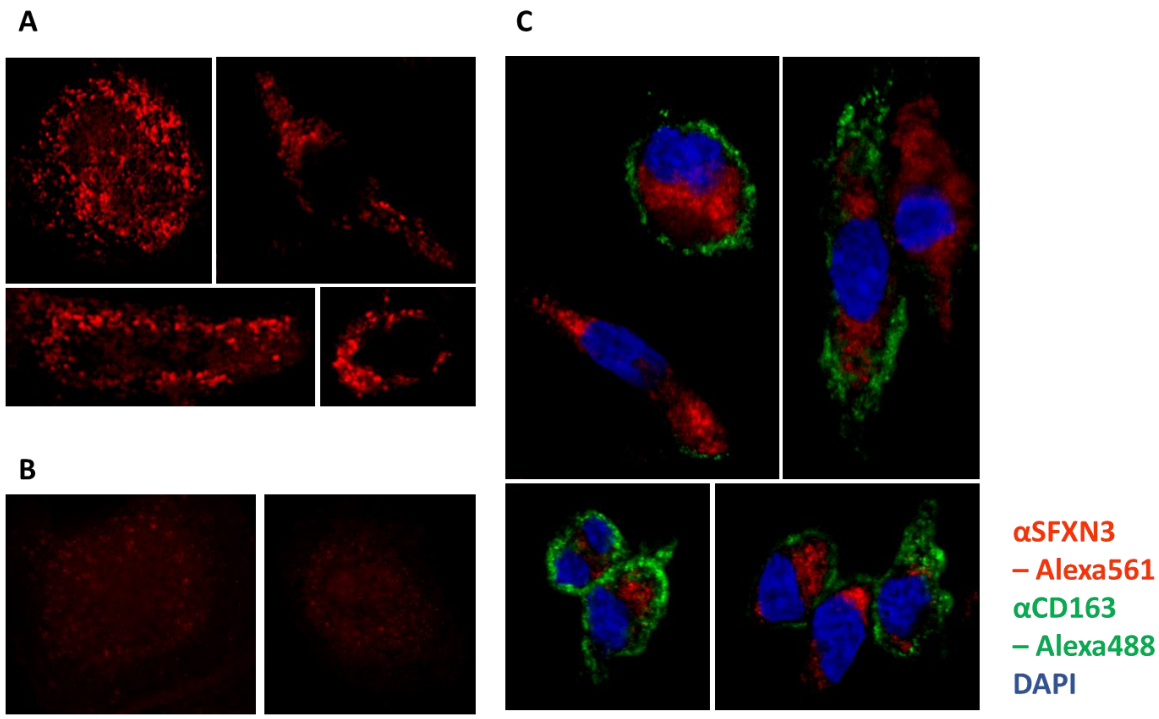

Figure 18. Intracellular and extracellular immunofluorescence labelling of M2-MDM with α-SFXN3 pAb*. A) Intracellular staining of mitochondria with anti-SFXN3 pAb. B) Plasma membrane staining with anti-SFXN3 antibody. C) co-staining of anti-SFXN3 antibody with plasma membrane marker CD163. Images were acquired with Zeiss 880 confocal microscope, using x63 objective.*

5.1.2 KO of SFXN3 in primary monocytes and macrophages, ultimate target invalidation

Previous failures in validation of SFXN3, raised serious concerns toward identity of 6-25 target. We knew that the best method to resolve these doubts, would be generation of gene KO in these cells. In order to do that, we incorporated we incorporated CRISPR-Cas9 ribonucleoprotein (RNP) electroporation technique, that finally allowed us to generate gene KO in primary myeloid cells.

To generate KO of SFXN3 in primary monocytes, three sgRNA targeting the gene of interest were combined for subsequent generation of RNP with Cas9. To increase the chances of the experiment, monocytes after negative and positive selection as well as CSF-1 activated MDM (at day 6 after plating) were used for electroporation. 5 days after the procedure, efficacy of the KO was evaluated by flow cytometry analysis of 6-25 staining, and by WB analysis of SFXN3 protein expression with commercial antibody (Fig. 19).

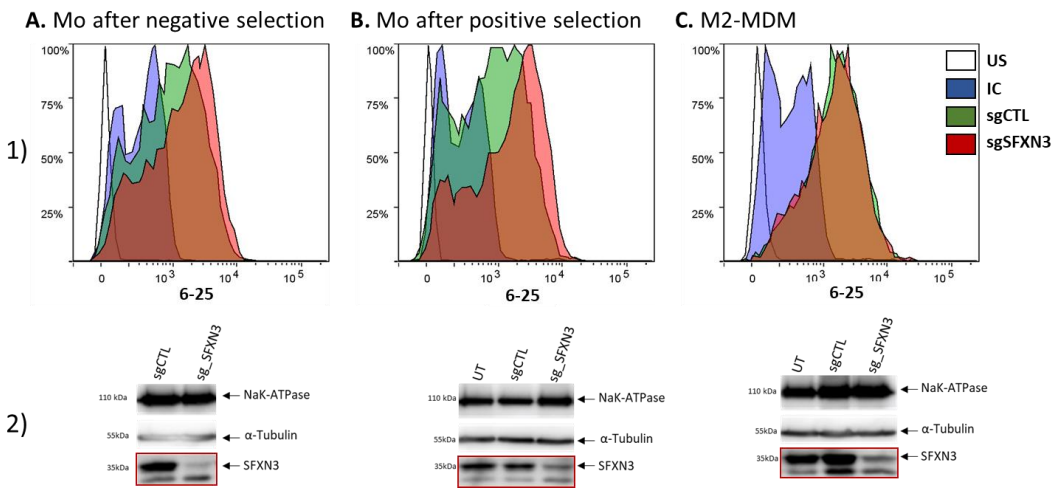

Figure 19. CRISPR-Cas9 KO of SFXN3 in primary monocytes and macrophages. *Monocytes (A, B) or M2-MDM (C) were electroporated with RNP targeting SFXN3 gene, and 5 days later analyzed by FC, after staining with 6-25 mAb (1) and by WB with anti-SFXN3 mAb (2). 1) US – unstained cells, IC – isotype control, SgCTL – sgRNA control, sgSFXN3 – sgRNA targeting SFXN3. 2) NaK-ATPase and α-Tubulin were used as a loading controls. Arrow indicates specific protein band.*

Based on flow cytometry analysis, no decrease in 6-25 staining in SFXN3 KO group was observed in comparison to cell treated with control sgRNA. On the other hand, WB results showed decrease of signal of SFXN3 protein in KO samples, confirming efficacy of the RNP-mediated KO. As downregulation of the SFXN3 gene did not affected staining of the 6-25 antibody, **SFXN3 was ultimately invalidated as a target of 6-25 antibody**.

The disqualification of SFXN3 as a target of 6-25 antibody required development of an alternative process aiming to identify a new target of the antibody.

5.2 Identification of a new target recognized by the 6-25 antibody

To evade possibility of another misidentification of 6-25 target, we decided to thoroughly retrace the initial analyses.

To re-evaluate the 6-25 target we have incorporated approaches:

1. indirect - RNA-seq based identification of differentially expressed genes (DEG) between control M2-MDM and cells treated with TNF (which abrogates expression of the 6-25 target),
2. direct – involving immunoprecipitation of M2-MDM lysates with 6-25 antibody combined with quantitative mass spectrometry.

Then we planned to combine results of both analyses and screen the list of potential target recognized by 6-25 antibody in CRISPR-Cas9 RNP-mediated KO of primary MDM.

5.2.1 Differential gene expression (DGE) analysis of MDM after treatment with TNF

According to optimization of MDM protocol (Study I), we knew that TNF abrogates expression of 6-25 target in CSF-1 activated cells. We decided to use this interaction and perform DEG analysis by RNAseq. Briefly, monocytes isolated from HD were activated with CSF-1, or combination of CSF-1 and TNF. After 8 days of culture, expression of 6-25 target was tested by FC (Fig. 20A).

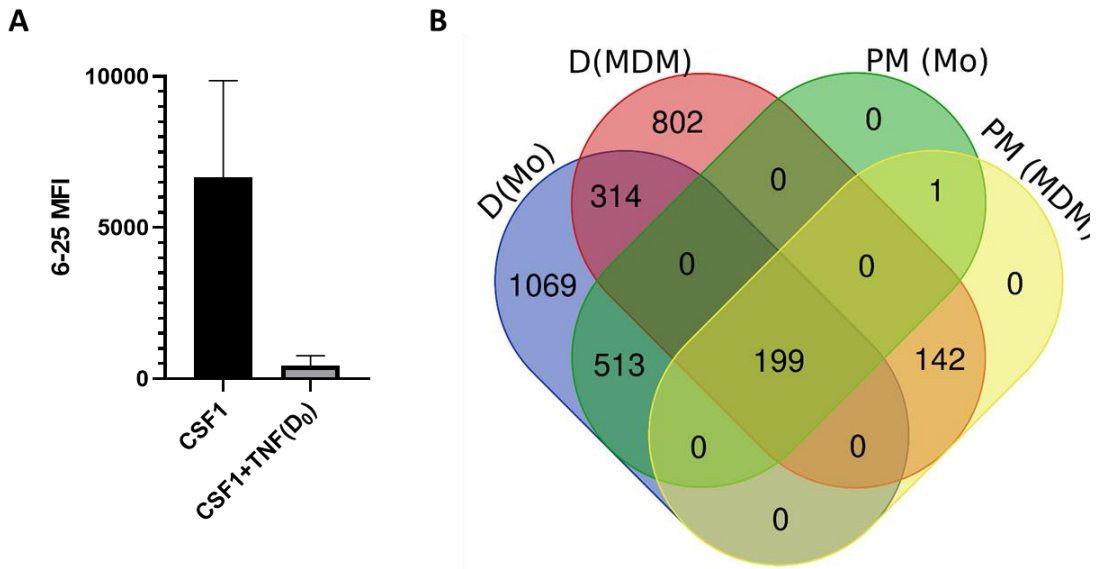

Figure 20. DEG analysis of plasma membrane-coding genes in CSF-1 activated-MDM treated with TNF*. A) Control of 6-25 target expression in MDM used for RNAseq analysis after treatment with TNF. Mean results for MDM from 4 different donors, used for further RNA extraction (MDM dataset). B) Venn diagram comparing 4 DEG lists: 2 from "MDM dataset" and 2 from GSE95588 data set ["Mo dataset"]. D(Mo) and PM (Mo) – list of all downregulated genes, and genes coding plasma membrane proteins respectively from Mo dataset; D(MDM), PM(MDM) – list of all downregulated genes, and genes coding plasma membrane proteins respectively from MDM dataset.*

After confirming downregulation of 6-25 target expression on TNF treated cells, RNA from the cells was extracted for subsequent RNAseq analysis. In order to perform quantitative analysis, RNA was extracted from MDM generated from 4 independent donors. Subsequently samples were analyzed by RNAseq, and data after processing ("MDM dataset") was used to perform DGE analysis. As a results of DEG analysis, list of significantly ($p < 0.001$) downregulated genes in TNF condition was extracted (list called D(MDM)). D(MDM) list, was then narrowed down to genes coding plasma membrane proteins (PM (DMD)). To increase the sensitivity of the analysis, analogous DGE analysis was performed on public data set (GSE95588) containing RNAseq results of monocytes activated for 24h with CSF-1 and another 24h with TNF. In the process additional two list of significantly downregulated genes in TNF conditions were generated – "D(Mo)" and "PM(Mo)". Finally, relation between all 4 gene lists were visualized with Venn diagram (Fig. 20B).

Comparison of 4 DGE lists, showed 199 genes coding plasma membrane proteins, that were commonly downregulated by the action of TNF in both datasets. One of this 199 gene was most probably responsible for expression of 6-25 target. We further defined the list based on the literature and experimental data on expression of various plasma membrane proteins.

5.2.2 Immunoprecipitation of M2 MDM membrane proteins with 6-25 antibody combined with quantitative mass spectrometry

After invalidation of the target, we come back to the results of initial IP-MS analysis that typed SFXN3 as protein recognized by the 6-25 antibody. We re-analyzed the list of remaining proteins and confronted them with the list of genes from RNA seq analysis (chapter 5.2.1) and data available in the literature. We did not find any potential candidates though. In this situation we decided perform a new IP-MS analysis for direct identification of the 6-25 target. First however, we wanted to confirm that 6-25 mAb is in fact recognizing protein antigen [243]. In order to do that, we generated the lysates from M2-MDM (after CSF-1 activation and IL-4 polarization) and subjected them to time-course of protease treatment. After inactivation of the proteases, we performed the dot blot analysis with the 6-25 detection (Fig. 21A).

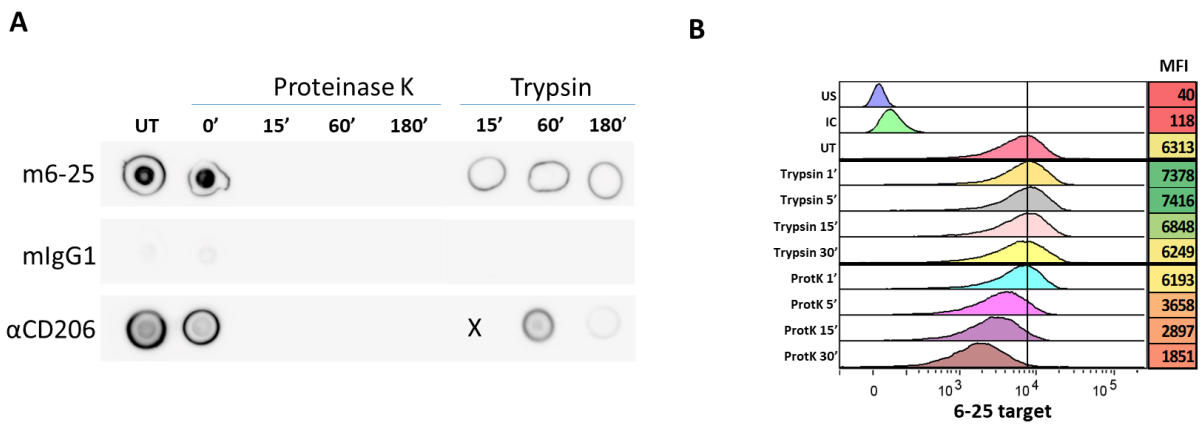

Figure 21. Confirmation of protein origin of the 6-25 target. *A) Dot blot analysis of the MDM lysates treated with Proteinase K or Trypsin. C) Flow cytometry analysis of the CSF-1 activated MDM treated with Trypsin of Proteinase K.*

Dot blot analysis revealed that a signal of 6-25 mAb in untreated samples, that is partially diminished with Trypsin and completely with Proteinase K. Analogical results were observed with anti-CD206 antibody, used as a positive control in the assay. These results confirmed protein nature of the 6-25 target. We also performed second analysis to further support this results, but this time we subjected intact M2-MDM to protease treatment schedule and analyzed the cells by flow cytometry (Fig. 21B). From that analysis we observed that Trypsin had a little effect on staining with 6-25 antibody, on the other hand Proteinase K led to strong decrease of the staining. We believe that weaker effect of proteases in flow cytometry analysis, may be caused be decreased availability of the proteins in intact plasma membrane compared to the lysate. Nevertheless, both analyses confirmed that the 6-25 is recognizing protein antigen. Additionally,

dot blot analyses showed that optimized lysis protocol, allowed to solubilize the target protein and preserve the binding with the 6-25 antibody, which was a crucial information for subsequent IP procedure.

Next, we decided to optimize the protocol of immunoprecipitation and downstream processing of the samples for MS. We used mouse 6-25 and matching isotype control for the procedure. For IP the same lysis protocol was used, as in case of dot blot analyses. After incubation of 6-25 or IC with the lysates antibodies were captured by magnetic Protein A beads. After extensive washing, samples were eluted with Laemmli buffer without reducing agent. For the downstream processing of the samples for MS, S-Trap™ spin column digestion protocol was used, instead of digestion of excised bands from SDS-PAGE analysis (which would more likely lead to loss of target protein in the process). To perform quantitative MS, 4 biological replicates for both 6-25 and IC control groups were used. As the result of the MS analysis, the list of significantly enriched proteins from both groups was obtained and results were plotted in the Volcano plot (Fig. 22).

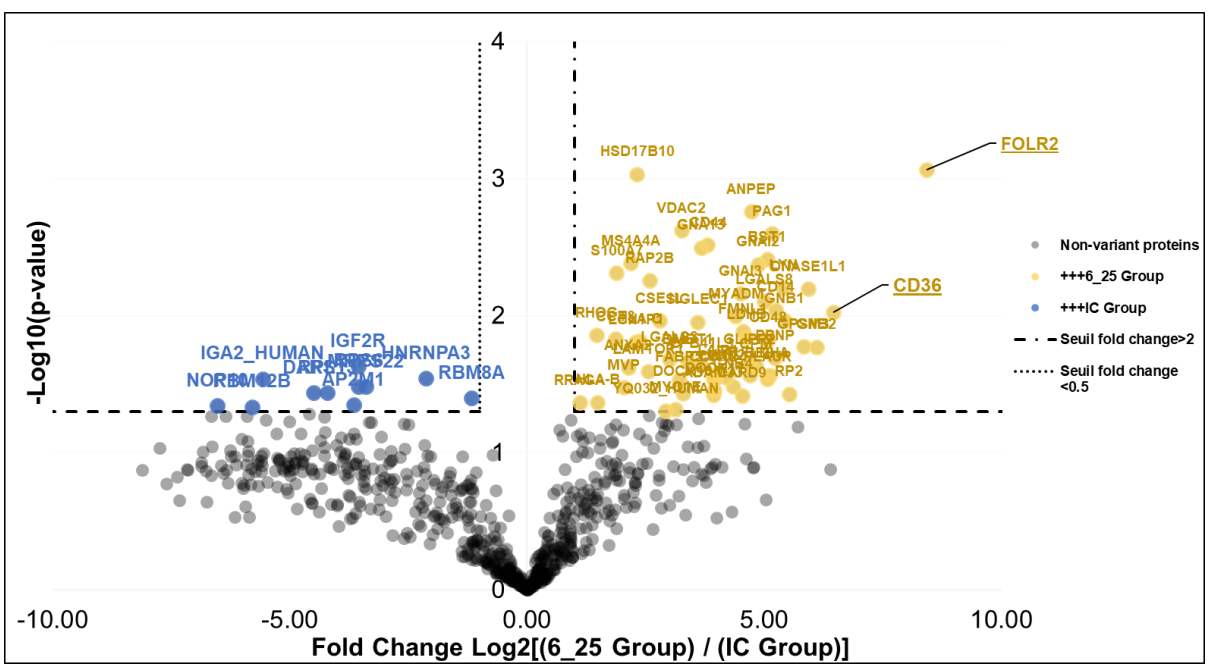

Figure 22. ***Volcano plot of proteins enriched in IP with 6-25 mAb****. Lysates from M2-MDM were used in IP procedure with 6-25 and IC antibodies. Eluates from IP, were analyzed by MS and identified proteins were used for differential quantitative analysis. Statistical analysis performed with T-test, p <0.05*

Overall 711 proteins were quantified during analysis, from which 6-25 group contained 59 significantly enriched protein compared to IC group. Moreover, most of the hits identified in the 6-25 group contained

membrane and in particular plasma membrane proteins, as oppose to IC group containing mostly nuclear proteins, which further validated the analysis.

By analyzing the lists obtained with IP-MS and RNAseq approach, we typed folate receptor β (abbreviation FRβ for protein and FOLR2 for the gene) and CD36 proteins as the most likely representing the target of 6-25 antibody.

5.2.3 Validation of the new 6-25 target

By combining the results from IP-MS and RNAseq approaches, FOLR2 and CD36 were typed as the most probable candidates recognized by the 6-25 mAb. Before performing gene KO in primary monocytes, two candidates were screened by flow cytometry.

5.2.3.1 *Comparison of the CD36 and FOLR2 with the 6-25 staining by FC*

In order to choose the more likely candidate for subsequent KO experiment we decided to first compare the staining of commercial α-FRβ and α-CD36 antibodies with 6-25 mAb. Thus we generated CSF-1 or GM-CSF activated MDM, treated with different M1 (TNF, IFNγ, LPS) or M2 (IL-4, IL-13, IL-10) agents in order to obtain cell selection with variable expression of the 6-25 target. Then, we stained the cells with previously mentioned mAbs and analyzed the samples by flow cytometry (Fig. 23).

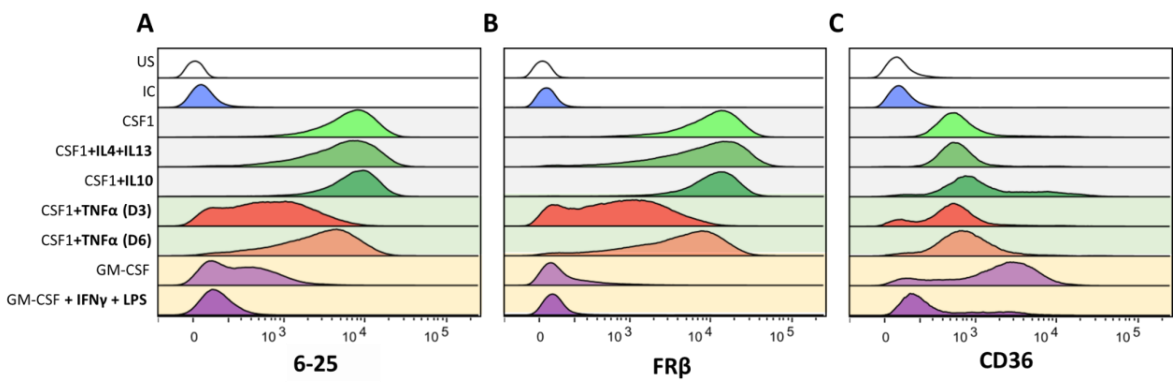

Figure 23. ***Comparison of staining of 6-25, αFRβ and αCD36 antibodies on MDM.*** *Human monocytes were activated with CSF-1 or GM-CSF, and polarized with M1 or M2 agents, to induce various subpopulations of M1 and M2 MDM. At day 8 cells were collected, stained with indicated antibodies and analyzed by FC. US – unstained cells, IC – isotype control.*

By comparing the results of the three staining, we observed that α-FRβ antibody is following the same pattern as the 6-25 antibody, irrespectively of the treatment. On the other hand, α-CD36 antibody showed

increased staining in GM-CSF-only activated MDM and no changes after TNF treatment. Hence, we chose FOLR2 to perform the KO experiments first.

5.2.3.2 *KO of FORL2 in primary monocytes and macrophages and ultimate target disqualification*

In the next step of validation of FOLR2, we performed RNP CRISPR Cas9 KO of the gene coding FOLR2 in primary monocytes, following analogical procedure as in case of SFXN3 gene. We isolated monocytes form HD, activated them with CSF-1 and the next day we performed RNP electroporation. This time we chose sgRNA against SFXN3 gene as a negative control of the test. 5 days after electroporation, we stained the cells with the 6-25 mAb or α-FRβ commercial antibody and analyzed the samples by flow cytometry (Fig. 24).

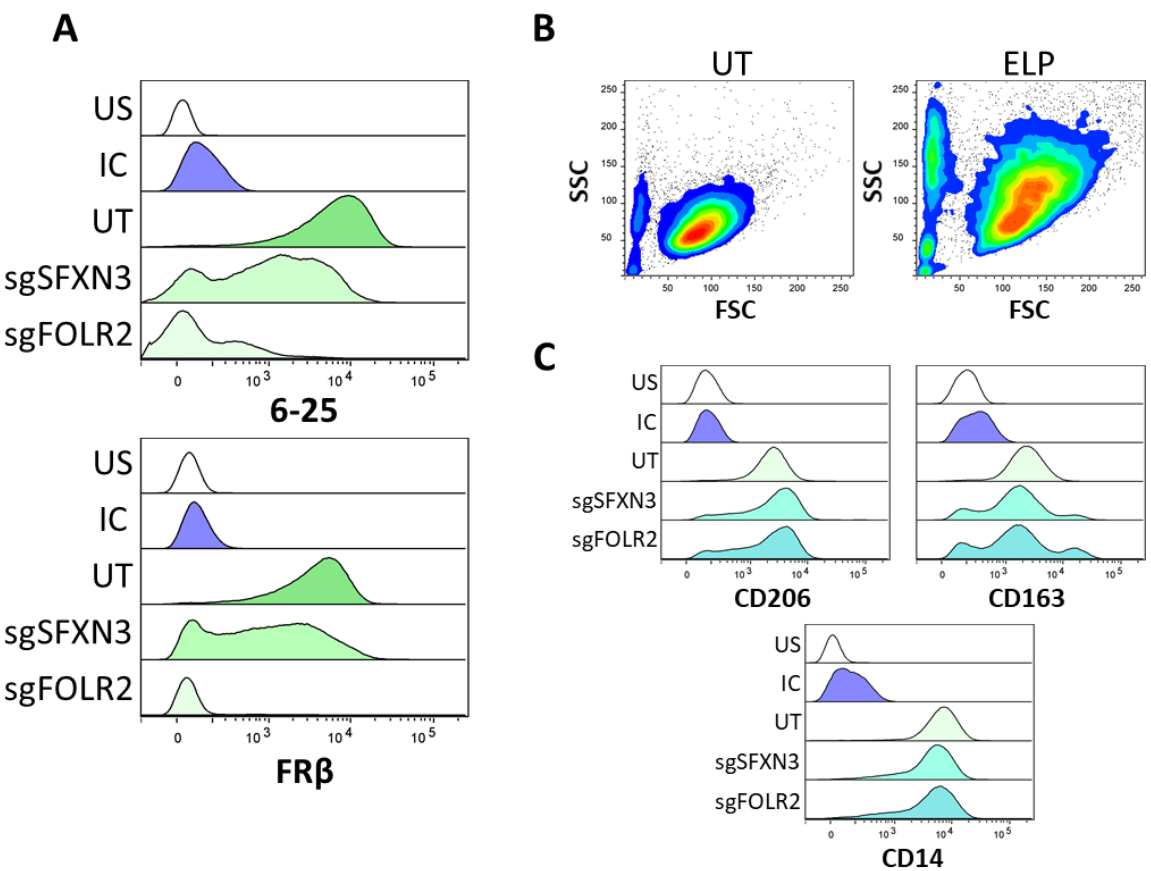

Figure 24. ***Validation of new 6-25 target by RNP mediated KO of FOLR2 gene in MDM.*** *Monocytes from HD were activated with CSF-1 for 24h and subsequently electroporated with RNP targeting FOLR2 gene. 5 days later cells were analyzed by FC, with 6-25 and α-FRβ (A). To account for electroporation stress, morphology (B) and phenotype (C) of UT and electroporated (ELP) cells were compared.*

Based on the flow cytometry analysis we observed abrogation of the staining with both 6-25 and commercial anti-FRβ antibody in FOLR2 KO cells, compared to SFXN3 KO control group (Fig. 24A). Additionally, downregulation of 6-25 and FRβ signal between UT and control electroporation (sgSFXN3) conditions was observed. As electroporation (ELP) is an aggressive procedure, the morphology (Fig. 24B) and phenotype (Fig. 24C) changes between UT and ELP cells were compared. It was noticed that ELP (even with control sgRNA) cause increase in size and granularity of the cells, and leads to comparable changes between FOLR2 and SFXN3 targeting sgRNA in expression of CD206, CD163 and CD14 markers. The specific decrease in the staining of anti-FRβ antibody and the 6-25 mAb in FOLR2 KO cells strongly suggested that **FRβ is the protein recognized by the 6-25 mAb**.

5.2.3.3 *Overexpression of FOLR2 gene in HEK-T cells*

To ultimately validate the FRβ as a target of the 6-25 antibody, FOLR2 was overexpressed in cell line with no expression of this gene. For this purpose, HEK-T cell line was chosen as these cells: do not express FOLR2 [244] and are susceptible to transfection. We chose to test three different transcripts variants of FOLR2 gene to additionally catch potential changes in staining between 6-25 and commercial anti-FRβ antibody, thus giving us potential information on the epitope recognized by 6-25 antibody. For transfection experiment, cells were plated 24h-prior the procedure in medium without antibiotics. Plasmid DNA transfection using Lipofectamine 2000 was performed according to manufacturer's protocol. 48h later cells were analyzed by FC, following staining with the 6-25 and α-FRβ antibodies (Fig. 25).

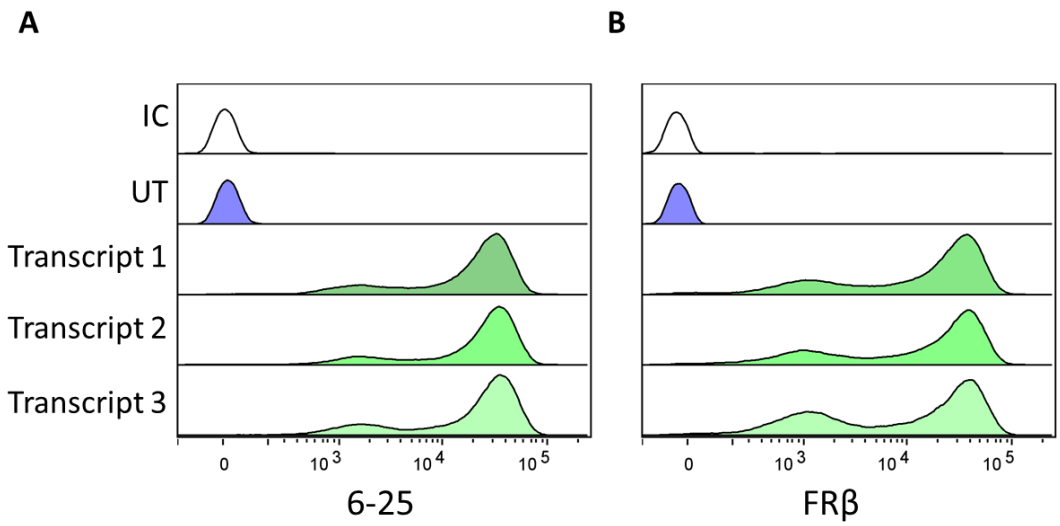

Figure 25. Overexpression of FOLR2 gene in HEK-T cell line. *HEK-T cells were transfected with plasmids coding different versions of FOLR2 gene, and analyzed by FC 48h later. Results presented as histogram plots of 6-25 (A) and α-FRβ (B) stained cells.*

Results of the flow cytometry analysis showed a strong signal with the 6-25 and anti-FRβ antibodies in cells transfected with each variant of the FOLR2 gene, in comparison to untreated cells (UT). These results were an ultimate confirmation that indeed, **the 6-25 antibody is recognizing FRβ protein**. Additionally, three different transcripts resulted in the same staining pattern for both 6-25 and anti-FRβ antibodies, indicating that the epitope recognized by both antibodies is localized in the common region of the three protein variants.

5.3 Conclusions

Identification of the 6-25 target – FRβ, has many implications for the future of the 6-25 mAb project. Not only FRβ was recently shown to be a M2 marker of macrophages, that could be used to target these cells [156–158], further validating our findings, but foremost it will allow us to study more directly and designedly the role of this protein in TAM, including NLC in CLL. Besides, it opens an opportunity to study "the 6-25 target" with various commercial tools, surpassing limitations of the 6-25 mAb in techniques involving protein denaturation, including WB or IHC.

It needs to be mentioned that validation of FRβ as a target of 6-25 mAb, was chronologically the most recent experiment presented in this thesis. Hence, all the results concerning 6-25 mAb specificity and functionality were designed and performed without this knowledge.

6 Study IV) Functionality of the 6-25 antibody

In between studies of expression of the 6-25 target in macrophages and identification target of the 6-25 antibody, we evaluated the functionality of the 6-25 antibody. It was crucial for us to know if naked 6-25 antibody: has an impact on viability of malignant and normal-human primary cells; can influence polarization of NLCs and MDM; can be internalized in the target cells (notably NLCs). These are all crucial parameters for pre-clinical evaluation of potential therapeutic antibody [245,246].

We had in our disposal two variants of 6-25 antibody, mouse and chimeric. Both with IgG1 isotype.

6.1 Effect of naked 6-25 antibody on the viability of the primary human cells

Evaluation of a toxicity is an essential step during drug development, and the situation is no different in case of therapeutic antibodies [247]. It is important to confirm that potential therapeutic antibody show toxic effect toxicity toward targeted cells, without affecting normal human cells (ideally). In case of the naked 6-25 mAb, its potential toxicity was evaluated on CLL and normal human PBMC, as well as M1 and M2 human MDM. First, the effect of the 6-25 mAb was studied on CLL cells and NLCs. In order to do that, CLL PBMC were cultured at 10×10^6 c/mL in the presence of 10 µg/mL of either mouse or chimeric version of the 6-25 mAb and matching isotype controls. The cultures were run for 12 days, and at day 8 and 12 viability of CLL cells was measured by flow cytometry with Annexin V/7-AAD staining, and cell concentration by haemocytometry (Fig 26). The flow cytometry analysis of CLL ($CD5^+$, $CD19^+$) cell viability, based on Annexin V/7-AAD staining, showed no statistical difference between PBMC cultured in the presence of either mouse or chimeric 6-25 mAb and corresponding isotype control MsIgG1 or HuIgG1 (Fig. 26A and 26B).

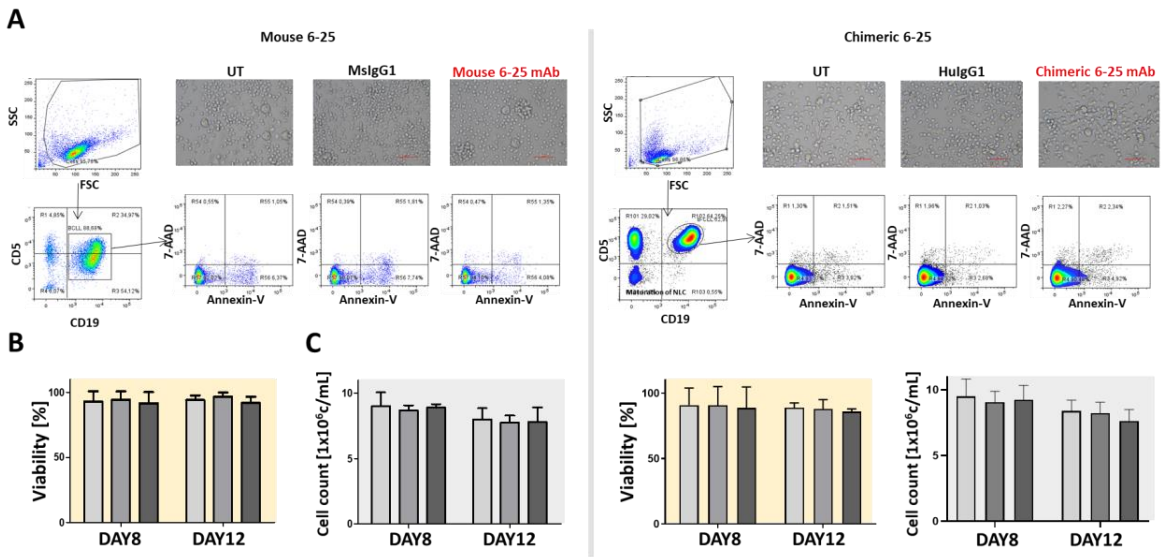

Figure 26. No toxicity of the 6-25 mAb toward CLL cells and NLCs. *PBMC isolated from CLL patients were cultured in vitro in the presence of mouse (left panel) or chimeric (right panel) version of 6-25 mAb and matching isotype controls, at the concentration of 10µg/mL. On day 8 and 12, cell concentration and viability were monitored by haemocytometer and flow cytometry (Annexin V/7-AAD staining) respectively. A) Gating strategy for evaluation of CLL cell viability with representative dotplot for: UT (untreated), Ms/HuIgG1 (mouse/human isotype control) and 6-25 conditions. Above dotplots, BF microscopy imaging of the culture at day 12 to confirmed presence of NLCs. B) statistical analysis of CLL cells viability based on 6 independent experiments. C) combined results of CLL PBMC cell concentration at day 8 and 12. Statistical analysis with one-way ANOVA showed no difference between tested groups (for p=0.05).*

Similarly, no effect on cell concentration was observed between treatment with 6-25 mAbs and corresponding isotype controls (Fig. 26 C). On the other hand, it was problematic to precisely evaluate the effect of the 6-25 mAb toward survival of NLC, as these cells usually represent ~0.5-2% of the whole culture, and their complete detachment requires scrapping (even after incubation with Trypsin) that inseparably damages the cells. Hence, the evaluation was limited to confirmation of the presence of NLC by the bright-field microscopy (BFM), considering distinct morphology of these cells, including increased size and adherence to plastic (Fig. 26 A). In the end no difference in NLC number was detected by BFM evaluation.

In the following series of experiments, we tested the effect of the 6-25 mAb on the viability of normal human PBMC. For that, PBMC were isolated from buffy-coats and plated at 1×10^6 c/mL. Then 10 µg/mL of either mouse or chimeric version of the 6-25 mAb and matching isotype controls were added to the cultures. Subsequently, the viability and cell number were measured at day 3, 6 and 9 of the culture. To evaluate effect of 6-25 antibody toward each of the main population of PBMC, the cells were first stained with anti-CD3, CD4, CD8, CD14 and CD56 antibodies, before incubation with Annexin V/7-AAD (Fig. 27).

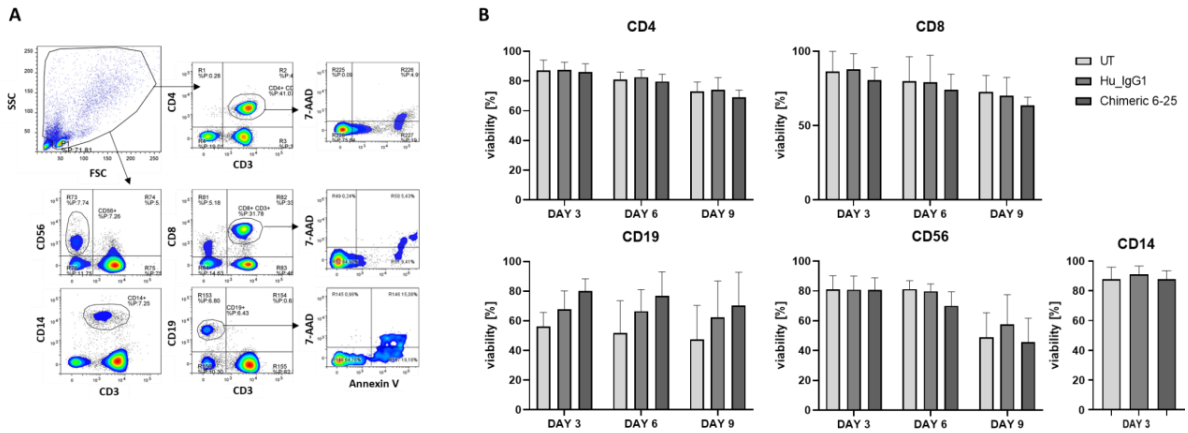

Figure 27. No toxicity of the 6-25 mAb toward healthy donor PBMC. *PBMC were cultured in vitro in the presence of chimeric 6-25 mAb and matching isotype control at the concentration of 10µg/mL, or left untreated. Cell viability was monitored by flow cytometry (Annexin V/7-AAD staining) on day 3, 6 and 9. A) Gating strategy for detection of 5 main cell subpopulation in PBMC. B) Analysis of combined data from FC assessment of cell viability by Annexin V/7-AAD staining. Statistical analysis with one-way ANOVA showed no difference between tested groups (for p=0.05). Legend: UT – untreated; HuIgG1 – human IgG1 isotype control antibody.*

Flow cytometry analysis of healthy donor PBMC (HD PBMC), showed no significant difference in viability of the indicated cell subpopulations, when cultivated in the presence of 6-25 mAb, isotype control or in untreated control. In case of monocytes we analyzed their viability only at day 3, as later they were attached strongly enough to hinder more precise flow cytometry analysis. BFM observations showed no clear difference in the population of these cells though (data not shown).

To account for incomplete results on 6-25 toxicity toward NLCs and monocytes in previous experiments, we performed 6-25 toxicity assay on M1 and M2 MDM, using Resazurin assay. M1 and M2 macrophages were prepared by activation of monocytes with GM-CSF and CSF-1 respectively and subsequent polarization with IFN-γ and LPS for M1 MDM, and IL-4, IL-13 for M2 MDM. At day 8 mature MDM were treated with either chimeric 6-25, human IC at 10 µg/mL or left untreated. 6 days later potential toxicity was evaluated by addition of Resazurin, followed by reading of the changes in the fluorescence for 24 h (Fig. 28).

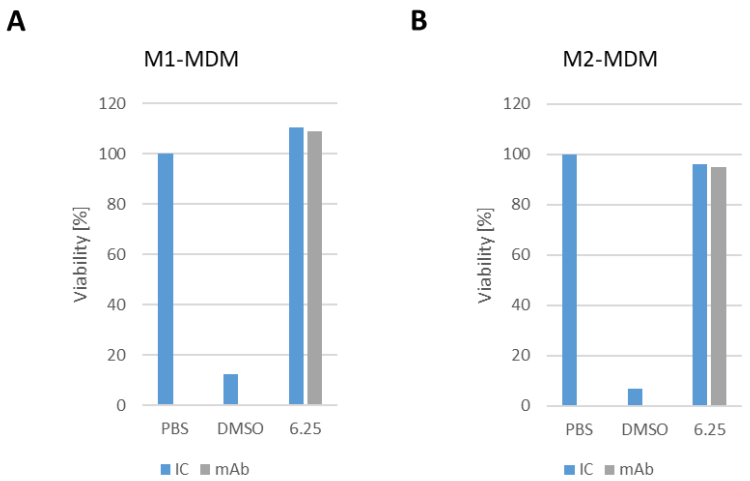

Figure 28. No toxicity of the 6-25 mAb toward M1 and M2-MDM. *M1 and M2-MDM were generated from HD monocytes. After 8 days of maturation, cells were treated with 10 µg/mL of chimeric 6-25 or isotype control. Additional PBS (UT condition) and 20% DMSO (to induce cell death) controls were used. After 6 days of treatment cells, Resazurine was added and fluorescence was measured for 24 h using plate reader. Bar plots show viability of cells calculated based on metabolic activity of the cells, normalized to PBS treated control. Results of 4 independent experiments for M1 (A) and M2 (B) MDM showed no statistical difference between 6-25 and control groups (for p=0.05).*

Both mouse and chimeric variants of 6-25 mAb showed no significant *in vitro* toxicity toward CLL and normal human PBMC and also M1 and M2-MDM.

6.2 Effect of naked 6-25 antibody on the maturation and polarization of macrophages

The next step in characterization of 6-25 functionality, was evaluation of its effect on maturation and polarization of NLCs. For that, we cultured CLL PBMC at 10×10^6 c/mL, and treated the cells with 10 µg/mL of the **mouse 6-25 mAb**. We tested two different approaches: 1) with cells treated at day 6, when NLC are already advanced in the maturation process, in order to evaluate potential effect of the antibody on the polarization of NLC; 2) at day 0, right after the beginning of the culture to evaluate the effect of the antibody on the maturation of NLCs. At day 13, phenotype of NLCs was analyzed by FC (Fig.29). Analysis of NLC from CLL cultures treated at day 6 (Fig. 29A), showed consistent staining with CD206, CD14, CD11c and HLA-DR between the cells cultured with the 6-25 antibody or isotype control. In case of CD163, DCSign (CD209), we observed very slight decrease in the signal and for CD16 increase in the signal in NLC cultured with the 6-25 mAb. In the end however, these changes were not significant.

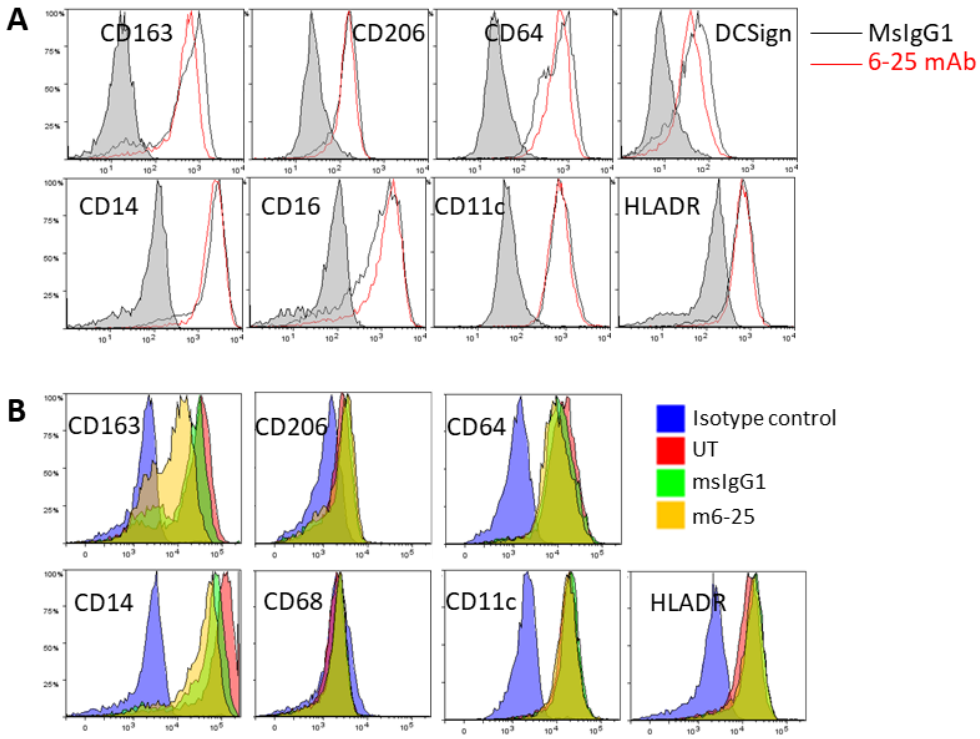

Figure 29. Effect of mouse 6-25 antibody on polarization (A) and maturation (B) of NLCs in vitro*. CLL PBMC were cultured at 10 × 10^6 c/mL with 10µg/mL of 6-25 mAb administrated from day 0 (A) or day 6 (B). Phenotype of NLCs was analyzed by FC. NLC were gated based on SSC/FSC parameters, and level of each marker was depicted as representative histogram.*

Analysis of phenotype of NLCs treated with 6-25 from day 0 (Fig. 29B), also showed consistent staining with CD206, CD11c and HLA-DR (Fig. 29B). Level of CD163, CD64 and CD14 was decreased in case of cells treated with the 6-25 mAb, however the effect was not significant (and not consistent between the donors). As evaluation of the NLCs phenotype was challenging in this setup, owing to low number of the cells (further decreased by low recovery of the cells during detachment), heterogeneity of the samples and potential effect of other cells from CLL PBMC (that represented > 97% of the overall population) we decided to further study effect of 6-25 antibody in MDM model, as it represents more basic and isolated environment, which also solves the problem of macrophages shortage.

We decided to evaluate the effect of the chimeric version of 6-25 mAb, as it is more relevant in case of human cells. We generated M1-MDM by GM-CSF activation for 6 days, followed by IFN-γ and LPS (LPS added 18h after IFN-γ) polarization for 2 days, and M2-MDM by CSF-1 activation for 6 days, followed by IL-4, IL-13 polarization for 2 days. Subsequently we treated the cells with 10 µg/mL of the 6-25 mAb for 3 days and analyzed the phenotype of the cells by flow cytometry. As we observed no changes in the

phenotype of M1-MDM upon the treatment (data not shown), we decided to further focus only on M2-MDM. We gathered the results from 9 independent experiments. To account for the heterogeneity between the phenotype of MDM from different donors, the MFI ratio of each tested marker was normalized to UT conditions for any given donor, and plotted together (Fig. 30)

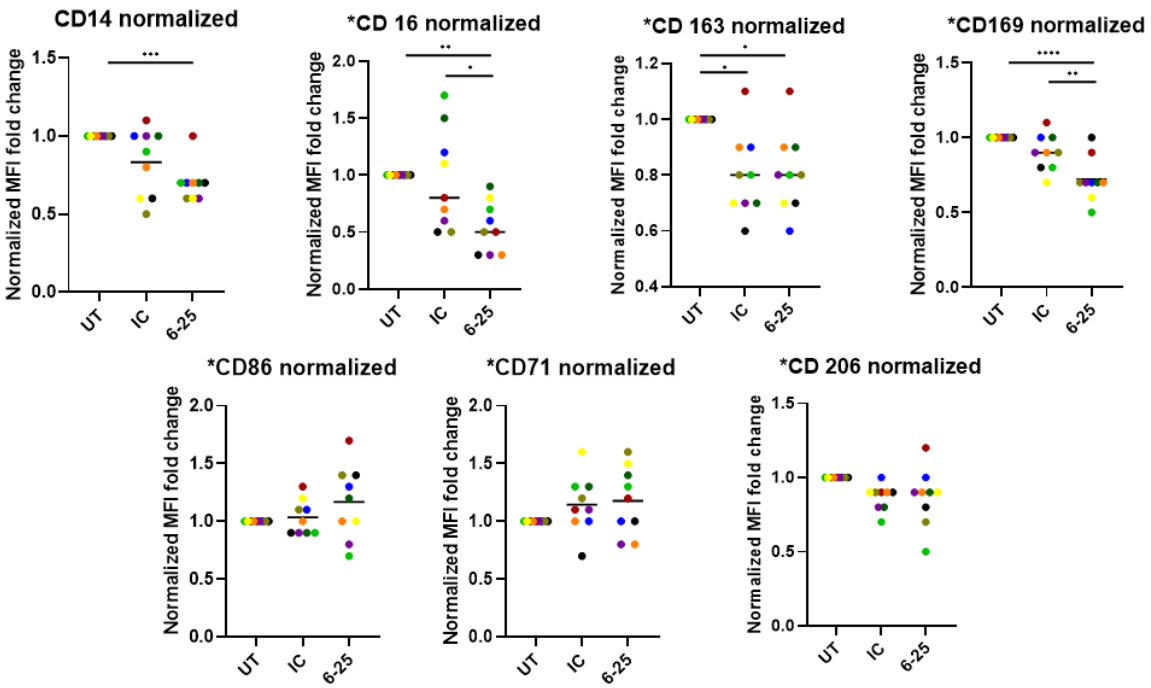

Figure 30. Chimeric 6-25 mAb cause changes in phenotype of mature M2 MDM. *$CD14^+$ cells isolated from healthy donor PBMC were activated for 6 days with 50ng/mL of CSF-1 and polarized for 2 days with 25 ng/mL of IL-4 and IL-13 into M2 MDM. Subsequently mature macrophages were treated or not (UT) for 3 days with 10ug/mL of 6-25 or corresponding isotype control (IC) and phenotype of the cells was analyzed by flow cytometry. Subsequently MFI of each tested sample was calculated and results of antibody treated groups were normalized to MFI of untreated cells from each independent experiment. Statistical analysis was performed with one-way ANOVA (*p<0.05, **p<0.01, ***p<0.005, ****p<0.001)*

Results presented on Fig. 30, show significant decrease of signal of CD16 and CD169 molecules upon the treatment with 6-25 mAb, compared to the UT and IC conditions. Level of CD14 and CD163 markers was also significantly decreased between UT and 6-25, but not 6-25 and IC conditions, which suggest that the effect is more specific to FC fragment of the antibodies (effect of 6-25 on CD14 decrease is much stronger, compared to IC though). Decrease of CD163 expression upon IgG1 administration was already reported [229]. Additionally, for some donors an increase in the expression CD86 was observed, upon administration of the 6-25 mAb, but the effect was not significant. As the CD14, CD16 and CD169 are overall associated with

M2 macrophages, the IgG1 version of chimeric 6-25 mAb showed to slightly depolarize M2-MDM to M1 side of the spectrum.

6.3 Internalization of 6-25 antibody

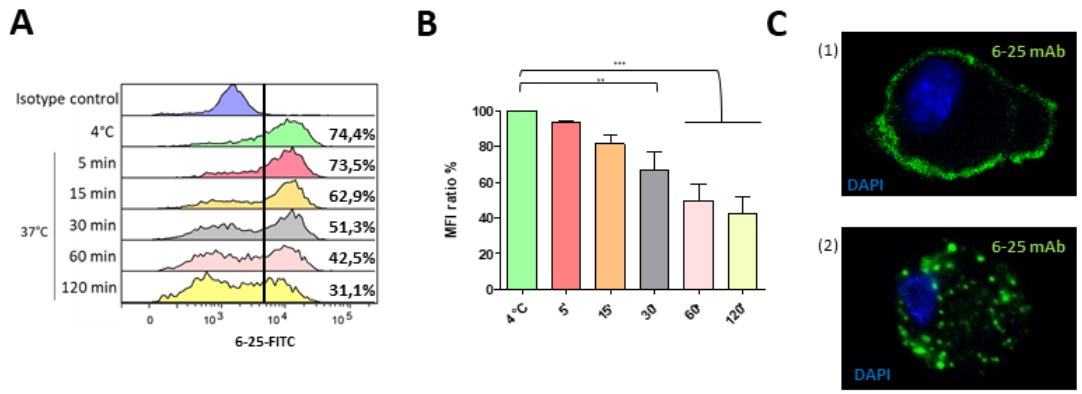

Figure 31. The 6-25 mAb is internalized by NLCs. *NLCs were incubated with 6-25 mAb, and incubated at 37°C for: 5', 15', 30', 1h and 2h. Subsequently cells were stained with II-antibody conjugated with fluorochrome and analyzed by FC; 4°C condition, used as a no-internalization control. A) Histograms with % of NLCs positive for 6-25, depending on incubation time at 37°C. B) Combined data from 5 independent experiments, represented by MFI ratio normalized to signal from 4°C control. Statistical significance calculated by one-way Anova. Confocal microscopy analysis (C) of 6-25 stained NLCs before (1) and after (2) two hours of incubation at 37°C.*

Another important functionality of the 6-25 we wanted to explore was internalization of the antibody in the NLC. To evaluate this phenomenon, we used in-house developed flow cytometry assay. Briefly, mature NLCs were collected, treated with FC block and incubated with unconjugated 6-25 mAb at 4°C. After extensive washing, cells were placed at 37°C to facilitate potential internalization for up to 2h. Subsequently cells were placed at 4°C and incubated with II-antibody conjugated with fluorochrome, to capture remaining 6-25 on the surface of the cells, and analyzed by FC.

The results presented on Fig 31. A) show decrease of the signal from 6-25 antibody, that depends on the incubation time at 37°C. Statistical analysis of normalized data from 5 independent experiments, confirmed significant decrease of 6-25 signal, already after 30 min of incubation at 37°C (Fig. 31B). To further complement FC results, we performed similar analysis using confocal microscopy. Slides with NLCs were stained with 6-25 conjugated with fluorochrome and incubated or not at 37°C. After samples were analyzed with confocal microscope. Pictures taken

after 1 min of incubation, show fluorescence signal from the 6-25 antibody, at the periphery of the cells. On the contrary, after 120 min of incubation, fluorescence can be detected in intracellular vesicles, further confirming internalization process (Fig. 31C).

Both flow cytometry and confocal microscope analyses confirmed that 6-25 antibody can be efficiently internalized in the NLCs.

6.4 Conclusions

Results presented in this chapter concern functionality of 6-25 target in the context of its effect on survival of primary human cells, polarization state of macrophages and internalization of antibody in the target cells. When tested on CLL and normal human PBMC, the 6-25 antibody showed no direct toxicity, leading to no changes in viability and cell concentration. While the antibody did not affect viability of the macrophages, it showed to modulate phenotype of M2 MDMs, by decrease of CD14, CD16 and CD169 markers. Finally, the 6-25 antibody turned out to be efficiently internalized in NLC. All of these characteristics indicated, that the 6-25 mAb might be a proper candidate for an antibody-drug conjugate (ADC) approach. And indeed, we generated the ADC versions of 6-25 antibody that was tested in the lab. Preliminary experiments indicated that 6-25-DC can selectively deplete M2 MDMs and NLCs in the *in vitro* cultures, without exerting toxic effect on healthy PBMC or M1 MDMs. These results are beyond the scope of this thesis however, and require additional development.

7 Discussion

TAMs belong to the major cell populations of TME [23,57], that not only support cancer cells in every step of tumor development [57], but are also regarded as one of the reasons for resistance of malignant cells to the treatment [78,95,102,103]. Multiple TAM-targeting strategies are currently in development or evaluation in I/II phases of clinical trials. The most advanced branch of these therapies revolves around targeting of CSF1R [78,95], one of the major receptors controlling biology of monocytes and macrophages [99]. Anti-CSF1R therapies were shown to deplete or reprogram TAMs in TME, leading to mixed clinical response [95,178,248]. At the same time, this receptor is also highly expressed by: monocytes, tissue-resident macrophages, and microglia, thus its targeting can lead to serious complications associated with decreased immunity, deregulation of the bone renewal [249] or neurotoxicity associated with microglia disruption [178]. This creates necessity to look for more specific markers of TAM and reduce toxicity of the potential therapeutic strategy (especially as TAM-targeting will most probably be part of combined therapy). With more specific targeting it will be also possible to deliver more potent drugs, that normally show unacceptable toxicity upon systemic administration.

The core results presented in this thesis revolves around the study of TAM-specific monoclonal antibody, called 6-25. 6-25 was previously generated by Team 09 of CRCT, using hybridoma technology with whole-cell immunization protocol, using NLCs as a model of TAM. This approach not only increased a chance to generate an antibody against an accessible epitope with native conformation, but also had a potential to find a novel target on NLCs [242]. Initial target identification and validation, typed SFXN3 as a molecule recognized by 6-25 mAb. SFXN3 is a poorly identified, inner-membrane mitochondrial protein, ubiquitously present in mammalian cell [250,251]. 6-25 mediated detection of this protein in plasma membrane of NLCs and other TAMs, represented not only a novel way of targeting these cells, but also showed a rare example of translocation of inner-membrane mitochondrial protein to plasma membrane of the cells. There are already examples of such phenomenon, notably as in the case of mitochondrial F1Fo-ATP synthase [252,253]. SFXN3 was also recognized to have a potential role in cancer. Recent findings identified SFXN3 to be an actor in one-carbon metabolism, as a transporter of serine [251], making it a potential receptor involved in supporting cancer cells in TME [254]. Moreover, a presence of αSFXN3 autoantibodies was reported in patients with squamous cell carcinoma [255]. As much as all these characteristics typed SFXN3 to be a very

attractive target for TAM targeting, in the course of this thesis growing body of evidence led us to initially doubt and ultimately **invalidate SFXN3 as a potential target recognized by 6-25 antibody**. Target disqualification was achieved thanks to CRISPR-Cas9 RNP mediated gene KO in primary MDM.

It is important to mention this technique, as primary macrophages represent problematic cells for gene manipulation, owing to their intrinsic ability to sense and destroy exogenous nucleic acid, initiate anti-viral response upon transduction procedure and general lack of proliferation [256,257]. RNP gene delivery is unique in that regard, as it ignores most of the mentioned obstacles [257], and is characterized by high efficiency with minimization of the negative effect on phenotype of the cells [256]. Adopting this technique, allowed us to easily generate gene KO in both primary monocytes and MDM, with acceptable changes to phenotype of the cells, at least in regard to surface marker expression, after CSF-1 activation (we will have to evaluate effect of this procedure on functionality of macrophages though). We used RNP technology not only to disqualify SFXN3 as a target of 6-25 mAb, but also **to validate a new target - FRβ**. We plan to further utilize RNP technology in studying FRβ in primary human macrophages, including NLCs.

Identification of FRβ has a huge implication for the future of 6-25 project, as it validates a lot of our previous findings. Additionally, FRβ represents a relatively recent discovery in the field of TAM targeting, giving us an opportunity for further studies (especially in the field of CLL).

7.1 Expression of FRβ

The gene family coding folate receptor consists of 4 members, FOLR1-4, that code FRα, FRβ, FRγ and FRδ respectively. All of these proteins show affinity to folic acid (high in case of FRα, FRβ) [258]. Both FRα and FRβ, are glycosylated proteins, attached to the plasma membrane of the cell through glycosylphosphatidylinositol (GPI) anchors [259]. FRα and FRβ are also the most relevant in the context of cancer. FRα is overexpressed on many human tumors, while FRβ shows expression mostly on activated macrophages [260] and myeloid leukemia cells [258,261]. Regarding macrophages, FRβ was reported to be highly expressed on TAM, found in: melanoma[262], breast cancer [262,263], colon cancer [263], hepatocarcinoma [264], lung squamous cell carcinoma, adenocarcinoma [259] and various mouse models of cancer [258,264,265]. Level of FRβ was shown to be correlated with higher stage of cancer and presence of LN metastases [260]. Moreover, expression of FRβ on TAM in a mouse model of ovarian cancer was reported to increase with cancer progression [258]. During the course of this thesis we also confirmed that NLCs show high expression of FRβ and that level of this protein is correlated with increased survival of CLL cells in vitro (chapter 4.2, Fig. 14).

In the context of autoimmune diseases, FRβ showed to be highly expressed on macrophages of patient with various autoimmune diseases, including: Crohn's disease, Ulcerative Colitis, Psoriasis, systemic lupus erythematosus [266], osteoarthritis (OA) and rheumatoid arthritis (RA) [267]. Besides, radiolabeled molecules specific to FRβ, showed that macrophages expressing this receptor are also enriched in atherosclerotic plaques [268]. All these findings signify connection of FRβ$^+$ macrophages with pathological inflammation. Nevertheless, FRβ$^+$ tissue-resident macrophages were also reported in normal tissues, like tonsils, colon and muscle[263]. Moreover, FOLR2 was shown to be highly expressed on the Hofbauer cells and to lesser extent in the Kupffer and Langerhans cells [244]. Expression of FRβ on healthy macrophages, especially on the Kupffer cells, needs to be carefully considered in case of potential targeted therapy.

Expression of FRβ$^+$ in macrophages was reported to be driven by CSF-1 signaling and maintained by IL-4 and IL-10. On the other hand, GM-CSF, IFN-γ and LPS were shown to downregulate this protein [262]. Additionally, PU.1 transcription factor was recently reported as an important element controlling expression of FOLR2 gene [263]. Another factor involved in control of folate transporters (including FRβ) is Activin A. This cytokine can be upregulated in GM-CSF activated MDMs, leading to downregulation of FRβ and overall promotion of M1 polarization in macrophages [269].

Mentioned results on the role of CSF-1 and other cytokines on expression of FRβ are in perfect agreement with our findings presented upon study of 6-25 target/FRβ$^+$ expression in MDM model (chapter 5.3). In the future, we consider further research on a signaling pathway driving expression FRβ. Our DEG analysis of CSF-1 activated MDMs treated with TNF (chapter 5.2.1), showed that PI3K-ATK-mTOR pathway to be most likely responsible for controlling expression of FOLR2. We also performed some preliminary results to validate this hypothesis. We confirmed that wide spectrum inhibitor – Ly294002 and specific mTOR inhibitor – Rapamycin, lead to dose-dependent downregulation of FRβ in primary monocytes and MDM. However, further tests with compounds specific to different isoforms of class I PI3K did not give us much clarification, and would require further experiments (data not shown). Especially given the complexity of PI3K-ATK-mTOR pathway, which represents one of the master regulators of many crucial cellular processes [260]. Considering that expression of FRβ is abrogated by the action of LPS, TNF and IFN-γ (chapter 3.3.3, fig. 9), finding genes commonly downregulated in these three conditions. It might provide a more precise answer, compared to our previous DGE analysis (chapter 4.2.1). Alternatively, single cell study, for example in a form of spatial transcriptomic could also help in typing the genes controlling FOLR2 expression.

Finally, FRβ pool in the cell is distributed between extra- and intracellular compartments [258,270], this is an aspect that we never considered during study on polarization of macrophages. Therefore, it is not clear if M1 agents like LPS, TNF and IFN-γ cause only gene downregulation, or also internalization of the receptor. It would be important to also establish how stable is an intracellular pool of FRβ, after treatment with M1 agents. That would also stress the importance of distinction between extra- and intra-cellular staining, especially in techniques less precise in distinguishing between both compartments, like IHC.

7.2 Phenotype of FRβ$^+$ macrophages

Most studies classify FRβ$^+$ macrophages as M2-like, anti-inflammatory cells with high expression of CD163 [259,262,263]. In the context of cancer, FRβ$^+$ TAM were shown as immunosuppressive subpopulation, with increased secretion of IL-10 and defective production of proinflammatory cytokines (including: GM-CSF, IL-1α, IL-1β, IL-12p70, or IL-23) upon stimulation with LPS. Consistently with cytokine expression profile, these macrophages were shown to inhibit antigen-specific T cell functions [258]. This is in agreement with another study that connected FOLR2 expression with MS4A6A, LILRB5, CD209, CD163, C1QC, a geneset characteristic for immunosuppressive macrophages [263]. We also confirmed that FRβ$^+$ NLCs are characterized with an overall M2-like phenotype (chapter 4.2, Fig. 15), ability to attract CLL cells (chapter 4.3, Fig. 1E) and perform efferocytosis (chapter 4.3, Fig. 2D).

In autoimmune diseases like osteoarthritis (OA) and rheumatoid arthritis (RA), researchers confirmed increased infiltration of FRβ^{high}, CD163$^+$ and FRβ^{dim}, CD163$^-$ macrophages. Both of these populations were characterized with high phagocytosis capacity (based on a dextran uptake). Additionally, authors showed that both FRβ$^+$ and CD163$^+$ macrophages can acquire mixed M1/M2 phenotype, based on the expression of TNF, iNOS (M1 signature) and IL-10, TGF-β (M2 signature), concluding that FRβ and CD163 markers, are not enough to classify polarization state of macrophages [267]. However, these results were performed only by 3 color IHC, with analysis of either CD163 or FRβ with M1 (TNF, iNOS) or M2 (IL-10, TGF-β) markers. It is well established, that polarization of macrophages is a continuum between M1-M2 side of the spectrum, and co-expression of classical M1 and M2 markers, such as TNF, iNOS and IL-10,TGF-β can be observed in some M2 macrophages [230,271]. In our studies, we observed that NLCs subjected to high doses of TNF, were able to maintain their M2-like/pro-tumoral phenotype, as long as they were co-treated with IL-10 (chapter 4.3), signifying an importance of interplay between various cytokines.

7.3 Role of folate and FRβ in macrophages

Folate (folic acid, vitamin B9) is an essential nutrient for humans, and plays a role in one-carbon metabolism, DNA synthesis and cell proliferation [269]. Folate was shown to be a donor of methyl groups and contribute to inflammatory responses of monocytes and macrophages, by downregulating expression of pro-inflammatory genes, including interleukin 1β and TNF [272]. Prolonged treatment with folic acid (synthetic form of folate) showed decreased production of pro-inflammatory cytokines in humans [272]. Another study indicated that folic acid diminished expression of TNF, IL-6, CSF-1, and CCL2 in GM-CSF activated M1 MDM upon LPS stimulation [269].

Role of FRβ in macrophages is still not entirely clear. The receptor is obviously responsible for binding of folate, and its high expression in M2-like macrophages suggest involvement in preservation of this phenotype. Especially as FRβ^{high} cells were shown to accumulate folate more efficiently, compared to M1-like macrophages, and folate was shown to blunt inflammatory responses [263]. This hypothesis is further supported by finding that Activin A, cytokine released by among others, GM-CSF activate macrophages that leads to downregulation of FOLR2 [269]. Besides, FRβ might have a role in modulation of macrophage adhesion, by functional interaction with CD11b/CD18 that in turn led to decreased attachment to collagen[273]. Another potential role of FRβ could be associated with bacterial microbiota. Many bacteria in the gastro-intestinal tract are responsible for synthesis of folate, and there FRβ could help in sensing the uncontrolled overgrowth of microbes [263].

7.4 Current state of FRβ-centered therapies

There are various characteristics that make FRβ a promising therapeutic target. This protein is exclusively expressed on myeloid cells, in particular on M2-like, immunosuppressive macrophages, connected with pathological inflammation [262,263]. In the context of cancer, these cells are shown to display protumoral functionality and their presence is correlated with bad prognosis and disease progression [258,260,262,263]. Additionally, FRβ shows high affinity to folate and undergo quick internalization upon binding of this vitamin, making it a great tool to deliver therapeutic agents into the target cells [258]. All these yield multiple therapeutic strategies, targeting FRβ in cancer and auto-immune diseases.

We can differentiate different therapeutic approaches in targeting FRβ in cancer. One of them resolves around an α-FRβ monoclonal antibody, called “m909” that showed ADCC-mediated efficacy in elimination of primary human TAM and AML cells in dose-dependent manner *in vitro*. Additionally, authors

demonstrated that m909 mAb treatment has a considerable impact on tumor growth in the humanized mouse model of AML, even without additional transfer of human NK cells [261]. In another study, authors used chimeric antigen receptor (CAR)-T cells, to selectively eliminate FRβ$^+$ TAM in the syngeneic mouse model of ovarian cancer. Targeting of FRβ$^+$ TAM, led in turn to increased infiltration with CD8$^+$ cytotoxic T-cells and tumor regression, further showing importance of TAM in immunosuppression. Also, authors stressed importance of targeting of FRβ$^+$ as preparative adjuncts, before administration of classical immunotherapies, to observe synergistic effect of both treatments [258]. Another approach, utilized FRβ$^+$ antibody fragment (Fv), coupled with *Pseudomonas exotoxin A*, to form immunotoxin specific toward cells expressing FRβ$^+$. This approach led to not only elimination of TAM, but also decreased tumor growth in the xenograft glioma mouse model [274]. Another study involved folate-modified lipoplex delivering BIM-s plasmid to FR expressing cells in a model of lung cancer. BIM stands for BCL-2-interacting mediator of cell death, which is a potent inducer of apoptosis. Administration of lipoplex with BIM-s plasmid turned out to effectively eliminate TAM and reduce tumor growth [259].

Compared to cancer treatment, targeting of FRβ in autoimmune diseases has an even longer history. It utilizes analogous strategies, including monoclonal antibodies [272], immunotoxins [275] and folic acid-drug conjugates [270,276]. Targeting of FRβ is these diseases demonstrated normalization of pathological inflammation, departure of pro-inflammatory cells, and symptom improvement in disease like rheumatoid arthritis (RA) [272,275,276].

Finally, different folate-conjugates are utilized to visualize either FRβ$^+$ macrophages or FRα$^+$ cancer cells. Compounds like [^{99}mTc]EC20[266] and [1^{8}F]fluoro-PEG-folate[277] have been successfully used to monitor active disease in joints affected with RA. Folate-conjugates with near-infrared fluorophores, are also tested for fluorescence-guided cancer-resection surgeries, showing positive results in case of superficial imaging [270].

All these promising results support the FRβ targeting in cancer, both as a mono- and combination therapy. Moreover, imaging techniques utilizing folate-conjugates confirm selectivity of potential treatment to pathological tissues. Hopefully soon we will be able to see the first clinical trials involving FRβ-targeting.

7.5 Perspectives for study of therapeutic potential of 6-25 mAb

As mentioned previously, all the results presented in this manuscript were designed and performed without knowledge of real specificity of 6-25 mAb. Hence we would like to discuss some of them from the perspective of FRβ, and propose possible improvements.

During our research we confirmed specificity of 6-25 mAb toward NLCs (Chapter 3.1.1), AML cell lines (3.2) and CSF-1 activated macrophages (3.3). Available data on FRβ expression further validated our finding. Especially encouraging is confirmation of FRβ expression on TAMs from various human cancers [273]. As we have an access to neoplastic tissues from various human hematological cancers (thanks to cooperation with Universitaire du Cancer de Toulouse-Oncopole (IUCT-O)), we could try to study FRβ$^+$ TAMs in these malignancies, especially as the most of a data in this topic is focused on TAM in solid tumors sources.

Furthermore, we would like to continue deciphering the role of FRβ in CLL. Since we confirmed that FRβ is a marker of protective NLCs, we want to investigate potential involvement of this receptor in their protumoral activity. First we plan to evaluate an effect of FOLR2 KO on functionality of NLCs, especially ability to attract cancer cells and perform efferocytosis. Next, we would like to study an influence of folate deficiency on the CLL PBMC culture dynamics. It would be interesting to establish if there is an effect of folate on polarization of NLCs, as it was previously reported that this vitamin can blunt proinflammatory responses in macrophages [269,272]. Regarding CLL cells, folate was recently revisited as an important metabolite in various leukemia. Confirmation of CLL cell lines sensitivity to antifolate therapy (with methotrexate) further supports this hypothesis [278]. We suggest that NLCs could potentially serve as a reservoir of folate for cancer cells. We plan to evaluate this hypothesis using fluorescent conjugates of folate. First, we would like to confirm that NLCs can actually accumulate folate, and if so establish if they can share it with cancer cells. Trogocytosis was reported before as a process involved in interaction between NLCs and CLL cells [206]. Perhaps it is also involved in the potential delivery of folate. Moreover, folate was shown to be especially important for dividing cells [269]. Since these cells do not proliferate in normal CLL PBMC setup, we could stimulate their division with CpG oligodeoxynucleotide and IL-15 [279].

With folate studies in the CLL PBMC model, we could also re-evaluate our experiments on functionality of 6-25 mAb (chapter 6.2). Admittedly, our previous results showed an unclear effect of 6-25 on phenotype of NLCs, and no effect on viability of CLL cells. This time, we could study if 6-25 mAb can block binding of folate to FRβ on NLCs or disrupt transfer of this metabolite to cancer cells. Also using confocal microscopy, we could study an effect of the antibody on the contact between NLCs and CLL cells.

Apart from standard IgG1 version of 6-25 antibody, we have also ADCC enhanced, FC silent and two antibody-drug conjugate (ADC) versions at our disposal. As mentioned previously, we already performed some in vitro experiments with DC-6-25 which showed high selectivity only toward cells expressing FRβ. In the case of the ADCC enhanced version of 6-25, we are planning to first perform experiments in vitro on AML and M2-MDM as target cells. After positive results in vitro, we are going to evaluate the efficacy of all 6-25 variants in vivo, either in monotherapy or in combination with immune checkpoint blockade, or classical chemotherapy. In our current approach we are mostly interested in studying elimination of TAM with 6-25 mAb. Nevertheless, by exploring other possible subclasses of IgG1 we could potentially cause repolarization of TAM instead [130].

Another crucial aspect for continuation of the 6-25 mAb project, is confirmation of 6-25 specificity toward mouse macrophages. Human and mouse FRβ share 81% similarity (based on alignment of aa sequences), which especially for monoclonal antibodies might result in lack of cross-reactivity or decreased affinity. Previously we were trying to evaluate specificity of 6-25 toward mouse BMDM and TAM from mouse tumors, but we never obtained a signal comparable to staining on human cells. At the same time, we did not have positive control for expression of the target of our antibody. For this reason, we plan to validate specificity of 6-25 toward a mouse version of FRβ, using commercial anti-FRβ antibody. Potential recognition of mouse FRβ by 6-25 antibody, would greatly ease in vivo experiments in mice, giving us freedom in choosing a mouse model of cancer. In vivo experiments will be necessary to further establish therapeutic potential of 6-25 mAb. However, if 6-25 mAb turns out to be unable to recognize the mouse version of the protein, we can still study its efficacy in vivo using a humanized model of AML. This approach was successfully used with other FRβ-targeting therapy [261].

7.5.1 Prognostic value of FRβ and 6-25 mAb in CLL

Previously our group showed that soluble CD163 can serve as indicator of NLCs burden and predictive marker of bad prognosis in CLL [214]. Considering that we found FRβ to share similar specificity as CD163 to mark protective NLCs, it would be interesting to also evaluate its prognostic value in clinical samples. First it would be necessary to confirm presence of soluble form of FRβ in plasma of the patients or supernatant of CLL PBMC cultures. Since soluble form of FRα was reported before [280] and both isoforms share structural similarity (including, being GPI-anchored to the plasma membrane [259]), there is a high chance that FRβ could also occur outside of the cells. This test could be easily made by direct or sandwich ELISA with 6-25 and commercial anti-FRβ antibodies or with use of surface plasmon resonance (e.g. BIAcore), given that

the structure of FRβ is preserved. Otherwise, detection could be made with WB or MS. In an optimistic scenario (there is a soluble form of FRβ and its concentration in plasma can be easily measured), we are going to evaluate the prognostic value of FRβ and soluble FRβ and compare it with other established markers like CD163.

Besides, we also need to analyze our current data from CLL PBMC cultures in respect to clinical data of the patients. Perhaps we could find a correlation between NLCs phenotype in vitro (expression of FRβ) and clinical picture of CLL.

8 Bibliography

1. Whiteside, T. L. The tumor microenvironment and its role in promoting tumor growth. *Oncogene* **27**, 5904–5912 (2008).
2. Balkwill, F. & Mantovani, A. Inflammation and cancer: back to Virchow? *Lancet* **357**, 539–545 (2001).
3. Akhtar, M., Haider, A., Rashid, S. & Al-Nabet, A. D. M. H. Paget's "seed and Soil" Theory of Cancer Metastasis: An Idea Whose Time has Come. *Adv. Anat. Pathol.* **26**, 69–74 (2019).
4. Valkenburg, K. C., De Groot, A. E. & Pienta, K. J. Targeting the tumour stroma to improve cancer therapy. *Nat. Rev. Clin. Oncol.* **15**, 366–381 (2018).
5. Jin, M. Z. & Jin, W. L. The updated landscape of tumor microenvironment and drug repurposing. *Signal Transduct. Target. Ther.* **5**, (2020).
6. Ramamonjisoa, N. & Ackerstaff, E. Characterization of the tumor microenvironment and tumor-stroma interaction by non-invasive preclinical imaging. *Front. Oncol.* **7**, 28–37 (2017).
7. Hanahan, D. & Weinberg, R. a. Hallmarks of cancer: The next generation. *Cell* **144**, 646–674 (2011).
8. Laplane, L., Duluc, D., Bikfalvi, A., Larmonier, N. & Pradeu, T. Beyond the tumour microenvironment. *Int. J. Cancer* **145**, 2611–2618 (2019).
9. Dvorak, H. F. Tumors: wounds that do not heal. Similarities between tumor stroma generation and wound healing. *N. Engl. J. Med.* **315**, 1650–9 (1986).
10. Westerbeck, C. & Meyerowitz, J. Bystander. *Art B.* **2**, 24a-24a (1995).
11. Dvorak, H. F. Tumors: Wounds That Do Not Heal--A Historical Perspective with a Focus on the Fundamental Roles of Increased Vascular Permeability and Clotting. *Semin. Thromb. Hemost.* **45**, 576–592 (2019).
12. Dvorak, H. F. Tumors: Wounds that do not heal-redux. *Cancer Immunol. Res.* **3**, 1–11 (2015).
13. Riss, J. *et al.* Cancers as wounds that do not heal: Differences and similarities between renal regeneration/repair and renal cell carcinoma. *Cancer Res.* **66**, 7216–7224 (2006).
14. Suijkerbuijk, S. J. E. & Rheenen, J. Van. From good to bad : Intravital imaging of the hijack of physiological processes by cancer cells. *Dev. Biol.* **428**, 328–337 (2017).
15. Freire, M. O. & Van Dyke, T. E. Natural resolution of inflammation. *Periodontol. 2000* **63**, 149–164 (2013).
16. Greten, F. R. & Grivennikov, S. I. Inflammation and Cancer: Triggers, Mechanisms, and Consequences. *Immunity* **51**, 27–41 (2019).
17. Medzhitov, R. Origin and physiological roles of inflammation. *Nature* **454**, 428–435 (2008).

18. Zhao, H. *et al.* Inflammation and tumor progression: signaling pathways and targeted intervention. *Signal Transduct. Target. Ther.* **6**, (2021).

19. Balkwill, F., Charles, K. A. & Mantovani, A. Smoldering and polarized inflammation in the initiation and promotion of malignant disease. *Cancer Cell* **7**, 211–217 (2005).

20. Galdiero, M. R., Marone, G. & Mantovani, A. Cancer inflammation and cytokines. *Cold Spring Harb. Perspect. Biol.* **10**, (2018).

21. Mantovani, A., Allavena, P., Sica, A. & Balkwill, F. Cancer-related inflammation. *Nature* **454**, 436–444 (2008).

22. Allavena, P., Garlanda, C., Borrello, M. G., Sica, A. & Mantovani, A. Pathways connecting inflammation and cancer. *Curr. Opin. Genet. Dev.* **18**, 3–10 (2008).

23. Sica, A., Allavena, P. & Mantovani, A. Cancer related inflammation: The macrophage connection. *Cancer Lett.* **267**, 204–215 (2008).

24. Trafford, A. M., Parisi, R., Kontopantelis, E., Griffiths, C. E. M. & Ashcroft, D. M. Association of Psoriasis with the Risk of Developing or Dying of Cancer: A Systematic Review and Meta-analysis. *JAMA Dermatology* **155**, 1390–1403 (2019).

25. Wang, K. & Karin, M. *Tumor-Elicited Inflammation and Colorectal Cancer*. *Advances in Cancer Research* **128**, (Elsevier Inc., 2015).

26. Brassart-Pasco, S. *et al.* Tumor Microenvironment: Extracellular Matrix Alterations Influence Tumor Progression. *Front. Oncol.* **10**, 1–13 (2020).

27. Binnewies, M. *et al.* Understanding the tumor immune microenvironment (TIME) for effective therapy. *Nat. Med.* **24**, 541–550 (2018).

28. Quail, D. F. & Joyce, J. A. Microenvironmental regulation of tumor progression and metastasis. *Nat. Med.* **19**, 1423–1437 (2013).

29. Wynn, T. A., Chawla, A. & Pollard, J. W. Macrophage biology in development, homeostasis and disease. *Nature* **496**, 445–455 (2013).

30. Ginhoux, F., Schultze, J. L., Murray, P. J., Ochando, J. & Biswas, S. K. perspective New insights into the multidimensional concept of macrophage ontogeny , activation and function. **17**, (2016).

31. Ginhoux, F. & Garel, S. The mysterious origins of microglia. *Nat. Neurosci.* **21**, 897–899 (2018).

32. Ajami, B., Bennett, J. L., Krieger, C., Tetzlaff, W. & Rossi, F. M. V. Local self-renewal can sustain CNS microglia maintenance and function throughout adult life. **10**, 1538–1543 (2007).

33. Passlick, B., Flieger, D. & Ziegler-heitbrock, H. W. L. Ã. Identification and Characterization of a Novel Monocyte Subpopulation in Human Peripheral Blood. *Blood* **74**, 2527–2534 (1989).

34. Patel, A. A. *et al.* The fate and lifespan of human monocyte subsets in steady state and systemic inflammation. 1–11 (2017).

35. Gautier, E. L. & Yvan-charvet, L. Understanding macrophage diversity at the ontogenic and

transcriptomic levels. 85–95 (2014).

36. Amit, I., Winter, D. R. & Jung, S. review The role of the local environment and epigenetics in shaping macrophage identity and their effect on tissue homeostasis. **17**, (2016).

37. Hulsmans, M. *et al.* Macrophages Facilitate Electrical Conduction in the Heart Article Macrophages Facilitate Electrical Conduction in the Heart. 510–522 (2017). doi:10.1016/j.cell.2017.03.050

38. Odegaard, J. I. *et al.* Article Alternative M2 Activation of Kupffer Cells by PPAR d Ameliorates Obesity-Induced Insulin Resistance. (2008). doi:10.1016/j.cmet.2008.04.003

39. Kohyama, M. *et al.* Role for Spi-C in the development of red pulp macrophages and splenic iron homeostasis. *Nature* **457**, 318–321 (2008).

40. Bruggen, R. Van. Of macrophages and red blood cells ; a complex love story. **5**, (2014).

41. Den Haan, J. M. M. & Kraal, G. Innate immune functions of macrophage subpopulations in the spleen. *J. Innate Immun.* **4**, 437–445 (2012).

42. Yoshimura, T. *et al.* Non-myeloid cells are major contributors to innate immune responses via production of monocyte chemoattractant protein-1 / CCL2. **4**, 1–7 (2014).

43. Anbazhagan, K., Duroux-richard, I., Jorgensen, C. & Apparailly, F. Transcriptomic Network Support Distinct Roles of Classical and Non-Classical Monocytes in Human. 470–489 (2014). doi:10.3109/08830185.2014.902453

44. Laskin, D. L., Sunil, V. R., Gardner, C. R. & Laskin, J. D. Macrophages and Tissue Injury : Agents of Defense or. 267–288 (2013). doi:10.1146/annurev.pharmtox.010909.105812.Macrophages

45. Martinez, F. O., Sica, A., Mantovani, A. & Locati, M. Macrophage activation and polarization. *Front. Biosci.* **13**, 453–461 (2008).

46. Macrophages, M.-M.- *et al.* M-1/M-2 Macrophages and the Th1/Th2 Paradigm 1. (2000).

47. Xue, J. *et al.* Transcriptome-Based Network Analysis Reveals a Spectrum Model of Human Macrophage Activation. *Immunity* **40**, 274–288 (2014).

48. Merad, M., Jung, S. & Amit, I. by the Local Microenvironment. **159**, 1312–1326 (2015).

49. Mould, K. J. *et al.* Single cell RNA sequencing identifies unique inflammatory airspace macrophage subsets Single cell RNA sequencing identifies unique inflammatory airspace macrophage subsets. **4**, (2019).

50. Kawai, T. & Akira, S. review The role of pattern-recognition receptors in innate immunity : update on Toll-like receptors. *Nat. Publ. Gr.* **11**, 373–384 (2010).

51. Mantovani, A. *et al.* The chemokine system in diverse forms of macrophage activation and polarization. **25**, (2004).

52. Vannella, K. M. & Wynn, T. A. Mechanisms of Organ Injury and Repair by Macrophages ∗. 1–25 (2016). doi:10.1146/annurev-physiol-022516-034356

53. Olingy, C. E. *et al.* Non-classical monocytes are biased progenitors of wound healing macrophages

during soft tissue injury. *Sci. Rep.* 1–16 (2017). doi:10.1038/s41598-017-00477-1

54. Martinez, F. O. *et al.* Genetic programs expressed in resting and IL-4 alternatively activated mouse and human macrophages : similarities and differences. (2013). doi:10.1182/blood-2012-06-436212

55. Vogel, D. Y. S. *et al.* Macrophages in inflammatory multiple sclerosis lesions have an intermediate activation status. 1–12 (2013).

56. Pettersen, J. S. *et al.* NIH Public Access. **131**, 1322–1330 (2012).

57. Mantovani, A., Marchesi, F., Malesci, A., Laghi, L. & Allavena, P. Tumour-associated macrophages as treatment targets in oncology. *Nat. Rev. Clin. Oncol.* **14**, 399–416 (2017).

58. Schreiber, R. D., Old, L. J. & Smyth, M. J. Cancer immunoediting: Integrating immunity's roles in cancer suppression and promotion. *Science (80-.).* **331**, 1565–1570 (2011).

59. Linde, N. *et al.* Vascular endothelial growth factor-induced skin carcinogenesis depends on recruitment and alternative activation of macrophages. **1**, 17–28 (2012).

60. Nandi, B. *et al.* Stromal CCR6 drives tumor growth in a murine transplantable colon cancer through recruitment of tumor-promoting macrophages. *Oncoimmunology* **5**, 1–11 (2016).

61. Manuscript, A. Cellular and Molecular Origin of Tam. *Changes* **29**, 997–1003 (2012).

62. Griffith, B. T. S. *et al.* Necrosis Factor – related Cytokine , TRAIL. *Cell* **189**, (1999).

63. De, I. *et al.* CSF1 Overexpression Promotes High-Grade Glioma Formation without Impacting the Polarization Status of Glioma-Associated Microglia and Macrophages. **76**, 2552–2561 (2016).

64. Li, D. *et al.* Tumor-associated macrophages secrete CC-chemokine ligand 2 and induce tamoxifen resistance by activating PI3K / Akt / mTOR in breast cancer. 47–58 (2020). doi:10.1111/cas.14230

65. Zhao, P. *et al.* Response gene to complement 32 (RGC-32) expression on M2-polarized and tumor-associated macrophages is M-CSF-dependent and enhanced by tumor-derived IL-4. **32**, 1–8 (2014).

66. Tripathi, C., Tewari, B. N. & Kanchan, R. K. Macrophages are recruited to hypoxic tumor areas and acquire a Pro-Angiogenic M2-Polarized phenotype via hypoxic cancer cell derived cytokines Oncostatin M and Eotaxin. **5**, (2014).

67. Solinas, G. *et al.* Tumor-Conditioned Macrophages Secrete Migration-Stimulating Factor: A New Marker for M2-Polarization, Influencing Tumor Cell Motility. (2014). doi:10.4049/jimmunol.1000413

68. Sica, A. *et al.* Autocrine Production of IL-10 Mediates Defective IL-12 Production and NF- κ B Activation in Tumor-Associated Macrophages. (2015). doi:10.4049/jimmunol.164.2.762

69. Sa, L., Estecha, A., Samaniego, R., Sa, S. & Sa, P. The chemokine CXCL12 regulates monocyte-macrophage differentiation and RUNX3 expression. **117**, 88–98 (2016).

70. Doedens, A. L. *et al.* Macrophage Expression of Hypoxia-Inducible Factor-1 α Suppresses T-Cell Function and Promotes Tumor Progression. 7465–7476 (2010). doi:10.1158/0008-5472.CAN-10-1439

71. Ito, M. *et al.* Tumor-Derived TGF β -1 Induces Dendritic Cell Apoptosis in the Sentinel Lymph Node. (2015). doi:10.4049/jimmunol.176.9.5637

72. Kato, Y. *et al.* Lenvatinib plus anti-PD-1 antibody combination treatment activates CD8 + T cells through reduction of tumor-associated macrophage and activation of the interferon pathway. 1–18 (2019).

73. Takenaka, M. C. *et al.* Control of tumor-associated macrophages and T cells in glioblastoma via AHR and CD39. *Nat. Neurosci.* **22**, 729–740 (2019).

74. Chen, C. *et al.* Induced expression of B7-H4 on the surface of lung cancer cell by the tumor-associated macrophages : A potential mechanism of immune escape. *Cancer Lett.* **317**, 99–105 (2012).

75. Prima, V., Kaliberova, L. N., Kaliberov, S., Curiel, D. T. & Kusmartsev, S. expression in tumor-associated macrophages and myeloid-derived suppressor cells. 2–7 (2016). doi:10.1073/pnas.1612920114

76. Kuang, D. *et al.* Activated monocytes in peritumoral stroma of hepatocellular carcinoma foster immune privilege and disease progression through PD-L1. **206**, 1327–1337 (2009).

77. Lievense, L. A. *et al.* Pleural Effusion of Patients with Malignant Mesothelioma Induces Macrophage-Mediated T Cell Suppression. *J. Thorac. Oncol.* (2016). doi:10.1016/j.jtho.2016.06.021

78. Wang, N. *et al.* Research trends in pharmacological modulation of tumor-associated macrophages. *Clin. Transl. Med.* **11**, (2021).

79. Lu, T. *et al.* Tumor-infiltrating myeloid cells induce tumor cell resistance to cytotoxic T cells in mice. **121**, 4015–4029 (2011).

80. Hung, K. E., Datz, C., Feng, Y. & Fearon, E. R. products drive IL-23 / IL-17-mediated tumour growth. (2012). doi:10.1038/nature11465

81. Kong, L. *et al.* Deletion of interleukin-6 in monocytes / macrophages suppresses the initiation of hepatocellular carcinoma in mice. *J. Exp. Clin. Cancer Res.* 1–11 (2016). doi:10.1186/s13046-016-0412-1

82. Jung, M., Mertens, C. & Tomat, E. Iron as a Central Player and Promising Target in Cancer Progression. 1–18 doi:10.3390/ijms20020273

83. Qian, B. & Pollard, J. W. Review Macrophage Diversity Enhances Tumor Progression and Metastasis. 39–51 (2010). doi:10.1016/j.cell.2010.03.014

84. Wen, Z. *et al.* Increased metabolites of 5-lipoxygenase from hypoxic ovarian cancer cells promote tumor-associated macrophage in fi ltration. 1–12 (2014). doi:10.1038/onc.2014.85

85. Lin, L. *et al.* CCL18 from tumor-associated macrophages promotes angio - genesis in breast cancer. **6**, (2015).

86. Wang, R. *et al.* Lung Cancer Tumor-associated macrophages provide a suitable microenvironment for non-small lung cancer invasion and progression. *Lung Cancer* **74**, 188–196 (2011).

87. Hong, L., Wang, S., Li, W., Wu, D. & Chen, W. Pathology - Research and Practice Tumor-associated macrophages promote the metastasis of ovarian carcinoma cells by enhancing CXCL16 / CXCR6 expression. *Pathol. - Res. Pract.* 0–1 (2018). doi:10.1016/j.prp.2018.07.009

88. Chen, J. *et al.* CCL18 from Tumor-Associated Macrophages Promotes Breast Cancer Metastasis via PITPNM3. *Cancer Cell* **19**, 541–555 (2011).

89. Liu, L. *et al.* Upregulation of IGF1 by tumor-associated macrophages promotes the proliferation and migration of epithelial ovarian cancer cells. *Oncol. Rep.* **39**, 818–826 (2018).

90. Yang, M. *et al.* Microvesicles secreted by macrophages shuttle invasion-potentiating microRNAs into breast cancer cells. *Mol. Cancer* **10**, 6–10 (2011).

91. Gao, L. U., Zhang, W. E. I., Zhong, W. E. N. Q. U. N., Liu, Z. J. U. E. & Li, H. U. I. M. I. N. Tumor associated macrophages induce epithelial to mesenchymal transition via the EGFR / ERK1 / 2 pathway in head and neck squamous cell carcinoma. 2558–2572 (2018). doi:10.3892/or.2018.6657

92. Fu, X. T. *et al.* Tumor - associated macrophages modulate resistance to oxaliplatin via inducing autophagy in hepatocellular carcinoma. *Cancer Cell Int.* 1–11 (2019). doi:10.1186/s12935-019-0771-8

93. Lebdai, S. *et al.* Potentiating vascular-targeted photodynamic therapy through CSF1R modulation of myeloid cells in a preclinical model of prostate cancer. *Oncoimmunology* **8**, 1–10 (2019).

94. Of, R., Microenvironment, T. H. E., Chronic, I. N. & Leukaemia, L. Role of the microenvironment in chronic lymphocytic leukaemia. 380–388 (2003).

95. Ceci, C., Atzori, M. G., Lacal, P. M. & Graziani, G. Targeting tumor-associated macrophages to increase the efficacy of immune checkpoint inhibitors: A glimpse into novel therapeutic approaches for metastatic melanoma. *Cancers (Basel).* **12**, 1–32 (2020).

96. Peranzoni, E., Lemoine, J., Vimeux, L., Feuillet, V. & Barrin, S. Macrophages impede CD8 T cells from reaching tumor cells and limit the efficacy of anti – PD-1 treatment. (2018). doi:10.1073/pnas.1720948115

97. Panni, R. Z. *et al.* Agonism of CD11b reprograms innate immunity to sensitize pancreatic cancer to immunotherapies. **9240**, (2019).

98. Domagala, M. *et al.* Cancer cells resistance shaping by tumor infiltrating myeloid cells. *Cancers (Basel).* **13**, 1–30 (2021).

99. Mun, S. H., Park, P. S. U. & Park-Min, K. H. The M-CSF receptor in osteoclasts and beyond. *Exp. Mol. Med.* **52**, 1239–1254 (2020).

100. Ma, X., Zhang, Y., Wang, S., Wei, H. & Yu, J. Immune checkpoint inhibitor (ICI) combination therapy compared to monotherapy in advanced solid cancer: A systematic review. *J. Cancer* **12**, 1318–1333 (2021).

101. Sterner, R. C. & Sterner, R. M. CAR-T cell therapy: current limitations and potential strategies. *Blood Cancer J.* **11**, (2021).

102. Komohara, Y., Fujiwara, Y., Ohnishi, K. & Takeya, M. Tumor-associated macrophages: Potential

therapeutic targets for anti-cancer therapy. *Adv. Drug Deliv. Rev.* **99**, 180–185 (2016).

103. Gentles, A. J. *et al.* The prognostic landscape of genes and infiltrating immune cells across human cancers. *Nat. Med.* **21**, 938–945 (2015).

104. Binnemars-Postma, K., Storm, G. & Prakash, J. Nanomedicine strategies to target tumor-associated macrophages. *Int. J. Mol. Sci.* **18**, (2017).

105. Ngambenjawong, C., Gustafson, H. H. & Pun, S. H. Progress in tumor-associated macrophage (TAM)-targeted therapeutics. *Adv. Drug Deliv. Rev.* **114**, 206–221 (2017).

106. Laplagne, C. *et al.* Latest advances in targeting the tumor microenvironment for tumor suppression. *Int. J. Mol. Sci.* **20**, (2019).

107. Ries, C. H. *et al.* Targeting tumor-associated macrophages with anti-CSF1R antibody reveals a strategy for cancer therapy. *Cancer Cell* **25**, 846–859 (2014).

108. Hume, D. A. & MacDonald, K. P. A. Therapeutic applications of macrophage colony-stimulating factor-1 (CSF-1) and antagonists of CSF-1 receptor (CSF1R) signaling. *Blood* **119**, 1810–1820 (2012).

109. Yan, D. *et al.* Inhibition of colony stimulating factor-1 receptor abrogates microenvironment-mediated therapeutic resistance in gliomas. *Oncogene* **36**, 6049–6058 (2017).

110. Stafford, J. H. *et al.* Colony stimulating factor 1 receptor inhibition delays recurrence of glioblastoma after radiation by altering myeloid cell recruitment and polarization. *Neuro. Oncol.* **18**, 797–806 (2016).

111. Rose Khavari Nicholas Dias, Y. P. 乳鼠心肌提取 HHS Public Access. *Physiol. Behav.* **176**, 139–148 (2017).

112. Butowski, N. *et al.* Orally administered colony stimulating factor 1 receptor inhibitor PLX3397 in recurrent glioblastoma: An Ivy Foundation Early Phase Clinical Trials Consortium phase II study. *Neuro. Oncol.* **18**, 557–564 (2016).

113. Denardo, D. G. *et al.* Functionally Regulates Response to Chemotherapy. *Cancer Discov.* 54–67 (2011). doi:10.1158/2159-8274.CD-10-0028.Leukocyte

114. Gomez-Roca, C. A. *et al.* Phase i study of emactuzumab single agent or in combination with paclitaxel in patients with advanced/metastatic solid tumors reveals depletion of immunosuppressive M2-like macrophages. *Ann. Oncol.* **30**, 1381–1392 (2019).

115. Weizman, N. *et al.* Macrophages mediate gemcitabine resistance of pancreatic adenocarcinoma by upregulating cytidine deaminase. *Oncogene* **33**, 3812–3819 (2014).

116. Lu, X. & Meng, T. Depletion of tumor-associated macrophages enhances the anti-tumor effect of docetaxel in a murine epithelial ovarian cancer. *Immunobiology* **224**, 355–361 (2019).

117. Pyonteck, S. M. *et al.* CSF1R inhibition alters macrophage polarization and blocks glioma progression HHS Public Access Author manuscript. *Nat Med* **19**, 1264–1272 (2013).

118. Michaelson, M. D. & Smith, M. R. Bisphosphonates for treatment and prevention of bone metastases. *J. Clin. Oncol.* **23**, 8219–8224 (2005).

119. van Rooijen, N. & Hendrikx, E. Liposomes for specific depletion of macrophages from organs and tissues. *Methods Mol. Biol.* **605**, 189–203 (2010).

120. Diel, I. J. *et al.* Reduction in New Metastases in Breast Cancer with Adjuvant Clodronate Treatment. *N. Engl. J. Med.* **339**, 357–363 (1998).

121. Van Acker, H. H., Anguille, S., Willemen, Y., Smits, E. L. & Van Tendeloo, V. F. Bisphosphonates for cancer treatment: Mechanisms of action and lessons from clinical trials. *Pharmacol. Ther.* **158**, 24–40 (2016).

122. Zeisberger, S. M. *et al.* Clodronate-liposome-mediated depletion of tumour-associated macrophages: A new and highly effective antiangiogenic therapy approach. *Br. J. Cancer* **95**, 272–281 (2006).

123. Wu, X. *et al.* Depletion of M2-like tumor-associated macrophages delays cutaneous T-cell lymphoma development in vivo. *J. Invest. Dermatol.* **134**, 2814–2822 (2014).

124. Hiraoka, K. *et al.* Inhibition of bone and muscle metastases of lung cancer cells by a decrease in the number of monocytes/macrophages. *Cancer Sci.* **99**, 1595–1602 (2008).

125. Qian, B. *et al.* A distinct macrophage population mediates metastatic breast cancer cell extravasation, establishment and growth. *PLoS One* **4**, (2009).

126. Gazzaniga, S. *et al.* Targeting tumor-associated macrophages and inhibition of MCP-1 reduce angiogenesis and tumor growth in a human melanoma xenograft. *J. Invest. Dermatol.* **127**, 2031–2041 (2007).

127. Germano, G. *et al.* Role of Macrophage Targeting in the Antitumor Activity of Trabectedin. *Cancer Cell* **23**, 249–262 (2013).

128. Banerjee, P. *et al.* Trabectedin reveals a strategy of immunomodulation in chronic lymphocytic leukemia. *Cancer Immunol. Res.* **7**, 2036–2051 (2019).

129. Liguori, M. *et al.* Functional TRAIL receptors in monocytes and tumor-associated macrophages: A possible targeting pathway in the tumor microenvironment. *Oncotarget* **7**, 41662–41676 (2016).

130. Georgoudaki, A. M. *et al.* Reprogramming Tumor-Associated Macrophages by Antibody Targeting Inhibits Cancer Progression and Metastasis. *Cell Rep.* **15**, 2000–2011 (2016).

131. Sommariva, M. *et al.* Activation of NK cell cytotoxicity by aerosolized CpG-ODN/poly(I:C) against lung melanoma metastases is mediated by alveolar macrophages. *Cell. Immunol.* **313**, 52–58 (2017).

132. Halama, N. *et al.* Tumoral Immune Cell Exploitation in Colorectal Cancer Metastases Can Be Targeted Effectively by Anti-CCR5 Therapy in Cancer Patients. *Cancer Cell* **29**, 587–601 (2016).

133. Long, K. B. *et al.* IFN-γ and CCL2 cooperate to redirect tumor-infiltrating monocytes to degrade fibrosis and enhance chemotherapy efficacy in pancreatic carcinoma. **6**, 400–413 (2017).

134. Maeda, A., Digifico, E., Andon, F. T., Mantovani, A. & Allavena, P. Poly(I:C) stimulation is superior than Imiquimod to induce the antitumoral functional profile of tumor-conditioned macrophages. *Eur. J. Immunol.* **49**, 801–811 (2019).

135. Yin, T., He, S. & Wang, Y. Toll-like receptor 7/8 agonist, R848, exhibits antitumoral effects in a breast cancer model. *Mol. Med. Rep.* **12**, 3515–3520 (2015).

136. Weihrauch, M. R. *et al.* Phase i clinical study of the toll-like receptor 9 agonist MGN1703 in patients with metastatic solid tumours. *Eur. J. Cancer* **51**, 146–156 (2015).

137. Lizotte, P. H. *et al.* Attenuated Listeria monocytogenes reprograms M2-polarized tumor-associated macrophages in ovarian cancer leading to iNOS-mediated tumor cell lysis. *Oncoimmunology* **3**, 1–12 (2014).

138. Tutt, A. L. *et al.* T Cell Immunity to Lymphoma Following Treatment with Anti-CD40 Monoclonal Antibody. *J. Immunol.* **168**, 2720–2728 (2002).

139. Rüter, J., Antonia, S. J., Burris, H. A., Huhn, R. D. & Vonderheide, R. H. Immune modulation with weekly dosing of an agonist CD40 antibody in a phase I study of patients with advanced solid tumors. *Cancer Biol. Ther.* **10**, 983–993 (2010).

140. Dheilly, E. *et al.* Selective Blockade of the Ubiquitous Checkpoint Receptor CD47 Is Enabled by Dual-Targeting Bispecific Antibodies. *Mol. Ther.* **25**, 523–533 (2017).

141. Mullins, D. W., Burger, C. J. & Elgert, K. D. Paclitaxel enhances macrophage IL-12 production in tumor-bearing hosts through nitric oxide. *J. Immunol.* **162**, 6811–6818 (1999).

142. Kortylewski, M. *et al.* TLR agonist-Stat3 siRNA cojugates: cell-specific. *Nat. Biotechnol.* **27**, 925–932 (2009).

143. Andersen, M. N. *et al.* STAT3 inhibition specifically in human monocytes and macrophages by CD163-targeted corosolic acid-containing liposomes. *Cancer Immunol. Immunother.* **68**, 489–502 (2019).

144. Binnemars-Postma, K., Bansal, R., Storm, G. & Prakash, J. Targeting the Stat6 pathway in tumor-associated macrophages reduces tumor growth and metastatic niche formation in breast cancer. *FASEB J.* **32**, 969–978 (2018).

145. Sonda, N. *et al.* MiR-142-3p Prevents Macrophage Differentiation during Cancer-Induced Myelopoiesis. *Immunity* **38**, 1236–1249 (2013).

146. Baer, C. *et al.* Suppression of microRNA activity amplifies IFN-γ-induced macrophage activation and promotes anti-tumour immunity. *Nat. Cell Biol.* **18**, 790–802 (2016).

147. Chen, W. *et al.* Macrophage-induced tumor angiogenesis is regulated by the TSC2-mTOR pathway. *Cancer Res.* **72**, 1363–1372 (2012).

148. Kaneda, M. M. *et al.* PI3Kγ 3 is a molecular switch that controls immune suppression. *Nature* **539**, 437–442 (2016).

149. Chakraborty, P. *et al.* Reprogramming of TAM toward proimmunogenic type through regulation of MAP kinases using a redox-active copper chelate. *J. Leukoc. Biol.* **91**, 609–619 (2012).

150. Tan, H. Y. *et al.* Autophagy-induced RelB/p52 activation mediates tumour-associated macrophage repolarisation and suppression of hepatocellular carcinoma by natural compound baicalin. *Cell Death Dis.* **6**, e1942-13 (2015).

151. Wang, C. *et al.* CYP4X1 inhibition by flavonoid CH625 normalizes glioma vasculature through reprogramming TAMs via CB2 and EGFR-STAT3 Axiss. *J. Pharmacol. Exp. Ther.* **365**, 72–83 (2018).

152. Guerriero, J. L. *et al.* Class IIa HDAC inhibition reduces breast tumours and metastases through anti-tumour macrophages. *Nature* **543**, 428–432 (2017).

153. Wanderley, C. W. *et al.* Paclitaxel reduces tumor growth by reprogramming tumor-associated macrophages to an M1 profile in a TLR4-dependent manner. *Cancer Res.* **78**, 5891–5900 (2018).

154. Perry, C. J. *et al.* Myeloid-targeted immunotherapies act in synergy to induce inflammation and antitumor immunity. *J. Exp. Med.* **215**, 877–893 (2018).

155. Smith, D. A. *et al.* Antitumor activity and safety of combination therapy with the Toll-like receptor 9 agonist IMO-2055, erlotinib, and bevacizumab in advanced or metastatic non-small cell lung cancer patients who have progressed following chemotherapy. *Cancer Immunol. Immunother.* **63**, 787–796 (2014).

156. Xu, A. *et al.* TLR9 agonist enhances radiofrequency ablation-induced CTL responses, leading to the potent inhibition of primary tumor growth and lung metastasis. *Cell. Mol. Immunol.* **16**, 820–832 (2019).

157. Ma, B. *et al.* The SIAH2-NRF1 axis spatially regulates tumor microenvironment remodeling for tumor progression. *Nat. Commun.* **10**, 1–17 (2019).

158. Chen, P. *et al.* Gpr132 sensing of lactate mediates tumor-macrophage interplay to promote breast cancer metastasis. *Proc. Natl. Acad. Sci. U. S. A.* **114**, 580–585 (2017).

159. Colegio, O. R. *et al.* Functional polarization of tumour-associated macrophages by tumour-derived lactic acid. *Nature* **513**, 559–563 (2014).

160. Verzella, D. *et al.* GADD45β loss ablates innate immunosuppression in cancer. *Cancer Res.* **78**, 1275–1292 (2018).

161. Wei, X. *et al.* Angiopoietin-like protein 2 facilitates non-small cell lung cancer progression by promoting the polarization of M2 tumor-associated macrophages. *Am. J. Cancer Res.* **7**, 2220–2233 (2017).

162. Racioppi, L. *et al.* CaMKK2 in myeloid cells is a key regulator of the immune-suppressive microenvironment in breast cancer. *Nat. Commun.* **10**, 1–16 (2019).

163. Zhang, Q. *et al.* Fatty acid oxidation contributes to IL-1β secretion in M2 macrophages and promotes macrophage-mediated tumor cell migration. 27–35 (2019). doi:10.1016/j.molimm.2017.12.011.Fatty

164. Goossens, P. *et al.* Membrane Cholesterol Efflux Drives Tumor-Associated Macrophage Reprogramming and Tumor Progression. *Cell Metab.* **29**, 1376-1389.e4 (2019).

165. Klichinsky, M. *et al.* Human chimeric antigen receptor macrophages for cancer immunotherapy. *Nat. Biotechnol.* **38**, 947–953 (2020).

166. Bartneck, M. *et al.* The CCR2 + Macrophage Subset Promotes Pathogenic Angiogenesis for Tumor Vascularization in Fibrotic Livers. *Cmgh* **7**, 371–390 (2019).

167. Li, F. *et al. Retinoblastoma inactivation induces a protumoral microenvironment via enhanced CCL2 secretion*. *Cancer Research* (2019). doi:10.1158/0008-5472.CAN-18-3604

168. Gui, P. *et al.* the Protease-Dependent Mesenchymal Migration of Tumor-Associated Macrophages As a Target in Cancer Immunotherapy. *Cancer Immunol. Res.* **6**, canimm.0746.2017 (2018).

169. Yang, Z. *et al.* CCL2/CCR2 Axis Promotes the Progression of Salivary Adenoid Cystic Carcinoma via Recruiting and Reprogramming the Tumor-Associated Macrophages. *Front. Oncol.* **9**, 1–13 (2019).

170. Nywening, T. M. *et al.* Targeting both tumour-associated CXCR2+ neutrophils and CCR2+ macrophages disrupts myeloid recruitment and improves chemotherapeutic responses in pancreatic ductal adenocarcinoma. *Gut* **67**, 1112–1123 (2018).

171. Vela, M., Aris, M., Llorente, M., Garcia-Sanz, J. A. & Kremer, L. Chemokine receptor-specific antibodies in cancer immunotherapy: Achievements and challenges. *Front. Immunol.* **6**, (2015).

172. Bonapace, L. *et al.* Cessation of CCL2 inhibition accelerates breast cancer metastasis by promoting angiogenesis. *Nature* **515**, 130–133 (2014).

173. Sandhu, S. K. *et al.* A first-in-human, first-in-class, phase i study of carlumab (CNTO 888), a human monoclonal antibody against CC-chemokine ligand 2 in patients with solid tumors. *Cancer Chemother. Pharmacol.* **71**, 1041–1050 (2013).

174. Pienta, K. J. *et al.* Phase 2 study of carlumab (CNTO 888), a human monoclonal antibody against CC-chemokine ligand 2 (CCL2), in metastatic castration-resistant prostate cancer. *Invest. New Drugs* **31**, 760–768 (2013).

175. Nywening, T. M. *et al.* Phase 1b study targeting tumour associated macrophages with CCR2 inhibition plus FOLFIRINOX in locally advanced and borderline resectable pancreatic cancer HHS Public Access. *Lancet Oncol* **17**, 651–662 (2016).

176. Leftin, A., Ben-Chetrit, N., Joyce, J. A. & Koutcher, J. A. Imaging endogenous macrophage iron deposits reveals a metabolic biomarker of polarized tumor macrophage infiltration and response to CSF1R breast cancer immunotherapy. *Sci. Rep.* **9**, 1–15 (2019).

177. Papadopoulos, K. P. *et al.* First-in-human study of AMG 820, a monoclonal anti-colony-stimulating factor 1 receptor antibody, in patients with advanced solid tumors. *Clin. Cancer Res.* **23**, 5703–5710 (2017).

178. Cassier, P. A. *et al.* CSF1R inhibition with emactuzumab in locally advanced diffuse-type tenosynovial giant cell tumours of the soft tissue: A dose-escalation and dose-expansion phase 1 study. *Lancet Oncol.* **16**, 949–956 (2015).

179. Sun, Y. *et al.* Phase i dose-escalation study of chiauranib, a novel angiogenic, mitotic, and chronic inflammation inhibitor, in patients with advanced solid tumors. *J. Hematol. Oncol.* **12**, 1–10 (2019).

180. Rosenbaum, E. *et al.* A Phase I Study of Binimetinib (MEK162) Combined with Pexidartinib (PLX3397) in Patients with Advanced Gastrointestinal Stromal Tumor. *Oncologist* theoncologist.2019-0418 (2019). doi:10.1634/theoncologist.2019-0418

181. Hegab, A. E. *et al.* Effect of FGF/FGFR pathway blocking on lung adenocarcinoma and its cancer-

associated fibroblasts. *J. Pathol.* **249**, 193–205 (2019).

182. Xia, Y. *et al.* Catecholamines contribute to the neovascularization of lung cancer via tumor-associated macrophages. *Brain. Behav. Immun.* **81**, 111–121 (2019).

183. Piao, C. *et al.* Complement 5a stimulates macrophage polarization and contributes to tumor metastases of colon cancer. *Exp. Cell Res.* **366**, 127–138 (2018).

184. Nakayama, R. *et al.* Clinical characteristics and treatment outcomes in six cases of malignant tenosynovial giant cell tumor: Initial experience of molecularly targeted therapy. *BMC Cancer* **18**, 1–9 (2018).

185. Yum, J. E. I. & Hong, Y. K. Terminating Cancer by Blocking VISTA as a Novel Immunotherapy: Hasta la vista, baby. *Front. Oncol.* **11**, 1–9 (2021).

186. Myers, K. V., Amend, S. R. & Pienta, K. J. Targeting Tyro3, Axl and MerTK (TAM receptors): Implications for macrophages in the tumor microenvironment. *Mol. Cancer* **18**, 1–14 (2019).

187. Kipps, T. J. *et al.* Chronic lymphocytic leukaemia. *Nat. Rev. Dis. Prim.* **3**, (2017).

188. Cancer Stat Facts: Leukemia — Chronic Lymphocytic Leukemia (CLL). Available at: https://seer.cancer.gov/statfacts/html/clyl.html.

189. de Faria-Moss, M. *et al.* Title: High frequency of chronic lymphocytic leukemia-like low-count monoclonal B-cell lymphocytosis in Japanese descendants living in Brazil. *Haematologica* **105**, 298–301 (2020).

190. Tissino, E. *et al.* CD49d promotes disease progression in chronic lymphocytic leukemia: New insights from CD49d bimodal expression. *Blood* **135**, 1244–1254 (2020).

191. Bulian, P. *et al.* CD49d is the strongest flow cytometry-based predictor of overall survival in chronic lymphocytic leukemia. *J. Clin. Oncol.* **32**, 897–904 (2014).

192. Poeta, G. Del *et al.* CD69 is independently prognostic in chronic lymphocytic leukemia: A comprehensive clinical and biological profiling study. *Haematologica* **97**, 279–287 (2012).

193. Gentile, M. *et al.* Predictive value of β2-microglobulin (β2-m) levels in chronic lymphocytic leukemia since Binet A stages. *Haematologica* **94**, 887–888 (2009).

194. Abruzzo, L. V. *et al.* Trisomy 12 chronic lymphocytic leukemia expresses a unique set of activated and targetable pathways. *Haematologica* **103**, 2069–2078 (2018).

195. Campo, E. *et al.* TP53 aberrations in chronic lymphocytic leukemia: An overview of the clinical implications of improved diagnostics. *Haematologica* **103**, 1956–1968 (2018).

196. ten Hacken, E. & Burger, J. A. Microenvironment interactions and B-cell receptor signaling in Chronic Lymphocytic Leukemia: Implications for disease pathogenesis and treatment. *Biochim. Biophys. Acta - Mol. Cell Res.* **1863**, 401–413 (2016).

197. Jaseb, K. *et al.* Prognostic significance of aberrant CD5 expression in B-cell leukemia. *Oncol. Rev.* **13**, 77–82 (2019).

198. Calissano, C. *et al.* Intraclonal complexity in chronic lymphocytic leukemia: Fractions enriched in recently born/divided and older/quiescent cells. *Mol. Med.* **17**, 1374–1382 (2011).

199. Mainou-Fowler, T., Miller, S., Proctor, S. J. & Dickinson, A. M. The levels of TNFα, IL4 and IL10 production by T-cells in B-cell chronic lymphocytic leukaemia (B-CLL). *Leuk. Res.* **25**, 157–163 (2001).

200. van Attekum, M. H. A. *et al.* CD40 signaling instructs chronic lymphocytic leukemia cells to attract monocytes via the CCR2 axis. *Haematologica* **102**, 2069–2076 (2017).

201. Burger, J. A. *et al.* Plenary paper Blood-derived nurse-like cells protect chronic lymphocytic leukemia B cells from spontaneous apoptosis through stromal cell – derived factor-1. *Blood* **96**, 2655–2663 (2000).

202. V, D. K. E. *et al.* Targeting of colony-stimulating factor 1 receptor (CSF1R) in the CLL microenvironment yields antineoplastic activity in primary patient samples. *Oncotarget* **9**, 24576–24589 (2018).

203. Polk, A. *et al.* Colony-stimulating factor-1 receptor is required for nurse-like cell survival in chronic lymphocytic leukemia. *Clin. Cancer Res.* **22**, 6118–6128 (2016).

204. Fiorcari, S. *et al.* Nurse-like cells and chronic lymphocytic leukemia b cells: A mutualistic crosstalk inside tissue microenvironments. *Cells* **10**, 1–12 (2021).

205. Jia, L. *et al.* Extracellular HMGB1 promotes differentiation of nurse-like cells in chronic lymphocytic leukemia. *Blood* **123**, 1709–1719 (2014).

206. Boissard, F. *et al.* Nurse-like cells promote CLL survival through LFA-3/CD2 interactions. *Oncotarget* **8**, 52225–52236 (2017).

207. Ysebaert, L. & Fournié, J. J. Genomic and phenotypic characterization of nurse-like cells that promote drug resistance in chronic lymphocytic leukemia. *Leuk. Lymphoma* **52**, 1404–1406 (2011).

208. Yang, X. *et al.* Repolarizing heterogeneous leukemia-associated macrophages with more M1 characteristics eliminates their pro-leukemic effects. *Oncoimmunology* **7**, (2018).

209. Boissard, F., Fournié, J. J., Laurent, C., Poupot, M. & Ysebaert, L. Nurse like cells: Chronic lymphocytic leukemia associated macrophages. *Leuk. Lymphoma* **56**, 1570–1572 (2015).

210. Nishio, M. *et al.* Nurselike cells express BAFF and APRIL , which can promote survival of chronic lymphocytic leukemia cells via a paracrine pathway distinct from that of SDF-1 ␣. **106**, 1012–1021 (2016).

211. Talbot, H. *et al.* BDNF belongs to the nurse-like cell secretome and supports survival of B chronic lymphocytic leukemia cells. *Sci. Rep.* **10**, 1–9 (2020).

212. van Attekum, M., Terpstra, S., Reinen, E., Kater, A. & Eldering, E. Macrophage-mediated chronic lymphocytic leukemia cell survival is independent of APRIL signaling. *Cell Death Discov.* **2**, (2016).

213. Binder, M. *et al.* Stereotypical chronic lymphocytic leukemia B-cell receptors recognize survival promoting antigens on stromal cells. *PLoS One* **5**, (2010).

214. Boissard, F. *et al.* Letter to the editor: Nurse-like cells impact on disease progression in chronic lymphocytic leukemia. *Blood Cancer J.* **6**, (2016).

215. Friedman, D. R. *et al.* study. **91**, 687–691 (2016).

216. Fiorcari, S. *et al.* <11782-177645-4-PB.pdf>. **7**, (2016).

217. Elliott, M. R., Koster, K. M. & Murphy, P. S. Efferocytosis Signaling in the Regulation of Macrophage Inflammatory Responses. *J. Immunol.* **198**, 1387–1394 (2017).

218. Ferrarini, I., Rigo, A., Montresor, A., Laudanna, C. & Vinante, F. Monocyte-to-macrophage switch reversibly impaired by Ibrutinib. *Oncotarget* **10**, 1943–1956 (2019).

219. Fiorcari, S. *et al.* Lenalidomide interferes with Tumor-Promoting properties of Nurse-Like cells in chronic lymphocytic leukemia. *Haematologica* **100**, 253–262 (2015).

220. *Phase II Trial of Revlimid® and Rituximab for Relapsed or Refractory Chronic Lymphocytic Leukemia (CLL)*.

221. Chanan-Khan, A. *et al.* Randomized phase 3 study of lenalidomide versus chlorambucil as first-line therapy for older patients with chronic lymphocytic leukemia (the ORIGIN trial). *Leukemia* **31**, 1240–1243 (2017).

222. Trabectedin and Venetoclax in Treating Patients With Chronic Lymphocytic Leukemia or Small Lymphocytic Lymphoma Resistant or Intolerant to a BTK Inhibitor.

223. Risnik, D. *et al.* Immunoregulatory effects of Lurbinectedin in chronic lymphocytic leukemia. *Cancer Immunol. Immunother.* **69**, 813–824 (2020).

224. Hanna, B. S. *et al.* Depletion of CLL-associated patrolling monocytes and macrophages controls disease development and repairs immune dysfunction in vivo. *Leukemia* **30**, 570–579 (2016).

225. Gautam, S. *et al.* Reprogramming nurse-like cells with interferon γ to interrupt chronic lymphocytic leukemia cell survival. *J. Biol. Chem.* **291**, 14356–14362 (2016).

226. Hailemariam, M. *et al.* S-Trap, an Ultrafast Sample-Preparation Approach for Shotgun Proteomics. *J. Proteome Res.* **17**, 2917–2924 (2018).

227. Almasri, N. M., Duque, R. E., Iturraspe, J., Everett, E. & Braylan, R. C. Reduced expression of CD20 antigen as a characteristic marker for chronic lymphocytic leukemia. *Am. J. Hematol.* **40**, 259–263 (1992).

228. Shanafelt, T. D. *et al.* Ibrutinib–Rituximab or Chemoimmunotherapy for Chronic Lymphocytic Leukemia. *N. Engl. J. Med.* **381**, 432–443 (2019).

229. Sievers, E. L. Targeted therapy of acute myeloid leukemia with monoclonal antibodies and immunoconjugates. *Cancer Chemother. Pharmacol.* **46**, 18–22 (2000).

230. Murray, P. J. *et al.* Macrophage Activation and Polarization: Nomenclature and Experimental Guidelines. *Immunity* **41**, 14–20 (2014).

231. Joshi, S. *et al.* Rac2 controls tumor growth, metastasis and M1-M2 macrophage differentiation in

vivo. *PLoS One* **9**, (2014).

232. Orecchioni, M., Ghosheh, Y., Pramod, A. B. & Ley, K. Macrophage polarization: Different gene signatures in M1(Lps+) vs. Classically and M2(LPS-) vs. Alternatively activated macrophages. *Front. Immunol.* **10**, 1–14 (2019).

233. Boulakirba, S. *et al.* IL-34 and CSF-1 display an equivalent macrophage differentiation ability but a different polarization potential. *Sci. Rep.* **8**, 1–11 (2018).

234. McWhorter, F. Y., Wang, T., Nguyen, P., Chung, T. & Liu, W. F. Modulation of macrophage phenotype by cell shape. *Proc. Natl. Acad. Sci. U. S. A.* **110**, 17253–17258 (2013).

235. Heinrich, F. *et al. Morphologic, phenotypic, and transcriptomic characterization of classically and alternatively activated canine blood-derived macrophages in vitro*. *PLoS ONE* **12**, (2017).

236. Depil, S., Duchateau, P., Grupp, S. A., Mufti, G. & Poirot, L. 'Off-the-shelf' allogeneic CAR T cells: development and challenges. *Nat. Rev. Drug Discov.* **19**, 185–199 (2020).

237. Zhou, X., Li, Z. & Zhou, J. Tumor necrosis factor α in the onset and progression of leukemia. *Exp. Hematol.* **45**, 17–26 (2017).

238. Aiyer, R. A. & Aggarwal, B. B. Tumor necrosis factors. *Cytolytic Lymphocytes Complement Eff. Immune Syst.* **2**, 105–134 (2018).

239. Boyette, L. B. *et al.* Phenotype, function, and differentiation potential of human monocyte subsets. *PLoS One* **12**, 1–20 (2017).

240. Munn, D. H. *et al.* Inhibition of T cell proliferation by macrophage tryptophan catabolism. *J. Exp. Med.* **189**, 1363–1372 (1999).

241. Droste, A., Sorg, C. & Högger, P. Shedding of CD163, a novel regulatory mechanism for a member of the scavenger receptor cysteine-rich family. *Biochem. Biophys. Res. Commun.* **256**, 110–113 (1999).

242. Moraes, J. Z. *et al.* Hybridoma technology: is it still useful? *Curr. Res. Immunol.* **2**, 32–40 (2021).

243. Wong-Baeza, C. *et al.* Anti-lipid IgG antibodies are produced via germinal centers in a murine model resembling human lupus. *Front. Immunol.* **7**, 1–13 (2016).

244. The human protein atlas. FOLR2. Available at: https://www.proteinatlas.org/ENSG00000165457-FOLR2.

245. Carmel M. Lynch, B. W. H. and I. S. G. Practical considerations for nonclinical safety evaluation of therapeutic monoclonal antibodies. *MAbs* **1**, 2–11 (2009).

246. Goulet, D. R. & Atkins, W. M. Considerations for the Design of Antibody-Based Therapeutics. *J. Pharm. Sci.* **109**, 74–103 (2020).

247. Lynch, C. M., Hart, B. W. & Grewal, I. S. Practical considerations for nonclinical safety evaluation of therapeutic monoclonal antibodies. *mAbs* **1**, 2–11 (2009).

248. Pradel, L. P. *et al.* Macrophage susceptibility to emactuzumab (RG7155) treatment. *Mol. Cancer*

Ther. **15**, 3077–3086 (2016).

249. Stanley, E. R. & Chitu, V. CSF-1 receptor signaling in myeloid cells. *Cold Spring Harb. Perspect. Biol.* **6**, 1–21 (2014).

250. Amorim, I. S. *et al.* Sideroflexin 3 is an α-synuclein-dependent mitochondrial protein that regulates synaptic morphology. *J. Cell Sci.* **130**, 325–331 (2017).

251. Kory, N. *et al.* SFXN1 is a mitochondrial serine transporter required for one-carbon metabolism. *Science (80-.).* **362**, eaat9528 (2018).

252. Ma, Z. *et al.* Mitochondrial F1Fo-ATP synthase translocates to cell surface in hepatocytes and has high activity in tumor-like acidic and hypoxic environment. *Acta Biochim. Biophys. Sin. (Shanghai).* **42**, 530–537 (2010).

253. Poyton, R. O., Duhl, D. M. J. & Clarkson, G. H. D. Protein export from the mitochondrial matrix. *Trends Cell Biol.* **2**, 369–375 (1992).

254. Banh, R. S. *et al.* Neurons Release Serine to Support mRNA Translation in Pancreatic Cancer. *Cell* **183**, 1202-1218.e25 (2020).

255. Murase, R. *et al.* Serum autoantibody to sideroflexin 3 as a novel tumor marker for oral squamous cell carcinoma. *Proteomics - Clin. Appl.* **2**, 517–527 (2008).

256. Freund, E. C. *et al.* Efficient gene knockout in primary human and murine myeloid cells by non-viral delivery of crispr-cas9. *J. Exp. Med.* **217**, (2020).

257. Reiner, N. E. Methods in molecular biology. Macrophages and dendritic cells. Methods and protocols. Preface. *Methods Mol. Biol.* **531**, 1–18 (2009).

258. Rodriguez-Garcia, A. *et al.* CAR-T cell-mediated depletion of immunosuppressive tumor-associated macrophages promotes endogenous antitumor immunity and augments adoptive immunotherapy. *Nat. Commun.* **12**, 1–17 (2021).

259. Tie, Y. *et al.* Targeting folate receptor β positive tumor-associated macrophages in lung cancer with a folate-modified liposomal complex. *Signal Transduct. Target. Ther.* **5**, 1–15 (2020).

260. Shen, J. *et al.* Assessment of folate receptor-β expression in human neoplastic tissues. *Oncotarget* **6**, 14700–14709 (2015).

261. Roy, A. G. *et al.* Folate receptor beta as a direct and indirect target for antibody-based cancer immunotherapy. *Int. J. Mol. Sci.* **22**, (2021).

262. Puig-Kröger, A. *et al.* Folate receptor β is expressed by tumor-associated macrophages and constitutes a marker for M2 anti-inflammatory/regulatory Macrophages. *Cancer Res.* **69**, 9395–9403 (2009).

263. 6;, R. S. 1; *; Á. D.-S. 2; M. R. 3; T. M. 4; P. S.-M. 5; Á. L. C. 2; † and A. P.-K. Folate Receptor β (FRβ) Expression in Tissue-Resident and Tumor-Associated Macrophages Associates with and Depends on the Expression of PU.1. *Cells* 1–17 (2020).

264. Sharma, A. *et al.* Onco-fetal Reprogramming of Endothelial Cells Drives Immunosuppressive

Macrophages in Hepatocellular Carcinoma. *Cell* **183**, 377-394.e21 (2020).

265. Park, Y. Il *et al.* pH-sensitive multi-drug liposomes targeting folate receptor β for efficient treatment of non-small cell lung cancer. *J. Control. Release* **330**, 1–14 (2021).

266. Hu, Y. *et al.* Depletion of activated macrophages with a folate receptor-beta-specific antibody improves symptoms in mouse models of rheumatoid arthritis. *Arthritis Res. Ther.* **21**, 1–14 (2019).

267. Tsuneyoshi, Y. *et al.* Functional folate receptor beta-expressing macrophages in osteoarthritis synovium and their M1/M2 expression profiles. *Scand. J. Rheumatol.* **41**, 132–140 (2012).

268. Moisio, O. *et al.* Radiosynthesis and preclinical evaluation of [68Ga]Ga-NOTA-folate for PET imaging of folate receptor β-positive macrophages. *Sci. Rep.* **10**, 1–10 (2020).

269. Samaniego, R. *et al.* Macrophage uptake and accumulation of folates are polarization-dependent in vitro and in vivo and are regulated by activin A. *J. Leukoc. Biol.* **95**, 797–808 (2014).

270. Chandrupatla, D. M. S. H., Molthoff, C. F. M., Lammertsma, A. A., van der Laken, C. J. & Jansen, G. The folate receptor β as a macrophage-mediated imaging and therapeutic target in rheumatoid arthritis. *Drug Deliv. Transl. Res.* **9**, 366–378 (2019).

271. Li, Y., You, M. J., Yang, Y., Hu, D. & Tian, C. The Role of Tumor-Associated Macrophages in Leukemia. *Acta Haematol.* **300011**, 1–6 (2019).

272. Samblas, M., Martínez, J. A. & Milagro, F. Folic Acid Improves the Inflammatory Response in LPS-Activated THP-1 Macrophages. *Mediators Inflamm.* **2018**, (2018).

273. Machacek, C. *et al.* Folate Receptor β Regulates Integrin CD11b/CD18 Adhesion of a Macrophage Subset to Collagen. *J. Immunol.* **197**, 2229–2238 (2016).

274. Nagai, T. *et al.* Targeting tumor-associated macrophages in an experimental glioma model with a recombinant immunotoxin to folate receptor β. *Cancer Immunol. Immunother.* **58**, 1577–1586 (2009).

275. Nagai, T., Kyo, A., Hasui, K., Takao, S. & Matsuyama, T. Efficacy of an immunotoxin to folate receptor beta in the intra-articular treatment of antigen-induced arthritis. *Arthritis Res. Ther.* **14**, R106 (2012).

276. Lu, Y. J. *et al.* Targeting folate receptor beta on monocytes/macrophages renders rapid inflammation resolution independent of root causes. *Cell Reports Med.* **2**, 100422 (2021).

277. Verweij, N. J. F. *et al.* First in man study of [18F]fluoro-PEG-folate PET: a novel macrophage imaging technique to visualize rheumatoid arthritis. *Sci. Rep.* **10**, 1–10 (2020).

278. Zarou, M. M., Vazquez, A. & Vignir Helgason, G. Folate metabolism: a re-emerging therapeutic target in haematological cancers. *Leukemia* **35**, 1539–1551 (2021).

279. Mongini, P. K. A. *et al.* TLR-9 and IL-15 Synergy Promotes the In Vitro Clonal Expansion of Chronic Lymphocytic Leukemia B Cells. *J. Immunol.* **195**, 901–923 (2015).

280. Kohlmeier, M. Water-Soluble Vitamins and Nonnutrients. *Nutr. Metab.* 567–671 (2015). doi:10.1016/b978-0-12-387784-0.00010-9

List of figures

Figure 1. Initial evaluation of 6-25 mAb specificity. 61

Figure 2 The 6-25 mAb FC analysis of primary human cells. 62

Figure 3. Expression of 6-25 target on NLCs. 65

Figure 4 Flow cytometry analysis of the staining of AML cell lines with 6-25 mAb. 66

Figure 5 Influence of GM-CSF, CSF-1 and IL-34 on polarization state of MDM and expression of 6-25 target 68

Figure 6. Influence of secondary M1 (IFN-γ or LPS) or M2 (IL-4, IL-13) polarization on expression of 6-25 target in CSF-1, IL-34 or GM-CSF activated MDM. 70

Figure 7. Effect of TNF on maturation and polarization of CSF-1 activated MDM, and expression of 6-25 target. 72

Figure 8 TNF blocks M2-polarization of macrophages induced by CSF-1 and IL-34, and abrogates expression of 6-25 target on MDM 73

Figure 9 Distinct effect of M1 polarizing agents (LPS, TNF and IFN-γ) on phenotype of CSF-1 activated MDM. 75

Figure 10. Kinetics of the 6-25 target appearance on the surface monocytes during the maturation into NLC in relation to other myeloid markers 78

Figure 11 Changes in the viability and CLL cell concentration during typical CLL PBMC culture.. 79

Figure 12. Correlation of the 6-25 target expression on NLC and viability of CLL cells. 80

Figure 13. Changes in the viability and CLL cell concentration in CLL PBMC culture from patient 5 (Fig. 12A) 81

Figure 14 Correlation of 6-25 target expression on NLCs and viability of CLL cells. 82

Figure 15. Comparison of phenotype NLCs from high and low viability CLL PBMC cultures. 83

Figure 16. Western blot analysis of 1) fragment of human SFXN3 and 2) mouse SFXN3 recombinant protein 100

Figure 17. Extracellular and intracellular immunofluorescence labelling of M2-MDM with 6-25 Ab. 102

Figure 18. Intracellular and extracellular immunofluorescence labelling of M2-MDM with a-SFXN3 pAb. 103

Figure 19. CRISPR-Cas9 KO of SFXN3 in primary monocytes and macrophages. 104

Figure 20. DEG analysis of plasma membrane-coding genes in CSF-1 activated-MDM treated with TNF. 106

Figure 21 Confirmation of protein origin of the 6-25 target. 107

Figure 22. Volcano plot of proteins enriched in IP with 6-25 mAb. 108

Figure 23. Comparison of staining of 6-25, aFRb and aCD36 antibodies on MDM. 109

Figure 24. Validation of new 6-25 target by RNP mediated KO of FOLR2 gene in MDM. 110

Figure 25. Overexpression of FOLR2 gene in HEK-T cell line. 112

Figure 26. No toxicity of the 6-25 mAb toward CLL cells and NLCs. 114

Figure 27 No toxicity of the 6-25 mAb toward healthy donor PBMC. 115

Figure 28. No toxicity of the 6-25 mAb toward M1 and M2-MDM. 116

Figure 29 Effect of mouse 6-25 antibody on polarization (A) and maturation (B) of NLCs in vitro.. 117

Figure 30. Chimeric 6-25 mAb cause changes in phenotype of mature M2 MDM. 118

Figure 31 The 6-25 mAb is internalized by NLCs. 119

List of abbreviations

AML	Acute myeloid leukemia
BPs	Bisphosphonates
CLL	Chronic lymphocytic leukemia
CRI	Cancer-related inflammation
CSF	Colony-stimulating factor
DAMP	Damage-associated molecular pattern
DGE	Differential gene expression
ECM	Extracellular matrix
FC	Flow cytometry
FRβ	Folate receptor beta
HD	Healthy donor
HIFs	Hypoxia inducible factors
ICB	Immune checkpoint blockade
IGHV	Immunoglobulin heavy-chain variable region gene
IP	Immuno-precipitation
KO	knock-out
LNs	Lymph nodes
LPS	Lipopolysaccharides
MDMs	Monocyte-derived macrophages
MDSC	Monocyte-derived suppressor cells
MS	Mass spectrometry
NLCs	Nurse-like cells
NSAIDs	Non-steroid anti-inflammatory drugs
PAMP	Pathogen-associated molecular patterns
PBMC	Peripheral blood mononuclear cell
PCs	Proliferation centers
RA	Rheumatoid arthritis
RNP	Ribonucleoprotein
ROS	reactive oxygen species
TAMs	Tumor-associated macrophages
TME	Tumor microenvironment
TNF	Tumor-necrosis factor
VEGF-A	Vascular endothelial growth factor A
WB	Western blot